Model Predictive Control Algorithms for Pen and Pump Insulin Administration

Boiroux, Dimitri

Publication date:
2012

Document Version
Publisher's PDF, also known as Version of record

Ph.D. Thesis

Model Predictive Control Algorithms for Pen and Pump Insulin Administration

Dimitri Boiroux

Department of Informatics and Mathematical Modelling
Technical University of Denmark
Kongens Lyngby
IMM-PHD-2012-283

DTU

Preface

This thesis was submitted at the Technical University of Denmark, Department of Informatics and Mathematical modelling in partial fulfilment of the PhD requirements. The work presented in this thesis was carried out from September 2009 to September 2012.
This project has been supervised by Associate Professors John Bagterp Jørgensen, Niels Kjølstad Poulsen and Professor Henrik Madsen.
This project has been founded by the Danish Council for Strategic Research (NABIIT project 2106-07-0034), which is gratefully acknowledged.

Acknowledgements

First of all, I would like to thank my supervisor John Bagterp Jørgensen and my co-supervisors Niels Kjølstad Poulsen and Henrik Madsen for their precious advice and their thorough insight into control theory, mathematical modeling, time series analysis and optimization. More generally, I thank all the past and current members of the Diabetes Consortium (DIACON) project for their collaboration and their involvement to the project, and particularly for having conducted the overnight clinical studies.
I also thank the whole Scientific Computing section of DTU Informatics for the interesting discussions and the active social life.
Last but not least, I would like to thank my friends and family for their moral support.

Summary

Despite recent developments within diabetes management such as rapid-acting insulin, continuous glucose monitors (CGM) and insulin pumps, tight blood glucose control still remains a challenge. A fully automated closed-loop controller, also known as an artificial pancreas (AP), has the potential to ease the life and reduce the risk of acute and chronic diabetic complications. However, the noise associated to CGMs, the long insulin action time for continuous subcutaneous infusion of insulin (CSII) pumps, and the high intra- and inter-patient variability significantly limits the performance of current closed-loop controllers.

In this thesis, we present different control strategies based on Model Predictive Control (MPC) for an artificial pancreas. We use Nonlinear Model Predictive Control (NMPC) in order to determine the optimal insulin and blood glucose profiles. The optimal control problem (OCP) is solved using a multiple-shooting based algorithm. We use an explicit Runge-Kutta method (DOPRI45) with an adaptive stepsize for numerical integration and sensitivity computation. The OCP is solved using a Quasi-Newton sequential quadratic programming (SQP) with a linesearch and a BFGS update for the Hessian of the Lagrangian. In addition, we apply a Continuous-Discrete Extended Kalman Filter (CDEKF) in order to simulate cases where the meal size is uncertain, or even unannounced.

We also propose a novel control strategy based on linear MPC for overnight stabilization of blood glucose. The model parameters are personalized using a priori available patient information. We consider an autoregressive integrated moving average with exogenous input (ARIMAX) model. We

summarize and the results of the overnight clinical studies conducted at Hvidovre Hospital. Based on these results, we propose improvements for the stochastic part of our controller model. We state and compare three different stochastic model structures. The first one is the ARIMAX structure that has been used for the clinical studies. The second one is an autoregressive moving average with exogenous input (ARMAX) model. The third one is an adaptive ARMAX model in which we estimate the parameters of the stochastic part using a Recursive Least Square (RLS) method. We test the controller in a virtual clinic of 100 patients. This virtual clinic is based on the Hovorka model. We consider the case where only half of the bolus is administrated at mealtime, and the case where the insulin sensitivity increases during the night.
This thesis consists of a summary report, glucose and insulin profiles of the clinical studies and research papers submitted, peer-reviewed and/or published in the period September 2009 - September 2012.

Contents

CHAPTER 1

Introduction

1.1 Motivation

1.1.1 Facts about diabetes

Insulin and glucagon are the main hormones involved in the blood glucose regulation. In case of high blood glucose concentration, the pancreas secretes insulin. Insulin promotes the uptake of glucose in the body cells and the storage of glucose in the liver as glycogen. If the blood glucose is lower than normal, the pancreas starts to produce glucagon. Glucagon has the opposite effect, ie. promotes the breakdown of glycogen into glucose. This regulatory mechanism is explicated in Fig. 1.1. In healthy people, these hormones maintain the blood glucose around 90 mg/dL ($\sim$5 mmol/L), and usually in the range 72-144 mg/dL ($\sim$4-8 mmol/L).
In 2010, approximately 280 million people suffered from diabetes, and this number is expected to increase by 150 million by 2030 [2]. In addition, the global health care expenditure to treat complications related to diabetes is also going to significantly increase within next years [3], from approximately 375 billion dollars to approximately 490 billion dollars. The evolution of the

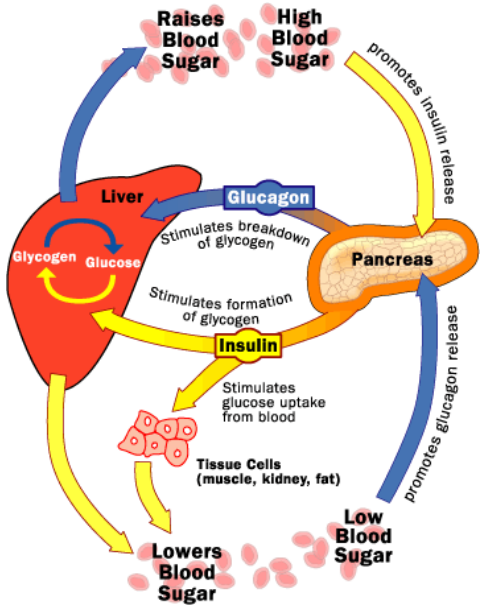

Figure 1.1: Blood glucose regulation in healthy people [1].

number of people with diabetes in the USA, Europe, India, China, Brazil and Africa for 2010 and 2030 is shown in Fig 1.2.

Type 1 diabetes (also previously known as juvenile diabetes or insulin-dependent diabetes) represent 5-10% of diabetes. In Denmark, the number of people with type 1 diabetes is estimated to 30,000 [4]. Type 1 diabetes is an autoimmune disease caused by the destruction of the insulin-producing β-cells in the pancreas. Therefore, people with type 1 diabetes do not produce insulin, and need frequent injections of exogenous insulin to survive.

Presently, people with type 1 diabetes have the responsibility of deciding on their insulin dosage. Too little insulin may lead to periods of high blood glucose (hyperglycemia), which has long-term complications, such as blindness, nerve disease or kidney disease. Conversely, overdosing the insulin may lead to low blood glucose, which has immediate effects, such as

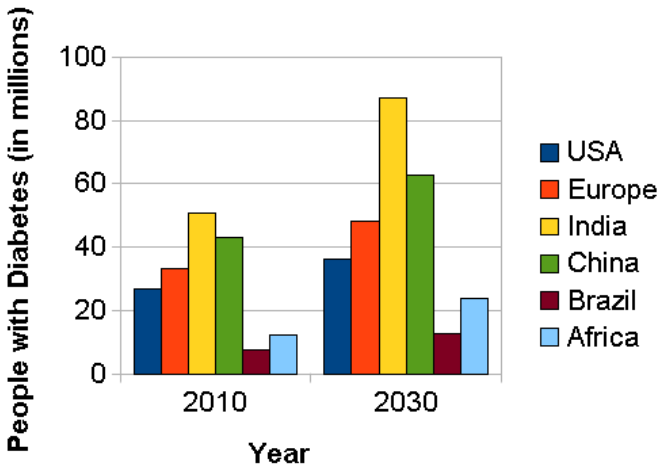

Figure 1.2: Estimation of the number of people with diabetes in the USA, Europe, India, China, Brazil and Africa in 2010 and 2030.

seizures or even death.

The traditional treatment for people with type 1 diabetes consists of multiple daily injections (MDI) of slow-acting insulin once per day and rapid-acting insulin several times per day with a needle. The decisions on the amount of injected insulin are based on discrete blood glucose measurements. The slow-acting insulin mitigates the endogenous glucose production from the liver. The rapid-acting insulin compensates for the carbohydrates coming from meals.

An increasing number of people with type 1 diabetes are using a Continuous Subcutaneous Insulin Infusion (CSII) pump combined with a Continuous Glucose Monitor (CGM). The insulin pump continuously injects small amounts of rapid-acting insulin during the day, and can inject larger amounts before mealtimes. The amount of basal insulin can be adjusted to fit the patient's daily variations in insulin needs. The CGM provides frequent measurements of the subcutaneous glucose. This therapy results

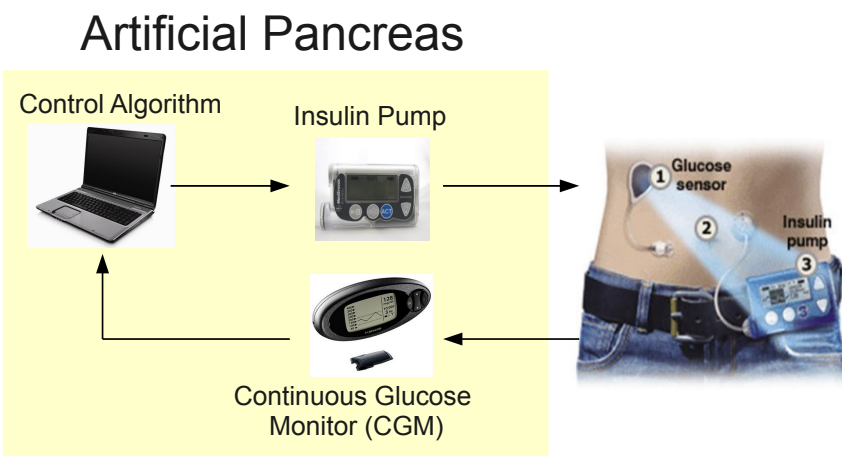

Figure 1.3: Design of an artificial pancreas.

in a better control of blood glucose compared to the one based on MDI [5].

1.1.2 The Artificial Pancreas

So far, the decision on the amount of insulin to be injected is still left to the patient. Closed-loop control of blood glucose, also known as an Artificial Pancreas (AP), can reduce the burden and the risk of complications associated to type 1 diabetes. Current versions of the AP use a CGM for glucose measurements, a control algorithm, and a CSII pump. Fig. 1.3 illustrates the principle of an AP.

The AP has been a subject of interest for almost 50 years [6–8]. Early versions of the AP like the Biostator^{TM}used intravenous (iv.) glucose measurements and iv. insulin and glucagon injections. However, this setup cannot be used for controlling the blood glucose in everyday life. In the recent years, the improvements in CSII pump technologies, insulin analogues and CGMs increased the potential of a fully automated AP [9–12].

Currently, the most popular control algorithms are proportional integral

derivative (PID) control [13, 14], model predictive control (MPC) [15, 16], sliding mode control [17], fuzzy logic [18, 19] and $\mathcal{H}_\infty$ control [20].
Currently, the main limitations towards the development of an AP are [21]

- The accuracy of CGMs. Erroneous CGM measurements represent the main limitation for closed-loop control [22, 23]. Currently available CGMs have a mean absolute relative error of approximately 15% [24]. Attempts to enhance CGM accuracy using currently available CGMs and novel approaches have been performed [25]. There also exists a lag in the interstitial fluid response to changes in plasma glucose. Usually, this lag is estimated to 15-20 minutes. However, [26] claimed that the actual lag is 5-10 minutes, and that additional lags are introduced by CGM filtering algorithms.

  Here, the difference between a lag and a delay should be explained. A delay is a period of time where the input has no influence on the response of the system. Conversely, a lag is for example a low-pass filter, where the response progressively reaches its final value. In the considered compartment models, the lags and delays are always modelled as lags. Fig. 1.4 illustrates the unit step response for a lag and a delay.

- The lag and delay associated to the subcutaneous route for insulin administration. The subcutaneously administrated insulin has its maximum effect on blood glucose after approximately 90-120 minutes, and can remain active in the body for 4-5 hours. Several ways are being investigated to make the insulin action faster. For example, the use of a local heating device at the insulin injection site can accelerate the insulin absorption [27]. Other routes, such as the intraperitoneal route, have also been considered [28]. These novel ways of administrating insulin can improve the control of blood glucose, but cannot be used in large populations of people with type 1 diabetes. They are more invasive than the CSII therapy, require more maintenance and can be subject to complications and infections.

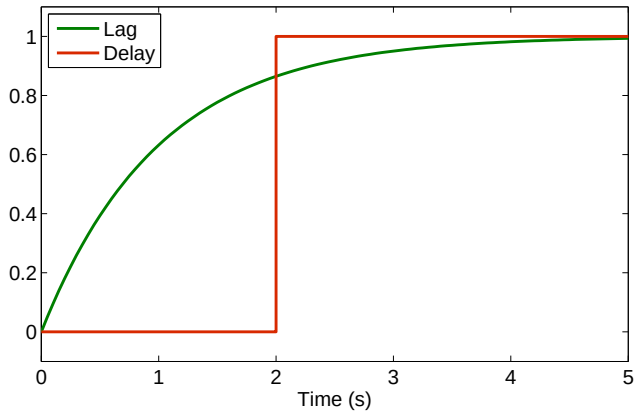

Figure 1.4: Example of lag and delay.

Glucagon can be used as a rescue in the case of an upcoming hypoglycemia. An example of AP using insulin and glucagon as manipulated variables is given in [29]. Further studies on APs using insulin and glucagon need to be performed, since glucagon has side effects at high concentration (nausea and vomiting), and aged glucagon is cytotoxic (ie. may alter or destroy cells) [30].

- The intra-patient variability. Many factors, such as insulin, meal intake, physical exercise, stress, illness, alcohol consumption etc. influence the blood glucose [31]. Also, hormone release during the night may cause elevated blood glucose in the early morning (also called dawn phenomenon).

1.1.3 Model Predictive Control

MPC is a control algorithm using a model to predict and optimize the future response of a plant. At each iteration, the controller solves an Optimal Control Problem (OCP). It computes the optimal sequence of inputs, based

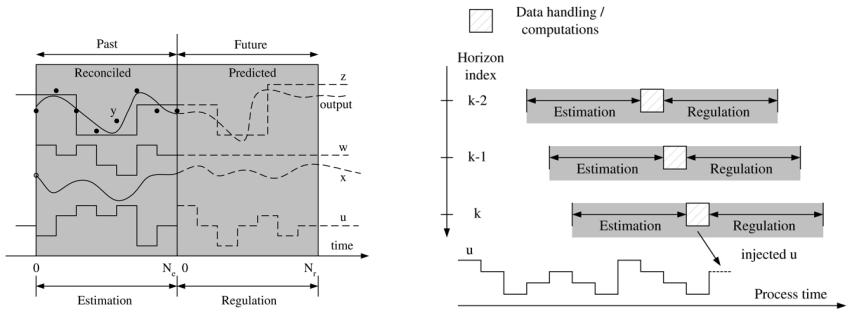

Figure 1.5: The principle of MPC.

on the current estimated state of the system, a prediction model and a desired reference trajectory. Then, the first value of the input is implemented to the plant and the new current state is estimated, eg. with a Kalman filter. The computation is repeated at the next sample using a receding horizon strategy. The principle of MPC and receding horizon is illustrated in Fig. 1.5. An overview of possible industrial applications of MPC can be found in [32].
MPC is a useful control method for the AP due to its ability to handle constraints on insulin administration and glucose level in a systematic and proactive way. In this thesis, we consider hard constraints on the insulin level and soft constraints on the glucose level. Prototypes of AP using MPC have been successfully tested both in silico [33] and in vivo [34].

1.1.4 Physiological models

Several physiological models have been developed to simulate virtual patients with type 1 diabetes. One of the oldest models is the Minimal Model developed by *Bergman et al.* [35]. The glucose-insulin dynamics model consists of three compartments in total. One compartment represents the plasma glucose level. The second one represents the action of insulin. Finally, the third one depicts the insulin concentration. Its simplicity makes it popular for modeling people with type 1 diabetes.

Another model for people with type 1 diabetes is the Sorensen model [36]. This model can simulate both healthy people and people with type 1 diabetes. This model consists of 19 states in total. This model is rarely used for simulations due to its high complexity. It is illustrated in Fig. 1.6. Examples of publications using the Sorensen model for modeling and/or control are [37–39].
One of the most used models is the Cobelli model [40]. The University of Virginia and the University of Padova developed a virtual clinic of people with type 1 diabetes based on the Cobelli model [41]. This clinic can simulate up to 300 patients (100 adults, 100 adolescents, 100 children), and is approved by the FDA (Food and Drugs Administration) as a substitution to animal trials. Consequently, this clinic is often used to test in silico closed-loop controllers for blood glucose. Examples of works using this virtual clinic are [42–44]. The main drawback of this model is the inability to vary model parameters (eg. insulin sensitivities) during the simulation.
A more recent model is the Medtronic Virtual Patient (MVP) model [45]. This model contains the same compartments as the minimal model. Its main difference is its identifiability. Thus, the 8 model parameters can be identified from a sufficiently large collection of clinical data.
In this thesis, we are using the model developed by *Hovorka et al.* in order to simulate patients with type 1 diabetes [46]. This model consists of 6 states for describing the glucose-insulin dynamics, 2 states for modeling the meal absorption, and 2 other states for modeling the sc. insulin infusion. As for the Cobelli model, a simulator has been developed for in silico clinical trials [47].
An overview of these models is available in [48].

1.2 Objective and main contributions

The main objective of this work is to implement and test in silico and in vivo control strategies for control of blood glucose in people with type 1 diabetes. In this project we limited ourselves to strategies based on MPC (both linear and nonlinear MPC). In addition, we only consider the sc.

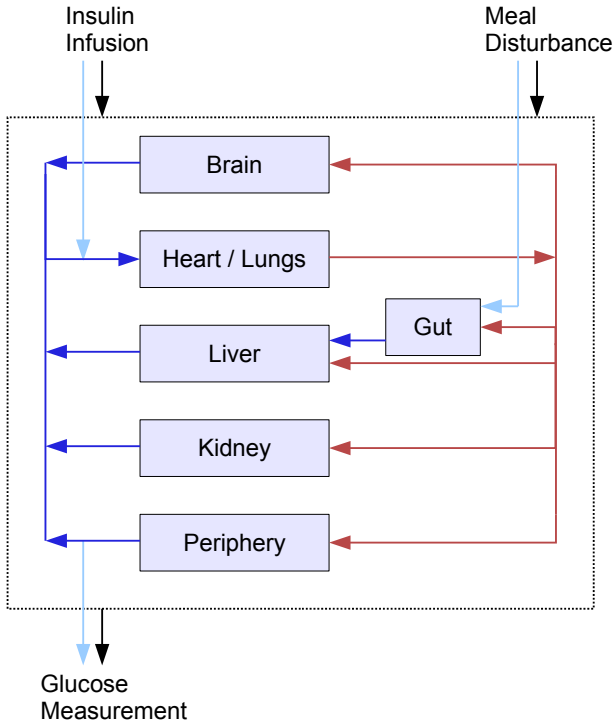

Figure 1.6: The Sorensen model.

route for insulin infusion and glucose measurements. We use the Hovorka model to simulate patients with type 1 diabetes.

The first goal of this work is to determine the maximal achievable performance of a closed-loop controller. In order to achieve this goal, we use a constrained non-linear optimal controller. The algorithm is a multiple shooting algorithm based on sequential quadratic programming (SQP) for optimization and an explicit Dormand-Prince Runge-Kutta method (DOPRI54) for numerical integration and sensitivity computation. We implement a toolbox for simulating a patient with type 1 diabetes for various

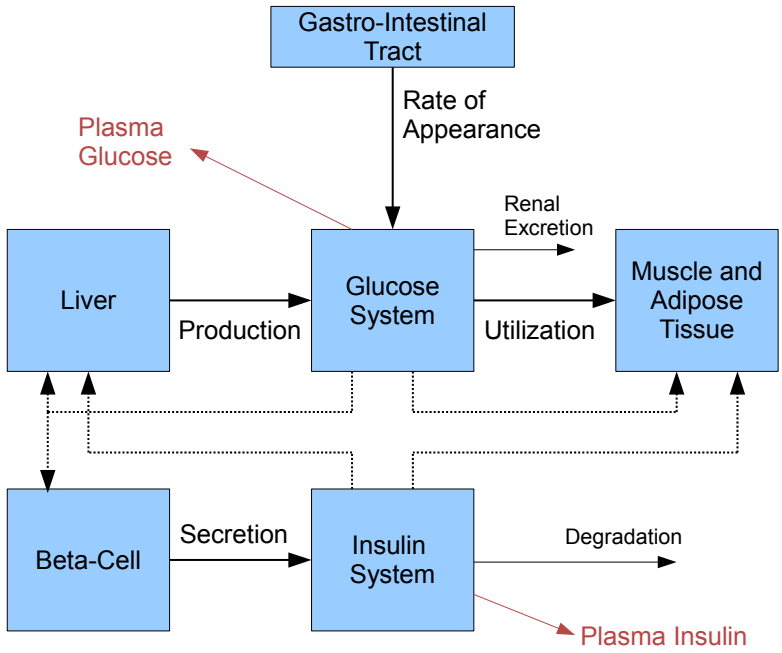

Figure 1.7: The Cobelli model.

scenarios. In the case where we assume that we do not know the current state, we use a continuous-discrete extended Kalman Filter (CDEKF) for state estimation.
The second goal is to implement a controller which can be used in a clinical study. The in vivo clinical studies require a simple and realistic method to estimate the model parameters. In this thesis we propose a simple and systematic method based on a priori patient parameters. We propose a robust controller to take into account the high intra-patient variability in insulin needs.

1.3 Outline

This thesis is structured as following.

Chapter 2 presents the Hovorka model. This model is used to simulate people with type 1 diabetes. We present the glucose-insulin dynamics model, the sc. insulin absorption model and the meal absorption model. We use a parameter distribution to generate cohorts of people with type 1 diabetes.

Chapter 3 discusses the limitations of closed-loop control for people with type 1 diabetes. We describe a control algorithm based on Nonlinear Model Predictive Control (NMPC). We test our controller in the cases where full meal information is available in advance, where the meal size is announced at mealtime only and where the meal sizes and mealtimes are unknown to the controller. We also compare a pump-based insulin therapy to a pen-based insulin therapy, and discuss the benefits of faster insulin on postprandial glucose excursions.

Chapter 4 proposes a control algorithm designed for in vivo clinical studies. This controller uses known patient information to determine the model parameters. We present the method for model computation, the results of numerical simulations and in vivo clinical studies. We also suggest possible improvements to the current controller. We compare and assess 3 different control strategies in the case where only half of the meal bolus is administrated at mealtime, and the case where the insulin sensitivity increases during the night.

Chapter 5 summarizes the main contributions of this thesis, and proposes possible future directions.

The appendices are structured as following.

- Appendix A shows the glucose and insulin profiles for the 25 clinical studies conducted at Hvidovre Hospital.

- Appendix B - C include a book chapter and a conference paper that has been peer-reviewed and published in proceedings. In these papers we describe the implementation of a controller based on NMPC. We provide and discuss the optimal glucose and insulin profiles in the case where the meal sizes and mealtimes are known in advance, and the case where the meal size is announced at mealtime only.

- In Appendix D, we apply receding horizon constrained optimal control to the computation of insulin administration for people with type 1 diabetes. We compare the glucose and insulin profiles for linear and nonlinear MPC. We also discuss the benefits of faster insulin on the postprandial glucose excursion.

- In Appendix E we estimate the sizes and the times of the meals using a continuous-discrete extended Kalman filter (EKF). We present study results based on the Hovorka model, where we consider the cases where the meal is correctly estimated, the case where the meal size is overestimated and the case where the meal is not announced at all. The paper describes the key aspects of the numerical implementation and provides quantitative insight into the factors limiting the achievement of acceptable closed-loop performance.

- In Appendix F, we apply a robust feedforward-feedback control strategy. The feedforward controller consists of a bolus calculator which compensates the disturbance coming from meals. The feedback controller is based on a linearized description of the model describing the patient. We minimize the risk of hypoglycemia by introducing a time-varying glucose setpoint based on the announced meal size and the physiological model of the patient. The simulation results include the cases where the insulin sensitivity changes, and mismatches in meal estimation. They demonstrate that the designed controller is able to achieve offset-free control when the insulin sensitivity changes, and that having a time-varying reference signal enables more robust control of blood glucose in the cases where the meal size is known, but also when the ingested meal does not match the announced one.

- In Appendix G, we summarize, compare and discuss the different control strategies presented in the previous papers.

- Appendix H is a technical report. In this report, we present a closed-loop control strategy for overnight glucose stabilization. The controller is a model predictive controller (MPC) based on a first-order extended Δ-ARX (autoregressive with exogenous input) model. We test this control strategy on a cohort of 7 virtual patients simulated by the Hovorka model.

- Appendix I - K include 2 peer-reviewed conference papers and a journal paper in submission. In these papers, we propose a control strategy based on linear MPC for overnight glucose stabilization. We propose a simple, systematic and patient-specific way of computing the model parameters based on a priori known patient information. The controller is evaluated in silico on a cohort of 100 randomly generated patients with a representative inter-subject variability. This cohort is simulated overnight with realistic variations in the insulin sensitivities and needs. We also provide results for the first tests of this controller in a real clinic.

- Appendix L consists of a journal paper in submission. In this paper we describe and compare 3 different control strategies for overnight stabilization of blood glucose. The first one is the ARIMAX model structure that has been used for the clinical studies on real patients. The second one is an ARMAX model structure. The third one is an adaptive ARMAX model structure, where we recursively estimate the model parameters for the stochastic part.

CHAPTER 2

The Hovorka Model for People with Type 1 Diabetes

This chapter describes the model that we use for our virtual clinic. The model has been developed by Hovorka et al., and we refer to it as the Hovorka model. First we state the differential equations describing the glucose-insulin dynamics, the subsystem describing the meal absorption, the subsystem describing the sc. insulin infusion and the subsystem modeling the glucose transport from plasma to interstitial tissues. We also propose a method for generating a cohort of people with type 1 diabetes representative of a real population by using a parameter distribution.

The Hovorka model has been identified on 6 healthy male patients during IVGTT (intravenous glucose tolerance test). In this study, traceable glucose is used to estimate the effect of insulin on glucose distribution/transport, glucose disposal, and endogenous glucose production (EGP) [49]. This model consists of 6 states. One state represents the glucose contained in plasma. The second state represents the glucose contained in peripheral tissues. Three other states represent the action of insulin on glucose distribution/transport, glucose disposal, and endogenous glucose production

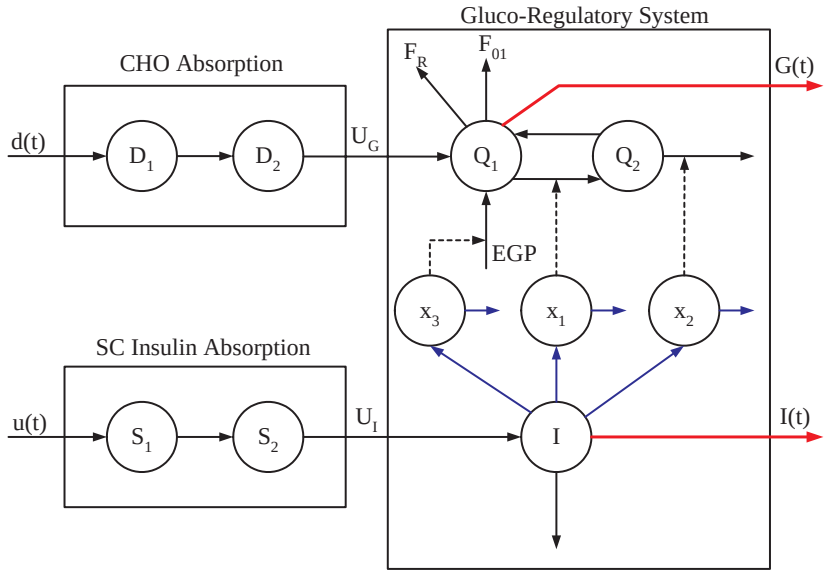

Figure 2.1: The Hovorka model.

(EGP). Finally, one state depicts the insulin concentration in plasma. This model is augmented with a two-compartment model for the meal absorption and another two-compartment model for sc. insulin absorption [46].
We also include a CGM model to simulate a sc. glucose sensor. This model simulates the glucose transport from blood to interstitial tissues, and the noise structure from the CGM. Hence, the full model used in this thesis to simulate a patient with type 1 diabetes contains 11 states.

2.1 Physiological subsystem

The blood glucose dynamics are modeled with two compartments. The two state variables are $Q_1(t)$ [mmol] and $Q_2(t)$ [mmol]. $Q_1(t)$ represents glucose in the main blood stream, while $Q_2(t)$ represents glucose in peripheral tissue such as muscles.

The model describing evolution of glucose in the main blood stream

$$\begin{aligned}\frac{dQ_1}{dt}(t) = U_G(t) - F_{01,c}(t) - F_R(t) \\ - x_1(t)Q_1(t) + k_{12}Q_2(t) \\ + EGP_0(1 - x_3(t))\end{aligned} \tag{2.1}$$

includes absorption from the gut, $U_G(t)$ [mmol/min], consumption of glucose by the central nervous system, $F_{01,c}$ [mmol/min], the renal excretion of glucose in the kidneys, $F_R(t)$ [mmol/min], the insulin dependent uptake of glucose in muscles, $x_1(t)Q_1(t)$ [mmol/min], transfer of glucose from peripheral tissue such as muscle to the blood, $k_{12}Q_2(t)$, and endogenous release of glucose by the liver, $EGP_0(1 - x_3(t))$. The uptake of glucose in muscles depends on insulin. $x_1(t)$ is a state representing insulin in muscle tissue. Release of glucose from the liver is also controlled by insulin. High concentrations of insulin suppress glucose release. $x_3(t)$ is used to model insulin in the liver.
Glucose in peripheral tissue such as muscle is modeled by the differential equation

$$\frac{dQ_2}{dt}(t) = x_1(t)Q_1(t) - (k_{12} + x_2(t))Q_2(t) \tag{2.2}$$

in which $x_1(t)Q_1(t)$ [mmol/min] is the transport of glucose from the main blood stream to the muscles, $k_{12}Q_2(t)$ [mmol/min], is transport of peripheral glucose to the main blood stream, and $x_2(t)Q_2(t)$ [mmol/min] is the insulin dependent disposal of glucose in the muscle cells. It depends on insulin modeled by $x_2(t)$.
The glucose concentration is

$$y(t) = G(t) = \frac{Q_1(t)}{V_G} \tag{2.3}$$

$y(t) = G(t)$ is the glucose concentration [mmol/L] and V_G [L] is the glucose distribution volume. It depends on body weight, BW [kg], of the individual.

The insulin-independent consumption of glucose by the central nervous systems and the red blood cells is modeled as

$$F_{01,c}(t) = \begin{cases} F_{01} & G(t) \geq 4.5 \text{ mmol/L} \\ F_{01}G(t)/4.5 & \text{otherwise} \end{cases} \tag{2.4}$$

At low glucose concentrations the consumption, $F_{01,c}$ [mmol/min], is proportional to the glucose concentration, $G(t)$, while it is constant when the glucose concentration is not low.
The excretion rate of glucose in the kidneys is zero unless the glucose concentration is high ($G(t) \geq 9$ mmol/L). In this case it is affine in the glucose concentration. Consequently, the glucose excretion rate, F_R [mmol/min], is modeled as

$$F_R(t) = \begin{cases} 0.003(G(t) - 9)V_G & G(t) \geq 9 \text{ mmol/L} \\ 0 & \text{otherwise} \end{cases} \tag{2.5}$$

The plasma insulin concentration, $I(t)$ [mU/L], evolves according to

$$\frac{dI}{dt}(t) = \frac{U_I(t)}{V_I} - k_e I(t) \tag{2.6}$$

The insulin action is governed by influence on transport and distribution $x_1(t)$, utilization and phosphorylation of glucose in adipose tissue $x_2(t)$, and endogenous production in the liver $x_3(t)$. These quantities are described by the differential equations

$$\frac{dx_1}{dt}(t) = -k_{a1}x_1(t) + k_{b1}I(t) \tag{2.7a}$$

$$\frac{dx_2}{dt}(t) = -k_{a2}x_2(t) + k_{b2}I(t) \tag{2.7b}$$

$$\frac{dx_3}{dt}(t) = -k_{a3}x_3(t) + k_{b3}I(t) \tag{2.7c}$$

2.2 Food Absorption Model

Food absorption models have been considered by a number of authors [50–53] and it has been observed that people with diabetes has abnormally slow gastric emptying [54].
We consider a two-compartment model describing carbohydrate (CHO) absorption and conversion to glucose. The model describes the effect of orally ingested carbohydrates on the rate of appearance of glucose in the blood stream. The model is

$$\frac{dD_1}{dt}(t) = A_G D(t) - \frac{1}{\tau_D} D_1(t) \tag{2.8a}$$

$$\frac{dD_2}{dt}(t) = \frac{1}{\tau_D} D_1(t) - \frac{1}{\tau_D} D_2(t) \tag{2.8b}$$

in which $D(t)$ [mmol/min] is the amount of oral carbohydrate intake at any time expressed as glucose equivalents, A_G is a factor describing the utilization of carbohydrates to glucose, τ_D [min] is the time constant, $D_1(t)$ [mmol] and $D_2(t)$ [mmol] are the states describing the amount of glucose in the two compartments. The rate of appearance of absorption of glucose in the blood stream is described by

$$U_G(t) = \frac{1}{\tau_D} D_2(t) \tag{2.9}$$

$U_G(t)$ [mmol/min] is the glucose absorption rate. The carbohydrate input rate, $D(t)$ [mmol/min], may be related to the carbohydrate input rate, $d(t)$ [g/min], by

$$D(t) = \frac{1000}{M_{wG}} d(t) \tag{2.10}$$

in which M_{wG} [g/mol] is the molecular weight of glucose. The glucose absorption profiles for different meal sizes are illustrated in Fig. 2.3.

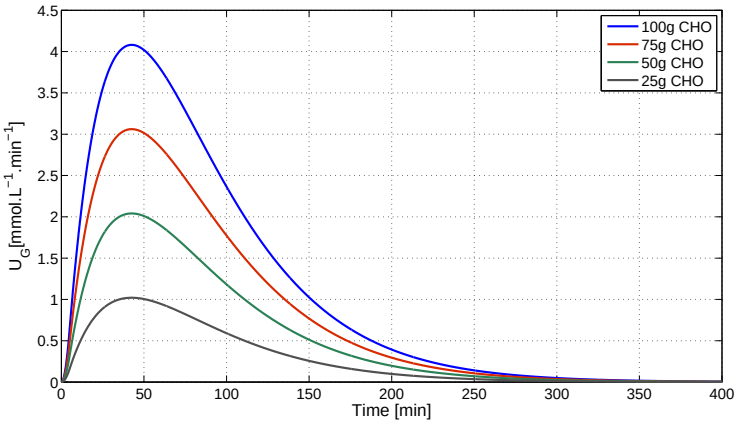

Figure 2.2: Glucose absorption profiles for 100, 75, 50 and 25g CHO. The model parameters are the average values.

2.3 Insulin Absorption Model

In this thesis, we assume that insulin is administered subcutaneously using a CSII pump. A number of models to describe the absorption rate of subcutaneously injected short acting insulin in the blood stream are available [55].

We consider a two compartment model describing the absorption rate of subcutaneously administered short acting insulin. The model is

$$\frac{dS_1}{dt}(t) = u(t) - \frac{1}{\tau_S} S_1(t) \tag{2.11a}$$

$$\frac{dS_2}{dt}(t) = \frac{1}{\tau_S} S_1(t) - \frac{1}{\tau_S} S_2(t) \tag{2.11b}$$

in which $u(t)$ [mU/min] is the amount of insulin injected, τ_S [min] is the time constant, $S_1(t)$ [mU] and $S_2(t)$ [mU] are the amounts of insulin in the

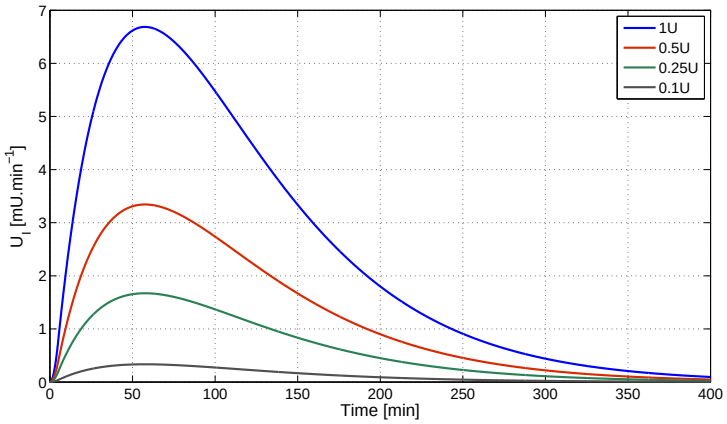

Figure 2.3: Insulin absorption profiles for 1U, 0.5U, 0.25U and 0.1U insulin boluses. The model parameters are the average values.

two compartments. The absorption rate of insulin in the blood stream is

$$U_I(t) = \frac{1}{\tau_S} S_2(t) \tag{2.12}$$

in which $U_I(t)$ [mU/min] is the absorption rate. The insulin absorption profiles for different bolus sizes are depicted in Fig. 2.3.

2.4 Parameters

The parameters in the Hovorka model (2.8)-(2.7) are listed in Table 2.1. The parameters $k_{b,i}$ are related to the insulin sensitivities, $S_{I,i}$, by

$$k_{b,i} = S_{I,i} k_{a,i} \qquad i = 1, 2, 3 \tag{2.13}$$

The European unit for glucose concentration is mmol/L and the American unit is mg/dL. One can convert between these units using the molecular weight of glucose ($C_6H_{12}O_6$): $M_{wG} = 180.1577$ g/mol.

Table 2.1: Parameters and distribution for the Hovorka model.

Parameter	Unit	Distribution
EGP_0	mmol/kg/min	$EGP_0 \sim N(0.0161, 0.0039^2)$
F_{01}	mmol/kg/min	$F_{01} \sim N(0.0097, 0.0022^2)$
k_{12}	min^{-1}	$k_{12} \sim N(0.0649, 0.0282^2)$
$k_{a,1}$	min^{-1}	$k_{a,1} \sim N(0.0055, 0.0056^2)$
$k_{a,2}$	min^{-1}	$k_{a,2} \sim N(0.0683, 0.0507^2)$
$k_{a,3}$	min^{-1}	$k_{a,3} \sim N(0.0304, 0.0235^2)$
$S_{I,1}$	min^{-1}/(mU/L)	$S_{I,1} \sim N(51.2, 32.09^2)$
$S_{I,2}$	min^{-1}/(mU/L)	$S_{I,2} \sim N(8.2, 7.84^2)$
$S_{I,3}$	L/mU	$S_{I,3} \sim N(520, 306.2^2)$
k_e	min^{-1}	$k_e \sim N(0.14, 0.035^2)$
V_I	L/kg	$V_I \sim N(0.12, 0.012^2)$
V_G	L/kg	$\exp(V_G) \sim N(1.16, 0.23^2)$
τ_I	min	$\frac{1}{\tau_I} \sim N(0.018, 0.0045^2)$
τ_G	min	$\frac{1}{\ln(\tau_G)} \sim N(-3.689, 0.25^2)$
A_g	Unitless	$A_g \sim U(0.7, 1.2)$
BW	kg	$BW \sim U(65, 95)$

2.4.1 Simulation of large populations of people with type 1 diabetes

In this thesis, we can use the parameter distribution presented in Table 2.1 to simulate a cohort of people with type 1 diabetes. We do it by generating a certain number of realizations of the parameter distribution. We limit ourselves to 100 patients in this work, but it is possible to generate a larger population.

Nevertheless, the parameter distribution presented in Table 2.1 does not include the parameter covariance. Also, some of the values are clearly not statistically significant as they are of the same order of magnitude as their standard deviation. In order to get a representative population of people with type 1 diabetes, we exclude a patient if

- One of their parameters is negative.
- Their insulin basal rate is below 0.35 U/hr.

2.5 CGM Model

In addition, we use a CGM for glucose feedback in our controller setup. For the numerical simulations, we generate noisy CGM data based on the model and the parameters determined by [56]. This model consists of two parts. The first part describes the glucose transport from blood to interstitial tissues, which is

$$\frac{dG_{sub}}{dt} = \frac{1}{\tau_{sub}} \left(G(t) - G_{sub}(t) \right) \tag{2.14}$$

$G_{sub}(t)$ is the subcutaneous glucose and $G(t)$ is the blood glucose. τ_{sub} is the time constant associated to glucose transport from blood to subcutaneous tissues.
The second part models non-Gaussian sensor noise. It is given by

$$\begin{cases} e_1 &= v_1 \\ e_k &= 0.7(e_{k-1} + v_n) \end{cases} \tag{2.15}$$

$$v_k \sim N_{iid}(0, 1) \tag{2.16}$$

$$\eta_k = \xi + \lambda \sinh \left(\frac{e_k - \gamma}{\delta} \right) \tag{2.17}$$

Fig. 2.4 provides an example of a CGM noise sequence η_k.
The glucose value returned by the CGM is

$$G_{CGM}(t_k) = G_{sub}(t_k) + \eta_k \tag{2.18}$$

Table 2.2: Parameters for the CGM model [56].

Parameter	Value
τ_{sub}	15 min
λ	15.96
ξ	-5.471
δ	1.6898
γ	-0.5444

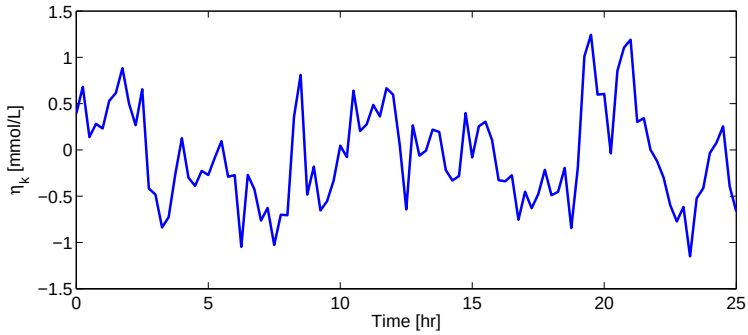

Figure 2.4: Example of a CGM noise realization.

2.6 Summary

In this chapter, we have presented the modified Hovorka model that we will use for all our simulations. This model includes a description of the glucose-insulin dynamics, a model for sc. insulin absorption, a model for meal absorption and a model for CGM glucose measurements. We use the parameter distribution to generate a representative population of people with type 1 diabetes.
However, the main drawback of this model is its non-identifiability.

CHAPTER 3

Nonlinear Model Predictive Control for Glucose Regulation in People with Type 1 Diabetes

In this chapter, we apply a nonlinear model predictive control (NMPC) strategy to people with type 1 diabetes. The optimal control problem (OCP) is solved using a multiple-shooting based algorithm described in [57–59]. We use an explicit Runge-Kutta method (DOPRI45) with an adaptive stepsize for numerical integration and sensitivity computation. The OCP is solved using a Quasi-Newton sequential quadratic programming (SQP) algorithm with line search and a BFGS update for the Hessian of the Lagrangian. We simulates the case where meals are announced in advance, and the case where meals are announced at mealtimes. We also apply a Continuous-Discrete Extended Kalman Filter (CDEKF) in order to simulate cases where the meal size is uncertain, or even unannounced. The developed framework is used to compare the glucose and insulin profiles for

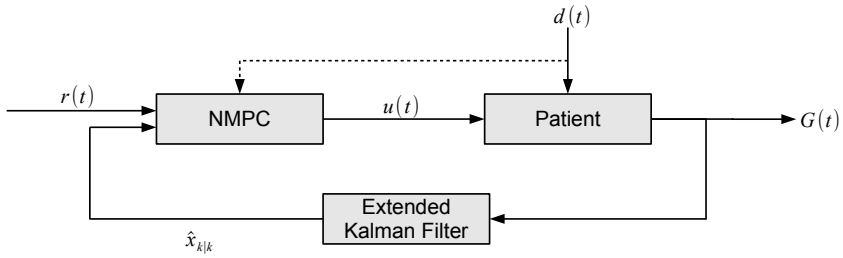

Figure 3.1: The general controller setup.

a pump-based and a pen-based insulin therapy, and is illustrated in Fig. 3.1.
Paper A and Paper B discuss the optimal insulin administration profiles. Paper C discusses the benefits of faster insulin on blood glucose regulation. In Paper D, we present and test the CDEKF for uncertain meal sizes.

3.1 Problem formulation

We discuss here the optimal control problem used to determine the optimal insulin injection profiles for people with type 1 diabetes. In this chapter, we use the constrained continuous-time Bolza problem

$$\min_{[x(t),u(t)]_{t_0}^{t_f}} \quad \phi = \int_{t_0}^{t_f} g(x(t),u(t))dt + h(x(t_f)) \tag{3.1a}$$

$$\text{s.t.} \quad x(t_0) = x_0 \tag{3.1b}$$

$$\dot{x}(t) = f(x(t),u(t),d(t)) \qquad t \in [t_0, t_f] \tag{3.1c}$$

$$u_{\min} \leq u(t) \leq u_{\max} \qquad t \in [t_0, t_f] \tag{3.1d}$$

to compute the optimal insulin administration. $x(t) \in \mathbf{R}^{n_x}$ is the state vector, $u(t) \in \mathbf{R}^{n_u}$ is the manipulated inputs, and $d(t) \in \mathbf{R}^{n_d}$ are known disturbances. $\dot{x}(t) = f(x(t),u(t),d(t))$ represents the model equations. The

initial time, t_0, and the final time, t_f, are specified parameters. The initial state, x_0, is a known parameter in (3.1). The inputs are bound constrained and must be in the interval $u(t) \in [u_{\min}, u_{\max}]$.
The objective function is stated generally with a stage cost term, $g(x(t), u(t))$, and a cost-to-go term, $h(x(t_f))$. The numerical algorithms for the problem are derived using this general structure of the objective function.
In the insulin administration problem, the stage cost term is a penalty function, the cost-to-go term is zero, and the model equations are represented by the Hovorka model described in Chapter 2. $u(t)$ represents the insulin infusion rate at time t and $d(t)$ represents the carbohydrates (CHO) intake rate at time t. Given an initial state, x_0, and a CHO intake rate profile, $[d(t)]_{t_0}^{t_f}$, the continuous-time Bolza problem (3.1) computes the optimal insulin injection rate profile, $[u(t)]_{t_0}^{t_f}$, as well as the optimal state trajectory, $[x(t)]_{t_0}^{t_f}$.

3.1.1 Choice of the cost function

The objective of the insulin administration is to mitigate glucose excursions caused by meals and variations in endogenous glucose production and utilization. We use an asymmetric penalty function defined as

$$\begin{aligned} g(x(t), u(t)) = \frac{\kappa_1}{2} |\max\{0, G(t) - \bar{G}\}|^2 + \frac{\kappa_2}{2} |\max\{0, \bar{G} - G(t)\}|^2 \\ + \frac{\kappa_3}{2} |\max\{0, G(t) - G_U\}|^2 + \frac{\kappa_4}{2} |\max\{0, G_L - G(t)\}|^2 \end{aligned} \tag{3.2}$$

$G(t)$ is the blood glucose concentration, $\bar{G} = 5$ mmol/L is the target value for the blood glucose concentration, $G_L = 4$ mmol/L is a lower acceptable limit on the glucose concentration, and $G_U = 8$ mmol/L is an upper acceptable limit on the blood glucose concentration. The weights κ_1-κ_4 are used to balance the desirability of different deviations from the target. As hypoglycemia is considered a more acute threat than hyperglycemia, $\kappa_1 < \kappa_2$ and $\kappa_3 < \kappa_4$. The cost function used in this Chapter is depicted in Fig. 3.2.

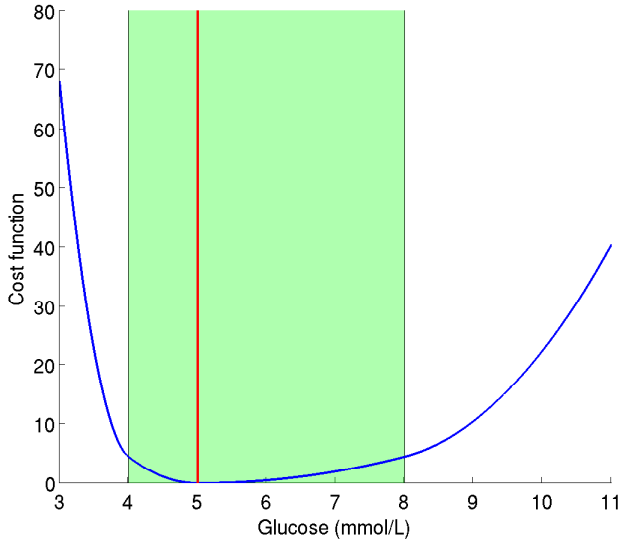

Figure 3.2: The cost function used to penalize glucose deviations from the target.

3.1.2 Discrete-time approximation

The continuous-time bound constrained Bolza problem (3.1) is approximated by a numerical tractable discrete-time bound constrained Bolza problem using the zero-order-hold input parametrisation of the manipulated variables, $u(t)$, as well as the known disturbance variables, $d(t)$. We divide the time interval, $[t_0, t_f]$, into N equidistant intervals each of length T_s. Let $\mathcal{N} = \{0, 1, ..., N-1\}$ and $t_k = t_0 + kT_s$ for $k \in \mathcal{N}$. The zero-order-hold restriction on the input variables, $u(t)$ and $d(t)$, imply

$$u(t) = u_k \qquad t_k \leq t < t_{k+1} \qquad k \in \mathcal{N} \tag{3.3a}$$
$$d(t) = d_k \qquad t_k \leq t < t_{k+1} \qquad k \in \mathcal{N} \tag{3.3b}$$

Using this zero-order-hold restriction on the inputs, the bound constrained continuous-time Bolza problem may be expressed as

$$\min_{\{x_{k+1},u_k\}_{k=0}^{N-1}} \quad \phi = \sum_{k=0}^{N-1} G_k(x_k, u_k, d_k) + h(x_N) \tag{3.4a}$$

$$\text{s.t.} \quad b_k = F_k(x_k, u_k, d_k) - x_{k+1} = 0 \quad k \in \mathcal{N} \tag{3.4b}$$

$$u_{\min} \leq u_k \leq u_{\max} \quad k \in \mathcal{N} \tag{3.4c}$$

The discrete-time state transition function is

$$F_k(x_k, u_k, d_k) = \{x(t_{k+1}) : \dot{x}(t) = f(x(t), u_k, d_k),\ x(t_k) = x_k\} \tag{3.5}$$

and the discrete time stage cost is

$$G_k(x_k, u_k, d_k) = \{\int_{t_k}^{t_{k+1}} g(x(t), u_k)dt : \dot{x}(t) = f(x(t), u_k, d_k),\ x(t_k) = x_k\} \tag{3.6}$$

3.2 Numerical Optimisation Algorithm

In this section, we develop a multiple-shooting based SQP algorithm for the numerical solution of (3.1). The SQP algorithm is based on line search. The structure of the quadratic sub-problems are utilised and they are solved by a primal-dual interior-point algorithm using Riccati iterations as in [60, 61]. The DOPRI54 scheme is used for numerical solution of the differential equation model and for computation of the sensitivities [62].

3.2.1 SQP algorithm

Define the parameter vector, p, as

$$p = \begin{bmatrix} u_0' & x_1' & u_1' & x_2' & \dots & x_{N-1}' & u_{N-1}' & x_N' \end{bmatrix}', \tag{3.7}$$

and the disturbance vector, $d = \begin{bmatrix} d_0' & d_1' & \dots & d_{N-1}' \end{bmatrix}'$, such that the discrete time dynamics may be represented by

$$b(p) = b(p; x_0, d) = \begin{bmatrix} F_0(x_0, u_0, d_0) - x_1 \\ F_1(x_1, u_1, d_1) - x_2 \\ \vdots \\ F_{N-1}(x_{N-1}, u_{N-1}, d_{N-1}) - x_N \end{bmatrix} \tag{3.8}$$

and the objective function may be denoted

$$\phi(p) = \phi(p; x_0, d) = \sum_{k=0}^{N-1} G_k(x_k, u_{k,d}) + h(x_N) \tag{3.9}$$

Let $c(p)$ denote the bound constraints, i.e.

$$c(p) = \begin{bmatrix} u_0 - u_{\min} \\ u_1 - u_{\min} \\ \vdots \\ u_{N-1} - u_{\min} \\ u_{\max} - u_0 \\ u_{\max} - u_1 \\ \vdots \\ u_{\max} - u_{N-1} \end{bmatrix}. \tag{3.10}$$

Then the bound constrained discrete-time Bolza problem may be expressed as a constrained optimisation problem in standard form

$$\min_p \quad \phi = \phi(p) \tag{3.11a}$$

$$\text{s.t.} \quad b(p) = 0 \tag{3.11b}$$

$$c(p) \geq 0 \tag{3.11c}$$

The concise formulation (3.11) is useful for presentation of the numerical optimisation algorithm used for solving the bound constrained continuous-time Bolza problem (3.1).

Algorithm 1 SQP Algorithm for (3.11)

Require: Initial guess: (p^0, y^0, z^0) with $z^0 \geq 0$.
Compute: $\phi(p^0)$, $\nabla_p \phi(p^0)$, $b(p^0)$, $\nabla_p b(p^0)$, $c(p^0)$, $\nabla_p c(p^0)$
Set $\lambda = 0$, $\mu = 0$, $W^0 = I$
while NOT stop **do**
Compute $(\Delta p^k, \tilde{y}^{k+1}, \tilde{z}^{k+1})$ by solution of:

$$\min_{\Delta p} \quad \frac{1}{2}\Delta p' W^k \Delta p + \nabla_p \phi'(p^k)\Delta p \tag{3.12a}$$

$$\text{s.t.} \quad \left[\nabla_p b(p^k)\right]' \Delta p = -b(p^k) \tag{3.12b}$$

$$\left[\nabla_p c(p^k)\right]' \Delta p \geq -c(p^k) \tag{3.12c}$$

Compute $\Delta y^k = \tilde{y}^{k+1} - y^k$ and $\Delta z^k = \tilde{z}^{k+1} - z^k$
Update the penalty parameter:
$\mu \leftarrow \max\{|z|, \frac{1}{2}(\mu + |z|)\}$ and $\lambda \leftarrow \max\{|y|, \frac{1}{2}(\lambda + |y|)\}$
Compute α using soft line search and Powell's ℓ_1 merit function (3.15).

$p^{k+1} = p^k + \alpha \Delta p^k$, $y^{k+1} = y^k + \alpha \Delta y^k$, $z^{k+1} = z^k + \alpha \Delta z^k$
Compute $\phi(p^{k+1}), \nabla_p \phi(p^{k+1})$, $c(p^{k+1})$, $\nabla_p c(p^{k+1})$, $b(p^{k+1})$ and $\nabla_p b(p^{k+1})$
Compute W^{k+1} by Powell's modified BFGS update. $k \leftarrow k + 1$.
end while

The Lagrangian of (3.11) is

$$\mathcal{L}(p, y, z) = \phi(p) - y' b(p) - z' c(p) \tag{3.13}$$

The first order KKT conditions

$$\nabla_p \mathcal{L}(p, y, z) = \nabla_p \phi(p) - \nabla_p b(p) y - \nabla_p c(p) z = 0 \tag{3.14a}$$
$$b(p) = 0 \tag{3.14b}$$
$$c(p) \geq 0 \tag{3.14c}$$
$$z \geq 0 \tag{3.14d}$$
$$c_i(p) = 0 \vee z_i = 0 \quad \forall i \tag{3.14e}$$

are used to test convergence of the SQP algorithm.
The steps for solution of (3.11) by an SQP algorithm with line search are listed in Algorithm 1.

3.2.2 Line search algorithm

The line search is based on Powell's ℓ_1 penalty function

$$P(p) = \phi(p) + \lambda' |b(p)| + \mu' |\min\{0, c(p)\}| \tag{3.15}$$

and the Armijo sufficient decrease condition. The penalty vectors, λ and μ, are selected such that they are numerically larger than the corresponding Lagrange multipliers, i.e. $\lambda \geq |y|$ and $\mu \geq z$ where y is the Lagrange multipliers associated with (3.11b) and z is the Lagrange multipliers associated with (3.11c). The line search algorithm is linted in Algorithm 2.

3.2.3 Gradient computation

The most time consuming computations in Algorithm 1 are computation of the objective function $\phi(p)$, computation of the derivatives of the objective function $\nabla_p \phi(p)$, computation of the dynamics $b(p)$, and computation of the sensitivities, $\nabla_p b(p)$, associated with the dynamics. $b(p)$ and $\phi(p)$ are computed by evaluation of (3.5) and (3.6), respectively. Consequently

$$b_k = b_k(x_k, x_{k+1}, u_k, d_k) = F_k(x_k, u_k, d_k) - x_{k+1} \tag{3.16a}$$
$$\nabla_{x_k} b_k = \nabla_{x_k} F_k(x_k, u_k, d_k) = S_{x_k}(t_{k+1})' = A_k' \tag{3.16b}$$
$$\nabla_{u_k} b_k = \nabla_{u_k} F_k(x_k, u_k, d_k) = S_{u_k}(t_{k+1})' = B_k' \tag{3.16c}$$
$$\nabla_{x_{k+1}} b_k = -I \tag{3.16d}$$

Algorithm 2 Line Search Algorithm

Require: $f(x^k)$, $\nabla_x f(x^k)$,Δx^k
Ensure: α
  $\alpha = 1$, $i = 1$, stop = false
  Compute $c = \phi(0) = f(x^k) + \mu' |\min\{0, g(x^k)\}|$
  Compute $b = \phi'(0) = \nabla_x f(x^k)\Delta x^k - \mu' |\min\{0, g(x^k)\}|$
  while NOT stop **do**
    Compute $x^{k+1} \leftarrow x^k + \alpha \Delta x^k$
    Evaluate$f(x^{k+1})$ and $g(x^{k+1})$
    Compute $\phi(\alpha) = f(x^{k+1}) + \mu' |\min\{0, g(x^{k+1})\}|$
    if $\phi(\alpha) \leq \phi(0) + 10^{-4}\phi'(0)\alpha$ (Armijo condition) **then**
      stop=true
    else
      Compute $a = \frac{\phi(\alpha) - (c + b\alpha)}{\alpha^2}$ and $\alpha_{min} = \frac{-b}{2a}$

$$\alpha \leftarrow \min\{0.9\alpha, \max\{\alpha_{min}, 0.1\alpha\}\}$$

    end if
  end while

where $x(t_{k+1}) = F(x_k, u_k, d_k)$ and

$$\dot{x}(t) = f(x(t), u_k, d_k) \tag{3.17a}$$

$$\dot{S}_{x_k}(t) = \left(\frac{\partial f}{\partial x}(x(t), u_k, d_k)\right) S_{x_k}(t) \tag{3.17b}$$

$$\dot{S}_{u_k}(t) = \left(\frac{\partial f}{\partial x}(x(t), u_k, d_k)\right) S_{u_k}(t) + \left(\frac{\partial f}{\partial u}(x(t), u_k, d_k)\right) \tag{3.17c}$$

with the initial conditions $x(t_k) = x_k$, $S_{x_k}(t_k) = I$, and $S_{u_k}(t_k) = 0$. The stage cost and the associated derivatives are computed as

$$G_k = G_k(x_k, u_k, d_k) = \int_{t_k}^{t_{k+1}} g(x(t), u_k, d_k)dt \tag{3.18a}$$

$$q_k = \nabla_{x_k} G_k = \int_{t_k}^{t_{k+1}} \left(\frac{\partial g}{\partial x}(x(t), u_k, d_k)\right) S_{x_k}(t)dt \tag{3.18b}$$

$$r_k = \nabla_{u_k} G_k = \int_{t_k}^{t_{k+1}} \left[\left(\frac{\partial g}{\partial x}(x(t), u_k, d_k)\right) S_{u_k}(t) + \left(\frac{\partial g}{\partial u}(x(t), u_k, d_k)\right)\right] dt \tag{3.18c}$$

The derivatives $\nabla_{x_k} b_k$ and $\nabla_{x_k} G_k$ are computed for $\{x_k\}_{k=1}^{N-1}$ and $k \in \mathcal{N}$. These derivatives are not computed for x_0 as $x_0 \notin p$, i.e. x_0 is a fixed parameter of the optimisation problem but not a decision variable. The derivatives $\nabla_{u_k} b_k$ and $\nabla_{u_k} G_k$ are computed for $k \in \mathcal{N}$. The derivatives with respect to x_N are

$$\nabla_{x_N} b_{N-1} = -I \tag{3.19a}$$

$$p_N = \nabla_{x_N} \phi = \nabla_{x_N} h(x_N) \tag{3.19b}$$

Therefore, the gradients of the equality constraints b_k with respect to the parameter vector p can be written as

$$\nabla_p b = \begin{bmatrix} B_0 & & & & & \\ -I & A_1 & & & & \\ & B_1 & & & & \\ & -I & A_2 & & & \\ & & B_2 & & & \\ & & -I & & & \\ & & & \ddots & & \\ & & & & A_{N-1} & \\ & & & & B_{N-1} & \\ & & & & -I & \end{bmatrix} \tag{3.20}$$

Table 3.1: Butcher tableau of an explicit Runge Kutta (ERK) scheme.

c_1	0	$\dots$	$\dots$	0
c_2	$a_{2,1}$	$\ddots$		$\vdots$
$\vdots$	$\vdots$	$\ddots$	$\ddots$	$\vdots$
c_s	$a_{s,1}$	$\dots$	$a_{s,s-1}$	0
x	b_1	b_2	$\dots$	b_s
$\hat{x}$	$\hat{b}_1$	$\hat{b}_2$	$\dots$	$\hat{b}_s$
e	d_1	d_2	$\dots$	d_s

3.2.4 Choice of the Runge-Kutta scheme

In evaluation of the functions and derivatives needed in the SQP algorithm, i.e. evaluation of $\phi(p)$, $\nabla_p\phi(p)$, $b(p)$, and $\nabla_p b(p)$, the major computational task is solution of the differential equations (3.17) and evaluation of the associated quadrature equations (3.18). These differential equations can be formulated as an Initial Value Problem (IVP)

$$\dot{x}(t) = f(x,t) \qquad x(t_0) = x_0 \tag{3.21}$$

The Hovorka model is a non-stiff system of differential equations. Therefore, we use an embedded explicit scheme for solution of the differential equations (3.17) and integration of the quadrature equations (3.18). The Butcher tableau of an explicit Runge Kutta (ERK) scheme is illustrated in Table 3.1 [63].

The main numerical steps in DOPRI54 for solution of (3.21) are

$$T_i = t_n + c_i h_n \qquad i = 1, 2, ..., s \tag{3.22a}$$

$$X_i = x_n + h_n \sum_{j=1}^{s-1} a_{i,j} f(T_j, X_j) \quad i = 1, 2, ..., s \tag{3.22b}$$

$$x_{n+1} = x_n + h_n \sum_{j=1}^{s-1} b_j f(T_j, X_j) \tag{3.22c}$$

$$e_{n+1} = h_n \sum_{j=1}^{s-1} d_j f(T_j, X_j) \tag{3.22d}$$

h_n is the step size. The step size is chosen adaptively using a PI-controller such that the resulting error estimate, e_{n+1}, meets the specifications [64]. The coefficients $a_{i,j}$, b_j, c_j and d_j for DOPRI54 are given by the Butcher tableau in Table 3.2 and in [62].
A special DOPRI54 method tailored for solution of (3.17)-(3.18) has been implemented. In this implementation, we re-use the internal stages computed by solution of (3.17) in the evaluation of the quadrature equation (3.18). The implementation uses an adaptive time step based on PI-control described in [64].
In order to avoid unnecessary computations when a stepsize is rejected, we solve the systems of ODEs sequentially. Its implementation is illustrated in Fig. 3.3.
When p is given as in the multiple shooting algorithm, evaluation of $c(p)$ and $\nabla_p c(p)$ becomes straightforward. As $c(p)$ represents the bound constraints, $u_{\min} \leq u_k \leq u_{\max}$ for $k \in \mathcal{N}$, $\nabla_p c(p)$ is a constant and the corresponding constraints in the quadratic program (3.12) become bound constraints as well.

3.2.5 Structure of the Hessian matrix

The BFGS update of the Hessian matrix usually produces a dense matrix W^k. However, for the multiple shooting algorithm for solution of (3.1),

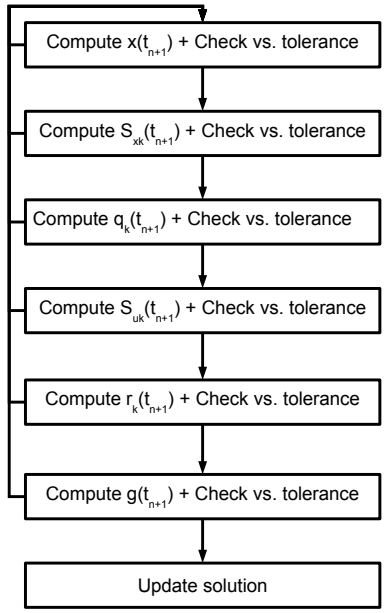

Figure 3.3: Flowchart of the Runge-Kutta method.

the Hessian of the Lagrangian $\nabla^2_{pp}\mathcal{L}$ is a block diagonal matrix. Therefore, we modify the BFGS update such that it also produces a block diagonal matrix.

Table 3.2: Butcher tableau for the DOPRI54 method.

0	0	0	0	0	0	0	0
$\frac{1}{5}$	$\frac{1}{5}$	0	0	0	0	0	0
$\frac{3}{10}$	$\frac{3}{40}$	$\frac{9}{40}$	0	0	0	0	0
$\frac{4}{5}$	$\frac{44}{55}$	$\frac{-56}{15}$	$\frac{32}{9}$	0	0	0	0
$\frac{8}{9}$	$\frac{19372}{6561}$	$\frac{-25360}{2187}$	$\frac{64448}{6561}$	$\frac{-212}{729}$	0	0	0
1	$\frac{9017}{3168}$	$\frac{-355}{33}$	$\frac{46732}{5247}$	$\frac{49}{176}$	$\frac{-5103}{18656}$	0	0
1	$\frac{35}{384}$	0	$\frac{500}{1113}$	$\frac{125}{192}$	$\frac{-2187}{6784}$	$\frac{11}{84}$	0
x	$\frac{5179}{57600}$	0	$\frac{7571}{16695}$	$\frac{393}{640}$	$\frac{-92097}{339200}$	$\frac{187}{2100}$	$\frac{1}{40}$
$\hat{x}$	$\frac{35}{384}$	0	$\frac{500}{1113}$	$\frac{125}{192}$	$\frac{-2187}{6784}$	$\frac{11}{84}$	0
e	$\frac{71}{57600}$	0	$\frac{-71}{16695}$	$\frac{71}{1920}$	$\frac{-17253}{339200}$	$\frac{22}{525}$	$\frac{-1}{40}$

The Lagrangian of (3.4) may be expressed as

$$\begin{aligned}\mathcal{L} &= \sum_{k=0}^{N-1} G_k(x_k, u_k, d_k) + h(x_N) \\ &\quad - \sum_{k=0}^{N-1} y'_{k+1}(F_k(x_k, u_k, d_k) - x_{k+1}) \\ &\quad - \sum_{k=0}^{N-1} z'_{L,k}\,(u_k - u_{\min}) + z'_{U,k}\,(u_{\max} - u_k) \\ &= \mathcal{H}_0 - z'_{L,0}(u_0 - u_{\min}) - z'_{U,0}(u_{\max} - u_0) \\ &\quad + \sum_{k=1}^{N-1} \mathcal{H}_k + y'_k x_k - z'_{L,k}(u_k - u_{\min}) - z'_{U,k}(u_{\max} - u_k) \\ &\quad + h_N(x_N) + y'_N x_N\end{aligned} \tag{3.23}$$

in which the Hamiltonians are

$$\begin{aligned}\mathcal{H}_k &= \mathcal{H}_k(x_k, u_k, d_k, y_{k+1}) \\ &= G_k(x_k, u_k, d_k) - y'_{k+1} F_k(x_k, u_k, d_k) \quad k \in \mathcal{N}\end{aligned} \tag{3.24}$$

Notice

$$\nabla_{x_k} \mathcal{H}_k(x_k, u_k, d_k, y_{k+1}) = q_k - A'_k y_{k+1} \quad k \in \mathcal{N} \setminus \{0\} \tag{3.25a}$$

$$\nabla_{u_k} \mathcal{H}_k(x_k, u_k, d_k, y_{k+1}) = r_k - B'_k y_{k+1} \quad k \in \mathcal{N} \tag{3.25b}$$

and that the Lagrangian, $\mathcal{L}$, is partially separable such that

$$\nabla^2_{pp}\mathcal{L} = \begin{bmatrix} R_0 & & & & & & \\ & Q_1 & M_1 & & & & \\ & M'_1 & R_1 & & & & \\ & & & \ddots & & & \\ & & & & Q_{N-1} & M_{N-1} & \\ & & & & M'_{N-1} & R_{N-1} & \\ & & & & & & P_N \end{bmatrix} \tag{3.26}$$

The block-matrices in $\nabla^2_{pp}\mathcal{L}$ are symmetric and given by

$$R_0 = \nabla^2_{u_0,u_0}\mathcal{H}_0 \approx W_0 \tag{3.27a}$$

$$\begin{bmatrix} Q_k & M_k \\ M'_k & R_k \end{bmatrix} = \begin{bmatrix} \nabla^2_{x_k,x_k}\mathcal{H}_k & \nabla^2_{x_k,u_k}\mathcal{H}_k \\ \nabla^2_{u_k,x_k}\mathcal{H}_k & \nabla^2_{u_k,u_k}\mathcal{H}_k \end{bmatrix} \approx W_k \tag{3.27b}$$

$$P_N = \nabla^2_{x_N,x_N} h_N \approx W_N \tag{3.27c}$$

for $k = 1, 2, \ldots, N-1$. Algorithm 3 describes a modified BFGS algorithm used to compute the approximate block matrices, $\{W_k\}_{k=0}^N$. The algorithm ensures that all these block matrices are symmetric positive definite. In implementations, we enforce symmetry explicitly by $W_k \leftarrow 0.5(W_k + W'_k)$.

3.2.6 Interior point algorithm

In this Chapter we use a structured primal-dual interior point algorithm for the solution of the constrained QP (3.12). We implement the centering

Algorithm 3 Block Structured Modified BFGS Update

Compute ($k = 1, 2, \ldots, N-1$)

$$q_0 = u_0^{j+1} - u_0^j$$
$$s_0 = \nabla_{u_0}\mathcal{H}_0(x_0, u_0^{j+1}, d_0, y_1) - \nabla_{u_0}\mathcal{H}_0(x_0, u_0^{j+1}, d_0, y_1)$$

$$q_k = \begin{bmatrix} x_k^{j+1} - x_k^j \\ u_k^{j+1} - u_k^j \end{bmatrix}$$
$$s_k = \begin{bmatrix} \nabla_{x_k}\mathcal{H}_k(x_k^{j+1}, u_k^{j+1}, d_k, y_{k+1}) - \nabla_{x_k}\mathcal{H}_k(x_k^j, u_k^j, d_k, y_{k+1}) \\ \nabla_{u_k}\mathcal{H}_k(x_k^{j+1}, u_k^{j+1}, d_k, y_{k+1}) - \nabla_{u_k}\mathcal{H}_k(x_k^j, u_k^j, d_k, y_{k+1}) \end{bmatrix}$$

$$q_N = x_N^{j+1} - x_N^j$$
$$s_N = \nabla_{x_N}h(x_N^{j+1}) - \nabla_{x_N}h(x_N^j)$$

for $k = 0, 1, ..., N$ **do**

Compute

$$\theta_k = \begin{cases} 1 & q_k' s_k' \geq 0.2 q_k' W_k q_k \\ \dfrac{0.8 q_k' W_k q_k}{q_k' W_k q_k - q_k' s_k} & q_k' s_k' < 0.2 q_k' W_k q_k \end{cases}$$
$$r_k = \theta_k s_k + (1 - \theta_k) W_k q_k$$
$$W_k \leftarrow \begin{cases} W_k & \|s_k\|_2 \leq \varepsilon_s \\ W_k - \dfrac{W_k q_k q_k' W_k}{q_k' W_k q_k} + \dfrac{r_k r_k'}{q_k' r_k} & \|s_k\|_2 > \varepsilon_s \end{cases}$$

end for

step correction proposed by Mehrotra [65]. We use the Riccati recusion presented in [60, 61] and [66] to factorize the KKT matrix. This factorization can be used to compute the optimal variation in the manipulated variables Δu_k, the optimal change in states variables Δx_{k+1}, and the Lagrange multipliers y_{k-1}.

We define the matrices $C = \nabla_p g(p^k)$ and $A = \nabla_p h(p^k)$, and the vectors $b = -h(p^k)$ and $d = -g(p^k)$. The QP in the local SQP algorithm (3.12) can be rewritten as

$$\begin{aligned} \min_{\Delta p} \quad & \frac{1}{2}\Delta p' G \Delta p + g'\Delta p \\ s.t. \quad & A'\Delta p = b \\ & C'\Delta p \geq d \end{aligned} \tag{3.28}$$

The Lagrangian for (3.28) is

$$\mathcal{L}(\Delta p, \tilde{y}, z) = \frac{1}{2}\Delta p' G \Delta p + g'\Delta p - \tilde{y}'(A'\Delta p - b) - z'(C'\Delta p - d) \tag{3.29}$$

and the optimality conditions (or first order KKT conditions) are

$$\begin{aligned} \nabla_{\Delta} p\mathcal{L}(\Delta p, \tilde{y}, z) &= G\Delta p + g - A\tilde{y} - Cz = 0 \\ \nabla_y \mathcal{L}(\Delta p, \tilde{y}, z) &= b - A'\Delta p = 0 \\ \nabla_z \mathcal{L}(\Delta p, \tilde{y}, z) &= -(C'\Delta p - d) \leq 0 \\ z &\geq 0 \\ (C'\Delta p - d)_i z_i &= 0, \quad i = 1, ..., m_c \end{aligned} \tag{3.30}$$

By introducing the slack variables $s = C'\Delta p - d \geq 0$, which is equivalent

to $s + d - C'\Delta p = 0$, the KKT conditions (3.30) become

$$r_L = G\Delta p + g - C\tilde{y} = 0 \tag{3.31a}$$
$$r_A = b - A'\Delta p = 0 \tag{3.31b}$$
$$r_C = -C'\Delta p + d + s = 0 \tag{3.31c}$$
$$z \geq 0 \tag{3.31d}$$
$$s \geq 0 \tag{3.31e}$$
$$s_i z_i = 0, \quad i = 1, ..., m_c \tag{3.31f}$$

The equality constraints (3.31a-3.31c, 3.31f) can be solved numerically by the Newton method. We write these constraints in a vector form

$$\begin{bmatrix} r_L = G\Delta p + g - C\tilde{y} \\ r_A = b - A'\Delta p \\ r_C = -C'\Delta p + d + s \\ r_{SZ} = SZe \end{bmatrix} = 0 \tag{3.32}$$

$S = diag(s)$, $Z = diag(z)$ and e is the unit vector. The Jacobian of (3.32) is

$$J = \begin{bmatrix} G & -A & -C & 0 \\ -A' & 0 & 0 & 0 \\ -C' & 0 & 0 & I \\ 0 & 0 & S & Z \end{bmatrix} \tag{3.33}$$

and the next Newton iteration is given by

$$\begin{bmatrix} G & -A & -C & 0 \\ -A' & 0 & 0 & 0 \\ -C' & 0 & 0 & I \\ 0 & 0 & S & Z \end{bmatrix} \begin{bmatrix} \Delta(\Delta p) \\ \Delta\tilde{y} \\ \Delta z \\ \Delta s \end{bmatrix} = - \begin{bmatrix} r_L = G\Delta p + g - C\tilde{y} \\ r_A = b - A'\Delta p \\ r_C = -C'\Delta p + d + s \\ r_{SZ} = SZe \end{bmatrix} \tag{3.34}$$

However, we need to check that the inequality constraints are satisfied for each Newton iteration. So, we compute first the search direction for the

optimization variables Δp, the Lagrange multipliers $\tilde{y}$ and z and the slack variables s and we find the biggest number $\alpha \in [0, 1]$ such that the new iteration satisfies $s \geq 0$ and $z \geq 0$, where the new iteration is given by

$$\begin{bmatrix} \Delta p \\ \tilde{y} \\ z \\ s \end{bmatrix} \leftarrow \begin{bmatrix} \Delta p \\ \tilde{y} \\ z \\ s \end{bmatrix} + \alpha \begin{bmatrix} \Delta(\Delta p) \\ \Delta\tilde{y} \\ \Delta z \\ \Delta s \end{bmatrix}$$

This algorithm defines the affine step

$$\begin{bmatrix} \Delta\Delta p^{aff} \\ \Delta\tilde{y}^{aff} \\ \Delta z^{aff} \\ \Delta s^{aff} \end{bmatrix} \tag{3.35}$$

However, the affine search often fails to find the optimal solution, since it does not prevent the components of (s, z) from moving too close to the boundary of the non-negative orthant.
The first improvement we can make is to correct the affine step. From the Newton iteration (3.34) and for the full affine step (i.e. when $\alpha = 1$), we obtain that for the next iteration, the i-th component in the complementarity condition is

$$\begin{aligned}(s_i^{aff} + \Delta s_i^{aff})(z_i^{aff} + \Delta z_i^{aff}) &= s_i^{aff} z_i^{aff} + s_i^{aff}\Delta z_i^{aff} + z_i^{aff}\Delta s_i^{aff} + \Delta s_i^{aff}\Delta z_i^{aff} \\ &= \Delta s_i^{aff}\Delta z_i^{aff}\end{aligned} \tag{3.36}$$

since $s_i^{aff}\Delta z_i^{aff} + z_i^{aff}\Delta s_i^{aff} = -s_i^{aff} z_i^{aff}$. However, we want to have

$$(s_i^{aff} + \Delta s_i^{aff})(z_i^{aff} + \Delta z_i^{aff}) = 0$$

So, we replace the last system of equations in the affine step by adding the corrector term $-\Delta S \Delta Z e$ and thus we obtain the modified linear system

$$\begin{bmatrix} G & -A & -C & 0 \\ -A' & 0 & 0 & 0 \\ -C' & 0 & 0 & I \\ 0 & 0 & S & Z \end{bmatrix} \begin{bmatrix} \Delta\Delta p^{cor} \\ \Delta\tilde{y}^{cor} \\ \Delta z^{cor} \\ \Delta s^{cor} \end{bmatrix} = \begin{bmatrix} 0 \\ 0 \\ 0 \\ -\Delta S \Delta Z e \end{bmatrix} \tag{3.37}$$

The second improvement for the interior point algorithm is suggested by Mehrotra [65]. Mehrotra adds a centering step

$$\begin{bmatrix} \Delta\Delta p^{cen} \\ \Delta\tilde{y}^{cen} \\ \Delta z^{cen} \\ \Delta s^{cen} \end{bmatrix} \tag{3.38}$$

The centering step is computed by solving the system

$$\begin{bmatrix} G & -A & -C & 0 \\ -A' & 0 & 0 & 0 \\ -C' & 0 & 0 & I \\ 0 & 0 & S & Z \end{bmatrix} \begin{bmatrix} \Delta\Delta p^{cen} \\ \Delta\tilde{y}^{cen} \\ \Delta z^{cen} \\ \Delta s^{cen} \end{bmatrix} = - \begin{bmatrix} 0 \\ 0 \\ 0 \\ \sigma\mu e \end{bmatrix} \tag{3.39}$$

μ is the duality measure given by

$$\mu = \frac{z's}{m_c} \tag{3.40}$$

σ is given by

$$\sigma = \left(\frac{\mu^{aff}}{\mu} \right)^3 \tag{3.41}$$

where μ^{aff} is the duality gap for the affine step

$$\frac{(z + \alpha^{aff}\Delta z^{aff})'(s + \alpha^{aff}\Delta s^{aff})}{m_c} \tag{3.42}$$

We can use the affine step combined with the corrected and the centering steps to implement the primal-dual interior point algorithm. The overall idea is to compute first the affine step and the coefficient α^{aff} by using the Newton iteration (3.34), to use this affine step to compute the corrector and the centering steps, and then to solve again the system of equations using a corrected term for r_{SZ} in (3.34) which includes the corrector step

(3.37) and the centering step (3.39). This corrected step is given by solving the linear system

$$\begin{bmatrix} G & -A & -C & 0 \\ -A' & 0 & 0 & 0 \\ -C' & 0 & 0 & I \\ 0 & 0 & S & Z \end{bmatrix} \begin{bmatrix} \Delta\Delta p \\ \Delta\tilde{y} \\ \Delta z \\ \Delta s \end{bmatrix} = - \begin{bmatrix} r_L = G\Delta p + g - C\tilde{y} \\ r_A = -A'\Delta p + b \\ r_C = -C'\Delta p + d + s \\ SZe + \Delta S\Delta Ze - \sigma\mu e \end{bmatrix} \tag{3.43}$$

This algorithm is presented in Algorithm 4.
The stopping criteria is given by the KKT-conditions (3.31), i.e.

$$\begin{cases} \|r_L\| \leq \varepsilon_L \\ \|r_A\| \leq \varepsilon_L \\ \|r_C\| \leq \varepsilon_C \\ \|r_{SZ}\| \leq \varepsilon_{SZ} \end{cases} \tag{3.44}$$

In Algorithm 4, the main computational task is to solve the linear systems of equations. The linear system of equations we have to solve is in the form (equations 3.34 and 3.43)

$$\begin{bmatrix} G & -A & -C & 0 \\ -A' & 0 & 0 & 0 \\ -C' & 0 & 0 & I \\ 0 & 0 & S & Z \end{bmatrix} \begin{bmatrix} \Delta p \\ \Delta\tilde{y} \\ \Delta z \\ \Delta s \end{bmatrix} = - \begin{bmatrix} r_L \\ r_A \\ r_C \\ \bar{r}_{SZ} \end{bmatrix} \tag{3.45}$$

$\bar{r}_{SZ}$ is either SZe for the affine step, or $SZe + \Delta S\Delta Ze - \sigma\mu e$ for the corrected step. The matrices S and Z are positive definite (and therefore invertible) since they are diagonal with positive terms. The Hessian matrix G is also positive definite, and therefore invertible.
The linear system (3.45) is equivalent to the augmented equation

$$\begin{bmatrix} G + C(S^{-1}Z)C' & -A \\ -A' & 0 \end{bmatrix} \begin{bmatrix} \Delta\Delta p \\ \Delta\tilde{y} \end{bmatrix} = \begin{bmatrix} -r_L + C(S^{-1}Z)\left(r_C - Z^{-1}\bar{r}_{SZ}\right) \\ -r_A \end{bmatrix} \tag{3.46}$$

Algorithm 4 Primal-Dual interior point algorithm

while not stop **do**

Solve (3.34)

$$\begin{bmatrix} G & -A & -C & 0 \\ -A' & 0 & 0 & 0 \\ -C' & 0 & 0 & I \\ 0 & 0 & S & Z \end{bmatrix} \begin{bmatrix} \Delta\Delta p^{aff} \\ \Delta\tilde{y}^{aff} \\ \Delta z^{aff} \\ \Delta s^{aff} \end{bmatrix} = - \begin{bmatrix} r_L = G\Delta p + g - C\tilde{y} \\ r_A = -A'\Delta p + b \\ r_C = -C'\Delta p + d + s \\ r_{SZ} = SZe \end{bmatrix}$$

Compute the largest α^{aff} such that: $z + \alpha^{aff}\Delta z^{aff} \geq 0$ and $s + \alpha^{aff}\Delta s^{aff} \geq 0$

Compute the affine duality gap: $\mu^{aff} = (z + \alpha^{aff}\Delta z^{aff})'(z + \alpha^{aff}\Delta z^{aff})/m_c$

Compute the centering parameter: $\sigma = (\mu^{aff}/\mu)^3$ with $\mu = z's/m_c$

Solve the modified Newton iteration

$$\begin{bmatrix} G & -A & -C & 0 \\ -A' & 0 & 0 & 0 \\ -C' & 0 & 0 & I \\ 0 & 0 & S & Z \end{bmatrix} \begin{bmatrix} \Delta\Delta p \\ \Delta\tilde{y} \\ \Delta z \\ \Delta s \end{bmatrix} = - \begin{bmatrix} r_L = G\Delta p + g - C\tilde{y} \\ r_A = -A'\Delta p + b \\ r_C = -C'\Delta p + d + s \\ SZe + \Delta S\Delta Ze - \sigma\mu e \end{bmatrix}$$

Compute the largest α such that: $z + \alpha\Delta z \geq 0$ and $s + \alpha\Delta s \geq 0$

$\eta = 0.995$. Update the solution:

$$\begin{bmatrix} \Delta p \\ \tilde{y} \\ z \\ s \end{bmatrix} \leftarrow \begin{bmatrix} \Delta p + \eta\Delta\Delta p \\ \tilde{y} + \eta\Delta\tilde{y} \\ z + \eta\Delta z \\ s + \eta\Delta s \end{bmatrix}$$

end while

combined with the equations

$$\Delta z = -\left(S^{-1}Z\right)C'\Delta\Delta p + \left(S^{-1}Z\right)\left(r_C - Z^{-1}\bar{r}_{SZ}\right) \tag{3.47a}$$

$$\Delta s = -Z^{-1}\bar{r}_{SZ} - -Z^{-1}S\Delta z \tag{3.47b}$$

Thus, we can compute $\Delta\Delta p$ and $\Delta\tilde{y}$ by solving the QP

$$\begin{aligned} \min_{\Delta\Delta p} \frac{1}{2} \quad & \Delta\Delta p' \left[G + C(S^{-1}Z)C'\right] \Delta\Delta p + \left[r_L - C(S^{-1}Z)\left(r_C - Z^{-1}\bar{r}_{SZ}\right)\right] \Delta\Delta p \\ \text{s.t.} \quad & A'\Delta\Delta p = r_A \end{aligned} \tag{3.48}$$

and compute Δz and Δs

$$\Delta z = -(S^{-1}Z)C'\Delta\Delta p + (S^{-1}Z)(r_C - Z^{-1}\bar{r}_{SZ}) \tag{3.49a}$$

$$\Delta s = -Z^{-1}\bar{r}_{SZ} - Z^{-1}S\Delta z \tag{3.49b}$$

In the multiple shooting, the KKT-matrix

$$\begin{bmatrix} G + C(S^{-1}Z)C' & -A \\ -A' & 0 \end{bmatrix} \tag{3.50}$$

has a special structure. This structure can be used to factorize it efficiently, and is described in [60, 61] and [66]. The factorization algorithm is summarized in Algorithm 5.

3.3 Continuous-discrete Extended Kalman Filter (CDEKF)

In this section, we introduce the extended Kalman filter (EKF) for continuous-discrete stochastic nonlinear systems [67–69]. The EKF is used to estimate the state of the system given a stochastic continuous-time model and measurements at discrete times, i.e.

$$dx(t) = f(t, x(t), u(t))dt + \sigma d\omega(t) \tag{3.51a}$$

$$y_k = h(t_k, x(t_k)) + v_k \tag{3.51b}$$

in which $\{\omega(t),\ t \geq 0\}$ is a standard Wiener process, i.e. a process with covariance Idt (intensity I). The matrix σ is time-invariant. The measurement noise v_k is normally distributed, $v_k \sim N_{iid}(0, R_k)$. We assume that the initial state x_0 is normally distributed with a known mean and covariance, $x_0 \sim N(\hat{x}_{0|-1}, P_{0|-1})$.

Algorithm 5 KKT matrix factorization

for $k = N-1, N-2, ..., 1$ **do**

Compute

$$\begin{aligned} R_{e,k} =& R_k + B_k P_{k+1} B_k' \\ K_k =& -R_{e,k}^{-1}(M_k' + B_k P_{k+1} A_k') \\ a_k =& -R_{e,k}^{-1}(r_k + B_k(P_{k+1} b_k + p_{k+1})) \\ P_k =& Q_k + A_k P_{k+1} A_k' - K_k' R_{e,k} K_k \\ P_k \leftarrow& \frac{1}{2}\left(P_k + P_k'\right) \\ p_k =& q_k + A_k(P_{k+1} b_k + p_{k+1}) + K_k'(r_k + B_k(P_{k+1} b_k + p_{k+1})) \end{aligned}$$

end for

Compute $a_0 = -(R_0 + B_0 P_1 B_0')^{-1}(r_0 + B_0(P_1 b_0 + p_1))$

for $k = 1, ..., N-1$ **do**

Compute $\Delta u_0 = a_0, \quad \Delta x_1 = B_0' \Delta u_0 + b_0$

and

$$\begin{aligned} \Delta u_k &= K_k \Delta x_k + a_k \\ \Delta x_{k+1} &= A_k' \Delta x_k + B_k' \Delta u_k + b_k \end{aligned}$$

end for

Compute the dual solution $\tilde{y}_{N-1} = -P_N \Delta x_N - p_N$

for $k = N-1, ..., 1$ **do**

Compute

$$\tilde{y}_{k-1} = A_k \tilde{y}_k - Q_k \Delta x_k - M_k \Delta u_k - q_k$$

end for

3.3.1 Filtering

Given an observation, y_k, at time t_k, the filtering in the EKF describes the steps used to compute the filtered state $\hat{x}_{k|k}$ and the corresponding covariance $P_{k|k}$. The filter step assumes availability of the one-step predicitons, $\hat{x}_{k|k-1}$ and $P_{k|k-1}$.
The filter gain is computed by

$$C_k = \frac{\partial h}{\partial x}(t_k, \hat{x}_{k|k-1}) \tag{3.52a}$$

$$R_{k|k-1} = C_k P_{k|k-1} C_k' + R_k \tag{3.52b}$$

$$K_k = P_{k|k-1} C_k' \left(R_{k|k-1}\right)^{-1} \tag{3.52c}$$

and the innovation is obtained by

$$e_k = y_k - \hat{y}_{k|k-1} = y_k - h(t_k, \hat{x}_{k|k-1}) \tag{3.53}$$

The filtered state $\hat{x}_{k|k}$ and its covariance $P_{k|k}$ are given by

$$\hat{x}_{k|k} = \hat{x}_{k|k-1} + K_k e_k \tag{3.54a}$$

$$P_{k|k} = P_{k|k-1} - K_k R_{k|k-1} K_k' \tag{3.54b}$$

3.3.2 Prediction

Given the observations $\mathcal{Y}_k = \{y_0, y_1, \ldots, y_k\}$, the predicted state vector $\hat{x}_{k+1|k} = \hat{x}_k(t_{k+1})$ and its associated covariance $P_{k+1|k} = P_k(t_{k+1})$ are computed as the solutions to the system of ordinary differential equations ([69])

$$\frac{d\hat{x}_k(t)}{dt} = f(t, \hat{x}_k(t), u_k) \tag{3.55a}$$

$$\frac{dP_k(t)}{dt} = A_k(t) P_k(t) + P_k(t) A_k(t)' + \sigma\sigma' \tag{3.55b}$$

with

$$A_k(t) = A(t, \hat{x}_k(t), u_k) = \frac{\partial f}{\partial x}(t, \hat{x}_k(t), u_k) \tag{3.56}$$

and the initial conditions

$$\hat{x}_k(t_k) = \hat{x}_{k|k} \tag{3.57a}$$

$$P_k(t_k) = P_{k|k} \tag{3.57b}$$

The numerical integration of (3.55) is computed using the explicit DOPRI54 method described in Section 3.2.4.

3.4 Application to People With Type 1 Diabetes

In this section, we use the Hovorka model described in Chapter 2 and the implemented multiple shooting algorithm presented in section 3.2 to compute optimal insulin profiles for people with type 1 diabetes.
We use $u_{\min} = 0$ and a large $u_{\max}$ such that the upper bound is never active. We do the optimisation in a 24 hour window, i.e. $t_0 = 0$ min and $t_f = 24 \cdot 60$ min, using a sampling time of $T_s = 5$ min. In the scenario considered, the simulated 70 kg subject has a 62 g CHO meal at 6:00, a 55 g CHO meal at 12:00, and a 50 g CHO meal at 18:00. To ensure an optimal blood glucose profile, a prediction horizon of six hours, i.e., $N = 6 \cdot 12 = 72$ samples, is employed in the receding horizon strategy.
In Section 3.4.1, we assume that the full state information is available at any time. In Section 3.4.2, we use the CDEKF presented in Section 3.3 to estimate the states of the system.

3.4.1 Optimal insulin administration

Fig. 3.4 illustrates an optimal insulin administration profile for the described scenario in the case where the controller knows the size and time of all meals in advance. Knowing the meal times and sizes allows the controller to deliver anticipatory insulin to pre-empt postprandial hyperglycaemia. However, the assumption that the patient would know in advance - and with accuracy - the meal times and sizes is not practical. Safety considerations would preclude significant amounts of insulin from being delivered prior to mealtime (as in this ideal scenario).

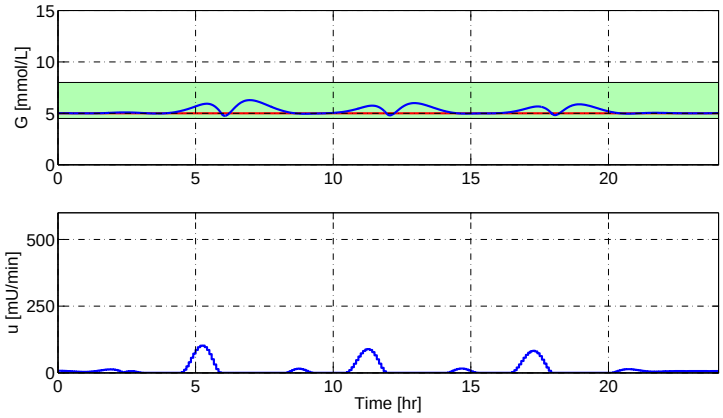

Figure 3.4: Optimal insulin administration for the case with meal announcement in advance of the meal. Most insulin is taken before the meals.

Fig. 3.5 shows the simulation results for the case in which the meals are announced to the MPC only at mealtime. Thus, the controller can deliver no anticipatory insulin prior to meals. The limitations for this case force the subject into (mild) hyperglycaemia, but hypoglycaemia is avoided. The insulin delivery profile for this case looks quite similar to bolus delivery of insulin by a pen; most of the meal-related insulin is delivered in bolus form in the few samples after the meals are taken (and announced). Simulated optimal bolus treatment with a pen in Fig. 3.6 provides glucose profiles comparable to the glucose profile in Fig. 3.5.

These results demonstrate that for cases for which meal information is unknown until mealtime, reasonably good control can still be obtained. Perhaps more importantly, the bolus like nature of the insulin profile in this case suggests that a pen-based system may be able to achieve control comparable to that of a pump.

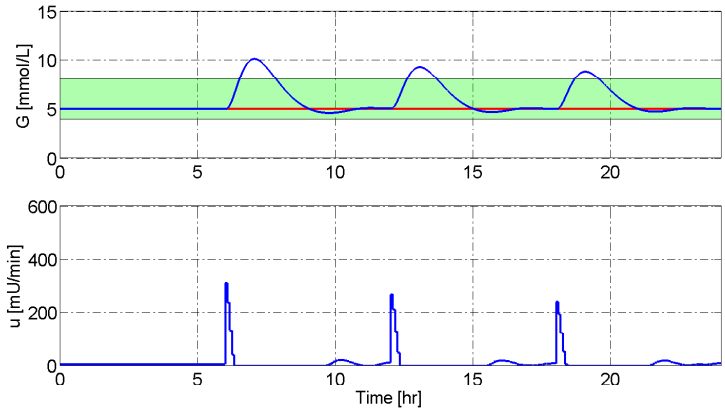

Figure 3.5: Optimal insulin administration with meal announcement at meal time. Most insulin is taken in bolus like form at meal time.

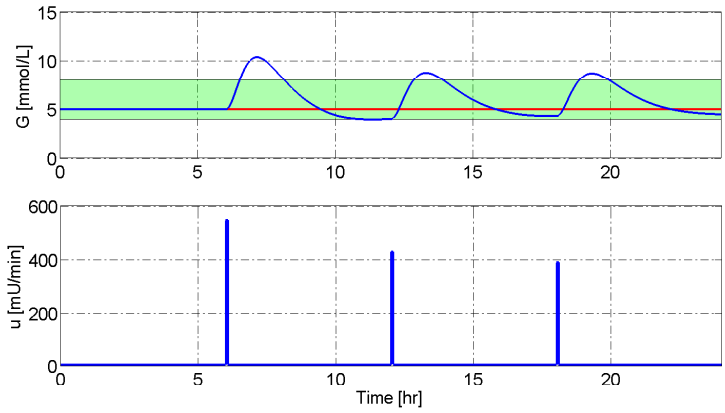

Figure 3.6: Optimal insulin administration with meal announcement at meal time.

3.4.2 Meal estimation

In real life, the mealtime and exact meal size cannot be exactly known. Here, we apply the CDEKF in order to estimate the states of the Hovorka model at every time step (i.e. every 5 minutes). Fig. 3.7(a) depicts the insulin and glucose profiles in the case where the meal is not announced. Fig. 3.7(b) depicts the actual and reconstructed profiles for the two compartments D_1 and D_2 in the CHO absorption subsystem. Although the peaks for the the first compartment D_1 are not correctly reconstructed by the continuous-discrete extended Kalman filter, it is possible to reconstruct the profile for the second compartment D_2.

3.4.3 Benefits of faster insulin on postprandial blood glucose

Fig. 3.8 shows the maximum blood glucose versus the insulin time constant τ_s for small-sized meals (25 g CHO), normal-sized meals (50 g CHO) and large-sized meals (100 g CHO) if the meal is announced only at mealtime. A faster insulin reduces the peak of glucose. For normal-sized meals, having an insulin absorption time constant at least equal to the glucose absorption time constant (i.e. $\tau_s = 40$ minutes) avoids hyperglycemic events.

3.5 Summary

In this chapter, we have applied NMPC to the control of blood glucose for people with type 1 diabetes. We have computed optimal insulin and glucose profiles in the cases where meals are announced beforehand, where meal are announced at mealtimes, and where meals are not announced at all. In the case where the meal size is announced at mealtime, the insulin profile is similar to a bolus-like profile.
Application of NMPC to real patients would require a sufficient amount of data and an identifiable model, such as the Medtronic Virtual Patient (MVP) model. In addition, we need a simpler control strategy to be used in a real clinic.

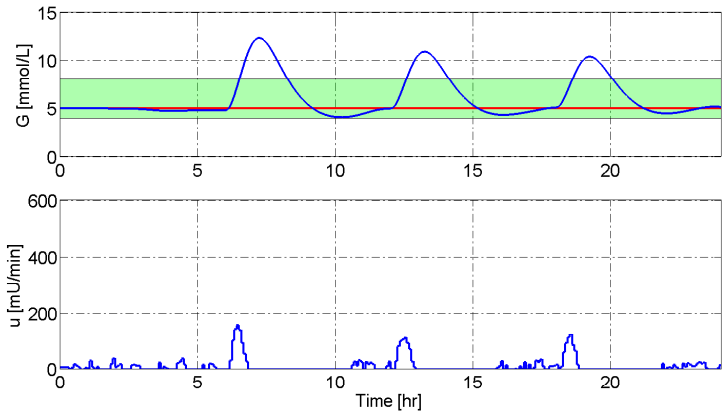

(a) Optimal insulin administration and glucose profile.

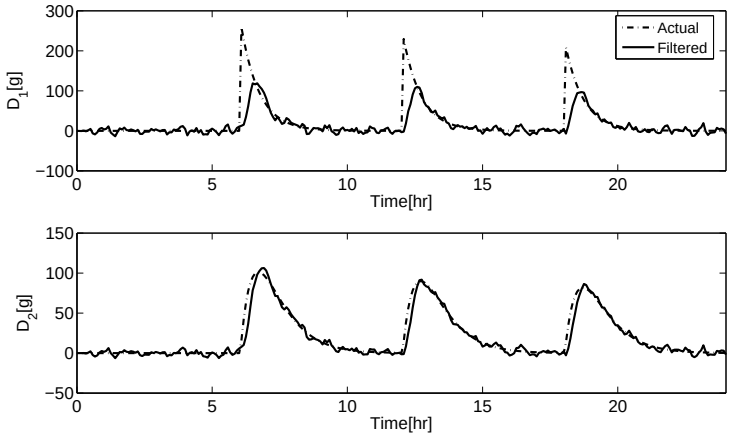

(b) Actual (dash-dotted line) and reconstructed (solid line) profiles for the two compartments in the CHO absorption subsystem.

Figure 3.7: Case in which the meals are not announced.

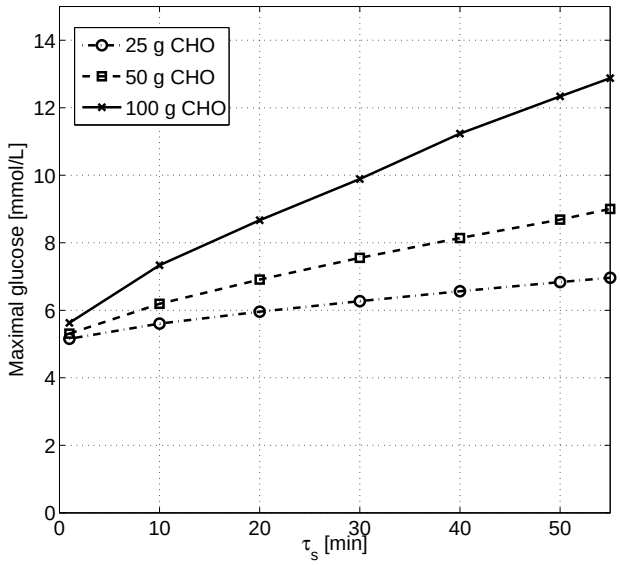

Figure 3.8: Maximal blood glucose versus insulin time constant τ_s for 25 g CHO (dash-dotted line, 50 g CHO (dashed line), and 100 g CHO meals (solid line).

CHAPTER 4

Model Predictive Control Algorithms for People with Type 1 Diabetes

In this chapter, we develop linear model predictive controllers based on models of the ARMAX-type. The deterministic part of the predictive model used by the controller is selected from already known clinical parameters. The parameters are the insulin sensitivity factor (ISF), the insulin action time, and the basal insulin. The stochastic part of the model is determined in different ways from data and cases with and without integrators are considered. All controllers are tested and compared for a cohort of 100 virtual patients. The controller based on the model with the integrator, i.e. the ARIMAX model, is also tested on 12 real patients at Hvidovre Hospital. Paper H presents the clinical protocol and results from the pilot in vivo studies. A detailed description of the controller and in silico simulations are presented in Paper I and Paper J. In Paper J we compare 3 different control strategies on overnight simulations. The glucose and insulin profiles of the in vivo clinical studies are presented in Appendix A.

4.1 Methods and material

This section describes the clinical protocol and the developed graphical user interface for the clinical studies. The aim of these studies is to demonstrate the ability of the controller to stabilize blood glucose in the euglycemic range during the study nights.

4.1.1 Clinical protocol

The patient is equipped with 2 Dexcom Seven Plus CGMs 2-4 days prior to the study and a Medtronic Paradigm Veo insulin pump. The CGMs provide glucose measurements every 5 minutes. The clinician decides on the sensor used by the controller, based on the accuracy of the sensor during the days before the study. The other CGM can be used as a backup device. Insulin is administrated to the patient through small discrete insulin injections (also called microboluses) every 15 minutes.
The pump used for the clinical studies has discrete increments of 0.025U, and a minimum continuous insulin injection (or basal rate) of 0.025 U/hr. The controller handles these restrictions by using hard constraints on the minimal insulin infusion rate and by rounding the suggested microbolus to the nearest 0.025U.
In addition, blood samples are taken at least every 30 minutes in order to measure the blood glucose. In case of a prolonged period of low blood glucose concentration, blood samples are taken and analyzed every 15 minutes. The blood samples are analyzed for blood glucose concentration immediately by Hemocue. These blood glucose measurements by Hemocue are included in the clinical protocol to ensure the patients' safety. These measurements provides reliable glucose measurements and enable the medical doctor to intervene and give IV glucose in case of critical low blood glucose concentrations. After the study, YSI measurements have been taken. YSI is the golden standard for blood glucose measurements. Neither the Hemocue blood glucose concentrations nor the YSI blood glucose concentrations are known to the controller. The controller receives feedback from one of the CGMs only.

The clinician has the authority to prevent severe hypoglycemia by injection of intravenous glucose. Such a decision is based on the glucose history.
The protocol is the following

- The patient arrives at the clinic at approximately 17.00. The insulin pump delivers the patient's usual basal rate. The clinician chooses the CGM that will be used for the study.
- At 18:00 an evening meal (white rice, curry sauce, boiled chicken breast, green salad) is served. The size of the meal is determined by the weight of the patient (1 gram carbohydrate/kg BW).
- At 22:00, the basal rate is reduced to its minimum (0.025 U/hr), and the controller is switched to closed-loop, ie. the insulin infusion rate is determined by the controller. The CGMs are calibrated using SMBG (Self Monitoring of Blood Glucose).
- The study ends at 07:00 the following day. The insulin pump delivers the patient's usual basal rate again.

4.1.2 Graphical User Interface

Fig 4.1 provides an overview of the graphical user interface developed for the artificial pancreas. The glucose sensor provides a glucose measurement every 5 minutes. The glucose measurements are transmitted from the sensor to the software via a wireless receiver.
The graphical user interface returns a new insulin microbolus suggestion every 15 minutes. At these times, it also returns the glucose prediction and insulin prediction profiles. The decision on the insulin microbolus can be overruled if there is a safety risk for the patient. The exact time before the next microbolus suggestion is provided by the graphical user interface.
The clinician also has the possibility to add comments if needed. These comments have no influence on the microboluses computation.

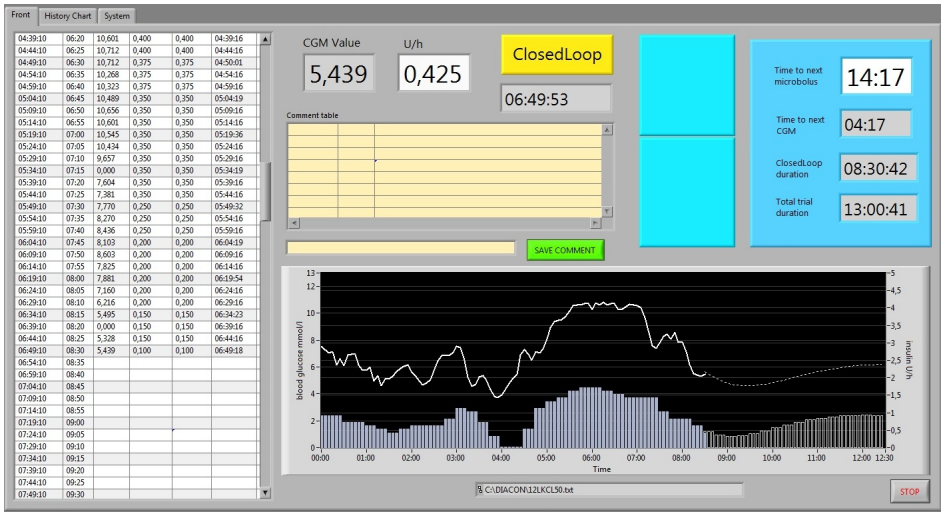

Figure 4.1: Graphical User Interface screenshot. The left panel provides the glucose and insulin history. The middle panel displays the current CGM value and insulin microbolus and the comments. The right panel indicates the time before the next microbolus administration, the time before the next CGM measurement, the duration of closed-loop and the total study duration. The plot depicts the glucose and insulin profiles (solid lines) and the predictions for glucose and insulin (dashed lines).

4.2 Modeling of Glucose-Insulin Dynamics

In this section, we derive a prediction model for subcutaneous glucose, $y(t)$. The model has a deterministic part describing the effect of sc. injected insulin, $u(t)$, and a stochastic part describing the effect of other unknown factors. This model identification technique turns out to give a good compromise between data requirements, performance and robustness of the resulting controller for the overnight study described in this chapter.

4.2.1 Choice of the deterministic model

All the physiological models listed in section 1.1.4 and in [48] contain a large number of parameters, and even the minimal model may be difficult to identify [70]. To overcome this issue, we use a low-order linear model to describe the glucose-insulin dynamics. Similar approaches have been investigated previously. [71] used a third order transfer function with an integrator, [72] used a third order discrete transfer function model and [73] applied a first order transfer function with a time delay. In this thesis we use a continuous-time second order transfer function

$$G(s) = \frac{Y(s)}{U(s)} = \frac{K_u}{(\tau s + 1)^2} \tag{4.1}$$

to model the effect of sc injected insulin on sc glucose. The gain, K_u, and the time constant, τ, are computed from known subject-specific parameters; the insulin action time and the insulin sensitivity factor (ISF).
The insulin action time and the insulin sensitivity factor are related to the response of blood glucose to an insulin bolus. If we assume that blood glucose is approximately identical to sc glucose, this is the impulse response of (4.1). The insulin action time is the time for blood glucose to reach its minimum. The ISF corresponds to the maximum decrease in blood glucose per unit of insulin bolus. These parameters are empirically estimated by the patient and his/her physician. These parameters may vary from day to day for a given patient but gives an estimate of the effect of insulin on blood glucose and sc glucose. An illustration of the ISF and the insulin action time is provided in Fig. 4.2.
Fig 4.3 depicts the impulse response for a virtual patient with type 1 diabetes and its second order approximation (4.1). This patient is simulated using the model developed by [46]. The figure demonstrates that a second order model provides an acceptable approximation of a patient with type 1 diabetes.
In the temporal domain, the impulse response of (4.1) is described by

$$y(t) = K_u \frac{t}{\tau^2} \exp(-t/\tau) \tag{4.2}$$

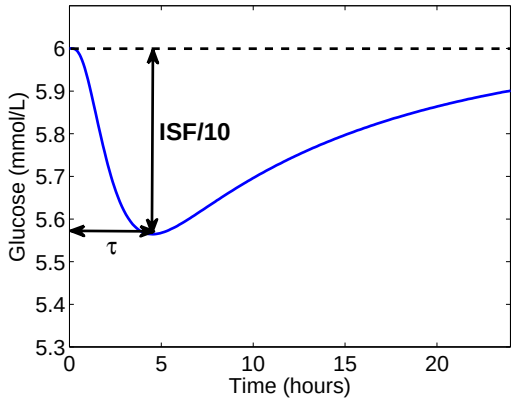

Figure 4.2: Impulse response for the nonlinear Hovorka model. The bolus size is 0.1U.

The insulin action time corresponds to the time to reach the minimum blood glucose. Consequently, this insulin action time is equal to τ. We determine K_u using (4.2) and the fact that the insulin sensitivity factor is equal to the minimal blood glucose (sc glucose), $y(\tau) = -ISF$, such that

$$K_u = -\tau \exp(1) ISF \tag{4.3}$$

We discretize the transfer function (4.1) in the form

$$y(t) = \frac{B(q^{-1})}{A(q^{-1})} u(t) \tag{4.4}$$

Using a zero-order-hold insulin profile, the continuous-time transfer function (4.1) may be used to determine the A and B polynomials in the model (4.4). They are

$$A(q^{-1}) = 1 + a_1 q^{-1} + a_2 q^{-2} \tag{4.5a}$$
$$B(q^{-1}) = b_1 q^{-1} + b_2 q^{-2} \tag{4.5b}$$

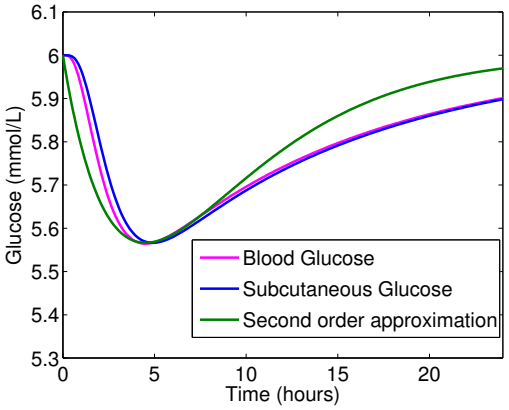

Figure 4.3: Impulse responses for a second order model and the nonlinear Hovorka model. The bolus size is 0.1U and the parameters for the second order model are: τ=4 hours and ISF = 0.4 mmol/L/0.1 U = 4.0 mmol/L/U.

with the coefficients a_1, a_2, b_1 and b_2 computed as [74]

$$a_1 = -2\exp(-T_s/\tau) \tag{4.6a}$$
$$a_2 = \exp(-2T_s/\tau) \tag{4.6b}$$
$$b_1 = K_u(1 - \exp(-T_s/\tau)(1 + T_s/\tau)) \tag{4.6c}$$
$$b_2 = K_u\exp(-T_s/\tau)(-1 + \exp(-T_s/\tau) + T_s/\tau) \tag{4.6d}$$

T_s is the sample time.

4.3 Stochastic Model

We take into account the process and measurement noise by adding a term describing the effect of unknown factors to the discrete-time model (4.4). We assume the model describing the glucose-insulin dynamics to be in the

form

$$A(q^{-1})y(t) = B(q^{-1})u(t) + \frac{C(q^{-1})}{D(q^{-1})}\varepsilon(t) \tag{4.7}$$

The model (4.7) has a deterministic part describing the effects of insulin injections $u(t)$ and a stochastic part. We assume either $D(q^{-1}) = 1 - q^{-1}$, which turns the model (4.7) into an ARIMAX model or $D(q^{-1}) = 1$, which turns the model (4.7) into an ARMAX model.
In this section we propose and discuss three different choices for the stochastic model in (4.7). The two first choices estimate the $C(q^{-1})$ based on a previous clinical study, while the last method estimate it recursively using a Recursive Least Square (RLS) algorithm.

4.3.1 ARIMAX modeling

The stochastic part, $C(q^{-1})$, of the ARIMAX model

$$A(q^{-1})y(t) = B(q^{-1})u(t) + \frac{C(q^{-1})}{1 - q^{-1}}\varepsilon(t) \tag{4.8}$$

is assumed to be a third order polynomial of the form

$$\begin{aligned} C(q^{-1}) &= 1 + c_1 q^{-1} + c_2 q^{-2} + c_3 q^{-3} \\ &= (1 - \alpha q^{-1})(1 - \beta_1 q^{-1})(1 - \beta_2 q^{-1}) \end{aligned} \tag{4.9}$$

$\alpha = 0.99$ is a fixed parameter. α has been determined based on performance studies of the resulting MPC. The choice of α is discussed in [75]. β_1 and β_2 are determined from clinical data for one real patient (see Paper H and [76]).
We compute β_1 and β_2 by estimating the process and measurement noise characteristics, σ and r, in the following continuous-discrete stochastic linear model

$$dx(t) = (A_c x(t) + B_c u(t))dt + \sigma d\omega(t) \tag{4.10a}$$

$$y_k = h(t_k, x(t_k)) + v_k \tag{4.10b}$$

A_c and B_c are realizations of (4.1). $\omega(t)$ is a standard Wiener process. The matrix σ is time-invariant and the measurement noise v_k is normally distributed, i.e. $v_k \sim N_{iid}(0, r^2)$. We estimate, σ and r, using a maximum likelihood criteria for the one-step prediction error [77, 78]. By zero-order hold (zoh) discretization, Kalman filter design, and z-transformation, (4.10) may be represented as

$$y_k = G(q^{-1})u_k + H(q^{-1})\epsilon_k \tag{4.11}$$

with

$$G(q^{-1}) = B(q^{-1})/A(q^{-1}) \tag{4.12a}$$
$$H(q^{-1}) = \tilde{C}(q^{-1})/A(q^{-1}) \tag{4.12b}$$

The parameters, β_1 and β_2, in

$$\tilde{C}(q^{-1}) = (1 - \beta_1 q^{-1})(1 - \beta_2 q^{-1}) \tag{4.13}$$

are extracted from $H(q^{-1})$. The coefficients β_1 and β_2 computed in this way are $\beta_{1,2} = 0.81 \pm 0.16i$.
The difference equation (4.11) corresponding to the SDE (4.10) is related to the ARIMAX model (4.8) by

$$\epsilon_k = \frac{1 - \alpha q^{-1}}{1 - q^{-1}} \varepsilon_k \tag{4.14}$$

This specification introduces a model-plant mismatch. ϵ_k is white noise in (4.11) while (4.14) models ϵ_k as filtered integrated white noise. This model-plant mismatch is necessary to have offset free control in the resulting predictive control system. (4.14) implies that

$$C(q^{-1}) = (1 - \alpha q^{-1})\tilde{C}(q^{-1}) \tag{4.15}$$

such that $c_1 = -2.61$, $c_2 = 2.28$ and $c_3 = -0.67$.

4.3.2 ARMAX modeling

The stochastic part, $C(q^{-1})$, of the ARMAX model

$$A(q^{-1})y(t) = B(q^{-1})u(t) + C(q^{-1})\varepsilon(t) \tag{4.16}$$

is now assumed to be a second order polynomial of the form

$$\begin{aligned} C(q^{-1}) &= 1 + c_1 q^{-1} + c_2 q^{-2} \\ &= (1 - \beta_1 q^{-1})(1 - \beta_2 q^{-1}) \end{aligned} \tag{4.17}$$

We use the same way as in Section 4.3.1 for computing β_1 and β_2, i.e. $\beta_{1,2} = 0.81 \pm 0.16i$.
Unlike the ARIMAX model structure described in Section 4.3.1, this model structure does not ensure offset-free control. However, it does not introduce a supplementary model-plant mismatch.

4.3.3 Adaptive control

Here, we consider again the ARMAX model structure (4.16). A similar approach has been proposed by [79].
The parameters c_1 and c_2 are estimated at each iteration using the recursive least square (RLS) method

$$y_k = \phi_k' \hat{\theta}_{k-1} + \varepsilon_k \tag{4.18a}$$

$$K_k = \frac{P_{k-1}\phi_k}{\mu + \phi_k' P_{k-1}\phi_k} \tag{4.18b}$$

$$\hat{\theta}_k = \hat{\theta}_{k-1} + K_k \left(y_k - \phi_k' \hat{\theta}_{k-1} \right) \tag{4.18c}$$

$$P_k = \frac{1}{\mu} \left(P_{k-1} - \frac{P_{k-1}\phi_k \phi_k' P_{k-1}}{\mu + \phi_k' P_{k-1}\phi_k} \right) \tag{4.18d}$$

ϕ_k is a vector of past observations

$$\phi_k = \begin{bmatrix} y_{k-1} & y_{k-2} & u_{k-1} & u_{k-2} & e_k & e_{k-1} \end{bmatrix} \tag{4.19}$$

θ_k is a vector of model parameters

$$\theta_k = \begin{bmatrix} -a_1 & -a_2 & b_1 & b_2 & c_1 & c_2 \end{bmatrix}' \tag{4.20}$$

P_k is the model parameters covariance matrix. Since we want to estimate c_1 and c_2 only, we initialize it with

$$P_0 = diag(0, 0, 0, 0, 100, 100) \tag{4.21}$$

Finally, μ is the forgetting factor. This parameter has an influence on the weight of previous observations. When $\mu = 1$, all the past observations are equally weighted. Smaller values of μ give more importance to recent observations [80].
An approximation of the memory length (in time samples) is

$$\frac{1}{1-\mu} \tag{4.22}$$

In this Chapter, we chose $\mu = 0.95$, ie. the corresponding memory length is approximately $1/(1 - 0.95) = 20$ time samples, or 100 minutes.
This model structure allows for a personalized stochastic model description.

4.3.4 Realization and predictions

The ARIMAX model (4.8) and the ARMAX model (4.16) may be represented as a discrete-time state space model in innovation form

$$x_{k+1} = Ax_k + Bu_k + K\varepsilon_k \tag{4.23a}$$
$$y_k = Cx_k + \varepsilon_k \tag{4.23b}$$

The observer canonical realization for the ARMAX model (4.16) is

$$A = \begin{bmatrix} -a_1 & 1 \\ -a_2 & 0 \end{bmatrix} B = \begin{bmatrix} b_1 \\ b_2 \end{bmatrix} K = \begin{bmatrix} c_1 - a_1 \\ c_2 - a_2 \end{bmatrix}$$
$$C = \begin{bmatrix} 1 & 0 \end{bmatrix}$$

and the observer canonical realization for the ARIMAX model (4.8) is

$$A = \begin{bmatrix} 1-a_1 & 1 & 0 \\ a_1-a_2 & 0 & 1 \\ a_2 & 0 & 0 \end{bmatrix} B = \begin{bmatrix} b_1 \\ b_2-b_1 \\ -b_2 \end{bmatrix} K = \begin{bmatrix} c_1+1-a_1 \\ c_2+a_1-a_2 \\ c_3+a_2 \end{bmatrix}$$
$$C = \begin{bmatrix} 1 & 0 & 0 \end{bmatrix}$$

The innovation of (4.23) is

$$e_k = y_k - C\hat{x}_{k|k-1} \tag{4.24}$$

and the corresponding predictions are [81]

$$\hat{x}_{k+1|k} = A\hat{x}_{k|k-1} + B\hat{u}_{k|k} + Ke_k \tag{4.25a}$$
$$\hat{x}_{k+1+j|k} = A\hat{x}_{k+j|k} + B\hat{u}_{k+j|k}, \quad j = 1, \ldots, N-1 \tag{4.25b}$$
$$\hat{y}_{k+j|k} = C\hat{x}_{k+j|k}, \qquad j = 1, \ldots, N \tag{4.25c}$$

The innovation (4.24) and the predictions (4.25) constitute the feedback and the predictions in the model predictive controller.

4.4 Model Predictive Control

Control algorithms for glucose regulation in people with type 1 diabetes must be able to handle intra- and inter-patient variability. In addition, the controller must administrate insulin in a safe way to minimize the risk of hypoglycemia. Due to the nonlinearity in the glucose-insulin interaction, the risk of hypoglycemic episodes as consequence of too much insulin is particularly prominent.
In this section we describe an MPC formulation with soft output constraints and hard input constraints. This formulation is based on the individualized prediction model for glucose computed in Section 4.3.2. Along with other features, we introduce a modified time-varying reference signal to robustify the controller and mitigate the effect of glucose-insulin nonlinearities and model-plant mismatch in the controller action.

The MPC algorithm computes the insulin dose by solution of an open-loop optimal control problem. Only the control action corresponding to the first sample interval is implemented and the process is repeated at the next sample interval. This is called a moving horizon implementation. The innovation (4.24) provides feedback from the CGM, y_k, and the open-loop optimal control problem solved in each sample interval is the convex quadratic program

$$\min_{\{\hat{u}_{k+j|k},\hat{v}_{k+j+1|k}\}_{j=0}^{N-1}} \phi \tag{4.26a}$$

$$s.t. \quad (4.25) \tag{4.26b}$$

$$u_{\min} \leq \hat{u}_{k+j|k} \leq u_{\max} \tag{4.26c}$$

$$\hat{y}_{k+j+1|k} \geq y_{\min} - \hat{v}_{k+j+1|k} \tag{4.26d}$$

$$\hat{v}_{k+j+1|k} \geq 0 \tag{4.26e}$$

with the objective function ϕ defined as

$$\begin{aligned}\phi =& \frac{1}{2}\sum_{j=0}^{N-1} \|\hat{y}_{k+j+1|k} - \hat{r}_{k+j+1|k}\|_2^2 \\ &+ \lambda\|\Delta\hat{u}_{k+j|k}\|_2^2 + \kappa\|\hat{v}_{k+j+1|k}\|_2^2\end{aligned} \tag{4.27}$$

N is the control and prediction horizon. We choose a prediction horizon equivalent to 10 hours, such that the insulin profile of the finite horizon optimal control problem (4.26) is similar to the insulin profile of the infinite horizon optimal control problem, (4.26) with $N \to \infty$. $\|\hat{y}_{k+j+1|k} - \hat{r}_{k+j+1|k}\|_2^2$ penalizes glucose deviation from the time-varying glucose setpoint and aims to drive the glucose concentration to 6 mmol/L. $\lambda\|\Delta u_{k+j|k}\|_2^2$ is a regularization term that prevents the insulin infusion rate from varying too aggressively. For the simulations and the in vivo clinical studies we set $\lambda = 100/u_{ss}^2$. The soft output constraint (4.26d) penalizes glucose values below 4 mmol/L. Since hypoglycemia is highly undesirable, we choose the weight on the soft output constraint to be rather high, i.e. $\kappa = 100$. The penalty function profile is illustrated in Fig. 4.4.

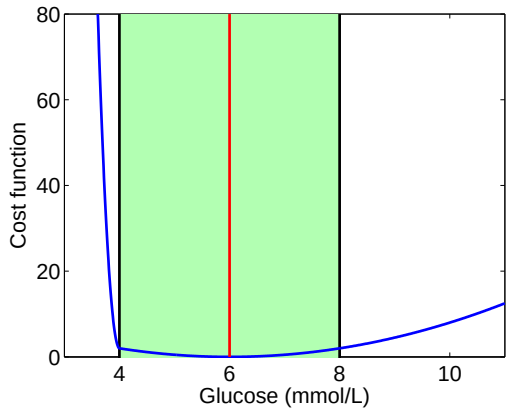

Figure 4.4: The penalty function $\rho = \|y - r\|_2^2 + \kappa \| \min\{y - y_{\min}, 0\}\|_2^2$.

To guard against model-plant mismatch we modify the maximal allowable insulin injection, $u_{\max}$, and let it depend on the current glucose concentration. If the glucose concentration is low (below the target of 6 mmol/L), we prevent the controller from taking future hyperglycemia into account by restricting the maximal insulin injection. If the glucose concentration is high (4 mmol/L above the target) we increase the maximal allowable insulin injection rate. In the range 0 - 4 mmol/L above target we allow the controller to double the basal insulin injection rate. These considerations lead to

$$u_{\max} = \begin{cases} 1.5u_{ss} & 4 \leq y_k \leq \infty \\ u_{ss} & 0 \leq y_k \leq 4 \\ 0.5u_{ss} & -\infty \leq y_k \leq 0 \end{cases} \tag{4.28}$$

in which u_{ss} is the basal insulin infusion rate. Due to pump restrictions, the minimum insulin injection rate, $u_{\min}$, is a low value but not exactly zero.

[17] and [79] use a time-varying glucose reference signal to robustify the controller and reduce the risk of hypoglycemic events. In this paper, we use an

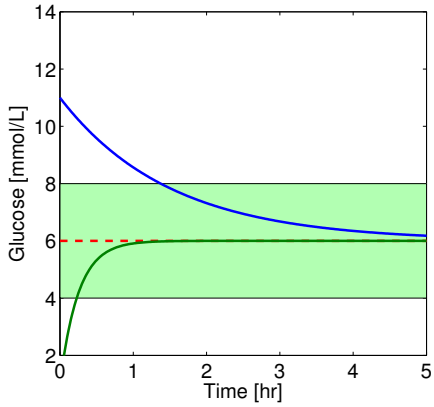

Figure 4.5: Time-varying reference signals for glucose above (blue curve) and below (green curve) the target of 6 mmol/L.

asymmetric time-varying glucose reference signal. The idea of the asymmetric reference signal is to induce safe insulin injections in hyperglycemic periods and fast recovery in hypoglycemic and below target periods. The asymmetric time-varying setpoint is given by

$$\hat{r}_{k+j|k}(t) = \begin{cases} y_k \exp\left(-t_j/\tau_r^+\right) & y_k \geq 0 \\ y_k \exp\left(-t_j/\tau_r^-\right) & y_k < 0 \end{cases} \tag{4.29}$$

Since we want to avoid hypoglycemia, we make the controller react more aggressively if the blood glucose level is below 6 mmol/L, so we choose $\tau_r^- = 15$ min and $\tau_r^+ = 90$ min. Fig 4.5 provides an illustration of the time-varying reference signal.

4.5 Result of clinical studies

In this section we present results from simulations on virtual patients and the clinical studies performed on real patients with type 1 diabetes.

4.5.1 Test of the controller on a virtual clinic

In this section we discuss the performance of the MPC for a randomly generated cohort of 100 patients. The 100 patients are generated from the probability distribution presented in Chapter 2. We compare the performance of the controller with simulated conventional insulin therapy in which the basal insulin infusion rate remains constant during the night. The change in insulin sensitivity is simulated by a step change in the insulin sensitivity parameters of the Hovorka model. We provide glucose and insulin profiles for a test clinical study using the MPC controller and the setup presented in Section 4.1.
The clinical protocol for the 100 in silico patients is:

- The patient arrives at the clinic at 17:00. The Kalman filter starts.
- The patient gets a 75 g CHO dinner and an insulin bolus at 18:00.
- The closed loop starts at 22:00. The regulator of the MPC starts.
- The insulin sensitivity is modified by ±30% at 01:00.
- The patient gets a 60 g CHO breakfast and an insulin bolus at 08:00. The controller is switched off.

The MPC is individualized using the insulin basal rate (u_{ss}), the insulin sensitivity factor (ISF), and the insulin action time for each virtual patient. In the virtual clinic these numbers are computed from an impulse response starting at a steady state. The meal boluses are determined using a bolus calculator similar to the one presented in Paper E. The glucose is provided to the controller every 5 minutes by a noise-corrupted CGM. The pump insulin infusion rate is changed every 5 minutes.
Fig. 4.6 shows the control variability grid analysis (CVGA) of the period between 22:00 and 08:00 for the case without MPC (white circles) and the case with MPC (black circles). In Fig. 4.6(a) we depict the case where the insulin sensitivity is increased by 30%, and in Fig. 4.6(b) we depict the case where the insulin sensitivity is decreased by 30%. These figures show that

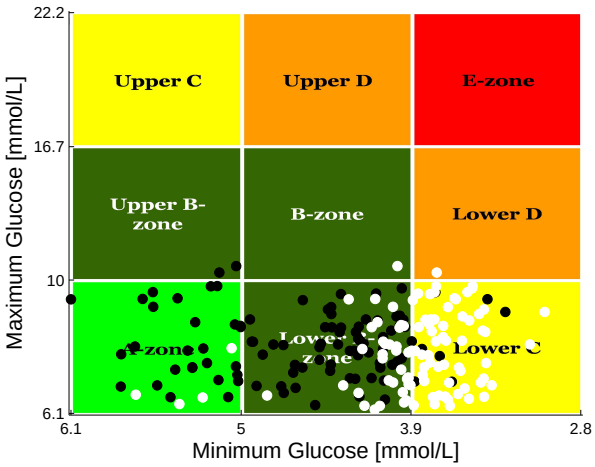

(a) Insulin sensitivity increases by 30%.

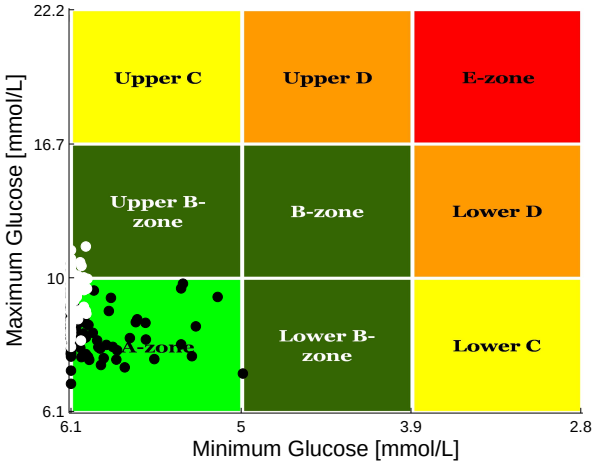

(b) Insulin sensitivity decreases by 30%.

Figure 4.6: CVGA ([82]) plot of the 100 in silico patients. White: Without MPC. Black: With MPC.

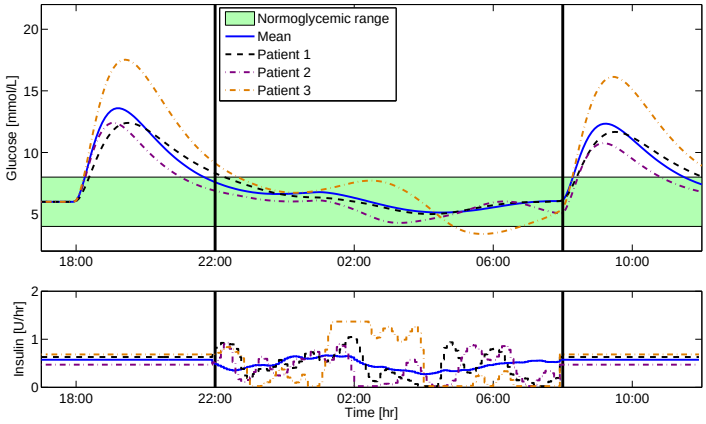

(a) Insulin sensitivity increases by 30%.

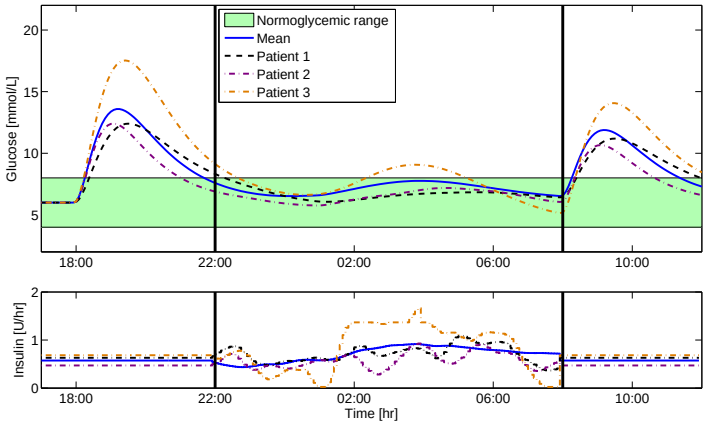

(b) Insulin sensitivity decreases by 30%.

Figure 4.7: Glucose and insulin profiles for 3 representative patients.

Table 4.1: Evaluation of the MPC versus constant insulin infusion rate in the case where the insulin sensitivity decreases by 30% during the night.

Glucose (mmol/L)	w/o. MPC	w. MPC
$G > 10$	2.1	<0.1
$G > 8$	30.7	13
$3.9 \leq G \leq 10$	97.9	100
$3.9 \leq G \leq 8$	69.3	87
$G < 3.9$	0	0
$G < 3.5$	0	0

our control algorithm reduces the risk of nocturnal hypoglycemia. Although the improvement is less significant, they also show that it can slightly reduce the risk of nocturnal hyperglycemia.
In the case where insulin sensitivity is increased by 30% (Fig. 4.6(a)), mild hypoglycemic events occur for some of the patients. However, almost no severe hypoglycemia (i.e. blood glucose concentrations below 3.5 mmol/L) is observed, and the choice of the tuning parameters in the controller allows for a fast recovery. In the case where insulin sensitivity is decreased by 30% (Fig. 4.6(b)), all the patients are well controlled during the study period.
Fig. 4.7 depicts the mean blood glucose and insulin profiles, along with blood glucose and insulin profiles for 3 representative patients. It shows a well-controlled patient (black curve), a decently controlled patient (purple curve) and a badly controlled patient (red curve), both in the case where insulin sensitivity increases (Fig. 4.7(a)) and in the case where insulin sensitivity decreases (Fig. 4.7(b)).
Table 4.1 and Table 4.2 provide the percentage of time spent in the period between 22:00 and 08:00 for the 100 simulated patients within range (3.9-10 mmol/L), in hyperglycemia(>10 mmol/L), in slight hypoglycemia(between 3.5 and 3.9 mmol/L) and in severe hypoglycemia (<3.5 mmol/L). This table show that MPC reduces the risk of hyperglycemia and significantly reduces the time spent in hypoglycemia in the case where the insulin sensitivity increases during the night.

Table 4.2: Evaluation of the MPC versus constant insulin infusion rate in the case where the insulin sensitivity increases by 30% during the night.

Glucose (mmol/L)	w/o. MPC	w. MPC
$G > 10$	<0.1	<0.1
$G > 8$	2.2	3.2
$3.9 \leq G \leq 10$	83.5	99.1
$3.9 \leq G \leq 8$	81.3	95.9
$G < 3.9$	16.5	0.9
$G < 3.5$	2.4	0.2

4.5.2 In vivo validation

We summarize here the main outcomes from the clinical studies conducted at Hvidovre Hospital. All study plots are available in Appendix A. In these studies, we used the ARIMAX controller design presented in 4.3.1. We compare closed-loop studies where the full meal bolus is administrated at mealtime, studies where half of the meal bolus is administrated at mealtime and studies where no meal bolus is administrated.

Fig. 4.8 shows the glucose and insulin profiles in a case where the CGM remains accurate during the study night. In this case, the controller is able to stabilize the glucose in the euglycemic range.

Fig. 4.9 illustrates a case where the CGM is not correctly calibrated. In this study, the self-monitoring of blood glucose (SMBG) underestimated the blood glucose value by 2-3 mmol/L. Although the CGM profile is correctly controlled, the YSI measurements are above the euglycemic range.

Fig. 4.10 illustrates a case where the CGM deviates from the YSI value. In this study night, the inaccuracy and malfunction of the sensor is not detected by the controller as we in the present controller have no monitoring and fault detection layer. Therefore, the controller uses the very inaccuraty glucose signal from the CGM. Accordingly, the patient was improperly controlled during this study night. or this study, detection of outliers such as an hypothesis test similar to the one provided in [79] may help for improving the controller. However, the consequence of bad sensors like this

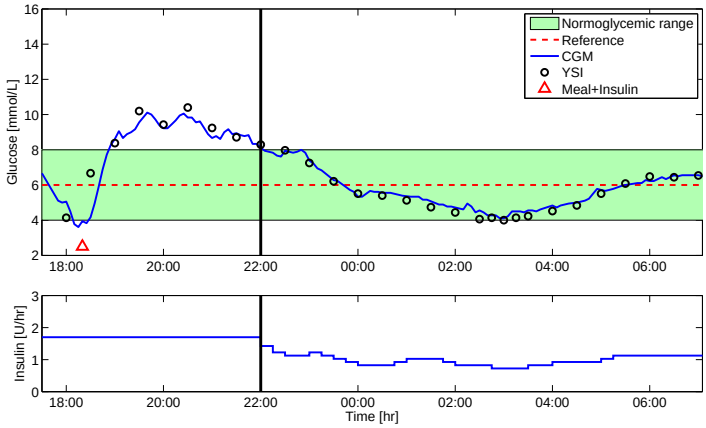

Figure 4.8: Glucose and insulin profiles for the study 11MMCLDouble.

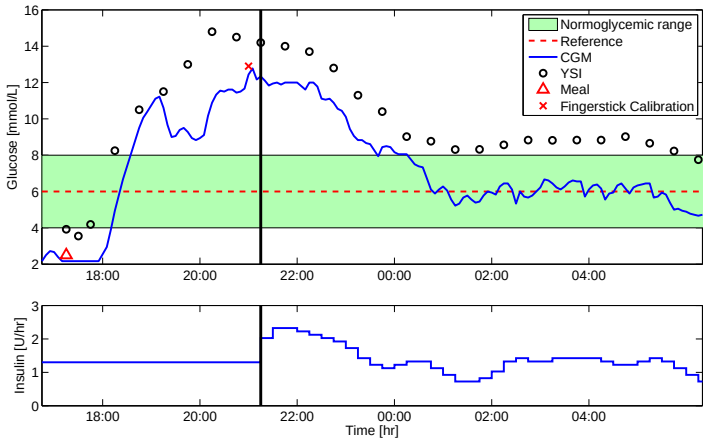

Figure 4.9: Glucose and insulin profiles for the study 09DKCL00.

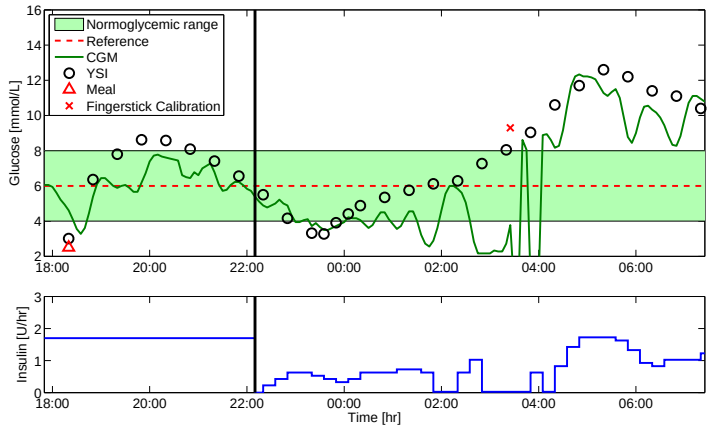

Figure 4.10: Glucose and insulin profiles for the study 11MMCL00.

will likely only be fully mitigated when redundant sensors are available. In such situations of sensor failure, a monitoring and fault detection layer may decide to suspend all insulin delivery and send an alarm. Also, it can be noticed that the closed-loop starts at approximately 21:00 instead of 22:00. This is due to the fact that the closed-loop starts 4 hours after the dinner. In this study, the patient had the meal before 18:00.

Fig. 4.11 provides the CVGA plot for the studies where the controller was used. The figure shows both the CGM and the YSI values for the 18 closed-loop studies and the YSI values for the 5 open-loop studies.

Table 4.3 shows the time spent inside and outside target for the 17 closed-loop studies. For comparison, results for a similar study have been published in [83].

The study plots in Appendix A show that the controller was able to stabilize the blood glucose concentration in the euglycemic range when the feedback from the CGM is accurate. However, it is also clear by these clinical studies that the limited accuracy and reliability of the current generation of CGM technology prevents routinely and unsupervised use of closed-loop glucose

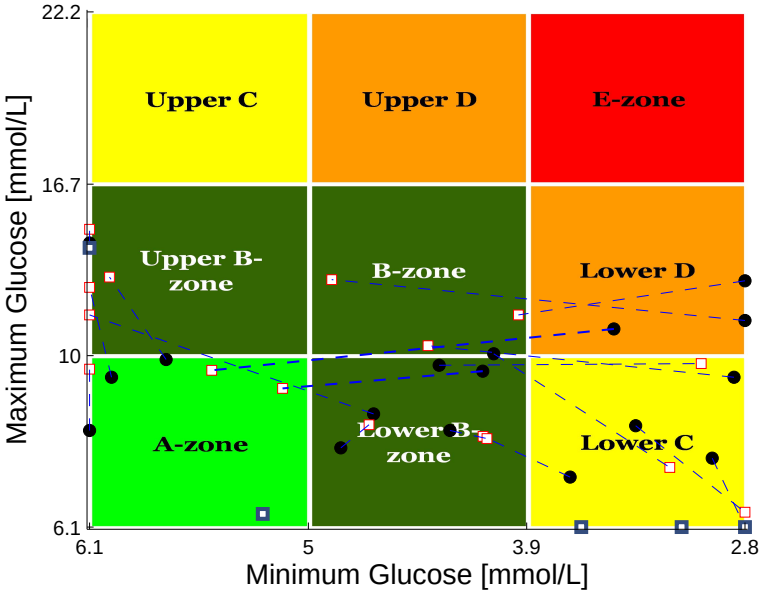

Figure 4.11: Control Variability Grid Analysis (CVGA) plot for the in vivo closed-loop studies. Black circles: CGM (Closed-loop studies). Red squares: YSI (Closed-loop studies). Blue squares: YSI (Open-loop studies)

control.

4.6 Comparison between ARIMAX, ARMAX and adaptive ARMAX model structures

In this section we compare three different versions of our Model Predictive Controller on a cohort of 100 virtual patients. These three versions are the ARIMAX formulation presented in Section 4.3.1, the ARMAX formulation presented in Section 4.3.2 and the adaptive ARMAX model formulation.

Table 4.3: Evaluation of the controller for the different bolus sizes (100% of the ideal bolus size, 50% of the ideal bolus size, unbolused meals). The number into brackets represent the number of available study nights for each category.

Glucose (mmol/L)	100% (6)	50% (5)	0% (6)	Overall (17)
$G > 10$	0.2	11.0	32.1	14.1
$G > 8$	10.8	29.0	53.7	30.6
$3.9 \leq G \leq 10$	91.1	82.1	61.1	78.4
$3.9 \leq G \leq 8$	80.4	64.0	39.5	61.8
$G < 3.9$	8.8	6.9	6.8	7.6
$G < 3.5$	3.7	5.2	3.5	4.1

The ARMAX based controllers do not contain an integrator and cannot guarantee steady-state offset-free control. However, the tuning of the MPC based ARMAX models may be simpler than the tuning of the MPC based on the ARIMAX model. The reason is that no artificial model-plant mismatch is introduced in the MPC based on ARMAX models, while the ARIMAX based controller deliberately include such a mismatch to ensure steady-state offset-free control.

4.6.1 Underbolused meal

Fig. 4.12 shows the CVGA plot for the three different strategies in the case where only 50% of the meal bolus is administrated at mealtime. The control strategy based on an ARIMAX model shows several cases of mild hypoglycemia due to an insulin overdose. The two control strategies based on an ARMAX model are able to avoid this undershoot. Fig. 4.13 illustrates an example of glucose and insulin profiles for the same patient using the three different control strategies.
Table 4.4 shows the time spent in the euglycemic range, hypoglycemia and hyperglycemia for the three different strategies in the case where only 50% of the meal bolus is administrated at mealtime. The results show that the control strategy based on an ARIMAX model structure reduce the time

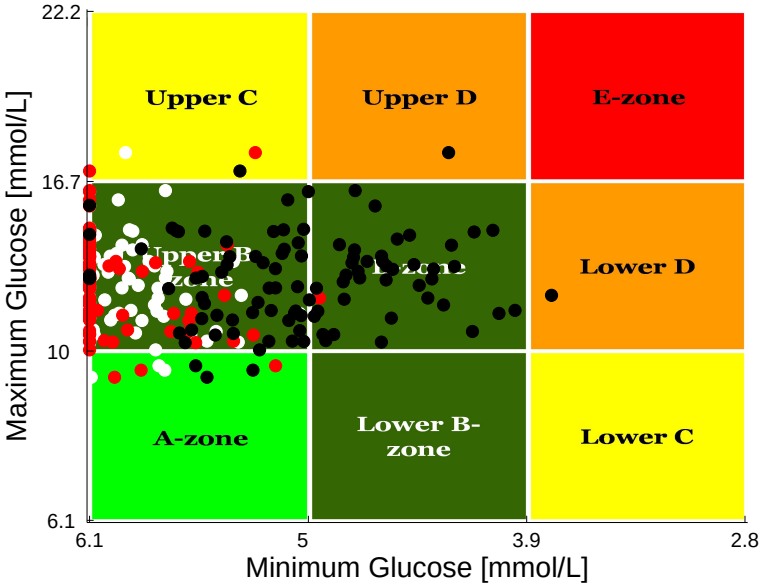

Figure 4.12: Control Variability Grid Analysis (CVGA) plot for the three different stochastic model structures. 50% of the meal bolus is administrated at mealtime. Black: ARIMAX. Red: ARMAX. White: Adaptive ARMAX.

spent in hyperglycemia. The adaptive ARMAX model structure shows the best compromise between the time spent in euglycemia and safety concerning the risk of insulin overdose.

4.6.2 Change in insulin sensitivity

Fig. 4.14 shows the CVGA plot for the three different strategies for the case where the insulin sensitivity is increased by 30% during the night. Table 4.5 shows the time spent in the euglycemic range, hypoglycemia and hyperglycemia for the three different strategies in the case where the insulin

Table 4.4: Evaluation of the controller for the different control strategies in the case where only 50% of the meal bolus is administrated at mealtime. The numbers show the total percentage of time spent in different glucose ranges for the 100 virtual patients during the period 22:00 - 08:00.

Glucose (mmol/L)	ARIMAX	ARMAX	Adaptive ARMAX
$G > 10$	17.8	23.9	20.8
$G > 8$	31.6	58.1	42.2
$3.9 \leq G \leq 10$	82.1	76.1	79.2
$3.9 \leq G \leq 8$	68.3	41.9	57.8
$G < 3.9$	0.1	0	0
$G < 3.5$	0	0	0

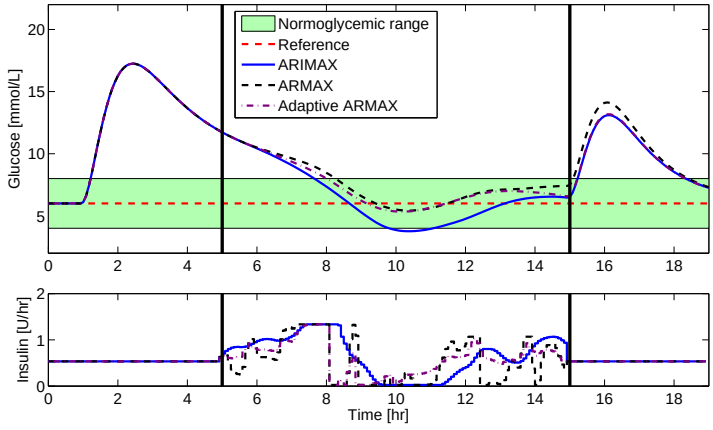

Figure 4.13: Glucose and insulin profiles of a specific patient for the different control strategies. The patients gets half of the optimal bolus at mealtime.

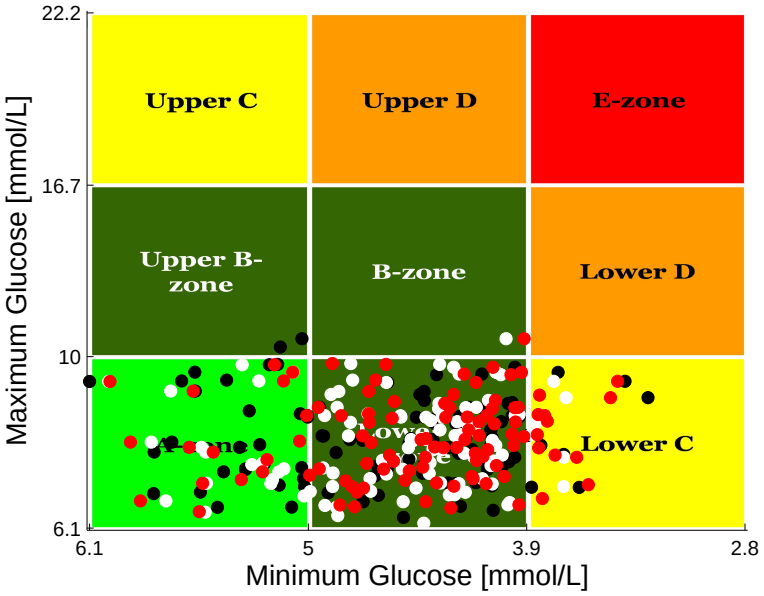

Figure 4.14: Control Variability Grid Analysis (CVGA) plot for the three different stochastic model structures in the case where the insulin sensitivity is increased by 30% during the night. Black: ARIMAX. Red: ARMAX. White: Adaptive ARMAX.

sensitivity is increased by 30% during the night. The control strategies based on an ARMAX model structure, i.e. the controllers without the integrator, reduces the occurrences of hypoglycemia, and avoid severe hypoglycemia (ie. glucose values below 3.5 mmol/L). Fig. 4.15 illustrates an example of glucose and insulin profiles for the same patient using the three different control strategies.

Table 4.5: Evaluation of the controller for the different control strategies in the case where the insulin sensitivity is increased by 30% during the night. The numbers show the total percentage of time spent in different glucose ranges for the 100 virtual patients during the period 22:00 - 08:00.

Glucose (mmol/L)	ARIMAX	ARMAX	Adaptive ARMAX
$G > 10$	<0.1	<0.1	<0.1
$G > 8$	3.2	2.5	2.2
$3.9 \leq G \leq 10$	99.1	99.4	99.7
$3.9 \leq G \leq 8$	95.9	96.9	97.5
$G < 3.9$	0.9	0.6	0.3
$G < 3.5$	0.2	0	0

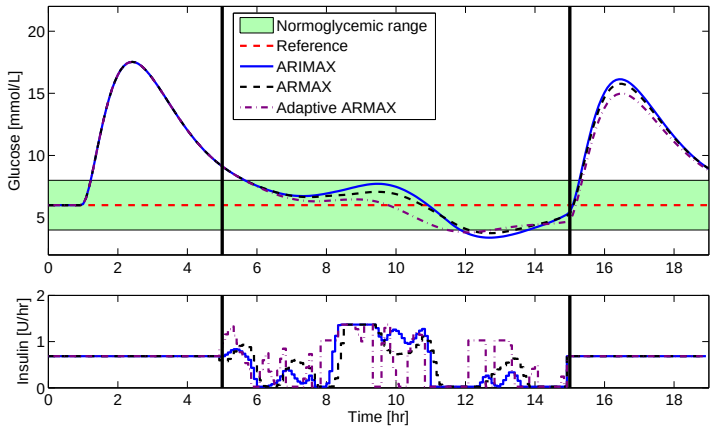

Figure 4.15: Glucose and insulin profiles of a specific patient for the different control strategies. The insulin sensitivity increases by 30% during the night.

4.7 Summary

The main advantage of the presented method is its simplicity. The use of safety layers and a robust MPC formulation reduces the risk of hypoglycemia. Therefore, the method presented in this Chapter can easily be reproduced or modified.
The results of the clinical studies suggest that the main limitation of the artificial pancreas is currently the lack of accuracy of CGMs. Consequently, a detection of outliers and an improved robustness of the controller could help to handle the CGM inaccuracy. However, such methods will likely only be sufficiently robust and safe when the glucose concentration is measured by redundant sensors.
The choice of the model structure for the stochastic part is a tradeoff between offset-free control and model-plant mismatch. In our case, the adaptive ARMAX formulation presented in this chapter has the potential to improve the controller performance, but would need a further investigation before being tested on real patients.

CHAPTER 5

Conclusion

This thesis illustrates the design and implementation of both linear and nonlinear model predictive control-based strategies for blood glucose in people with type 1 diabetes. The main contributions of this thesis are summarized below.

- We have developed a virtual clinic that can be used to evaluate and screen insulin administration strategies. The virtual clinic uses a modified version of the Hovorka model to simulate a large population of people with type 1 diabetes. The model consists of a subsystem modeling the glucose-insulin dynamics, a subsystem modeling the sc. insulin absorption, a subsystem modeling the meal absorption and a subsystem modeling a noise-corrupted CGM. We use the parameter distribution published by *Hovorka et al.* to generate a cohort of people with type 1 diabetes.
- We have implemented Nonlinear Model Predictive Control (NMPC). We have used a multiple-shooting algorithm to solve the optimal control problem (OCP) and an explicit Runge-Kutta method (DOPRI54) with an adaptive step size for numerical integration and sensitivity

computation. The OCP is solved using a Quasi-Newton sequential quadratic programming (SQP) with line search and a BFGS update for the Hessian of the Lagrangian. We have used this controller to generate optimal blood glucose and insulin profiles in the cases where the meals are announced in advance, and where meals are announced at mealtimes. We also apply a Continuous-Discrete Extended Kalman Filter (CDEKF) in order to simulate cases where the meal size is uncertain, or even unannounced. The numerical simulations demonstrate that a pen may give similar performance to a pump.

- We have developed linear model predictive controllers based on ARMAX type of models. We have proposed a simple and systematic way of computing model parameters based on a priori known patient information. The required patient information are the insulin sensitivity factor (ISF), the insulin action time and the basal insulin infusion rate. We discussed three alternatives for the stochastic part of our model. The three resulting controllers are tested on virtual patients, and their performance is assessed.

- We have validated our control strategy on real patients with type 1 diabetes. We have tested the ability of our controller to stabilize the glucose overnight. The simulations on virtual patients and the clinical studies on real patients show that the current lack of accuracy of the CGMs is the main limitation of the artificial pancreas.

Future possible research directions may include

- Model identification from another physiological model. The Medtronic Virtual Patient (MVP) model or any model identified from previously collected clinical data could be used to generate a population of people with type 1 diabetes [45].

- Test of adaptive NMPC on virtual patients. The model used for the controller can be for example the Medtronic Virtual Patient (MVP) model.

- Improvements of the control strategy for clinical studies on real patients. The replacement of the ARIMAX model structure with an adaptive ARMAX model structure presented in Chapter 4 and the detection of CGM outliers may improve the controller performance. Also, a monitoring layer to adjust the basal insulin comparable to run-to-run control pioneered by Palerm et al. can achieve offset-free control [84].
- Further clinical studies. The purpose of these clinical studies would be to validate the possible improvements presented in Chapter 4.

Bibliography

[1] B. W. Bequette. A critical assessment of algorithms and challenges in the development of a closed-loop artificial pancreas. *Diabetes Technology and Therapeutics*, 7:28 – 47, 2005.

[2] J. Shaw, R. Sicree, and P. Zimmet. Global estimates of the prevalence of diabetes for 2010 and 2030. *Diabetes Research and Clinical Practice*, 87:4 – 14, 2010.

[3] P. Zhang, X. Zhang, J. Brown, D. Vistisen, R. Sicree, J. Shaw, and G. Nichols. Global healthcare expenditure on diabetes for 2010 and 2030. *Diabetes Research and Clinical Practice*, 87:293 – 301, 2010.

[4] Diabetes Foreningen. Facts about type 1 diabetes, 2012. Website: http://www.diabetes.dk/English/Facts_about_Diabetes_in_Denmark/Type_1_diabetes.aspx.

[5] R. M. Bergenstal, W. V. Tamborlane, A. Ahmann, J. B. Buse, G. Dailey, S. N. Davis, C. Joyce, T. Peoples, B. A. Perkins, J. B. Welsh, S. M. Willi, and M. A. Wood. Effectiveness of sensor-augmented insulin-pump therapy in type 1 diabetes. *New England Journal of Medicine*, 363:311 – 320, 2010.

[6] A. H. Kadish. Automation control of blood sugar. I. a servomechanism for glucose monitoring and control. *American Journal of Medical Electronics*, 3:82 – 86, 1964.

[7] A. Albisser, B. Leibel, T. Ewart, Z. Davidovac, C. Botz, and W. Zingg. An artificial endocrine pancreas. *Diabetes*, 23:389 – 396, 1974.

[8] E. Pfeiffer, C. Thum, and A. Clemens. The artificial beta cell - a continuous control of blood sugar by external regulation of insulin infusion (glucose controller insulin infusion system). *Hormone and Metabolic Research*, 6(5):339 – 342, 1974.

[9] R. Hovorka, M. E. Wilinska, L. J. Chassin, and D. B. Dunger. Roadmap to the artificial pancreas. *Diabetes Research and Clinical Practice*, 74:178 – 182, 2006.

[10] C. Cobelli, C. Dalla Man, G. Sparacino, L. Magni, G. De Nicolao, and B. P. Kovatchev. Diabetes: Models, signals, and control. *IEEE Reviews in Biomedical Engineering*, 2:54–96, 2009.

[11] C. Cobelli, E. Renard, and B. Kovatchev. Artificial pancreas: past, present, future. *Diabetes*, 60:2672 – 2682, 2011.

[12] G. De Nicolao, L. Magni, C. Dalla Man, and C. Cobelli. Modeling and control of diabetes: Towards the artificial pancreas. In *Preprints of the 18th IFAC World Congress*, pages 7092 – 7101, 2011.

[13] G. Marchetti, M. Barolo, L. Jovanovič, H. Zisser, and D. E. Seborg. An improved PID switching control strategy for type 1 diabetes. In *2006 International Conference of the IEEE Engineering in Medicine and Biology Society*, pages 5041–5044, New York City, USA, 2006.

[14] S.A. Weinzimer, G.M. Steil, K.L. Swan, J. Dziura, N. Kurtz, and W.V. Tamborlane. Fully automated closed-loop insulin delivery versus semi-automated hybrid control in pediatric patients with type 1 diabetes using an artificial pancreas. *Diabetes Care*, 31(5):934 – 939, 2008.

[15] E. Dassau, C.C. Palerm, H. Zisser, B.A. Buckingham, L. Jovanovič, , and F.J. Doyle III. In silico evaluation platform for artificial pancreatic beta-cell development - a dynamic simulator for closed-loop con-

trol with hardware-in-the-loop. *Diabetes Technology and Therapeutics*, 11(3):187 – 194, 2009.

[16] L. Magni, D. M. Raimondo, L. Bossi, C. Dalla Man, G. De Nicolao, B. Kovatchev, and C. Cobelli. Model predictive control of type 1 diabetes: An *in silico* trial. *Journal of Diabetes Science and Technology*, 1:804–812, 2007.

[17] W. Garcia-Gabin, J. Vehí, J. Bondia, C. Tarín, and R. Calm. Robust sliding mode closed-loop glucose control with meal compensation in type 1 diabetes mellitus. In *Proceedings of the 17th World Congress, The International Federation of Automatic Control*, pages 4240 – 4245, 2008.

[18] R. Mauseth, Y. Wang, E. Dassau, R. Kircher, D. Matheson Jr., H. Zisser, L. Jovanovič, , and F.J. Doyle III. Proposed clinical application for tuning fuzzy logic controller of artificial pancreas utilizing a personalization factor. *Journal of Diabetes Science and Technology*, 4(4):913–922, 2010.

[19] E. Atlas, R. Nimri, S. Miller, E.A. Grunberg, and M. Phillip. Md-logic artificial pancreas system: a pilot study in adults with type 1 diabetes. *Diabetes Care*, 33(4):1072–1076, 2010.

[20] L. Kovács, P. Szalay, B. Benyó, and J.G. Chase. Robust tight glycaemic control of icu patients. In *Proceedings of the 17th World Congress, The International Federation of Automatic Control*, pages 4995 – 5000, 2011.

[21] H. Thabit and R. Hovorka. Closed-loop insulin delivery in type 1 diabetes. *Endocrinology Metabolism Clinics of North America*, 41:105 – 117, 2012.

[22] R. Hovorka. Continuous glucose monitoring and closed-loop systems. *Diabetic Medicine*, 23:1 – 12, 2005.

[23] G. M. Steil and K. Rebrin. Closed-loop insulin delivery - what lies between where we are and where we are going. *Expert Opinion on Drug Delivery*, 2(2):353 – 362, 2005.

[24] D. B. Keenan, R. Cartaya, and J. J. Mastrototaro. Accuracy of a new real-time continuous glucose monitoring algorithm. *Journal of Diabetes Science and Technology*, 4(1):111 – 118, 2010.

[25] S. Guerra, A. Facchinetti, G. Sparacino, G. De Nicolao, and C. Cobelli. Enhancing the accuracy of subcutaneous glucose sensors: A real-time deconvolution-based approach. *IEEE transactions on biomedical engineering*, 59(6):1658 – 1669, 2012.

[26] K. Rebrin, N. F. Sheppard Jr., and G. M. Steil. Use of subcutaneous interstitial fluid glucose to estimate blood glucose: Revisiting delay and sensor offset. *Journal of Diabetes Science and Technology*, 4(5):1087 – 1098, 2010.

[27] I. Raz, R. Weiss, Y. Yegorchikov, G. Bitton, R. Nagar, and B. Pesach. Effect of a local heating device on insulin and glucose pharmacokinetic profiles in an opel-label, randomised, two-period, one-way crossover study in patients with type 1 diabetes using continuous subcutaneous insulin infusion. *Clinical Therapeutics*, 31:980 – 987, 2009.

[28] E. Renard, J. Place, M. Cantwell, H. Chevassus, and C. C. Palerm. Closed-loop insulin delivery using a subcutaneous glucose sensor and intraperitoneal insulin delivery: feasibility study testing a new model for the artificial pancreas. *Diabetes Care*, 33:121 – 127, 2010.

[29] J. R. Castle, K. C. J. Yuen, J. M. Engle, R. Kagan, J. El youssef, W. K. Ward, and R. G. Massoud. Novel use of glucagon in a closed-loop system for prevention of hypoglycemia in type 1 diabetes. *Diabetes Care*, 33(6):1282 – 1287, 2010.

[30] W. K. Ward, J. R. Castle, and J. El Youssef. Safe glycemic management during closed-loop treatment of type 1 diabetes: the role of

glucagon, use of multiple sensors, and compensation for stress hyperglycemia. *Journal of Diabetes Science and Technology*, 5(6):1373 – 1380, 2011.

[31] B. C. Turner, E. Jenkins, D. Kerr, R. S. Sherwin, and D. A. Cavan. The effect of evening alcohol consumption on next-morning glucose control in type 1 diabetes. *Diabetes Care*, 24:1888 – 1893, 2001.

[32] S. J. Qin and T. A. Badgwell. A survey of industrial model predictive control technology. *Control Engineering Practice*, 11:733 – 764, 2003.

[33] L. Magni, D. M. Raimondo, C. Dalla Man, G. De Nicolao, B. P. Kovatchev, and C. Cobelli. Model predictive control of glucose concentration in type I diabetic patients: An in silico trial. *Biomedical Signal Processing and Control*, 4(4):338–346, 2009.

[34] R. Hovorka, K. Kumareswaran, J. Harris, J. M. Allen, D. Elleri, D. Xing, C. Kollman, M. Nodale, H. R. Murphy, D. B. Dunger, S. A. Amiel, S. R. Heller, M. E. Wilinska, and M. L. Evans. Overnight closed loop insulin delivery (artificial pancreas) in adults with type 1 diabetes: crossover randomised controlled studies. *British Medical Journal*, (342):d1855, 2011.

[35] R. N. Bergman, L. S. Phillips, and C. Cobelli. Physiologic evaluation of factors controlling glucose tolerance in man: measurement of insulin sensitivity and beta-cell glucose sensitivity from the response to intravenous glucose. *Journal of Clinical Investigation*, 68(6):1456 – 1467, 1981.

[36] J. T. Sorensen. *A physiologic model of glucose metabolism in man and its use to design and assess improved insulin therapies for diabetes.* PhD thesis, Massachusetts Institute of Technology, 1985.

[37] R. S. Parker, F. J. Doyle III, J. H. Ward, and N. A. Peppas. Robust H_∞ glucose control in diabetes using a physiological model. *AIChE Journal*, 46(12):2537 – 2549, 2000.

[38] E. Ruiz-Velasquez, R. Femat, and D. U. Campos-Delgado. Blood glucose control for type 1 diabetes mellitus: a robust tracking H_∞ problem. *Control Engineering Practice*, 12:1170 – 1195, 2004.

[39] L. Kovács and B. Kulcsár. LPV modeling of type 1 diabetes mellitus. In *8th International Symposium of Humgarian Researchers on Computational Intelligence and Informatics*, 2007.

[40] C. Dalla Man, R. Rizza, and C. Cobelli. Meal simulation model of the glucose-insulin system. *IEEE Transactions on Biomedical Engineering*, 54(10):1740–1749, 2007.

[41] B. P. Kovatchev, M. Breton, C. Dalla Man, and C. Cobelli. In silico preclinical trials: A proof of concept in closed-loop control of type 1 diabetes. *Journal of Diabetes Science and Technology*, 3(1):44 – 55, 2009.

[42] H. Lee, B. A. Buckingham, D. M. Wilson, and W. Bequette. A closed-loop artificial pancreas using model predictive control and a sliding meal size estimator. *Journal of Diabetes Science and Technology*, 3:1082 – 1090, 2009.

[43] S. Miller, R. Nimri, E. Atlas, E. A. Grunberg, and M. Philip. Automatic learning algorithm for the MD-logic artificial pancreas system. *Diabetes technology and therapeutics*, 13(10):983 – 990, 2011.

[44] G. Campetelli, E. Musulin, M. S. Basualdo, and A. Rigalli. A novel index to evaluate the blood glucose controllability of type I diabetic patients. In *Preprints of the 18th IFAC world congress*, pages 14223 – 14228, Milano, Italy, 2011. IFAC 2011.

[45] S. S. Kanderian, S. Weinzimer, G. Voskanyan, and G. M. Steil. Identification of intraday metabolic profiles during closed-loop glucose control in individuals with type 1 diabetes. *Journal of Diabetes Science and Technology*, 3(5):1047 – 1057, 2009.

[46] R. Hovorka, V. Canonico, L. J. Chassin, U. Haueter, M. Massi-Benedetti, M. O. Federici, T. R. Pieber, H. C. Schaller, L. Schaupp, T. Vering, and M. E. Wilinska. Nonlinear model predictive control of glucose concentration in subjects with type 1 diabetes. *Physiological Measurement*, 25:905–920, 2004.

[47] M. E. Wilinska, L. J. Chassin, C. L. Acerini, J. M. Allen, D. B. Dunger, and R. Hovorka. Simulation environment to evaluate closed-loop insulin delivery systems in type 1 diabetes. *Journal of Diabetes Science and Technology*, 4(1):132 – 144, 2010.

[48] M. E. Wilinska and R. Hovorka. Simulation models for in silico testing of closed-loop glucose controllers in type I diabetes. *Drug Discovery Today: Disease Models*, 5(4):289 – 298, 2008.

[49] R. Hovorka, F. Shojaee-Moradie, P. V. Caroll, L. J. Chassin, I. J. Gowrie, N. C. Jackson, R. S. Tudor, A. M. Umpleby, and R. H. Jones. Partitioning glucose distribution/transport, disposal, and endogenous production during IVGTT. *Am. J. Physiol.*, 282:992–1007, 2002.

[50] J. D. Elashoff, T. J. Reedy, and J. H. Meyer. Analysis of gastric emptying data. *Gastroenterology*, 83:1306–1312, 1982.

[51] E. D. Lehmann and T. Deutsch. A physiological model of glucose-insulin interaction in type 1 diabetes mellitus. *Journal of Biomedical Engineering*, 14:235–242, 1992.

[52] C. Dalla Man, M. Camilleri, and C. Cobelli. A system model of oral glucose absorption: Validation on gold standard data. *IEEE Transactions on Biomedical Engineering*, 53:2472–2478, 2006.

[53] O. Goetze, A. Steingoetter, D. Menne, I. R. van der Voort, M. A. Kwiatek, P. Boesiger, D. Weishaupt, M. Thumshirn, M. Fried, and W. Schwizer. The effect of macronutrients on gastric volume responses and gastric emptying in humans: A magnetic resonance imaging study. *Am J Physiol Gastrointest Liver Physiol*, 292:G11–G17, 2007.

[54] M. Horowitz, D. O'Donovan, K. L. Jones, C. Feinle, C. K. Rayner, and M. Samsom. Gastric emptying in diabetes: Clinical significance and treatment. *Diabetic Medicine*, 19:177–194, 2002.

[55] M. E. Wilinska, L. J. Chassin, H. C. Schaller, L. Schaupp, T. R. Pieber, and R. Hovorka. Insulin kinetics in type 1 diabetes: Continuous and bolus delivery of rapid acting insulin. *IEEE Transactions on Biomedical Engineering*, 52:3–12, 2005.

[56] M. Breton and B. Kovatchev. Analysis, modeling, and simulation of the accuracy of continuous glucose sensors. *Journal of Diabetes Science and Technology*, 2:853–862, 2008.

[57] H.G. Bock and K.J. Plitt. A multiple shooting method for direct solution of optimal control problems. In *Proc. of the IFAC 9th World Congress*, pages 242–247, Budapest, Hungary, 1984.

[58] T. Binder, L. Blank, H. G. Bock, R. Burlisch, W. Damen, M. Diehl, T. K., W. Marquardt, J. P. Schlöder, and O. von Stryk. Introduction to model based optimization of chemical processes on moving horizons. In M. Grötschel, S. O. Krumke, and J. Rambau, editors, *Online Optimization of Large Scale Systems*, pages 295–339. Springer, Berlin, 2001.

[59] M. Diehl, J. Ferreau, and N. Haverbeke. Efficient numerical methods for nonlinear MPC and moving horizon estimation. In *Nonlinear Model Predictive Control. Towards New Challenging Applications*, pages 391–417. Springer, Berlin, Germany, 2009.

[60] C. V. Rao, S.J. Wright, and J. B. Rawlings. Application of interior-point methods to model predictive control. *Journal of Optimization Theory and Applications*, 99(3):723 – 757, 1998.

[61] J. B. Jørgensen. *Moving Horizon Estimation and Control*. PhD thesis, Department of Chemical Engineering, Technical University of Denmark, 2005.

[62] J. R. Dormand and P. J. Prince. A family of embedded runge-kutta formulae. *Journal of Computational and Applied Mathematics*, 6(1):19 – 26, 1980.

[63] J. C. Butcher. *Numerical Methods for Ordinary Differential Equations*. Wiley, Chichester, England, 2003.

[64] K. Gustafsson. *Control of Error and Convergence in ODE Solvers*. PhD thesis, Department of Automatic Control, Lund Institute of Technology, 1992.

[65] S. Mehrotra. On the implementation of a primal-dual interior point method. *SIAM Journal of Optimization*, 2(4):575–601, 1992.

[66] D. Boiroux. *Nonlinear Model Predictive Control for an Artificial Pancreas*. PhD thesis, DTU Informatics, Technical University of Denmark, 2009.

[67] A. H. Jazwinski. *Stochastic Processes and Filtering Theory*. Academic Press, San Diego, CA, 1970.

[68] M. Nørgaard, N. K. Poulsen, and O. Ravn. New developments in state estimation for nonlinear systems. *Automatica*, 36:1627–1638, 2000.

[69] J. B. Jørgensen, M. R. Kristensen, P. G. Thomsen, and H. Madsen. A numerically robust ESDIRK-based implementation of the continuous-discrete extended kalman filter. In *European Control Conference 2007*, Kos, Greece, 2007. ECC 2007.

[70] G. Pillonetto, G. Sparacino, and C. Cobelli. Numerical non-identifiability regions of the minimal model of glucose kinetics: superiority of bayesian estimation. *Mathematical Biosciences*, 184:53 – 67, 2003.

[71] H. Kirchsteiger, G. C. Estrada, S. Pölzer, E. Renard, and L. del Re. Estimating interval process models for type 1 diabetes for robust control design. In *Preprints of the 18th IFAC World Congress*, pages 11761 – 11766, 2011.

[72] K. van Heusden, E. Dassau, H. C. Zisser, D. E. Seborg, and F. J. Doyle III. Control-relevant models for glucose control using a priori patient characteristics. *IEEE transactions on biomedical engineering*, 59(7):1839 – 1849, 2012.

[73] M. W. Percival, W. C. Bevier, Y. Wang, E. Dassau, H Zisser, L. Jovanovič, and F. J. Doyle III. Modeling the effects of subcutaneous insulin administration and carbohydrate consumption on blood glucose. *Diabet Sci Technol*, 4(5):1214–1228, 2010.

[74] B. Wittenmark, K. J. Åström, and K.-E. Årzén. Computer control: An overview. In *IFAC Professional Brief*.

[75] J. K. Huusom, N. K. Poulsen, S. B. Jørgensen, and J. B. Jørgensen. Tuning SISO offset-free model predictive control based on ARX models. *Journal of Process Control*, 2012. Web-address: http://dx.doi.org/10.1016/j.jprocont.2012.08.007.

[76] A. K. Duun-Henriksen, D. Boiroux, S. Schmidt, K. Nørgaard, S. Madsbad, O. Skyggebjerg, P. R. Jensen, N. K. Poulsen, J. B. Jørgensen, and H. Madsen. Tuning of controller for type 1 diabetes treatment with stochastic differential equations. In *8th IFAC Symposium on Biological and Medical Systems*, Budapest, Hungary, 2012. BMS 2012.

[77] N. R. Kristensen, H. Madsen, and S. B. Jørgensen. Parameter estimation in stochastic grey-box models. *Automatica*, 40:225 – 237, 2004.

[78] J. B. Jørgensen and S. B. Jørgensen. Comparison of prediction-error modelling criteria. In *Proceedings of the 2007 American Control Conference (ACC 2007)*, pages 140–146, 2007.

[79] M. Eren-Oruklu, A. Cinar, L. Quinn, and D. Smith. Adaptive control strategy for regulation of blood glucose levels in patients with type 1 diabetes. *Journal of Process Control*, 19:1333 – 1346, 2009.

[80] J. K. Huusom, N. K. Poulsen, S. B. Jørgensen, and J. B. Jørgensen. Adaptive disturbance estimation for offset-free SISO model predictive

control. In *2011 American Control Conference on O'Farrell Street, San Francisco, CA, USA*, pages 2417–2422. ACC 2011, 2011.

[81] J. B. Jørgensen, J. K. Huusom, and J. B. Rawlings. Finite horizon MPC for systems in innovation form. In *50th IEEE Conference on Decision and Control and European Control Conference (CDC-ECC 2011)*, pages 1896 – 1903, 2011.

[82] L. Magni, D. Raimondo, C. Dalla Man, M. Breton, S. Patek, G. De Nicolao, C. Cobelli, and B. Kovatchev. Evaluating the efficacy of closed-loop glucose regulation via control-variability grid analysis. *Journal of Diabetes Science and Technology*, 2(4):630 – 635, 2008.

[83] B. P. Kovatchev, C. Cobelli, E. Renard, S. Anderson, M. Breton, S. Patek, W. Clarke, D. Bruttomesso, A. Maran, S. Costa, A. Avogaro, C. Dalla Man, A. Facchinetti, L. Magni, G. De Nicolao, J. Place, and A. Farret. Multinational study of subcutaneous model-predictive closed-loop control in type 1 diabetes mellitus: summary of the results. *Journal of Diabetes Science and Technology*, 4(6):1374 – 1381, 2010.

[84] L. Jovanovič C. C. Palerm, H. Zisser and F. J. Doyle III. A run-to-run control strategy to adjust basal insulin infusion rates in type 1 diabetes. *Journal of Process Control*, 18:258–265, 2008.

Appendices

APPENDIX A

Clinical study plots

In this Appendix, we show all the glucose and insulin profiles for the 25 clinical studies (2 pilot studies + 23 overnight studies) conducted at Hvidovre Hospital during the period November 2011 - May 2012.

- The studies whose name ends by "CL" are closed-loop studies where full meal bolus is provided.
- The studies whose name ends by "OL" are studies where the controller is not used and the usual basal insulin infusion rate is provided by the pump.
- The studies whose name ends by "CL00" are closed-loop studies where no meal bolus is provided.
- The studies whose name ends by "CL50" are closed-loop studies where full meal bolus is provided.
- The study whose name ends by "11MMCLdouble" is a particular study where the patient got a larger meal (95g CHO), no insulin bolus and 2 apple juice glasses (15g CHO and 10g CHO respectively).

A.1 First pilot study

In this study, the right CGM has been used for feedback. The insulin overdose at the beginning of the closed-loop phase led to a severe hypoglycemia around midnight.

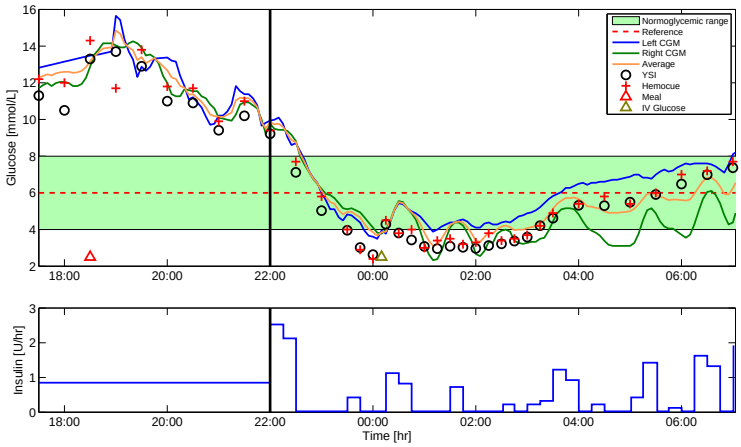

A.2 Second pilot study

In this study, we used the left CGM for feedback. Unlike all other studies, this study was performed during the day.

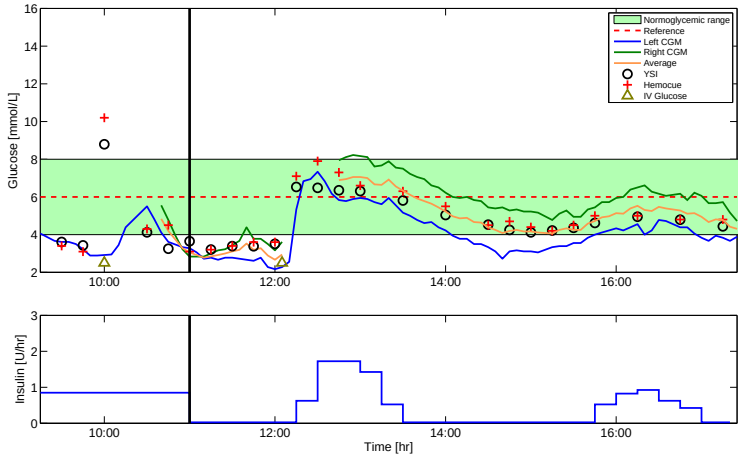

A.3 01PBCL - Plot

In this study, we used the left CGM for feedback. Although the CGM signal is inside the euglycemic range for almost the whole study night, the YSI remains outside the euglycemic range for most of the study night.

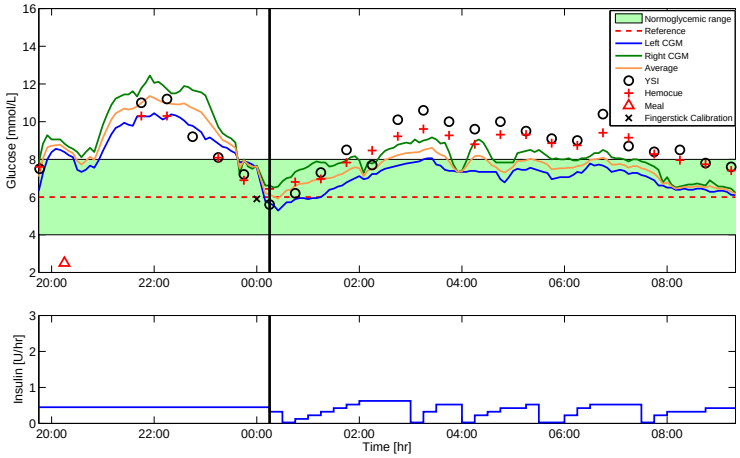

A.4 01PBOL - Plot

In this open-loop study, the patient was in hypoglycemia during most of the night. Intravenous glucose has been administrated 5 times.

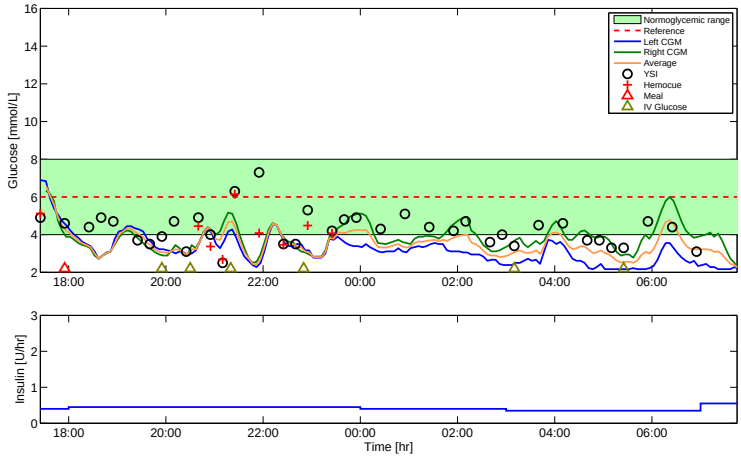

A.5 02KSCL - Plot

In this study, we used the left CGM for feedback. The CGM value remains stable at approximately 5 mmol/L from 22:00 until midnight.

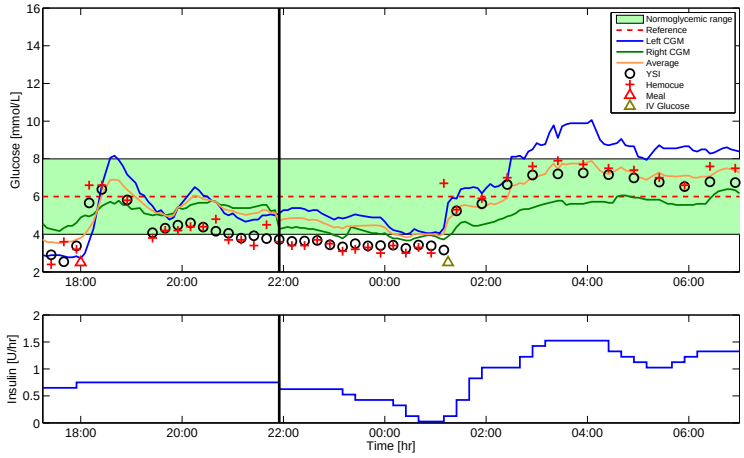

A.6 02KSOL - Plot

During this study, IV glucose has been administrated 2 times. The patient was in hyperglycemia during most of the study night.

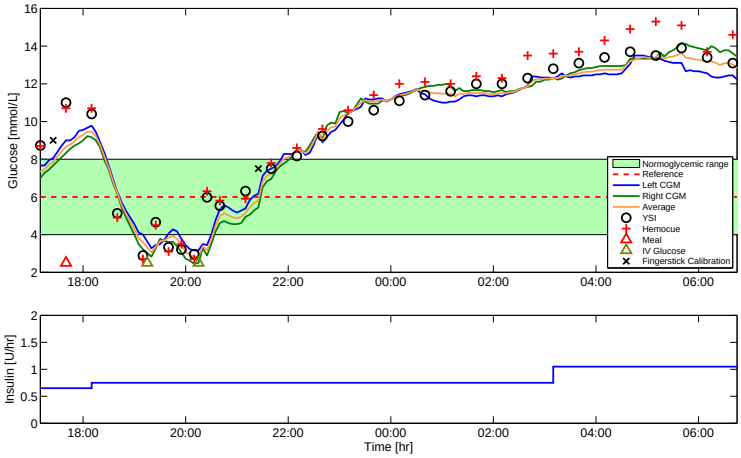

A.7 03AHCL - Plot

Intravenous glucose has been administrated 2 times before the closed-loop phase starts, probably due to an overbolused meal. However, the controller managed to stabilize blood glucose during the night.

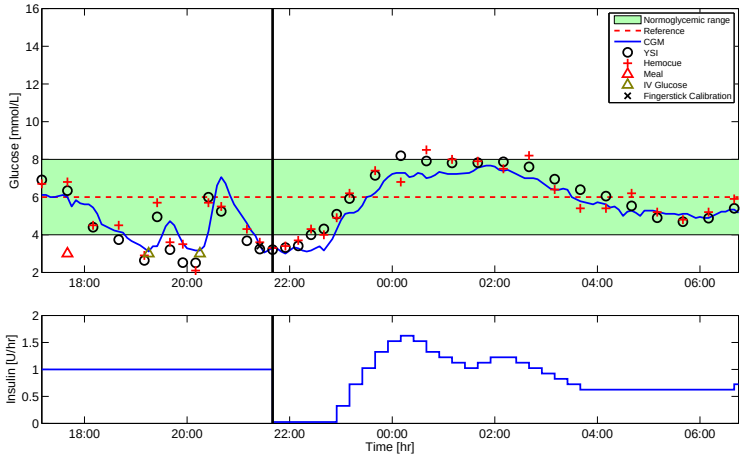

A.8 03AHOL - Plot

As in the closed-loop study, intravenous glucose has been administrated 2 times. However, the glucose remained stable during the study night.

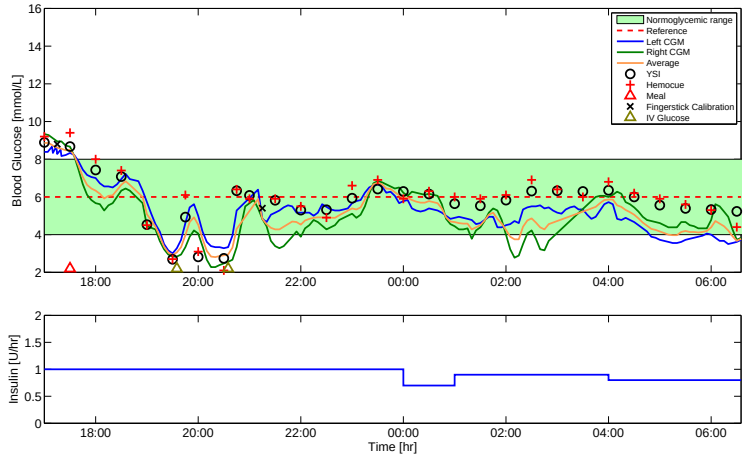

A.9 04BACL - Plot

In this study, we used the left CGM for feedback. The CGM has been accurate for the whole study night, therefore the controller was able to keep the glucose in the euglycemic range.

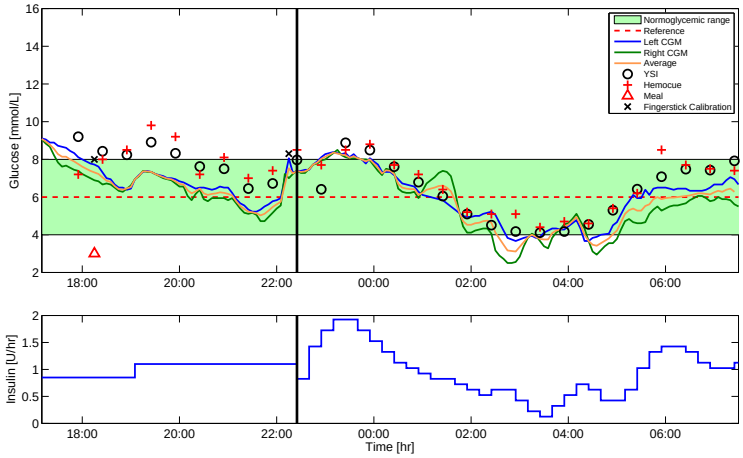

A.10 04BAOL - Plot

In this study, IV glucose were administrated once. In addition, the patient was in a mild hypoglycemia from 03:00 approximately until the end of the study.

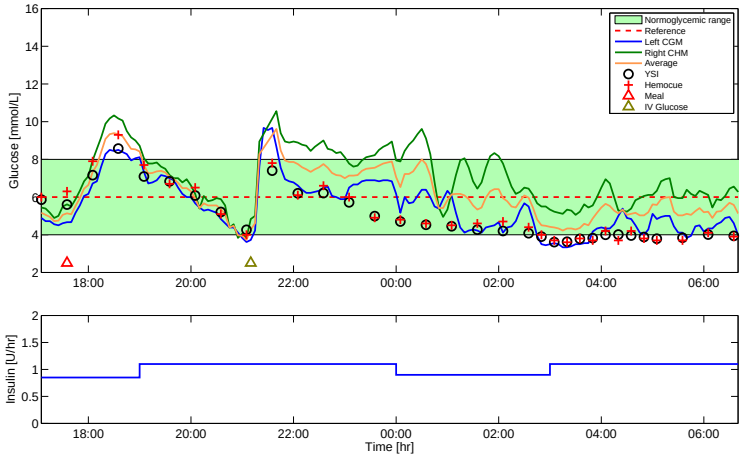

A.11 05KFCL - Plot

In this study, the patient got 7 IV glucose injections due to low postprandial blood glucose values. The controller was able to stabilize the blood glucose concentration despite the disturbances induced by these injections.

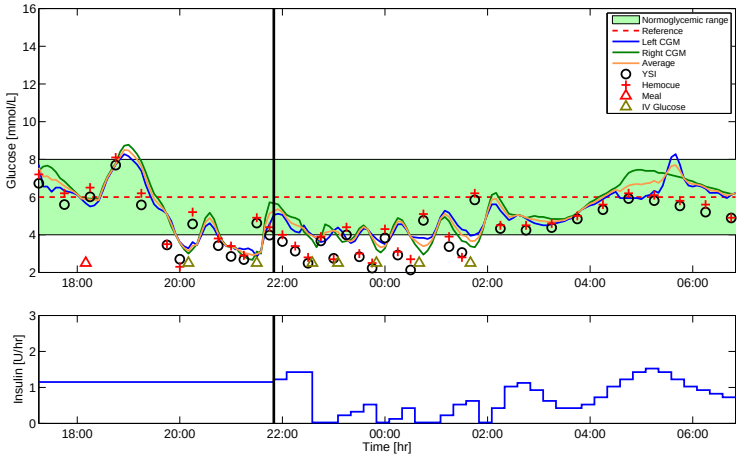

A.12 05KFOL - Plot

In this study, the patient got 8 IV glucose injections due to low postprandial blood glucose values.

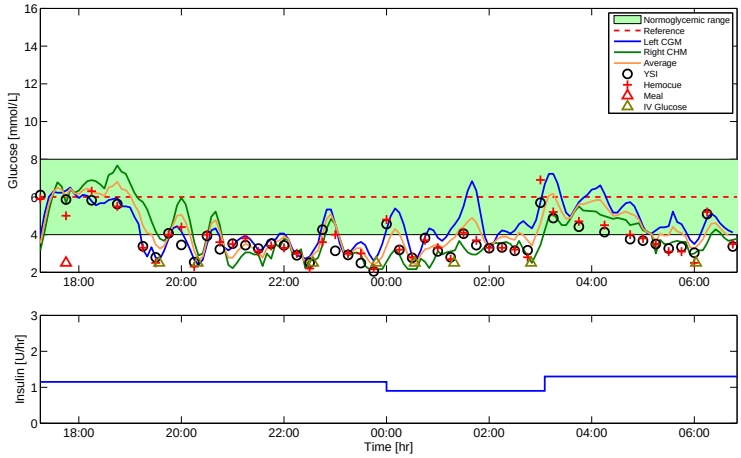

A.13 06MMCL - Plot

In this study, we used the left CGM for feedback. IV glucose has been administrated 3 times during the study night. Globally, the CGM overestimated the actual blood glucose concentration.

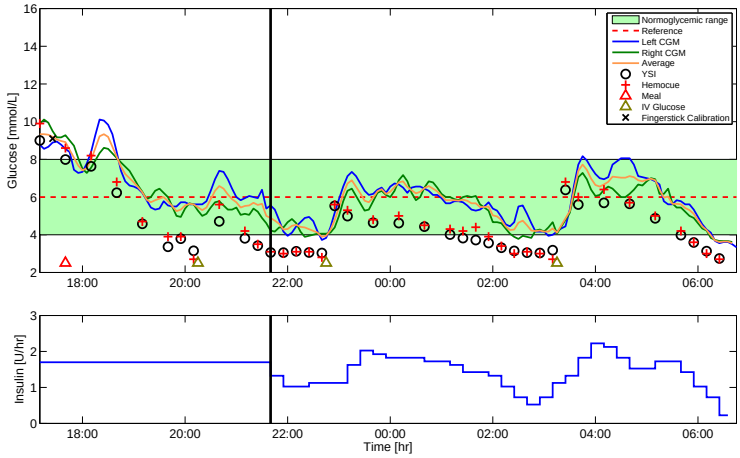

A.14 07CKCL00 - Plot

In this study, we used the left CGM for feedback. Both CGMs were accurate during the study night, and the controller was able to stabilize the glucose.

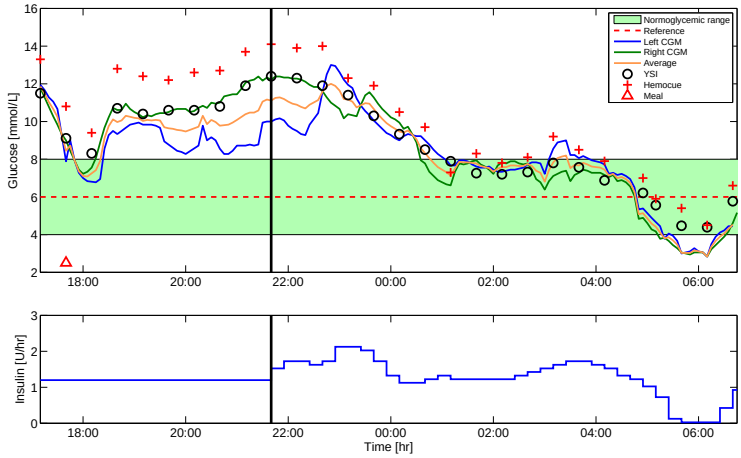

A.15 07CKCL50 - Plot

In this study, we used the right CGM for feedback. Both CGMs were accurate during the study night, and the controller was able to stabilize the glucose.

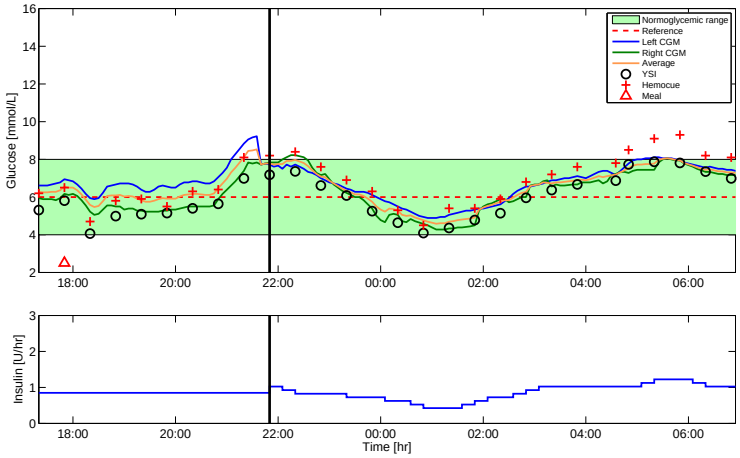

A.16 08TSCL00 - Plot

In this study, we used the right CGM for feedback. The pump were shut down between 23:00 and midnight approximately due to undetected outliers.

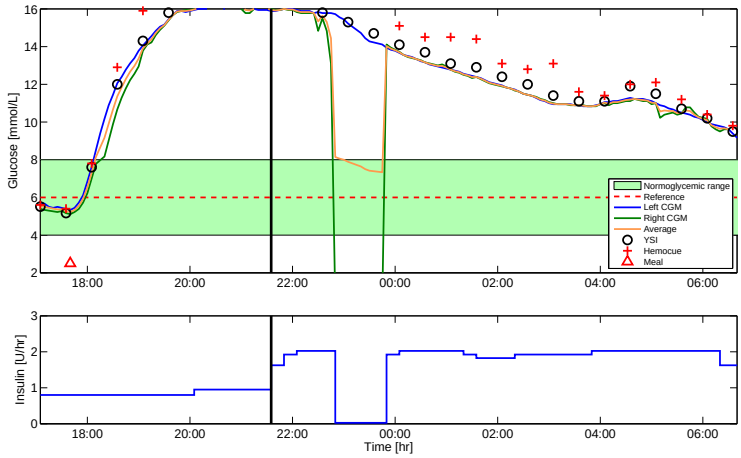

A.17 08TSCL50 - Plot

The CGM remained inside or close to the euglycemic range during the study night. However, the YSI showed values above 10 mmol/L.

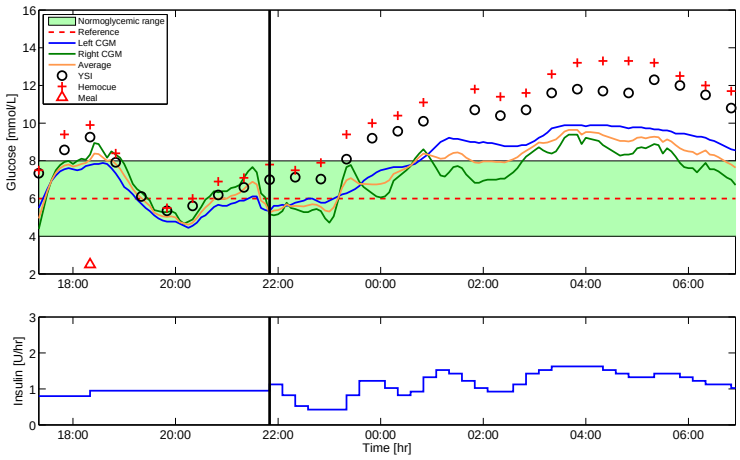

A.18 09DKCL00 - Plot

In this study, we used the left CGM for feedback. Although the glucose values from the CGM were tightly held around 6 mmol/L, the actual blood glucose concentration was around 9 mmol/L. This offset is due to the wrong calibration value before the beginning of the closed-loop sequence.

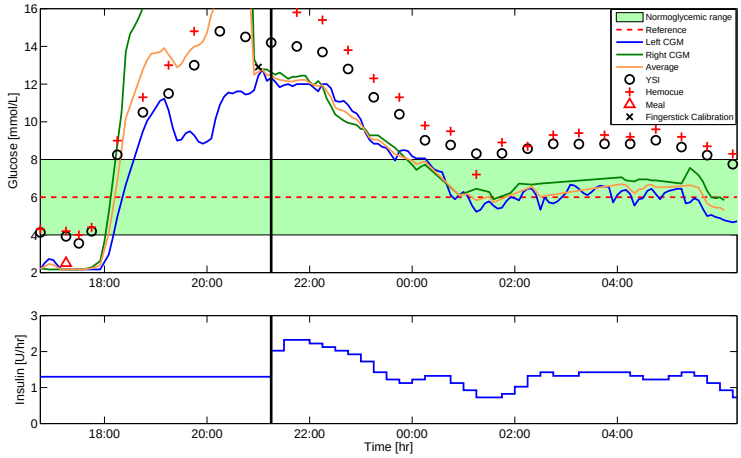

A.19 09DKCL50 - Plot

The CGM sensor values dropped at approximately midnight. This sudden drop inducted a mild hyperglycemia. Apart from this, the patient was well-controlled during the study night.

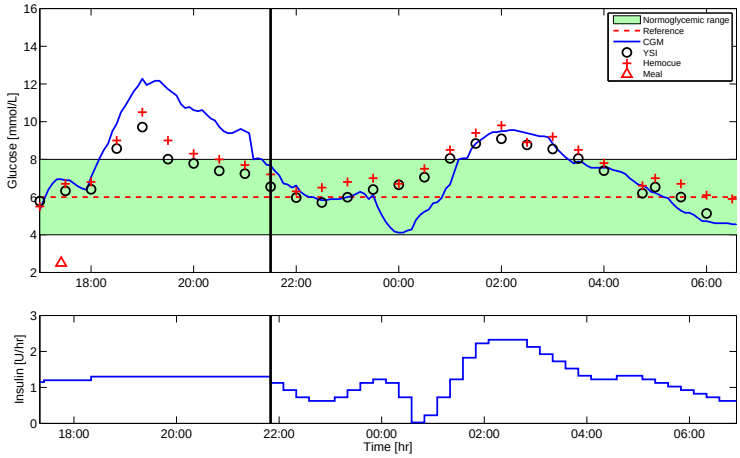

A.20 10HTCL00 - Plot

In this study, we used the left CGM for feedback. The insulin was slightly overdosed, consequently the subject was in hypoglycemia at the end of the study night.

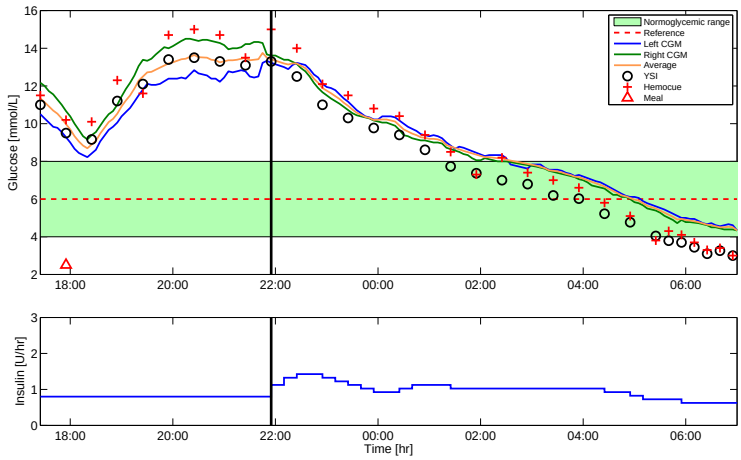

A.21 10HTCL50 - Plot

In this study, we used the left CGM for feedback. IV glucose has been administrated three times during the study time.

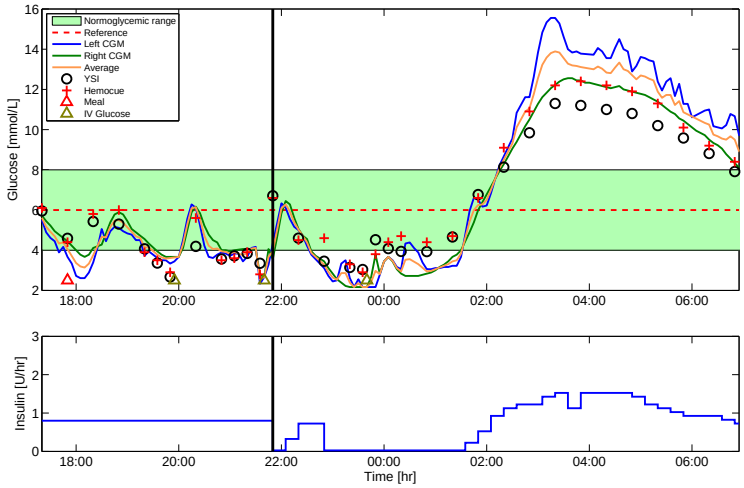

A.22 11MMCL00 - Plot

In this study, we used the right CGM for feedback. Oscillations in CGM values from midnight until the end of the study and undetected outliers caused an hyperglycemic event.

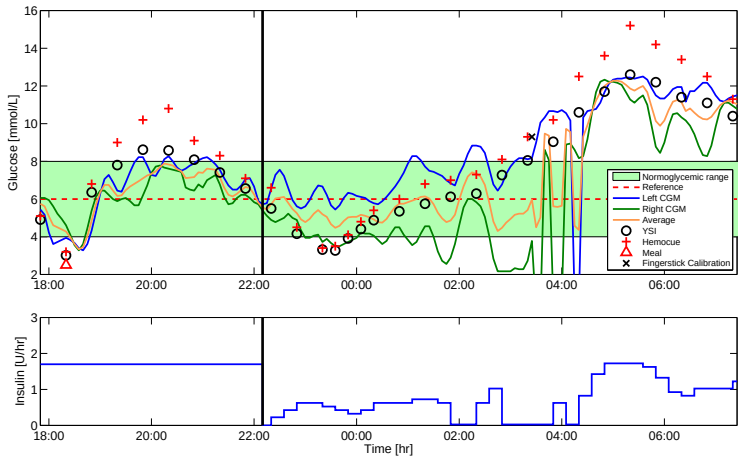

A.23 11MMCLdouble - Plot

In this study, we used the right CGM for feedback. The CGM has been accurate for the whole study night, therefore the controller was able to keep the glucose in the euglycemic range.

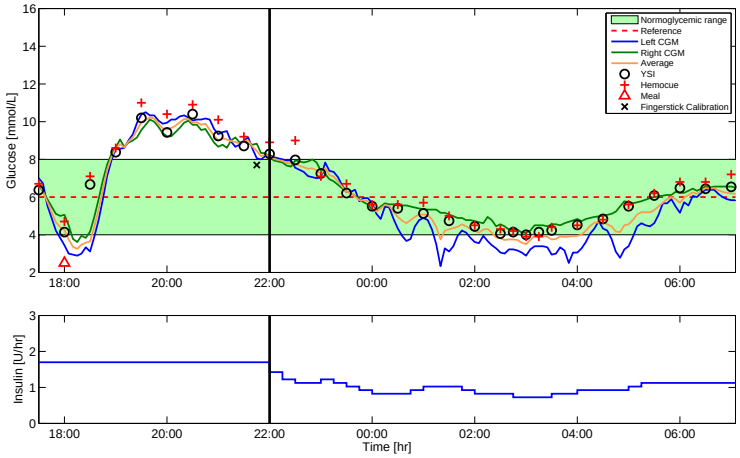

A.24 12LKCL00 - Plot

In this study, we used the left CGM for feedback. The CGM has been quite accurate for the whole study night, therefore the controller was able to keep the glucose concentration in the euglycemic range.

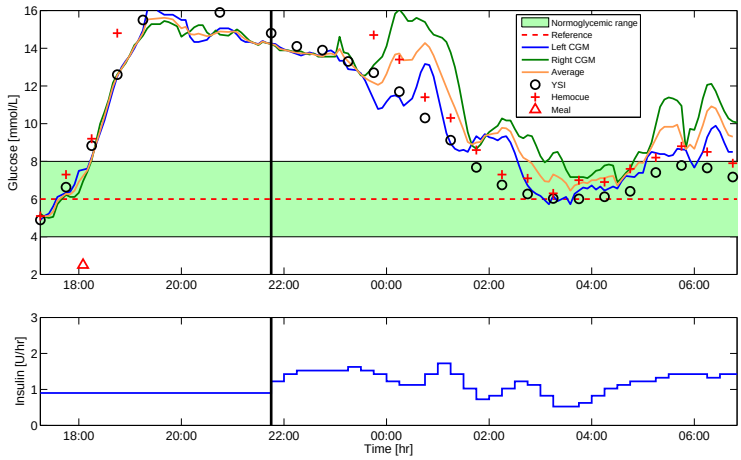

A.25 12LKCL50 - Plot

In this study, we used the left CGM for feedback. The blood glucose concentration remained in the euglycemic range for most of the study night. However, a sudden drop in the CGM value at approximately 02:00 caused a mild hyperglycemic event.

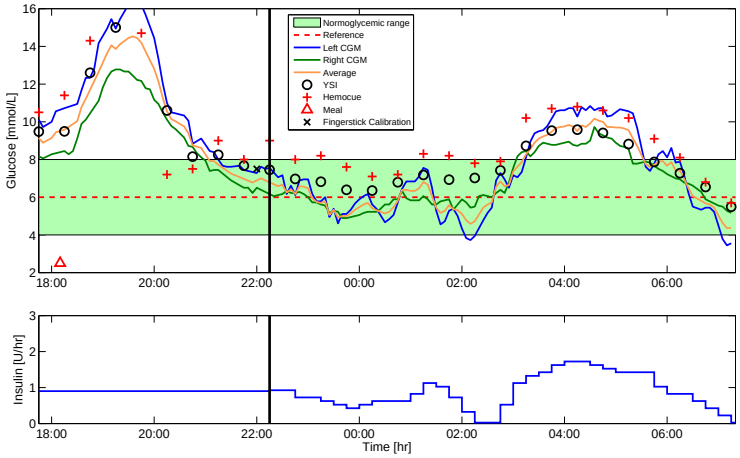

APPENDIX B

Paper A

Nonlinear Model Predictive Control for an Artificial Beta-Cell

Authors:

Dimitri Boiroux, Daniel Aaron Finan, John Bagterp Jørgensen, Niels Kjølstad Poulsen, and Henrik Madsen

Published in:

Recent Advances in Optimization and its Applications in Engineering, pages 299-308. Springer, 2010

Nonlinear Model Predictive Control for an Artificial β-cell

Dimitri Boiroux, Daniel A. Finan, John B. Jørgensen, Niels K. Poulsen, and Henrik Madsen

DTU Informatics, Technical University of Denmark, 2800 Kgs. Lyngby, Denmark,
{dibo, dafi, jbj, nkp, hm}@imm.dtu.dk

Summary. In this contribution we apply receding horizon constrained nonlinear optimal control to the computation of insulin administration for people with type 1 diabetes. The central features include a multiple shooting algorithm based on sequential quadratic programming (SQP) for optimization and an explicit Dormand-Prince Runge-Kutta method (DOPRI54) for numerical integration and sensitivity computation. The study is based on a physiological model describing a virtual subject with type 1 diabetes. We compute the optimal insulin administration in the cases with and without announcement of the meals (the major disturbances). These calculations provide practical upper bounds on the quality of glycemic control attainable by an artificial β-cell.

1 Introduction

The World Health Organization estimates that more than 220 million people worldwide have diabetes, and this number is growing quickly [13]. The number of people with diabetes is projected to double between 2005 and 2030. In addition to the obvious physical and personal effects of diabetes, the disease also has a detrimental economic impact. In the USA, for example, the budget for diabetes care represents 10% of the health care budget, or more than $130 billion ($132 billion in 2002).

In people without diabetes, the pancreas regulates the blood glucose concentration tightly near 90 mg/dL ($\sim$5 mmol/L). Type 1 diabetes is a chronic disease characterized by the autoimmune destruction of the insulin-producing β-cells in the pancreas. Consequently, without insulin—a hormone whose key physiological role is to facilitate the uptake of glucose from the blood into the cells where it is metabolized—elevated concentrations of blood glucose, or *hyperglycemia*, occur. Prolonged hyperglycemia is known to cause a litany of complications: eye, nerve, and kidney disease, to name a few. Thus, exogenous insulin must be injected to lower the blood glucose. This treatment must be done carefully, however, because overinsulinization results in low blood glucose

M. Diehl et al. (eds.), *Recent Advances in Optimization and its Applications in Engineering*,
DOI 10.1007/978-3-642-12598-0_26,

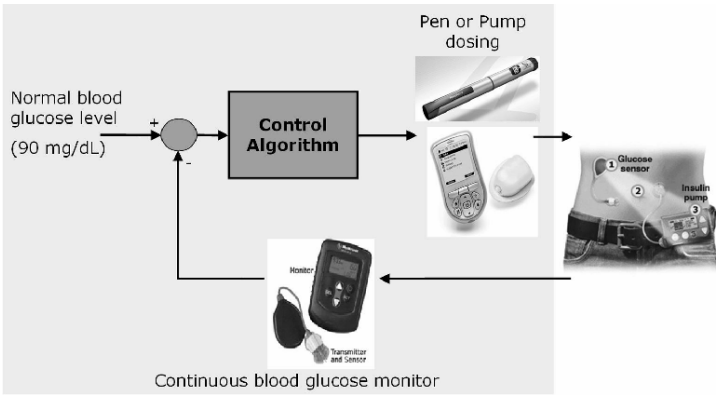

Fig. 1. Closed-loop glucose control for an artificial β-cell. Glucose is measured subcutaneously using a continuous glucose monitor (CGM). Insulin is dosed either continuously (using a pump) or in discrete instances (using a pen), based on the control algorithm.

concentrations, or *hypoglycemia*, which can pose immediate and severe health threats. Ideally, the blood glucose concentration should be kept within the *normoglycemic* range of approximately 70–140 mg/dL (or 3.9–7.8 mmol/L).

By today's standards, treatment consists of administration of exogenous insulin either continuously using an insulin pump or in discrete instances using an insulin pen (or syringe). In any case, the insulin is infused or injected into the subcutaneous tissue of the user, and thus must absorb into the intravenous system before being dispersed throughout the body. A critical component of this insulin therapy is the delivery of boluses (i.e., rapid injections) to offset the effects of carbohydrate (CHO) meals. The size of the bolus is based on a measurement of the current blood glucose and the (estimated) size of the meal, i.e., the amount of CHO in the meal.

Unfortunately, estimating the size of a meal can be a difficult task. Furthermore, having measurements only at meal times does not provide enough information about blood glucose. Hypoglycemic and hyperglycemic events can be missed due to these infrequent blood glucose measurements. In addition, such a measurement process does not provide any information about the dynamic trends of the blood glucose. Consequently, people with diabetes often tolerate frequent hyperglycemia in order to avoid hypoglycemia and its drastic effects.

An artificial β-cell is a biomedical device which would provide automatic regulation of blood glucose (in the case of a pump-based system), or at least optimal treatment suggestions (in the case of a pen-based system), based on a robust control algorithm [4]. A vital element to the success of such a device is the continuous glucose monitor (CGM), which will be used as the sensor in the closed-loop controller. A schematic of the artificial β-cell algorithm is shown in Fig. 1.

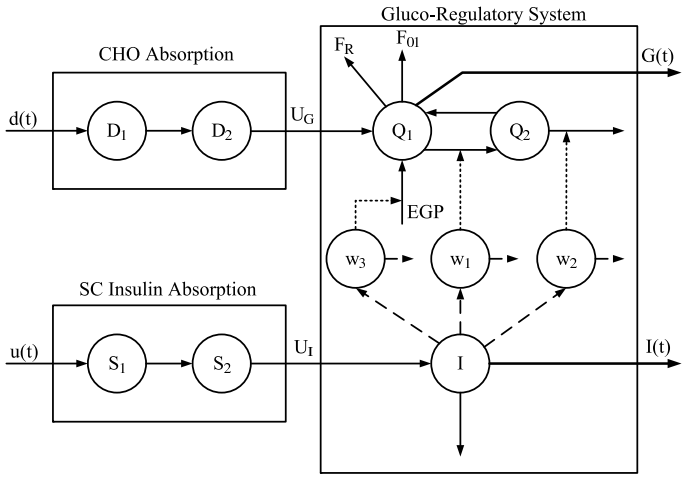

Fig. 2. Diagram of the physiological Hovorka model [8].

From a control perspective, insulin administration via an insulin pump offers a key advantage over insulin pens. Since an insulin pump is permanently attached to the patient, it is suitable for truly automatic, user-free control. That is, a pump-based system has the ability to adjust the manipulated variable, insulin infusion rate, at any time, independent of the patient. In contrast, a pen-based system ultimately relies on the patient physically delivering the insulin dose. There is, of course, an associated tradeoff: insulin pens are less invasive and cheaper for patients with type 1 diabetes.

2 Model Description

A prominent physiological model of the glucose-insulin dynamics in type 1 diabetes developed by Hovorka and colleagues [8] is depicted in Fig. 2. We use this Hovorka model to simulate a virtual subject with type 1 diabetes. In brief, it is a nonlinear model describing the effect of exogenous insulin, $u(t)$, on plasma insulin concentration, $I(t)$, and ultimately on blood glucose concentration, $G(t)$. In addition, the model accounts for the appearance of glucose in the blood due to CHO meals, $d(t)$, and endogenous insulin production, EGP, and removal due to insulin-independent cellular uptake, F_{01}, and renal excretion, F_R.

The model includes descriptions of subcutaneous (SC)-to-intravenous insulin absorption and CHO absorption from a meal, which are both represented as two-compartment (i.e., second order) submodels with time constants of $\tau_S = 55$ min and $\tau_D = 40$ min, respectively. The "slower" appearance of insulin in the blood, relative to meal-related glucose, has important and limiting control implications. These implications are elucidated through one of our key results, which is discussed in Optimization Results.

The nonlinearity in the Hovorka model is due primarily to the time-varying actions of insulin on glucose processes (namely, glucose transport, disposal, and endogenous production), denoted by w_1–w_3 in Fig. 2. Two other sources of nonlinearity are the insulin-independent glucose consumption F_{01} and the renal excretion of glucose F_R, which are both (modeled as) piecewise affine functions of the glucose concentration.

3 Problem Formulation

In this section, we state and discuss the continuous-time optimal control problem that is the basis for computing the insulin injection profiles for people with type 1 diabetes. We also discuss a numerically tractable discrete-time approximation to the continuous-time optimal control problem. The optimal insulin administration is formulated as the bound-constrained continuous-time Bolza problem

$$\min_{[x(t),u(t)]_{t_0}^{t_f}} \quad \phi = \int_{t_0}^{t_f} g(x(t),u(t))dt + h(x(t_f)) \tag{1a}$$

$$\text{s.t.} \quad x(t_0) = x_0 \tag{1b}$$

$$\dot{x}(t) = f(x(t),u(t),d(t)) \qquad t \in [t_0,t_f] \tag{1c}$$

$$u_{\min} \leq u(t) \leq u_{\max} \qquad t \in [t_0,t_f] \tag{1d}$$

in which $x(t) \in \mathbf{R}^{n_x}$ is the state vector, $u(t) \in \mathbf{R}^{n_u}$ is the vector of manipulated inputs, and $d(t) \in \mathbf{R}^{n_d}$ is a vector of known disturbances. $\dot{x}(t) = f(x(t),u(t),d(t))$ represents the model equations. The initial time, t_0, and the final time, t_f, are specified parameters. The initial state, x_0, is a known parameter in (1). The inputs are bound-constrained and must be in the interval $[u_{\min}, u_{\max}]$.

The objective function is stated generally with a stage cost term, $g(x(t),u(t))$, and a cost-to-go term, $h(x(t_f))$. The numerical algorithms for the problem are based on this general structure of the objective function.

3.1 Discrete-time Approximation

The continuous-time bound-constrained Bolza problem (1) is approximated by a numerically tractable discrete-time bound-constrained Bolza problem using the zero-order-hold input parameterization of the manipulated variables, $u(t)$, as well as the known disturbance variables, $d(t)$. We divide the time interval, $[t_0, t_f]$, into N intervals, each of length T_s. Let $\mathcal{N} = \{0,1,...,N-1\}$ and $t_k = t_0 + kT_s$ for $k \in \mathcal{N}$. The zero-order-hold restriction on the input variables, $u(t)$ and $d(t)$, implies

$$u(t) = u_k \qquad t_k \le t < t_{k+1} \qquad k \in \mathcal{N} \tag{2a}$$

$$d(t) = d_k \qquad t_k \le t < t_{k+1} \qquad k \in \mathcal{N} \tag{2b}$$

Using this zero-order-hold restriction on the inputs, the bound constrained continuous-time Bolza problem (1) may be approximated by

$$\min_{\{x_{k+1},u_k\}_{k=0}^{N-1}} \quad \phi = \sum_{k=0}^{N-1} G_k(x_k, u_k, d_k) + h(x_N) \tag{3a}$$

$$\text{s.t.} \qquad b_k := F_k(x_k, u_k, d_k) - x_{k+1} = 0 \quad k \in \mathcal{N} \tag{3b}$$

$$u_{\min} \le u_k \le u_{\max} \qquad k \in \mathcal{N} \tag{3c}$$

The discrete-time state transition function is

$$F_k(x_k, u_k, d_k) = \{x(t_{k+1}) : \dot{x}(t) = f(x(t), u_k, d_k),\, x(t_k) = x_k\} \tag{4}$$

and the discrete time stage cost is

$$G_k(x_k, u_k, d_k) = \{\int_{t_k}^{t_{k+1}} g(x(t), u_k)dt : \dot{x}(t) = f(x(t), u_k, d_k),\, x(t_k) = x_k\} \tag{5}$$

4 Numerical Optimization Algorithm

In this section, we implement a multiple-shooting based SQP algorithm for the numerical solution of (1) [1, 5, 10]. The SQP algorithm is based on line search and structured high rank BFGS updates of the Hessian matrix [1, 10]. The structures of the quadratic subproblems are utilized and they are solved by a primal-dual interior-point algorithm using Riccati iterations [9, 11]. DOPRI54 is used for numerical solution of the differential equation model and sensitivities [3, 6, 7].

4.1 SQP Algorithm

We define the parameter vector, p, as $p = \begin{bmatrix} u_0' & x_1' & u_1' & x_2' & \dots & x_{N-1}' & u_{N-1}' & x_N' \end{bmatrix}'$, and the disturbance vector, d, as $d = \begin{bmatrix} d_0' & d_1' & \dots & d_{N-1}' \end{bmatrix}'$.

Then the bound constrained discrete-time Bolza problem (3) may be expressed as a constrained optimization problem in standard form

$$\min_{p} \quad \phi = \phi(p) \tag{6a}$$

$$\text{s.t.} \quad b(p) = 0 \tag{6b}$$

$$c(p) \ge 0 \tag{6c}$$

The concise formulation (6) is useful for presentation of the numerical optimization algorithm used for solving the bound constrained continuous-time Bolza problem (1).

The steps for solution of (6) by an SQP algorithm with line search are listed in Algorithm 1.

Algorithm 0.1 1 SQP Algorithm for (6)

Require: Initial guess: (p^0, y^0, z^0) with $z^0 \geq 0$.
Compute: $\phi(p^0)$, $\nabla_p \phi(p^0)$, $b(p^0)$, $\nabla_p b(p^0)$, $c(p^0)$, $\nabla_p c(p^0)$
Set $\lambda = 0$, $\mu = 0$, $W^0 = I$
while NOT stop **do**
Compute $(\Delta p^k, \tilde{y}^{k+1}, \tilde{z}^{k+1})$ by solution of:

$$\min_{\Delta p} \quad \frac{1}{2}\Delta p' W^k \Delta p + \nabla_p \phi'(p^k)\Delta p \tag{7a}$$

$$\text{s.t.} \quad \left[\nabla_p b(p^k)\right]' \Delta p = -b(p^k) \tag{7b}$$

$$\left[\nabla_p c(p^k)\right]' \Delta p \geq -c(p^k) \tag{7c}$$

Compute $\Delta y^k = \tilde{y}^{k+1} - y^k$ and $\Delta z^k = \tilde{z}^{k+1} - z^k$
Update the penalty parameter:
$\mu \leftarrow \max\{|z|, \frac{1}{2}(\mu + |z|)\}$ and $\lambda \leftarrow \max\{|y|, \frac{1}{2}(\lambda + |y|)\}$
Compute α using soft line search and Powell's ℓ_1 merit function.
$p^{k+1} = p^k + \alpha \Delta p^k$, $y^{k+1} = y^k + \alpha \Delta y^k$, $z^{k+1} = z^k + \alpha \Delta z^k$
Compute $\phi(p^{k+1})$, $\nabla_p \phi(p^{k+1})$, $c(p^{k+1})$, $\nabla_p c(p^{k+1})$, $b(p^{k+1})$ and $\nabla_p b(p^{k+1})$
Compute W^{k+1} by Powell's modified BFGS update. $k \leftarrow k + 1$.
end while

4.2 Gradient Computation

The most demanding computations in Algorithm 1 are those of the objective function $\phi(p)$, the derivatives of the objective function $\nabla_p \phi(p)$, the dynamics $b(p)$, and the sensitivities, $\nabla_p b(p)$, associated with the dynamics. $b(p)$ and $\phi(p)$ are computed by evaluation of (4) and (5), respectively. Consequently

$$b_k = b_k(x_k, x_{k+1}, u_k, d_k) = F_k(x_k, u_k, d_k) - x_{k+1} \tag{8a}$$

$$\nabla_{x_k} b_k = \nabla_{x_k} F_k(x_k, u_k, d_k) \tag{8b}$$

$$\nabla_{u_k} b_k = \nabla_{u_k} F_k(x_k, u_k, d_k) \tag{8c}$$

$$\nabla_{x_{k+1}} b_k = -I \tag{8d}$$

The gradients $\nabla_{x_k} F_k(x_k, u_k, d_k)$ $\nabla_{u_k} F_k(x_k, u_k, d_k)$ are computed by numerical integration of the sensitivity equations [2].

In the evaluation of the functions and derivatives needed in the SQP algorithm, i.e., $\phi(p)$, $\nabla_p \phi(p)$, $b(p)$, and $\nabla_p b(p)$, the major computational task is solving the sensitivity equations and evaluating the associated quadrature equations. The Hovorka model is a non-stiff system of differential equations. Therefore, we use an embedded Dormand-Prince explicit Runge-Kutta scheme (DOPRI54) for solving the differential equations and integrating the quadrature equations. A special DOPRI54 method has been implemented [2] in which we use the internal stages already computed by solving $\dot{x}(t) = f(x(t), u_k, d_k)$ in the evaluation of the quadrature equation. The implementation uses an adaptive time step based on PI-control [7].

5 Application to an Artificial β-cell

In this section we state and discuss the objective function and the scenarios used in the simulations. We also state the strategy for the nonlinear model predictive controller.

5.1 Nonlinear Model Predictive Control (NMPC)

NMPC is a receding horizon control technology that repeatedly solves open-loop nonlinear optimal control problems and implements the computed optimal control associated to the current time period [12]. In this contribution, we use a receding horizon strategy to compute the ideal insulin administration profile for people with type 1 diabetes. In order to obtain the ideal insulin profile, the NMPC uses state feedback and relative long prediction horizons.

5.2 Objective Function with Soft Output Constraints

The objective of the insulin administration is to compensate for glucose excursions caused by meals and by variations in endogenous glucose production and utilization. We use a penalty function defined as

$$\begin{aligned}\rho(G(t)) = \frac{\kappa_1}{2}|\max\{0, G(t) - \bar{G}\}|^2 + \frac{\kappa_2}{2}|\max\{0, \bar{G} - G(t)\}|^2 + \\ \frac{\kappa_3}{2}|\max\{0, G(t) - G_U\}|^2 + \frac{\kappa_4}{2}|\max\{0, G_L - G(t)\}|^2\end{aligned} \tag{9}$$

where $G(t)$ is the blood glucose concentration, $\bar{G} = 5$ mmol/L is the target value for the blood glucose concentration, $G_L = 4$ mmol/L is a lower acceptable limit, and $G_U = 8$ mmol/L is an upper acceptable limit. The weights κ_1–κ_4 are used to balance the desirability of different deviations from the target. As hypoglycemia is considered a more immediate risk than hyperglycemia, $\kappa_1 < \kappa_2$ and $\kappa_3 < \kappa_4$. The penalty function used in the simulations is illustrated in Fig. 3. Even though the penalty function (9) is not twice differentiable, we use the standard BFGS update procedure. $G(t)$ is a function of the state, $x(t)$, in the Hovorka model. Therefore, the penalty function (9) may be expressed as a stage cost in the form $g(x(t), u(t))$. The objective function used in the simulations is

$$\phi = \int_{t_0}^{t_f} g(x(t), u(t))dt + \frac{\eta}{2}\sum_{k=0}^{N-1} \|\Delta u_k\|_2^2 \tag{10}$$

where $u(t)$ represents the rate of insulin injection at any time and $\Delta u_k = u_{k+1} - u_k$. Given an initial state, x_0, and a CHO intake rate profile, $[d(t)]_{t_0}^{t_f}$, the continuous-time Bolza problem (1) computes the optimal insulin injection rate profile, $[u(t)]_{t_0}^{t_f}$, as well as the optimal state trajectory, $[x(t)]_{t_0}^{t_f}$. This

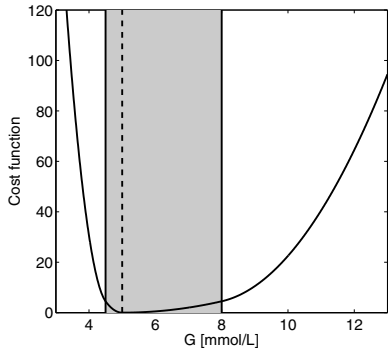

Fig. 3. Penalty as a function of the blood glucose concentration. The shaded region is the interval of acceptable glucose concentrations. The target glucose concentration is 5 mmol/L. Blood glucose concentrations less than 3 mmol/L are very undesirable as severe hypoglycemia can result in immediate dangers for the patient.

objective function has no cost-to-go function, i.e., $h(x(t_f)) = 0$, and can be brought into the standard form (3a) using state augmentation [12].

We use $u_{\min} = 0$ and a large $u_{\max}$ such that the upper bound is never active. (The former bound is self-evident, and the latter is consistent with realistic insulin pump and pen specifications.) We perform the optimization over a 24-hour window, i.e., $t_0 = 0$ min and $t_f = 24 \cdot 60 = 1440$ min, using a sampling time of $T_s = 5$ min (consistent with realistic CGM and insulin pump specifications). In the scenario considered, the simulated 70-kg subject has a 62-g CHO meal at 6:00, a 55-g CHO meal at 12:00, and a 50-g CHO meal at 18:00. To ensure an optimal blood glucose profile, a prediction horizon of six hours, i.e., $N = 6 \cdot 12 = 72$ samples, is employed in the receding horizon strategy.

6 Optimization Results

In this section, we use the Hovorka model and the developed multiple shooting SQP algorithm for (1) to compute insulin administration profiles for a virtual patient with type 1 diabetes.

Fig. 4(a) depicts the optimal insulin administration profile for the scenario in which the controller knows the size and time of all meals in advance. It illustrates the absolutely best insulin dosage and the corresponding glucose profile. This profile is obtained by solving the discrete-time constrained optimal control problem (3) given the disturbance vector d. It is evident from Fig. 4(a) that, due to the slower absorption of insulin relative to meal-related glucose (see Model Description), the optimal glucose concentration is achieved by administering the insulin in advance of the meal. Knowing the meal times and sizes allows the controller to deliver this anticipatory insulin to preempt

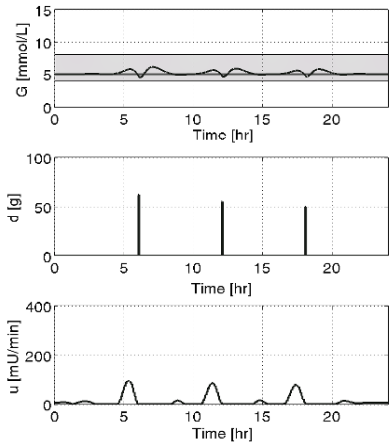

(a) Optimal insulin administration for the case with meal announcement in advance of the meal. Most insulin is taken before the meals.

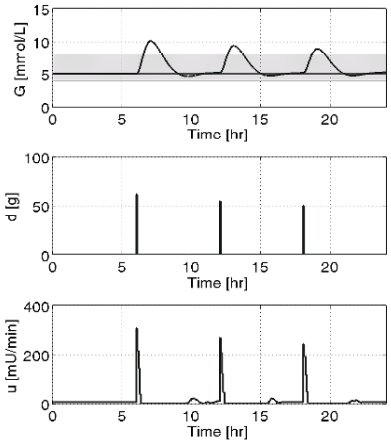

(b) Optimal insulin administration with meal announcement at mealtime. Most insulin is taken in bolus like form at meal time.

Fig. 4. Optimal insulin administration and blood glucose profiles.

postprandial hyperglycemia. However, the assumption that the patient would know in advance—and with accuracy—the meal times and sizes is not practical. Safety considerations would preclude significant amounts of insulin from being delivered prior to mealtime.

Fig. 4(b) shows the simulation results for the more practical case in which the meals are announced to the MPC only at mealtime. Thus, the controller can deliver no anticipatory insulin prior to meals. The limitations for this case force the subject into (mild) hyperglycemia, but hypoglycemia is avoided. The insulin delivery profile for this case looks qualitatively similar to bolus delivery of insulin by a pen; most of the meal-related insulin is delivered in bolus form within the few samples after the meals are taken (and announced). Simulated optimal bolus treatment with a pen provides glucose profiles comparable to the glucose profile in Fig. 4(b) (results not shown).

These results demonstrate that for realistic cases, e.g., cases for which meal information is unknown until mealtime, acceptable control can still be obtained.

7 Conclusion

In this paper, we described a multiple shooting SQP algorithm for the solution of a bound-constrained discrete-time Bolza problem. Based on the Hovorka model for people with type 1 diabetes, we use an optimal control algorithm

to compute insulin administration profiles for the cases with and without meal announcement in advance. The blood glucose profiles provide information about the best achievable performance in the case where anticipatory insulin administration is allowed, and in the case where insulin is delivered at mealtimes. The insulin profile for the realistic case with announcement of meals at mealtime is reminiscent of a bolus-based treatment regimen. This suggests that, for certain situations, insulin treatment based on pen systems may be nearly as effective as insulin treatment based on pump systems.

References

1. H.G. Bock and K.J. Plitt (1984) A multiple shooting method for direct solution of optimal control problems. Proc. of the IFAC 9th World Congress, pp. 242-247. Budapest, Hungary
2. D. Boiroux (2009) Nonlinear Model Predictive Control for an Artificial Pancreas. MSc Thesis, DTU Informatics, Technical University of Denmark
3. J. C. Butcher (2003) Numerical Methods for Ordinary Differential Equations. Wiley, Chichester, England
4. C. Cobelli, C. Dalla Man, G. Sparacino, L. Magni, G. De Nicolao and B. P. Kovatchev (2009) Diabetes: Models, Signals, and Control. IEEE Reviews in Biomedical Engineering, vol. 2, pp. 54-96
5. M. Diehl, H. G. Bock, J. P. Schlöder, R. Findeisen, Z. Nagy and F. Allgöwer (2002) Real-time optimization and nonlinear model predictive control of processes governed by differential-algebraic equations. Journal of Process Control, vol. 12, pp. 577-585
6. J. R. Dormand and P. J. Prince (1980) A family of embedded Runge-Kutta formulae. Journal of Computational and Applied Mathematics, vol. 6, no. 1, pp. 19-26
7. K. Gustafsson (1992) Control of Error and Convergence in ODE Solvers. PhD Thesis, Department of Automatic Control, Lund Institute of Technology
8. R. Hovorka, V. Canonico, L. J. Chassin, U. Haueter, M. Massi-Benedetti, M. Orsini Federici, T. R. Pieber, H. C. Schaller, L. Schaupp, T. Vering and M. E. Wilinska (2004) Nonlinear Model Predictive Control of Glucose Concentration in Subjects with Type 1 Diabetes. Physiological Measurement, vol. 25, pp. 905-920
9. J. B. Jørgensen (2005) Moving Horizon Estimation and Control. PhD Thesis, Department of Chemical Engineering, Technical University of Denmark
10. D. B. Leineweber, I. Bauer, H. G. Bock, J. P. Schlöder (2003) An efficient multiple shooting based reduced SQP strategy for large-scale dynamic process optimization. Part 1: theoretical aspects. Computers and Chemical Engineering, vol. 27, pp. 157-166
11. C. V. Rao, S.J. Wright and J. B. Rawlings (1998) Application of Interior-Point Methods to Model Predictive Control. Journal of Optimization Theory and Applications, vol. 99, nr. 3, pp. 723-757.
12. J. B. Rawlings and D. Q. Mayne (2009) Model Predictive Control: Theory and Design. Nob Hill Publishing. Madison, Wisconsin, USA
13. World Health Organization (2009) Diabetes (fact sheet no. 312). Website: `http://www.who.int/mediacentre/factsheets/fs312/en/`.

APPENDIX C

Paper B

Implications and Limitations of Ideal Insulin Administration for People with Type 1 Diabetes

Authors:

Dimitri Boiroux, Daniel Aaron Finan, John Bagterp Jørgensen, Niels Kjølstad Poulsen, and Henrik Madsen

Published in:

UKACC International Conference on Control 2010, pages 156-161, 2010.

Implications and Limitations of Ideal Insulin Administration for People with Type 1 Diabetes ⋆

Dimitri Boiroux * **Daniel A. Finan** * **John Bagterp Jørgensen** *
Niels Kjølstad Poulsen * **Henrik Madsen** *

* *Department of Informatics and Mathematical Modelling, Technical University of Denmark, DK-2800 Kgs Lyngby, Denmark (e-mail: {dibo,dafi,jbj,nkp,hm}@imm.dtu.dk)*

Abstract:
In this paper we use open-loop constrained non-linear optimal control to compute insulin administration profiles for people with type 1 diabetes. The algorithm is a multiple shooting algorithm based on sequential quadratic programming (SQP) for optimisation and an explicit Dormand-Prince Runge-Kutta method (DOPRI54) for numerical integration and sensitivity computation. We describe the numerical details of the constrained non-linear optimal control algorithm. The Hovorka model is used to describe a person with type 1 diabetes. We use the model and the algorithm to compute insulin administration profiles for people with type 1 diabetes in the cases with and without meal announcement in advance. The case with advance meal announcement results in almost perfect glucose control, but is undesirable as an insulin therapy due to the fact that most of the meal-related insulin is injected before the meal is actually taken. In the second, more realistic case, information about the meal is provided to the controller as the meal is taken. In this case, the optimal insulin administration profile is characterised by bolus-like injections of insulin coincident with the meals. These results indicate that, for certain conditions, insulin pens may be able to provide glucose control comparable to that of insulin pumps.

Keywords: type 1 diabetes, non-linear model predictive control, meal announcement

1. INTRODUCTION

The World Health Organization (2009) estimates that 180 million people worldwide have diabetes. This number is projected to double by 2030. In the USA, the budget for diabetes represents approximately 10% of the health care budget, i.e., more than 130 billion dollars.

People with type 1 diabetes produce negligible amounts of pancreatic insulin. To maintain normal blood glucose concentrations, or normoglycaemia (approximately 60–140 mg/dL or 3.3–7.8 mmol/L), exogenous insulin must be injected. The glucose concentration must be regulated around 90 mg/dL and kept in the normoglycaemic range in order to avoid diabetes-related complications. Persistent high blood glucose concentrations above 140 mg/dL (hyperglycaemia) cause vascular, nerve, eye and kidney diseases. On the other hand, very low blood glucose concentrations (hypoglycaemia) can cause insulin shock or coma.

Insulin reduces the glucose concentration in the blood by facilitating the uptake of glucose into liver cells, where it can be stored as glycogen, and into peripheral tissue cells (muscles and adipose), where it can be stored or metabolised. Two types of insulin secretion patterns are used by a normal, fully functional pancreas. First, a low, relatively constant basal rate of insulin is needed to counteract the glucose secreted by the conversion of glycogen to glucose in the liver (endogenous glucose production, or EGP). In addition to EGP, the major disturbance affecting the blood glucose levels is the absorption of carbohydrates (CHO) from meals. To offset these large loads of glucose, insulin is secreted in rapidly released boluses.

The challenge, then, for people with type 1 diabetes, is to try to mimic these insulin delivery patterns of a normal pancreas as closely as possible. Exogenous insulin therapy is often based on several (say, 4–8) blood glucose measurements per day, some of which are typically taken just before meals. Rapid-acting insulin analogues are injected as boluses to compensate for the CHO in the meal and correct the current blood glucose level if necessary. Long-acting insulin analogues are taken infrequently (say, once per day) to counteract EGP. In well controlled subjects, the outcome of this therapy is illustrated in Fig. 1. Fig. 1 shows the daily glucose concentration tracings for one subject for seven consecutive days. Clearly, there is much room for improvement in the degree of glucose control. Significant parts of days are spent in the hyperglycaemic range, and occasionally hypoglycaemic events do occur.

Digestion and absorption of CHO from the gastrointestinal tract into the blood is generally faster than absorption of

⋆ Funding for this research as part of the DIACON project from the Danish Council for Strategic Research is gratefully acknowledged.

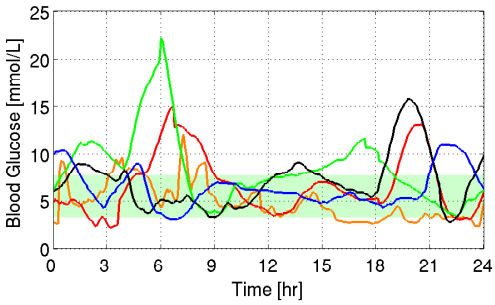

Fig. 1. Glucose concentration variations in a person with type 1 diabetes for 5 consecutive days using conventional insulin therapy based on discrete glucose measurements and discrete insulin injections. The green-shaded area represents the normoglycaemic range.

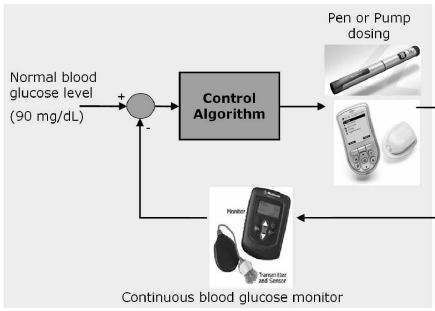

Fig. 2. Closed-loop glucose control. Glucose is measured subcutaneously using a continuous glucose monitor (CGM). Insulin is dosed either continuously by an insulin pump or discretely using an insulin pen.

subcutaneously injected insulin into the blood. Furthermore, the glucose-insulin dynamics are complex and non-linear. Thus, with infrequent, discrete measurements of blood glucose and estimates of the CHO content in meals, it is not surprising that the degree of control depicted in Fig. 1 is typical of conventional insulin therapy.

To improve the glycaemic control by fine-tuning their insulin therapy, people with type 1 diabetes are using continuous glucose monitors (CGMs) more prevalently. These CGMs continuously (every one to few minutes) measure the subcutaneous glucose concentration. In addition, insulin pumps that can continuously infuse rapid-acting insulin are becoming more popular. The combination of these two medical devices has inspired much research interest in an artificial beta-cell (pancreas) that automatically adjusts the insulin dosage to control the blood glucose in people with type 1 diabetes. This concept is illustrated in Fig. 2. Several research groups worldwide are investigating aspects of control algorithms integrating the CGM and the insulin pump to automatically adjust insulin administration for people with type 1 diabetes, such as Klonoff et al. (2009).

The quality of the glucose control is limited by the time lag associated with subcutaneous-to-intravenous insulin absorption. In some mathematical descriptions of the physiology, such as that of Hovorka et al. (2004), the absorption and transport of subcutaneously injected insulin to systemic circulation is modeled as linear second order process with time constants of $\tau_S = 55$ min. Digestion and absorption of CHO is similarly modelled as a linear second order process, but with time constants of $\tau_D = 40$ min. These absorption models and their relation to glucose-insulin dynamics in the Hovorka model are illustrated in Fig. 3. This system property fundamentally limits the control quality that can be achieved in closed-loop insulin administration.

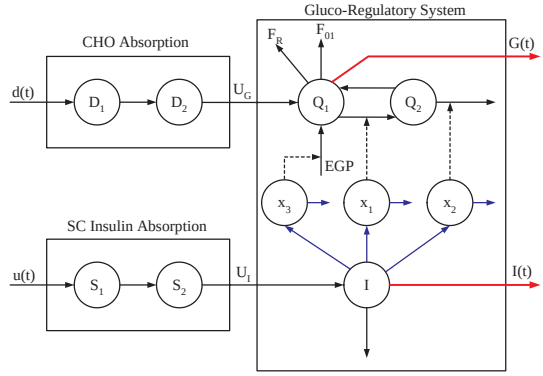

Fig. 3. Diagram of the Hovorka model.

In this paper, we use constrained non-linear optimal control theory to compute the optimal insulin injection rates during a day. The computed profiles are open loop profiles and are not based on feedback. We consider the case when the meals throughout the day are announced to the controller in advance, and the case when the meals are only announced to the controller when they are taken. Knowing the ideal insulin administration profiles, we compare and discuss the advantages, disadvantages, and implications of these solutions. In particular, we address the issue of whether we can expect fundamentally better insulin therapy with pumps than with pens in the limiting case of perfect meal information.

The paper is structured as follows. The constrained non-linear optimal control problem is presented in Section 2. Section 3 presents an quasi-Newton SQP algorithm with line search for solution of the discrete-time constrained non-linear Bolza problem. The numerical procedures for integration of the differential equations and computation of their sensitivities are also presented in Section 3. The non-linear model predictive controller and the scenarios are stated in Section 4. Section 5 applies the constrained non-linear optimal control algorithm to compute insulin administration profiles for virtual subjects with type 1 diabetes. Conclusions are provided in Section 6.

2. PROBLEM FORMULATION

In this section, we state and discuss the continuous-time optimal control problem that we use to compute the insulin injection profiles for people with type 1 diabetes. We also discuss a numerically tractable discrete-time approximation to the continuous-time optimal control problem.

The bound constrained continuous-time Bolza problem

$$\min_{[x(t),u(t)]_{t_0}^{t_f}} \quad \phi = \int_{t_0}^{t_f} g(x(t),u(t))dt + h(x(t_f)) \tag{1a}$$

$$\text{s.t.} \quad x(t_0) = x_0 \tag{1b}$$

$$\dot{x}(t) = f(x(t),u(t),d(t)) \qquad t \in [t_0,t_f] \tag{1c}$$

$$u_{\min} \le u(t) \le u_{\max} \qquad t \in [t_0,t_f] \tag{1d}$$

is used to compute the optimal insulin administration. $x(t) \in \mathbf{R}^{n_x}$ is the state vector, $u(t) \in \mathbf{R}^{n_u}$ is the manipulated inputs, and $d(t) \in \mathbf{R}^{n_d}$ are known disturbances. $\dot{x}(t) = f(x(t),u(t),d(t))$ represents the model equations. The initial time, t_0, and the final time, t_f, are specified parameters. The initial state, x_0, is a known parameter in (1). The inputs are bound constrained and must be in the interval $u(t) \in [u_{\min}, u_{\max}]$.

The objective function is stated generally with a stage cost term, $g(x(t),u(t))$, and a cost-to-go term, $h(x(t_f))$. The numerical algorithms for the problem are derived using this general structure of the objective function.

In the insulin administration problem, the stage cost term is a penalty function, the cost-to-go term is zero, and the model equations are represented by the Hovorka model Hovorka et al. (2004). $u(t)$ represents the rate of insulin injection at any time and $d(t)$ represents the carbohydrates (CHO) intake rate at any time. Given an initial state, x_0, and a CHO intake rate profile, $[d(t)]_{t_0}^{t_f}$, the continuous-time Bolza problem (1) computes the optimal insulin injection rate profile, $[u(t)]_{t_0}^{t_f}$, as well as the optimal state trajectory, $[x(t)]_{t_0}^{t_f}$.

2.1 Discrete-Time Approximation

The continuous-time bound constrained Bolza problem (1) is approximated by a numerical tractable discrete-time bound constrained Bolza problem using the zero-order-hold input parametrisation of the manipulated variables, $u(t)$, as well as the known disturbance variables, $d(t)$. We divide the time interval, $[t_0, t_f]$, into N equidistant intervals each of length T_s. Let $\mathcal{N} = \{0,1,...,N-1\}$ and $t_k = t_0 + kT_s$ for $k \in \mathcal{N}$. The zero-order-hold restriction on the input variables, $u(t)$ and $d(t)$, imply

$$u(t) = u_k \qquad t_k \le t < t_{k+1} \qquad k \in \mathcal{N} \tag{2a}$$

$$d(t) = d_k \qquad t_k \le t < t_{k+1} \qquad k \in \mathcal{N} \tag{2b}$$

Using this zero-order-hold restriction on the inputs, the bound constrained continuous-time Bolza problem may be expressed as

$$\min_{\{x_{k+1},u_k\}_{k=0}^{N-1}} \quad \phi = \sum_{k=0}^{N-1} G_k(x_k,u_k,d_k) + h(x_N) \tag{3a}$$

$$\text{s.t.} \quad b_k := F_k(x_k,u_k,d_k) - x_{k+1} = 0 \quad k \in \mathcal{N} \tag{3b}$$

$$u_{\min} \le u_k \le u_{\max} \qquad k \in \mathcal{N} \tag{3c}$$

The discrete-time state transition function is

$$F_k(x_k,u_k,d_k) = \{x(t_{k+1}) : \dot{x}(t) = f(x(t),u_k,d_k),\, x(t_k) = x_k\} \tag{4}$$

and the discrete time stage cost is

$$G_k(x_k,u_k,d_k) = \{\int_{t_k}^{t_{k+1}} g(x(t),u_k)dt : \dot{x}(t) = f(x(t),u_k,d_k),\, x(t_k) = x_k\} \tag{5}$$

3. NUMERICAL OPTIMISATION ALGORITHM

In this section, we develop a multiple-shooting based SQP algorithm described in Diehl et al. (2009) and in Bock and Plitt (1984) for the numerical solution of (1). The SQP algorithm is based on line search. The structure of the quadratic sub-problems are utilised and they are solved by a primal-dual interior-point algorithm using Riccati iterations, as in Jørgensen (2005) and Rao et al. (1998). The DOPRI54 scheme derived in Dormand and Prince (1980) is used for numerical solution of the differential equation model and sensitivities.

3.1 SQP Algorithm

Define the parameter vector, p, as

$$p = \begin{bmatrix} u_0' & x_1' & u_1' & x_2' & \dots & x_{N-1}' & u_{N-1}' & x_N' \end{bmatrix}', \tag{6}$$

and the disturbance vector, $d = \begin{bmatrix} d_0' & d_1' & \dots & d_{N-1}' \end{bmatrix}'$, such that the discrete time dynamics may be represented by

$$b(p) = b(p;x_0,d) = \begin{bmatrix} F_0(x_0,u_0,d_0) - x_1 \\ F_1(x_1,u_1,d_1) - x_2 \\ \vdots \\ F_{N-1}(x_{N-1},u_{N-1},d_{N-1}) - x_N \end{bmatrix} \tag{7}$$

and the objective function may be denoted

$$\phi(p) = \phi(p;x_0,d) = \sum_{k=0}^{N-1} G_k(x_k,u_{k,d}) + h(x_N) \tag{8}$$

Let $c(p)$ denote the bound constraints, i.e.

$$c(p) = \begin{bmatrix} u_0 - u_{\min} \\ u_1 - u_{\min} \\ \vdots \\ u_{N-1} - u_{\min} \\ u_{\max} - u_0 \\ u_{\max} - u_1 \\ \vdots \\ u_{\max} - u_{N-1} \end{bmatrix}. \tag{9}$$

Then the bound constrained discrete-time Bolza problem may be expressed as a constrained optimisation problem in standard form

$$\min_p \quad \phi = \phi(p) \tag{10a}$$

$$\text{s.t.} \quad b(p) = 0 \tag{10b}$$

$$c(p) \ge 0 \tag{10c}$$

The concise formulation (10) is useful for presentation of the numerical optimisation algorithm used for solving the bound constrained continuous-time Bolza problem (1).

The Lagrangian of (10) is

$$\mathcal{L}(p,y,z) = \phi(p) - y'b(p) - z'c(p) \tag{12}$$

Algorithm 1 SQP Algorithm for (10)

Require: Initial guess: (p^0, y^0, z^0) with $z^0 \geq 0$.
Compute: $\phi(p^0)$, $\nabla_p\phi(p^0)$, $b(p^0)$, $\nabla_p b(p^0)$, $c(p^0)$, $\nabla_p c(p^0)$
Set $\lambda = 0$, $\mu = 0$, $W^0 = I$
while NOT stop **do**
Compute $(\Delta p^k, \tilde{y}^{k+1}, \tilde{z}^{k+1})$ by solution of:

$$\min_{\Delta p} \quad \frac{1}{2}\Delta p' W^k \Delta p + \nabla_p \phi'(p^k)\Delta p \tag{11a}$$

$$\text{s.t.} \quad \left[\nabla_p b(p^k)\right]' \Delta p = -b(p^k) \tag{11b}$$

$$\left[\nabla_p c(p^k)\right]' \Delta p \geq -c(p^k) \tag{11c}$$

Compute $\Delta y^k = \tilde{y}^{k+1} - y^k$ and $\Delta z^k = \tilde{z}^{k+1} - z^k$
Update the penalty parameter:
$\mu \leftarrow \max\{|z|, \frac{1}{2}(\mu + |z|)\}$ and $\lambda \leftarrow \max\{|y|, \frac{1}{2}(\lambda + |y|)\}$
Compute α using soft line search and Powell's ℓ_1 merit function (14).
$p^{k+1} = p^k + \alpha\Delta p^k$, $y^{k+1} = y^k + \alpha\Delta y^k$, $z^{k+1} = z^k + \alpha\Delta z^k$
Compute $\phi(p^{k+1}), \nabla_p\phi(p^{k+1})$, $c(p^{k+1})$, $\nabla_p c(p^{k+1})$, $b(p^{k+1})$ and $\nabla_p b(p^{k+1})$
Compute W^{k+1} by Powell's modified BFGS update.
$k \leftarrow k + 1$.
end while

and the first order KKT conditions

$$\nabla_p \mathcal{L}(p, y, z) = \nabla_p\phi(p) - \nabla_p b(p) y - \nabla_p c(p) z = 0 \tag{13a}$$

$$b(p) = 0 \tag{13b}$$

$$c(p) \geq 0 \tag{13c}$$

$$z \geq 0 \tag{13d}$$

$$c_i(p) = 0 \vee z_i = 0 \quad \forall i \tag{13e}$$

are used to test convergence of the SQP algorithm (Alg. 1).

The steps for solution of (10) by an SQP algorithm with line search are listed in Algorithm 1. The line search is based on Powell's ℓ_1 penalty function

$$P(p) = \phi(p) + \lambda'|b(p)| + \mu'|\min\{0, c(p)\}| \tag{14}$$

and the Armijo sufficient decrease condition. The penalty vectors, λ and μ, are selected such that they are numerically larger than the corresponding Lagrange multipliers, i.e. $\lambda \geq |y|$ and $\mu \geq z$ where y is the Lagrange multipliers associated with (10b) and z is the Lagrange multipliers associated with (10c).

3.2 Gradient Computation

The most time consuming computations in Algorithm 1 are computation of the objective function $\phi(p)$, computation of the derivatives of the objective function $\nabla_p\phi(p)$, computation of the dynamics $b(p)$, and computation of the sensitivities, $\nabla_p b(p)$, associated with the dynamics. $b(p)$ and $\phi(p)$ are computed by evaluation of (4) and (5), respectively. Consequently

$$b_k = b_k(x_k, x_{k+1}, u_k, d_k) = F_k(x_k, u_k, d_k) - x_{k+1} \tag{15a}$$

$$\nabla_{x_k} b_k = \nabla_{x_k} F_k(x_k, u_k, d_k) = S_{x_k}(t_{k+1})' = A_k' \tag{15b}$$

$$\nabla_{u_k} b_k = \nabla_{u_k} F_k(x_k, u_k, d_k) = S_{u_k}(t_{k+1})' = B_k' \tag{15c}$$

$$\nabla_{x_{k+1}} b_k = -I \tag{15d}$$

where $x(t_{k+1}) = F(x_k, u_k, d_k)$ and

$$\dot{x}(t) = f(x(t), u_k, d_k) \tag{16a}$$

$$\dot{S}_{x_k}(t) = \left(\frac{\partial f}{\partial x}(x(t), u_k, d_k)\right) S_{x_k}(t) \tag{16b}$$

$$\dot{S}_{u_k}(t) = \left(\frac{\partial f}{\partial x}(x(t), u_k, d_k)\right) S_{u_k}(t) + \left(\frac{\partial f}{\partial u}(x(t), u_k, d_k)\right) \tag{16c}$$

with the initial conditions $x(t_k) = x_k$, $S_{x_k}(t_k) = I$, and $S_{u_k}(t_k) = 0$. The stage cost and the associated derivatives are computed as

$$G_k = G_k(x_k, u_k, d_k) = \int_{t_k}^{t_{k+1}} g(x(t), u_k, d_k) dt \tag{17a}$$

$$q_k = \nabla_{x_k} G_k = \int_{t_k}^{t_{k+1}} \left(\frac{\partial g}{\partial x}(x(t), u_k, d_k)\right) S_{x_k}(t) dt \tag{17b}$$

$$r_k = \nabla_{u_k} G_k = \int_{t_k}^{t_{k+1}} \left[\left(\frac{\partial g}{\partial x}(x(t), u_k, d_k)\right) S_{u_k}(t) + \left(\frac{\partial g}{\partial u}(x(t), u_k, d_k)\right)\right] dt \tag{17c}$$

The derivatives $\nabla_{x_k} b_k$ and $\nabla_{x_k} G_k$ are computed for $\{x_k\}_{k=1}^{N-1}$ and $k \in \mathcal{N}$. These derivatives are not computed for x_0 as $x_0 \notin p$, i.e. x_0 is a fixed parameter of the optimisation problem but not a decision variable. The derivatives $\nabla_{u_k} b_k$ and $\nabla_{u_k} G_k$ are computed for $k \in \mathcal{N}$. The derivatives with respect to x_N are

$$\nabla_{x_N} b_{N-1} = -I \tag{18a}$$

$$p_N = \nabla_{x_N}\phi = \nabla_{x_N} h(x_N) \tag{18b}$$

In evaluation of the functions and derivatives needed in the SQP algorithm, i.e. evaluation of $\phi(p)$, $\nabla_p\phi(p)$, $b(p)$, and $\nabla_p b(p)$, the major computational task is solution to the differential equations (16) and evaluation of the associated quadrature equations (17). The Hovorka model is a non-stiff system of differential equations. Therefore, we use an embedded Dormand-Prince explicit Runge-Kutta scheme (DOPRI54) described in Dormand and Prince (1980) for solution of the differential equations (16) and integration of the quadrature equations (17). The Butcher tableau (see Butcher (2003)) of the DOPRI54 method is listed in Table 1. The DOPRI54 method has 7 stages, the advancing step, x, has order 5, and the error estimator, e, has order 4. A special DOPRI54 method tailored for solution of (16)-(17) has been implemented. In this implementation, we re-use the internal stages computed by solution of (16) in the evaluation of the quadrature equation (17). The implementation uses an adaptive time step based on PI-control developed by Gustafsson (1992).

When p is given as in the multiple shooting algorithm, evaluation of $c(p)$ and $\nabla_p c(p)$ becomes trivial. As $c(p)$ represents the bound constraints, $u_{\min} \leq u_k \leq u_{\max}$ for $k \in \mathcal{N}$, $\nabla_p c(p)$ is a constant and the corresponding constraints in the quadratic program (11) become bound constraints as well.

4. APPLICATION TO AN ARTIFICIAL PANCREAS

In this section we state and discuss the objective function and the scenarios used in the simulations. We also state the strategy for the non-linear model predictive controller.

Table 1. Butcher tableau for the DOPRI54 method.

0	0	0	0	0	0	0	0
$\frac{1}{5}$	$\frac{1}{5}$	0	0	0	0	0	0
$\frac{3}{10}$	$\frac{3}{40}$	$\frac{9}{40}$	0	0	0	0	0
$\frac{4}{5}$	$\frac{44}{55}$	$\frac{-56}{15}$	$\frac{32}{9}$	0	0	0	0
$\frac{8}{9}$	$\frac{19372}{6561}$	$\frac{-25360}{2187}$	$\frac{64448}{6561}$	$\frac{-212}{729}$	0	0	0
1	$\frac{9017}{3168}$	$\frac{-355}{33}$	$\frac{46732}{5247}$	$\frac{49}{176}$	$\frac{-5103}{18656}$	0	0
1	$\frac{35}{384}$	0	$\frac{500}{1113}$	$\frac{125}{192}$	$\frac{-2187}{6784}$	$\frac{11}{84}$	0
x	$\frac{5179}{57600}$	0	$\frac{7571}{16695}$	$\frac{393}{640}$	$\frac{-92097}{339200}$	$\frac{187}{2100}$	$\frac{1}{40}$
$\hat{x}$	$\frac{35}{384}$	0	$\frac{500}{1113}$	$\frac{125}{192}$	$\frac{-2187}{6784}$	$\frac{11}{84}$	0
e	$\frac{71}{57600}$	0	$\frac{-71}{16695}$	$\frac{71}{1920}$	$\frac{-17253}{339200}$	$\frac{22}{525}$	$\frac{-1}{40}$

4.1 Non-linear Model Predictive Control (NMPC)

NMPC is a receding horizon control technology that repeatedly solves open-loop non-linear optimal control problems and implements the computed optimal control associated to the current time period (see e.g. Rawlings and Mayne (2009)). In this contribution, we use a receding horizon strategy to compute the ideal insulin administration profile for people with type 1 diabetes. In order to obtain the ideal insulin profile, the NMPC uses state feedback and relative long prediction horizons.

4.2 Objective Function with Soft Output Constraints

The objective of the insulin administration is to compensate glucose excursions caused by meals and variations in endogenous glucose production and utilisation. We use a penalty function defined as

$$\begin{aligned}\rho(G(t)) = &\frac{\kappa_1}{2}|\max\{0, G(t) - \bar{G}\}|^2 \\ &+ \frac{\kappa_2}{2}|\max\{0, \bar{G} - G(t)\}|^2 \\ &+ \frac{\kappa_3}{2}|\max\{0, G(t) - G_U\}|^2 \\ &+ \frac{\kappa_4}{2}|\max\{0, G_L - G(t)\}|^2\end{aligned} \tag{19}$$

$G(t)$ is the blood glucose concentration, $\bar{G} = 5$ mmol/L is the target value for the blood glucose concentration, $G_L = 4$ mmol/L is a lower acceptable limit on the glucose concentration, and $G_U = 8$ mmol/L is an upper acceptable limit on the blood glucose concentration. The weights κ_1-κ_4 are used to balance the desirability of different deviations from the target. As hypoglycaemia is considered worse than hyperglycaemia, $\kappa_1 < \kappa_2$ and $\kappa_3 < \kappa_4$. The penalty function used in the simulations is illustrated in Fig. 4. $G(t)$ is a function of the state, $x(t)$, in the Hovorka model. Therefore, the penalty function (19) may be expressed as a stage cost in the form $g(x(t), u(t))$. The objective function used in the simulations is

$$\phi = \int_{t_0}^{t_f} g(x(t), u(t))dt + \frac{\eta}{2}\sum_{k=0}^{N-1} \|\Delta u_k\|_2^2 \tag{20}$$

where $\Delta u_k = u_k - u_{k-1}$. This objective function has no cost-to-go function, i.e. $h(x(t_f)) = 0$, and can be brought into the standard form (3a) using state augmentation formulated by Rawlings and Mayne (2009).

We use $u_{\min} = 0$ and a large $u_{\max}$ such that the upper bound is never active. We do the optimisation in a 24 hour window, i.e. $t_0 = 0$ min and $t_f = 24 \cdot 60$ min, using a sampling time of $T_s = 5$ min. In the scenario considered, the simulated 70 kg subject has a 62 g CHO meal at 6:00, a 55 g CHO meal at 12:00, and a 50 g CHO meal at 18:00. To ensure an optimal blood glucose profile, a prediction horizon of six hours, i.e., $N = 6 \cdot 12 = 72$ samples, is employed in the receding horizon strategy.

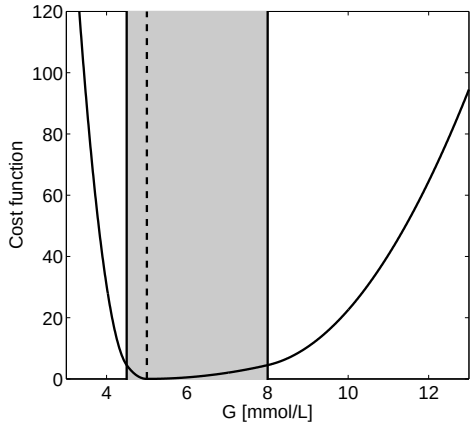

Fig. 4. Penalty as a function of the blood glucose concentration. The green shaded area is an interval of acceptable glucose concentrations. The target glucose concentration is 5 mmol/L. Blood glucose concentrations less than 3 mmol/L is very undesirable as people may fall into coma at this low blood glucose concentration.

5. SIMULATION RESULTS

In this Section, we use the model developed by Hovorka et al. (2004) and the developed multiple shooting SQP algorithm for (1) to compute insulin administration profiles for people with type 1 diabetes.

Fig. 5 illustrates an optimal insulin administration profile for the described scenario in the case where the controller knows the size and time of all meals in advance. Knowing the meal times and sizes allows the controller to deliver anticipatory insulin to pre-empt postprandial hyperglycaemia. However, the assumption that the patient would know in advance - and with accuracy - the meal times and sizes is not practical. Safety considerations would preclude significant amounts of insulin from being delivered prior to mealtime (as in this ideal scenario).

Fig. 6 shows the simulation results for the case in which the meals are announced to the MPC only at mealtime. Thus, the controller can deliver no anticipatory insulin prior to meals. The limitations for this case force the subject into (mild) hyperglycaemia, but hypoglycaemia is avoided. The insulin delivery profile for this case looks quite similar to bolus delivery of insulin by a pen; most of the meal-related insulin is delivered in bolus form in the few samples after the meals are taken (and announced). Simulated optimal bolus treatment with a pen provides glucose profiles comparable to the glucose profile in Fig. 6.

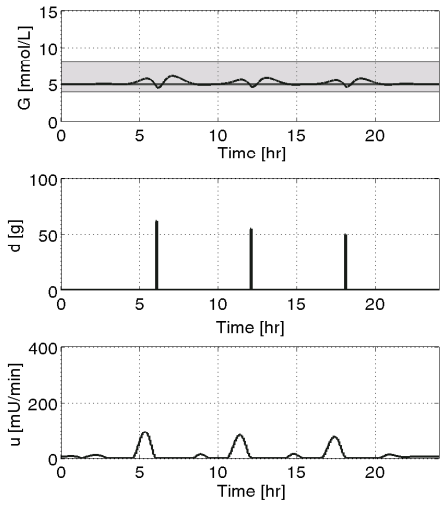

Fig. 5. Glucose profile (top), meal disturbances (middle) and optimal insulin administration profile (bottom) for the case with meal announcement in advance of the meal. Most insulin is taken before the meals.

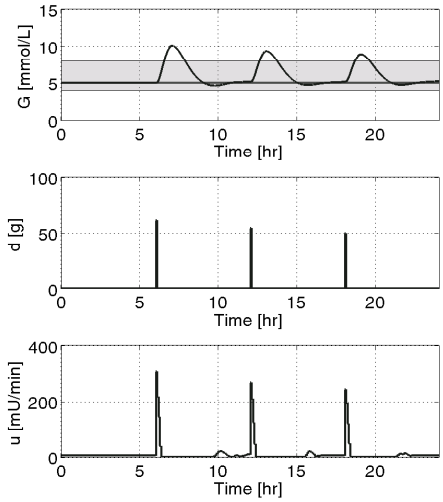

Fig. 6. Glucose profile (top), meal disturbances (middle) and optimal insulin administration profile (bottom) with meal announcement at meal time. Most insulin is taken in bolus like form at meal time.

These results demonstrate that for realistic cases, i.e., cases for which meal information is unknown until mealtime, reasonably good control can still be obtained. Perhaps more importantly, the bolus like nature of the insulin profile in this case suggests that a pen-based system may be able to achieve control comparable to that of a pump.

6. CONCLUSION

In this paper, we described a multiple shooting SQP algorithm for solution of a bound constrained continuous-time Bolza problem. Based on the model developed by Hovorka et al. (2004) for people with type 1 diabetes, we use our optimal control algorithm to compute insulin administration profiles for the cases with and without meal announcement in advance. The insulin profile for the realistic case with announcement of meals at mealtime is bolus like. This suggests that insulin treatment based on pen-systems may be nearly as effective as insulin treatment based on pump systems.

REFERENCES

Bock, H. and Plitt, K. (1984). A multiple shooting method for direct solution of optimal control problems. 242–247. Proc. of the IFAC 9th World Congress, Budapest, Hungary.

Butcher, J.C. (2003). *Numerical Methods for Ordinary Differential Equations*. Wiley, Chichester, England.

Diehl, M., Ferreau, J., and Haverbeke, N. (2009). Efficient numerical methods for nonlinear MPC and moving horizon estimation. In L. Magni, D.M. Raimondo, and F. Allgöwer (eds.), *Nonlinear Model Predictive Control. Towards New Challenging Applications*, 391–417. Springer, Berlin, Germany.

Dormand, J.R. and Prince, P.J. (1980). A family of embedded runge-kutta formulae. *Journal of Computational and Applied Mathematics*, 6(1), 19 – 26.

Gustafsson, K. (1992). *Control of Error and Convergence in ODE Solvers*. Ph.D. thesis, Department of Automatic Control, Lund Institute of Technology.

Hovorka, R., Canonico, V., Chassin, L.J., Haueter, U., Massi-Benedetti, M., Federici, M.O., Pieber, T.R., Schaller, H.C., Schaupp, L., Vering, T., and Wilinska, M.E. (2004). Nonlinear model predictive control of glucose concentration in subjects with type 1 diabetes. *Physiological Measurement*, 25, 905–920.

Jørgensen, J.B. (2005). *Moving Horizon Estimation and Control*. Ph.D. thesis, Department of Chemical Engineering, Technical University of Denmark.

Klonoff, D.C., Cobelli, C., Kovatchev, B., and Zisser, H.C. (2009). Progress in development of an artificial pancreas. *Journal of Diabetes Science and Technology*, 3, 1002–1004.

Rao, C.V., Wright, S., and Rawlings, J.B. (1998). Application of interior-point methods to model predictive control. *Journal of Optimization Theory and Applications*, 99(3), 723 – 757.

Rawlings, J.B. and Mayne, D.Q. (2009). *Model Predictive Control: Theory and Design*. Nob Hill Publishing, Madison, Wisconsin, USA.

World Health Organization (2009). Diabetes (fact sheet no. 312). WHO Web site: http://www.who.int/mediacentre/factsheets/fs312/en/.

APPENDIX D

Paper C

Optimal insulin administration for People with Type 1 Diabetes

Authors:

Dimitri Boiroux, Daniel Aaron Finan, John Bagterp Jørgensen, Niels Kjølstad Poulsen, and Henrik Madsen

Published in:

Proceedings of the 9th International Symposium on Dynamics and Control of Process Systems (DYCOPS 2010), pages 234-239, 2010.

Proceedings of the 9th International Symposium on
Dynamics and Control of Process Systems (DYCOPS 2010),
Leuven, Belgium, July 5-7, 2010
Mayuresh Kothare, Moses Tade, Alain Vande Wouwer, Ilse Smets (Eds.)

Optimal Insulin Administration for People with Type 1 Diabetes

Dimitri Boiroux * **Daniel A. Finan** * **John Bagterp Jørgensen** *
Niels Kjølstad Poulsen * **Henrik Madsen** *

* *Department of Informatics and Mathematical Modeling, Technical University of Denmark, DK-2800 Kgs Lyngby, Demmark (e-mail: {dibo,dafi,jbj,nkp,hm}@imm.dtu.dk)*

Abstract: In this paper we apply receding horizon constrained optimal control to the computation of insulin administration for people with type 1 diabetes. The study is based on the Hovorka model, which describes a virtual subject with type 1 diabetes. First of all, we compute the optimal insulin administration for the linearized system using quadratic programming (QP) for optimization. The optimization problem is a discrete-time problem with soft state constraints and hard input constraints. The computed insulin administration is applied to the nonlinear model, which represents the virtual patient. Then, a nonlinear discrete-time Bolza problem is stated and solved using sequential quadratic programming (SQP) for optimization and an explicit Dormand-Prince Runge-Kutta method (DOPRI54) for numerical integration and sensitivity computation. Finally, the effects of faster acting insulin on the postprandial (i.e., post-meal) blood glucose peak are discussed.

Keywords: Type 1 diabetes, model predictive control, physiological modeling, simulation

1. INTRODUCTION

The World Health Organization (2008) estimates that 180 million people worldwide have diabetes. This number is predicted to double by 2030. In the USA, the budget for diabetes alone represents 10% of the health care budget, or more than 130 billion dollars (132 billion dollars in 2002).

In people without diabetes, the blood glucose is controlled tightly around 90 mg/dL (∼5 mmol/L). Type 1 diabetes is a chronic disease characterized by an insufficient (effectively nonexistent) endogenous production of insulin, which leads to poor regulation of glucose concentrations in the blood. In particular, the deficiency of insulin causes sustained high glucose levels (hyperglycemia) that result in serious long-term health problems like eye, nerve, and kidney disease. On the other hand, too much insulin can result in very low glucose levels (hypoglycemia) which can pose immediate health risks. Exogenous insulin, then, must be injected to regulate the blood glucose concentration as tightly as possible.

Usually, insulin treatment consists of the administration of rapid acting insulin through boluses (i.e., discrete insulin administration) at the time of meals. The size of the bolus is based on a measurement of the current blood glucose at mealtime and the (estimated) size of the meal. However, having measurements only at mealtime does not provide enough information about blood glucose. Hypoglycemic and hyperglycemic events can go unobserved due to the infrequent blood glucose measurements. In addition, such a measurement process does not give any information about the dynamic trend of the blood glucose. Consequently, people with diabetes often tolerate hyperglycemia in order to avoid hypoglycemia and its immediate effects.

⋆ Funding for this research as part of the DIACON project from the Danish Council for Strategic Research is gratefully acknowledged.

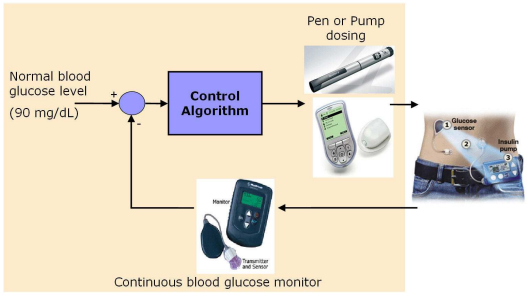

Fig. 1. Closed-loop glucose control. Glucose is measured subcutaneously using a continuous glucose monitor (CGM). Insulin is dosed either continuously by an insulin pump or discretely using an insulin pen.

Continuous glucose monitors (CGM) can help to provide a better control of blood glucose. They measure the glucose concentration in the subcutaneous depot. Insulin pumps that continuously inject fast acting insulin have also been developed. Combining a CGM with an insulin pump can enable automatic insulin administration for people with type 1 diabetes. Such a medical device is called an artificial pancreas and is illustrated in Fig. 1. Several research groups work on aspects of control algorithms integrating the CGM and the insulin pump to automatically adjust insulin administration for people with type 1 diabetes (see e.g. Klonoff et al. (2009)).

In this paper we describe the Hovorka model and use this description to point to the factors limiting ideal glucose

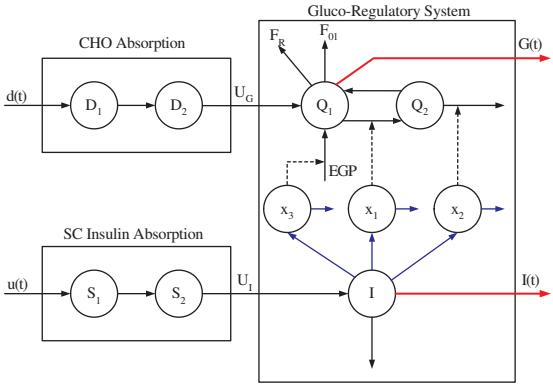

Fig. 2. Diagram of the Hovorka model.

control by insulin administration. One factor limiting the performance is the relative long absorption time of insulin. Using open-loop NMPC we describe quantitatively the maximal postprandial glucose in relation to the insulin absorption rate.

The paper is structured as following. Section 2 presents the model developed by Hovorka et al. (2004). Section 3 states an optimal control problem in the linear case. Section 4 presents the nonlinear optimal control problem and discusses the benefits of having faster-acting insulin. Conclusions are provided in Section 5.

2. MODEL

For the study of insulin administration and its effect on glucose concentrations we use a model developed by Hovorka et al. (2002, 2004). The model consists of a submodel describing food absorption, a submodel describing subcuteneous-to-intravenous absorption of insulin, a simple lumped model describing the glucose dynamics, and simple lumped models describing insulin dynamics and action mechanisms. In the following we describe these models.

2.1 Food Absorption

Food absorption models have been considered by a number of authors (Elashoff et al., 1982; Lehmann and Deutsch, 1992; Dalla Man et al., 2006; Goetze et al., 2007) and it has been observed that people with diabetes has abnormally slow gastric emptying (Horowitz et al., 2002).

In this paper, we consider a two-compartment model describing carbohydrate (CHO) absorption and conversion to glucose. The model describes the effect of orally ingested carbohydrates on the rate of appearance of glucose in the blood stream. The model is

$$\frac{dD_1}{dt}(t) = A_G D(t) - \frac{1}{\tau_D} D_1(t) \tag{1a}$$

$$\frac{dD_2}{dt}(t) = \frac{1}{\tau_D} D_1(t) - \frac{1}{\tau_D} D_2(t) \tag{1b}$$

in which $D(t)$ [mmol/min] is the amount of oral carbohydrate intake at any time expressed as glucose equivalents, A_G is a factor describing the utilization of carbohydrates to glucose, τ_D [min] is the time constant, $D_1(t)$ [mmol] and $D_2(t)$ [mmol] are the states describing the amount of glucose in the two compartments. The rate of appearance of absorption of glucose in the blood stream is described by

$$U_G(t) = \frac{1}{\tau_D} D_2(t) \tag{2}$$

$U_G(t)$ [mmol/min] is the glucose absorption rate. The carbohydrate input rate, $D(t)$ [mmol/min], may be related to the carbohydrate input rate, $d(t)$ [g/min], by

$$D(t) = \frac{1000}{M_{wG}} d(t) \tag{3}$$

in which M_{wG} [g/mol] is the molecular weight of glucose.

2.2 Insulin Absorption

Insulin is administered subcutaneously. A number of models to describe the absorption rate of subcutaneously injected short acting insulin in the blood stream are available (Wilinska et al., 2005).

In this paper we consider a two compartment model describing the absorption rate of subcutaneously administered short acting insulin. The model is

$$\frac{dS_1}{dt}(t) = u(t) - \frac{1}{\tau_S} S_1(t) \tag{4a}$$

$$\frac{dS_2}{dt}(t) = \frac{1}{\tau_S} S_1(t) - \frac{1}{\tau_S} S_2(t) \tag{4b}$$

in which $u(t)$ [mU/min] is the amount of insulin injected, τ_S [min] is the time constant, $S_1(t)$ [mU] and $S_2(t)$ [mU] are the amounts of insulin in the two compartments. The absorption rate of insulin in the blood stream is

$$U_I(t) = \frac{1}{\tau_S} S_2(t) \tag{5}$$

in which $U_I(t)$ [mU/min] is the absorption rate.

2.3 Glucose Subsystem

The blood glucose dynamics are modeled with two compartments. The two state variables are $Q_1(t)$ [mmol] and $Q_2(t)$ [mmol]. $Q_1(t)$ represents glucose in the main blood stream, while $Q_2(t)$ represents glucose in peripheral tissue such as muscles.

The model describing evolution of glucose in the main blood stream

$$\begin{aligned}\frac{dQ_1}{dt}(t) = {} & U_G(t) - F_{01,c}(t) - F_R(t) \\ & - x_1(t)Q_1(t) + k_{12}Q_2(t) \\ & + EGP_0(1 - x_3(t))\end{aligned} \tag{6}$$

includes absorption from the gut, $U_G(t)$ [mmol/min], consumption of glucose by the central nervous system, $F_{01,c}$ [mmol/min], the renal excretion of glucose in the kidneys, $F_R(t)$ [mmol/min], the insulin dependent uptake of glucose in muscles, $x_1(t)Q_1(t)$ [mmol/min], transfer of glucose from peripheral tissue such as muscle to the blood, $k_{12}Q_2(t)$, and endogenous release of glucose by the liver, $EGP_0(1-x_3(t))$. The uptake of glucose in muscles depends on insulin. $x_1(t)$ is a state representing insulin in muscle tissue. Release of glucose from the liver is also controlled by insulin. High concentrations of insulin suppress glucose release. $x_3(t)$ is used to model insulin in the liver.

Glucose in peripheral tissue such as muscle is modeled by the differential equation

$$\frac{dQ_2}{dt}(t) = x_1(t)Q_1(t) - (k_{12} + x_2(t))Q_2(t) \tag{7}$$

in which $x_1(t)Q_1(t)$ [mmol/min] is the transport of glucose from the main blood stream to the muscles, $k_{12}Q_2(t)$ [mmol/min], is transport of peripheral glucose to the main blood stream, and $x_2(t)Q_2(t)$ [mmol/min] is the insulin dependent disposal of glucose in the muscle cells. It depends on insulin modeled by $x_2(t)$.

The glucose concentration is

$$y(t) = G(t) = \frac{Q_1(t)}{V_G} \tag{8}$$

$y(t) = G(t)$ is the glucose concentration [mmol/L] and V_G is the glucose distribution volume. It depends on body weight, BW [kg], of the individual.

The consumption of glucose by the central nervous systems is modeled as

$$F_{01,c}(t) = \begin{cases} F_{01} & G(t) \geq 4.5 \text{ mmol/L} \\ F_{01}G(t)/4.5 & \text{otherwise} \end{cases} \tag{9}$$

At low glucose concentrations the consumption, $F_{01,c}$ [mmol/min], is proportional to the glucose concentration, $G(t)$, while it is constant when the glucose concentration is not low.

The excretion rate of glucose in the kidneys is zero unless the glucose concentration is high ($G(t) \geq 9$ mmol/L). In this case it is affine in the glucose concentration. Consequently, the glucose excretion rate, F_R [mmol/min], is modeled as

$$F_R(t) = \begin{cases} 0.003(G(t) - 9)V_G & G(t) \geq 9 \text{ mmol/L} \\ 0 & \text{otherwise} \end{cases} \tag{10}$$

2.4 Insulin Subsystem

Then the plasma insulin concentration, $I(t)$ [mU/L], evolves according to

$$\frac{dI}{dt}(t) = \frac{U_I(t)}{V_I} - k_e I(t) \tag{11}$$

The insulin action is governed by influence on transport and distribution $x_1(t)$, utilization and phosphorylation of glucose in adipose tissue $x_2(t)$, and endogenous production in the liver $x_3(t)$. These quantities are described by the differential equations

$$\frac{dx_1}{dt}(t) = -k_{a1}x_1(t) + k_{b1}I(t) \tag{12a}$$

$$\frac{dx_2}{dt}(t) = -k_{a2}x_2(t) + k_{b2}I(t) \tag{12b}$$

$$\frac{dx_3}{dt}(t) = -k_{a3}x_3(t) + k_{b3}I(t) \tag{12c}$$

2.5 Parameters

The parameters in the Hovorka model (1)-(12) are listed in Table 1. The parameters $k_{b,i}$ are related to the insulin sensitivities, $S_{I,i}$, by

$$k_{b,i} = S_{I,i}k_{a,i} \qquad i = 1, 2, 3 \tag{13}$$

Table 1. Parameters in the Hovorka Model.

	Symbol	Value	Unit
Transfer rate	k_{12}	0.066	1/min
Deactivation rate	k_{a1}	0.006	1/min
Deactivation rate	k_{a2}	0.06	1/min
Deactivation rate	k_{a3}	0.03	1/min
Insulin elimination rate	k_e	0.138	1/min
CHO absorption constant	τ_D	40	min
Insulin absorption constant	τ_S	55	min
CHO utilization	A_G	0.8	-
Transport insulin sensitivity	$S_{I,1}$	$51.2 \cdot 10^{-4}$	L/mU
Disposal insulin sensitivity	$S_{I,2}$	$8.2 \cdot 10^{-4}$	L/mU
EGP insulin sensitivity	$S_{I,3}$	$520 \cdot 10^{-4}$	L/mU
Insulin distribution volume	$\frac{V_I}{BW}$	0.12	L/kg
Glucose distribution volume	$\frac{V_G}{BW}$	0.16	L/kg
Liver glucose production	$\frac{EGP_0}{BW}$	0.0161	$\frac{\text{mmol}}{\text{min}}$/kg
CNS glucose consumption	$\frac{F_{01}}{BW}$	0.0097	$\frac{\text{mmol}}{\text{min}}$/kg

Some parameters are related to the body weight, BW [kg], of the individual being considered. For a 70 kg person ($BW = 70$ kg), these parameters are

$$V_I = 0.12 \text{ L/kg} \cdot 70 \text{ kg} = 8.4 \text{ L} \tag{14a}$$

$$V_G = 0.16 \text{ L/kg} \cdot 70 \text{ kg} = 11.2 \text{ L} \tag{14b}$$

$$EGP_0 = 0.0161 \frac{\text{mmol}}{\text{min}}/\text{kg} \cdot 70 \text{ kg} = 1.1270 \frac{\text{mmol}}{\text{min}} \tag{14c}$$

$$F_{01} = 0.0097 \frac{\text{mmol}}{\text{min}}/\text{kg} \cdot 70 \text{ kg} = 0.6790 \frac{\text{mmol}}{\text{min}} \tag{14d}$$

The European unit for glucose concentration is mmol/L and the American unit is mg/dL. One can convert between these units using the molecular weight of glucose ($C_6H_{12}O_6$): $M_{wG} = 180.1577$ g/mol.

3. LINEAR MODEL PREDICTIVE CONTROL

In this section, we formulate and discuss the linearized optimal control problem. Let $x(t) \in \mathbf{R}^{n_x}$ be the state vector, $u(t) \in \mathbf{R}^{n_u}$ be the manipulated inputs, and $d(t) \in \mathbf{R}^{n_d}$ be known disturbances.

A zero-order hold parametrization for the manipulated variables function u and the disturbance function d is used. We divide the time interval, $[t_0, t_f]$, into N equidistant intervals, each of length T_s. We denote $\mathcal{N} = \{0, 1, ..., N-1\}$ and $t_k = t_0 + kT_s$ for $k \in \mathcal{N}$. The zero-order hold restrictions on d and u imply

$$u(t) = u_k \qquad t_k \leq t < t_{k+1} \qquad k \in \mathcal{N} \tag{15a}$$

$$d(t) = d_k \qquad t_k \leq t < t_{k+1} \qquad k \in \mathcal{N} \tag{15b}$$

3.1 Hard Output Constraints

Using the zero-order hold parametrization (15), the linear discrete-time optimal control problem may be expressed as

$$\min_{\{u_k\}_{k=0}^{N-1}} \quad \phi = \phi\left(\{u_k, y_{k+1}, r_{k+1}\}_{k=0}^{N-1}\right) \tag{16a}$$

$$s.t. \quad x_{k+1} = Ax_k + Bu_k + Ed_k \tag{16b}$$

$$y_k = Cx_k \tag{16c}$$

$$u_{\min} \leq u_k \leq u_{\max} \tag{16d}$$

$$\Delta u_{\min} \leq \Delta u_k \leq \Delta u_{\max} \tag{16e}$$

$$y_{\min} \leq y_k \leq y_{\max} \tag{16f}$$

in which $x_k \in \mathbf{R}^{n_x}$ is the state vector at time t_k, and y_k is the measured output at time t_k. The manipulated inputs u_k and the difference $\Delta u_k = u_{k+1} - u_k$ must lie in the interval $[u_{\min},\ u_{\max}]$ and $[\Delta u_{\min},\ \Delta u_{\max}]$ respectively.

The objective function ϕ is in the form

$$\phi = \frac{1}{2}\sum_{k=0}^{N-1} \|y_{k+1} - r_{k+1}\|_2^2 + \lambda\|\Delta u_k\|_2^2 \tag{17}$$

Furthermore, the measured output y_k must lie in the interval $[y_{\min},\ y_{\max}]$. In the insulin administration problem, it means that the blood glucose at sample times must be kept in the normoglycemic range (60-140 mg/dL or 3.3-7.8 mmol/L).

However, infeasibility of (16) might arise due to the hard constraints on the measured output y_k. Consequently, it is preferable to replace the hard constraints (16f) with soft output constraints.

3.2 Soft Output Constraints

The hard constraints (16f) are replaced by soft constraints using the slacks variables v_k and w_k. The new objective function is

$$\phi = \frac{1}{2}\sum_{k=0}^{N-1} \|y_{k+1} - r_{k+1}\|_2^2 + \lambda\|\Delta u_k\|_2^2 + \kappa_1\|v_k\|_2^2 + \kappa_2\|w_k\|_2^2 \tag{18}$$

The two new terms $\kappa_1\|v_k\|_2^2 + \kappa_2\|w_k\|_2^2$ correspond to penalty costs for hyperglycemia and hypoglycemia respectively.

The linear discrete-time optimal control problem with soft constraints that has to be solved may be expressed as

$$\min_{\{u_k, v_k, w_k\}_{k=0}^{N-1}} \quad \phi = \phi\left(\{u_k, y_{k+1}, r_{k+1}, v_k, w_k\}_{k=0}^{N-1}\right) \tag{19a}$$

$$s.t. \quad x_{k+1} = Ax_k + Bu_k + Ed_k \tag{19b}$$

$$y_k = Cx_k \tag{19c}$$

$$u_{\min} \leq u_k \leq u_{\max} \tag{19d}$$

$$\Delta u_{\min} \leq \Delta u_k \leq \Delta u_{\max} \tag{19e}$$

$$y_{\min} - y_k \leq w_k \tag{19f}$$

$$y_k \leq y_{\max} + v_k \tag{19g}$$

$$v_k \geq 0 \tag{19h}$$

$$w_k \geq 0 \tag{19i}$$

in which the hard output constraint (16f) has been replaced with penalty terms in the objective function (18) and the inequality constraints (19f - 19i).

3.3 Linear simulation results

We use the Hovorka et al. (2004) model linearized at the steady state corresponding to the target blood glucose concentration $\bar{G} = 5$ mmol/L to compute the optimal insulin administration profiles. Then, we apply this profile to the Hovorka et al. (2004) model.

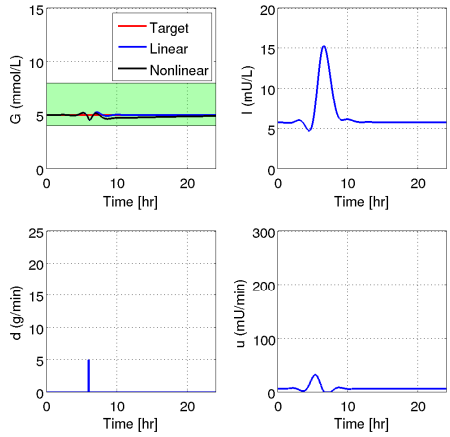

Fig. 3. MPC with soft output constraints on glucose concentration. The small meal case. Upper left corner: Blood glucose concentration. Upper right corner: Insulin concentration. Lower left corner: Disturbance (Meals). Lower right corner: Injected insulin

The objective of the insulin administration is to compensate glucose excursions caused by meals and variations in endogenous glucose production and utilization. We use a penalty function defined by (18). y_k is the blood glucose concentration, $r_k = 5$ mmol/L is the target value for the blood glucose concentration, $y_{min} = 4$ mmol/L is a lower acceptable limit on the glucose concentration, and $y_{max} = 8$ mmol/L is an upper acceptable limit on the blood glucose concentration. The weights κ_1 and κ_2 are used to balance the desirability of different deviations from the target. As hypoglycemia is considered a more immediate danger than hyperglycemia, $\kappa_1 < \kappa_2$.

The choice of the weight λ should not change the shape of the optimal blood glucose profile. It is used to avoid ill-conditioning of the problem. For all the simulations, we use $\lambda = 10^{-2}$.

We use $u_{\min} = 0$ and a large $u_{\max}$ such that the upper bound is never active. We do the optimization in a 24 hour window, i.e. $t_0 = 0$ min and $t_f = 24 \cdot 60$ min, using a sampling time of $T_s = 5$ min. In the three scenarios considered, the simulated 70 kg subject has a meal at 6:00. The meal sizes for each scenario are 25 g CHO, 50 g CHO and 100 g CHO, respectively. We compute the optimal insulin administration using the linearized model, and simulate a virtual patient using this sequence of insulin administration on the Hovorka model (Hovorka et al. (2004)).

Fig. 3 illustrates an optimal insulin administration profile for the case where the meal size is relatively small. Having a small meal implies a small deviation to the steady state. Consequently, the linear and nonlinear solutions are quite similar.

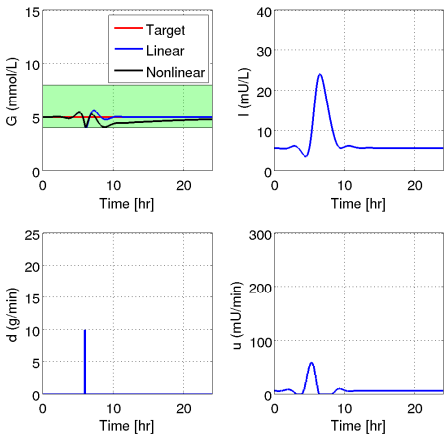

Fig. 4. MPC with soft output constraints on glucose concentration. The normal-sized meal case.

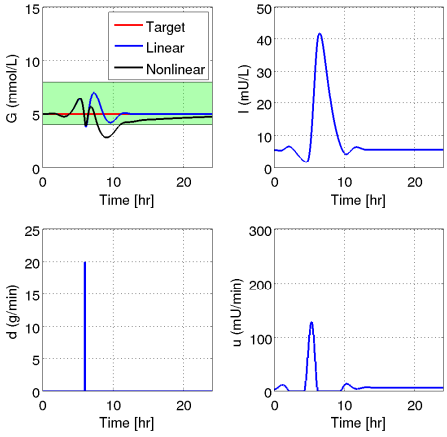

Fig. 5. MPC with soft output constraints on glucose concentration. The large meal case.

Fig. 4 illustrates an optimal insulin administration profile for the case where the meal size is normal. Although the mismatch between the linear and the nonlinear model becomes more evident, hypoglycemia is avoided.

Fig. 5 illustrates an optimal insulin administration profile for the case where the meal size is large. A hypoglycemic event occurs when the computed insulin is injected to the virtual patient.

4. NONLINEAR MODEL PREDICTIVE CONTROL

In this section, we state and discuss the continuous-time nonlinear optimal control problem that we use to compute the insulin injection profiles for people with type 1 diabetes. The bound-constrained continuous-time optimal control problem

$$\min_{\{u_k\}_{k=0}^{N-1}} \quad \phi = \phi\left(\{u(t), y(t), r(t)\}_{t=t_0}^{t=t_f}\right) \tag{20a}$$

$$s.t. \quad x(t_0) = x_0 \tag{20b}$$

$$\dot{x}(t) = f(x(t), u(t), d(t)) \tag{20c}$$

$$y(t) = g(x(t)) \tag{20d}$$

$$u(t) = u_k \qquad t_k \le t < t_{k+1} \tag{20e}$$

$$u_{\min} \le u_k \le u_{\max} \tag{20f}$$

$$\Delta u_{\min} \le \Delta u_k \le \Delta u_{\max} \tag{20g}$$

is used to compute the optimal insulin administration. $x(t) \in \mathbf{R}^{n_x}$ is the state vector, $u(t) \in \mathbf{R}^{n_u}$ is the vector of manipulated inputs for $t_k \le t < t_{k+1}$, $y(t) \in \mathbf{R}^{n_y}$ is the vector of measured outputs and $d(t) \in \mathbf{R}^{n_d}$ are known disturbances. $\dot{x}(t) = f(x(t), u(t), d(t))$ represents the model equations. The initial time, t_0, and the final time, t_f, are specified parameters. The initial state, x_0, is a known parameter in (20). The inputs are bound-constrained and must lie in the interval $[u_{\min}, u_{\max}]$, and the difference $\Delta u_k = u_{k+1} - u_k$ must lie in the interval $[\Delta u_{\min}, \Delta u_{\max}]$.

The objective of the insulin administration is to mitigate glucose excursions caused by meals and variations in endogenous glucose production and utilization. We use a penalty function defined as

$$\begin{aligned}\phi = &\frac{1}{2}\sum_{k=0}^{N-1}\Big[\int_{t_k}^{t_{k+1}} (y(t) - r_{k+1})^2 + \\ &\kappa_1 \| \max\{y_{\min} - y(t), 0\}\|_2^2 + \\ &\kappa_2 \| \max\{y(t) - y_{\max}, 0\}\|_2^2 \Big]\, \mathrm{d}t + \lambda \|\Delta u_k\|_2^2\end{aligned} \tag{21}$$

4.1 Optimal insulin administration

Fig. 6 illustrates an optimal insulin administration profile in the case where the controller knows the size and time of all meals in advance. Computing the solution using the nonlinear model allows the controller to avoid mismatches. However, the assumption that the patient would know in advance the meal times and sizes is not practical. Safety considerations would preclude significant amounts of insulin from being delivered prior to mealtime.

Fig. 7 shows the simulation results for the case in which the meals are announced to the MPC only at mealtime. Thus, the controller can deliver no anticipatory insulin prior to meals. The limitations for this case force the subject into hyperglycemia, but hypoglycemia is avoided.

Fig. 8 shows the maximum blood glucose versus the insulin time constant τ_s for small-sized meals (25 g CHO), normal-sized meals (50 g CHO) and large-sized meals (100 g CHO) if the meal is announced only at mealtime. A faster insulin reduces the peak of glucose. For normal-sized meals, having an insulin absorption time constant at least equal to the glucose absorption time constant (i.e. $\tau_s = 40$ minutes) avoids hyperglycemic events.

5. CONCLUSION

In this paper, we described a model developed by Hovorka et al. (2004) to study the effects of insulin administration on glucose concentration for people with type 1 diabetes. Based on a linearized version of this model, we use an

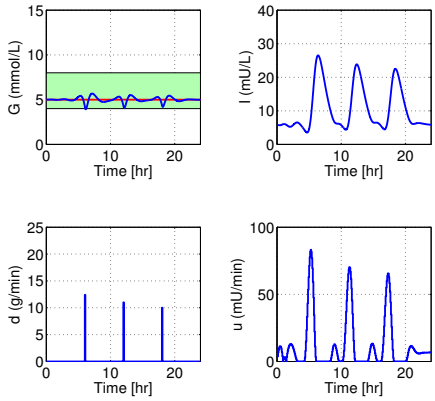

Fig. 6. Optimal insulin administration profile obtained using NMPC.

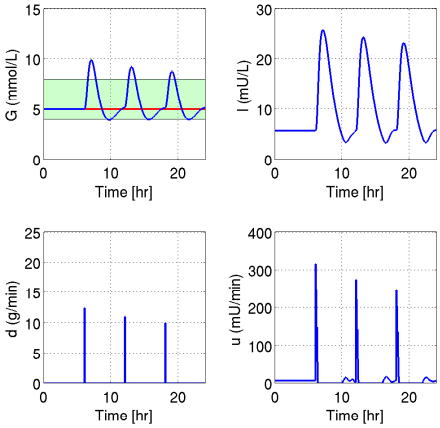

Fig. 7. Optimal insulin administration with meal announcement at meal time.

optimal control algorithm to compute insulin administration profiles for the case with meal announcement in advance. The insulin profile simulated on the nonlinear model does not match the optimal insulin administration for the linearized model only if the meal is too large.

We use our optimal control algorithm to compute insulin administration profiles for the cases with and without meal announcement in advance, and we also compute the maximum blood glucose versus the insulin time constant for small-, normal- and large-sized meals. The results suggest that having faster acting insulin can significantly increase the control quality of blood glucose.

REFERENCES

Dalla Man, C., Camilleri, M., and Cobelli, C. (2006). A system model of oral glucose absorption: Validation on gold standard data. *IEEE Transactions on Biomedical Engineering*, 53, 2472–2478.

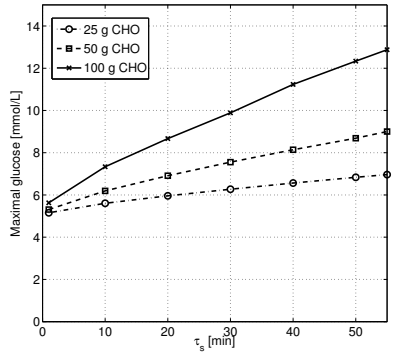

Fig. 8. Maximal blood glucose versus insulin time constant τ_s for 25 g CHO (dash-dotted line, 50 g CHO (dashed line), and 100 g CHO meals (solid line).

Elashoff, J.D., Reedy, T.J., and Meyer, J.H. (1982). Analysis of gastric emptying data. *Gastroenterology*, 83, 1306–1312.

Goetze, O., Steingoetter, A., Menne, D., van der Voort, I.R., Kwiatek, M.A., Boesiger, P., Weishaupt, D., Thumshirn, M., Fried, M., and Schwizer, W. (2007). The effect of macronutrients on gastric volume responses and gastric emptying in humans: A magnetic resonance imaging study. *Am J Physiol Gastrointest Liver Physiol*, 292, G11–G17.

Horowitz, M., O'Donovan, D., Jones, K.L., Feinle, C., Rayner, C.K., and Samsom, M. (2002). Gastric emptying in diabetes: Clinical significance and treatment. *Diabetic Medicine*, 19, 177–194.

Hovorka, R., Shojaee-Moradie, F., Caroll, P.V., Chassin, L.J., Gowrie, I.J., Jackson, N.C., Tudor, R.S., Umpleby, A.M., and Jones, R.H. (2002). Partitioning glucose distribution/transport, disposal, and endogenous production during IVGTT. *Am. J. Physiol.*, 282, E992–E1007.

Hovorka, R., Canonico, V., Chassin, L.J., Haueter, U., Massi-Benedetti, M., Federici, M.O., Pieber, T.R., Schaller, H.C., Schaupp, L., Vering, T., and Wilinska, M.E. (2004). Nonlinear model predictive control of glucose concentrations in subjects with type 1 diabetes. *Physiological Measurement*, 25, 905–920.

Klonoff, D.C., Cobelli, C., Kovatchev, B., and Zisser, H.C. (2009). Progress in development of an artificial pancreas. *Journal of Diabetes Science and Technology*, 3, 1002–1004.

Lehmann, E.D. and Deutsch, T. (1992). A physiological model of glucose-insulin interaction in type 1 diabetes mellitus. *Journal of Biomedical Engineering*, 14, 235–242.

Wilinska, M.E., Chassin, L.J., Schaller, H.C., Schaupp, L., Pieber, T.R., and Hovorka, R. (2005). Insulin kinetics in type-1 diabetes: Continuous and bolus delivery of rapid acting insulin. *IEEE Transactions on Biomedical Engineering*, 52, 3–12.

World Health Organization (2008). Diabetes (fact sheet no. 312). WHO Web site: http://www.who.int/mediacentre/factsheets/fs312/en/.

APPENDIX E

Paper D

Meal Estimation in Nonlinear Model Predictive Control for Type 1 Diabetes

Authors:

Dimitri Boiroux, Daniel Aaron Finan, John Bagterp Jørgensen, Niels Kjølstad Poulsen, and Henrik Madsen

Published in:

Preprints of the 8th IFAC Symposium on Nonlinear Control Systems, pages 1052-1057. Springer, 2010

Meal Estimation in Nonlinear Model Predictive Control for Type 1 Diabetes

Dimitri Boiroux * **Daniel A. Finan** * **John Bagterp Jørgensen** *
Niels Kjølstad Poulsen * **Henrik Madsen** *

* *Department of Informatics and Mathematical Modeling, Technical University of Denmark, DK-2800 Kgs Lyngby, Denmark (e-mail: {dibo,dafi,jbj,nkp,hm}@imm.dtu.dk)*

Abstract: In this paper we apply receding horizon constrained nonlinear optimal control to the computation of insulin administration for people with type 1 diabetes. In particular, the sizes and the times of the meals are assumed to be unknown, and have to be estimated using a continuous-discrete extended Kalman filter (EKF). The optimization problem is a discrete-time Bolza problem with soft state constraints and hard input constraints. This problem is solved using a sequential quadratic programming (SQP) algorithm. An explicit Dormand-Prince Runge-Kutta method (DOPRI54) is used for numerical integration, including integration of the mean-covariance pair, and sensitivity computation. The study is based on the Hovorka model, which is a continuous-time physiological model describing a virtual subject with type 1 diabetes. The paper describes the key aspects of the numerical implementation and provides quantitative insight into the factors limiting the achievement of acceptable closed-loop performance.

Keywords: Model predictive control, biomedical systems, type 1 diabetes mellitus, extended Kalman filter.

1. INTRODUCTION

Insulin is a hormone that reduces the glucose concentration in blood. It facilitates the uptake of glucose into cells (adipose tissues, muscles, etc.) and the storage of glucose in the liver. In people without diabetes, the blood glucose is tightly regulated around 90 mg/dL (or 5 mmol/L). Diabetes is a disease characterized by an insufficient production of insulin, a decrease in its effectiveness, or both. Thus, the most common consequence of the disease is having blood glucose levels that are too high, but blunted counterregulatory responses also result in levels that are too low.

Type 1 (also known as insulin-dependent) diabetes—the most severe form of the disease—is characterized by total lack of insulin production. Exogenous insulin must be injected to keep the glucose concentration in the normal (i.e., normoglycemic) range (say, 60-140 mg/dL or 3.3-7.8 mmol/L). If the glucose concentration falls below the normoglycemic range (hypoglycemia), the subject may suffer seizures, fall into a coma or even die. On the other hand, a blood glucose concentration chronically above the normoglycemic range (hyperglycemia) has long-term complications like vascular, nerve, eye and kidney diseases.

A basal infusion of insulin is necessary to counterbalance the continuous production of glucose by the liver. Glucose production from the liver is a two-part process: glycogenolysis (breakdown of glycogen to glucose) and gluconeogenesis (synthesis of glucose from amino acids). The main disturbances affecting the blood glucose levels are meal carbohydrates (CHO) absorbed in the gut, physical activity (Breton (2008)), and variations in insulin sensitivity.

Today, proper treatment for people with type 1 diabetes involves at least 3–4 blood glucose measurements per day. It is common to take these measurements shortly before meal times. It is also common to inject rapid acting insulin at meal time in order to compensate for ingested meal CHO, thus regulating the blood glucose level. Digestion and absorption of CHO from the gastrointestinal tract to the blood is generally faster than absorption of subcutaneously injected insulin into the blood. Furthermore, the glucose-insulin dynamics are complex and nonlinear. Consequently, the ability to control the blood glucose using the conventional insulin therapy is limited. The outcome of a conventional insulin therapy is illustrated in Fig. 1.

The amount of injected insulin is based on the current blood glucose and a (rough) estimation of the amount of CHO in the meal. However, discrete measurements of blood glucose do not account for its local trend, and estimating the carbohydrates of a meal may be difficult. The conception and development of continuous glucose monitors (CGMs), and continuous subcutaneous insulin infusion (CSII) pumps, have improved considerably the insulin therapy for people with type 1 diabetes. Moreover, these technologies can be used in an artificial pancreas, which will automatically adjust the insulin dosage to control blood glucose. Several research groups work on aspects of control algorithms integrating the CGM and the insulin pump; see, e.g. Klonoff et al. (2009), Cobelli et al. (2009) and Magni et al. (2009).

⋆ Funding for this research as part of the DIACON project from the Danish Council for Strategic Research is gratefully acknowledged.

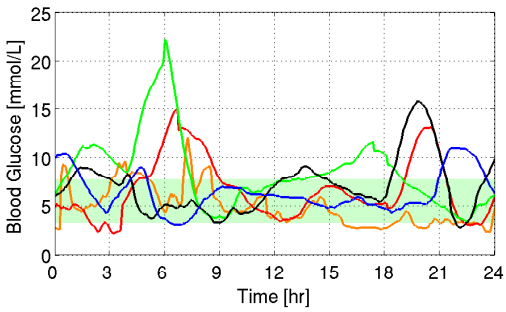

Fig. 1. Glucose concentration tracings in an individual with type 1 diabetes for five consecutive days using conventional insulin therapy based on discrete glucose measurements and discrete insulin injections. The green-shaded area corresponds to the normoglycemic range.

However, the quality of the controller is limited by the lag associated with the subcutaneous injection of insulin. In the Hovorka et al. (2004) model, the absorption and transport of subcutaneously injected insulin to systemic circulation in the blood is modeled as a two-compartment model with time constants of $\tau_S = 55$ min. The absorption of meal CHO is also modeled as a two-compartment model, but with time constants of $\tau_D = 40$ min. The difference in these lags limits the quality of the closed-loop control.

In this paper, we use constrained nonlinear optimal control theory to compute the optimal insulin injection rates during a day. We compare the blood glucose profiles in the cases where A) full state information is available (meals are announced to the controller at meal time), and B) meals are not announced to the controller. In the case where full state information is not available, the state is reconstructed by the continuous-discrete EKF. In particular, we try to estimate the glucose rate of appearance accurately. Furthermore, we assume that the measured glucose is subject to noise.

The paper is structured as follows. The continuous-discrete time extended Kalman filter (EKF) is presented in section 2. Section 3 states and discusses the constrained nonlinear program (NLP) which determines the optimal insulin profiles. Section 4 presents the algorithm for filtering and prediction, and the scheme used for numerical integration. Section 5 applies the continuous-discrete EKF algorithm to compute insulin administration profiles for virtual subjects with type 1 diabetes in the case where meals are not announced to the controller, or in the case where the meal is announced with an overestimated meal size. Conclusions are provided in Section 6.

2. THE CONTINUOUS-DISCRETE EKF

In this section, we introduce the extended Kalman filter (EKF) for continuous-discrete stochastic nonlinear systems (Jazwinski, 1970; Nørgaard et al., 2000; Jørgensen et al., 2007). The EKF is used to estimate the state of the system given a stochastic continuous-time model and measurements at discrete times, i.e.

$$d\boldsymbol{x}(t) = f(t, \boldsymbol{x}(t), u(t))dt + \sigma d\boldsymbol{\omega}(t) \tag{1a}$$
$$\boldsymbol{y}_k = h(t_k, \boldsymbol{x}(t_k)) + \boldsymbol{v}_k \tag{1b}$$

in which $\{\boldsymbol{\omega}(t),\ t \geq 0\}$ is a standard Wiener process, i.e. a process with covariance Idt (intensity I). The matrix σ is time-invariant. The measurement noise $\boldsymbol{v}_k$ is normally distributed, $\boldsymbol{v}_k \sim N_{iid}(0, R_k)$. We assume that the initial state $\boldsymbol{x}_0$ is normally distributed with a known mean and covariance, $\boldsymbol{x}_0 \sim N(\hat{x}_{0|-1}, P_{0|-1})$.

2.1 Filtering

Given an observation, y_k, at time t_k, the filtering in the EKF describes the steps used to compute the filtered state $\hat{x}_{k|k}$ and the corresponding covariance $P_{k|k}$. The filter step assumes availability of the one-step predicitons, $\hat{x}_{k|k-1}$ and $P_{k|k-1}$.

The filter gain is computed by

$$C_k = \frac{\partial h}{\partial x}(t_k, \hat{x}_{k|k-1}) \tag{2a}$$
$$R_{k|k-1} = C_k P_{k|k-1} C_k' + R_k \tag{2b}$$
$$K_k = P_{k|k-1} C_k' \left(R_{k|k-1}\right)^{-1} \tag{2c}$$

and the innovation is obtained by

$$e_k = y_k - \hat{y}_{k|k-1} = y_k - h(t_k, \hat{x}_{k|k-1}) \tag{3}$$

The filtered state $\hat{x}_{k|k}$ and its covariance $P_{k|k}$ are given by

$$\hat{x}_{k|k} = \hat{x}_{k|k-1} + K_k e_k \tag{4a}$$
$$P_{k|k} = P_{k|k-1} - K_k R_{k|k-1} K_k' \tag{4b}$$

2.2 Prediction

Given the observations $\mathcal{Y}_k = \{y_0, y_1, \ldots, y_k\}$, the predicted state vector $\hat{x}_{k+1|k} = \hat{x}_k(t_{k+1})$ and its associated covariance $P_{k+1|k} = P_k(t_{k+1})$ are computed as the solutions to the system of ordinary differential equations (Jørgensen et al. (2007))

$$\frac{d\hat{x}_k(t)}{dt} = f(t, \hat{x}_k(t), u_k) \tag{5a}$$
$$\frac{dP_k(t)}{dt} = A_k(t)P_k(t) + P_k(t)A_k(t)' + \sigma\sigma' \tag{5b}$$

with

$$A_k(t) = A(t, \hat{x}_k(t), u_k) = \frac{\partial f}{\partial x}(t, \hat{x}_k(t), u_k) \tag{6}$$

and the initial conditions

$$\hat{x}_k(t_k) = \hat{x}_{k|k} \tag{7a}$$
$$P_k(t_k) = P_{k|k} \tag{7b}$$

The numerical integration of (5) is computed using an explicit DOPRI54 method described in Section 4.1.

3. THE OPTIMAL CONTROL PROBLEM

At each time sample, Nonlinear Model Predictive Control solves an open-loop optimal control problem. We consider the continuous-time optimal control problem

$$\min_{x(\cdot), u(\cdot)} \ \phi = \int_{t_k}^{t_k+T} g(x(t), u(t))dt + \frac{1}{2}\sum_{i=k}^{k+N-1} \|\Delta u_i\|^2_{2,S} \tag{8a}$$

$$s.t. \quad x(t_k) = \hat{x}_{k|k} \tag{8b}$$
$$\dot{x}(t) = f(t, x(t), u(t)) \qquad t \in [t_k, t_k + T[\tag{8c}$$
$$u_{\min} \leq u(t) \leq u_{\max} \qquad t \in [t_k, t_k + T[\tag{8d}$$

parameterized using a zero-order hold

$$u(t) = u_k \qquad t_k \leq t < t_{k+1} \tag{9}$$

such that $\Delta u_k = u_k - u_{k-1}$ is well defined. The systems is discretized by $t_{i+1} = t_i + T_s$ with T_s being the sample time. The control horizon, T, and the sample time, T_s, are related by $T = NT_s$.

The optimal control problem (8) is solved using a multiple shooting algorithm (Bock and Plitt, 1984; Binder et al., 2001; Diehl et al., 2009). Our implementation of the multiple shooting algorithm is based on sequential quadratic programming (SQP) for optimization and an explicit Dormand-Prince Runge-Kutta method (DOPRI54) for numerical integration and sensitivity computation (Boiroux et al., 2009a). DOPRI54 is described in Section 4.1.

The objective of the insulin administration is to mitigate glucose excursions caused by meals and variations in endogenous glucose production and utilization. We use a penalty function defined as

$$\begin{aligned} g(x(t), u(t)) = &\frac{\kappa_1}{2} |\max\{0, G(t) - \bar{G}\}|^2 \\ &+ \frac{\kappa_2}{2} |\max\{0, \bar{G} - G(t)\}|^2 \\ &+ \frac{\kappa_3}{2} |\max\{0, G(t) - G_U\}|^2 \\ &+ \frac{\kappa_4}{2} |\max\{0, G_L - G(t)\}|^2 \end{aligned} \tag{10}$$

$G(t)$ is the blood glucose concentration, $\bar{G} = 5$ mmol/L is the target value for the blood glucose concentration, $G_L = 4$ mmol/L is a lower acceptable limit on the glucose concentration, and $G_U = 8$ mmol/L is an upper acceptable limit on the blood glucose concentration. The weights κ_1-κ_4 are used to balance the desirability of different deviations from the target. As hypoglycemia is considered a more acute threat than hyperglycemia, $\kappa_1 < \kappa_2$ and $\kappa_3 < \kappa_4$.

We call the second term of the objective function (8a) a regularization term. This term is used to smooth the solution and avoid too sudden variations in the insulin administration. For the simulations we use $S = 10^{-2}$.

4. NUMERICAL IMPLEMENTATION

In this section we describe our algorithm for output based Nonlinear Model Predictive Control. We also introduce the numerical method used for integration of the systems of differential equations arising in output based Nonlinear Model Predictive Control. The numerical integration is an important part of the continuous-discrete EKF as well as the optimal control problem.

4.1 The DOPRI54 Method

The Hovorka model is a non-stiff system of differential equations. Therefore, we use an embedded explicit Runge-Kutta scheme derived by Dormand and Prince (1980) (DOPRI54) for the solution of the model equations, the sensitivity computation and the computation of the mean-covariance pair in the extended Kalman filter. Explicit Runge-Kutta schemes are described in Gustafsson (1992). They are characterized by a Butcher tableau as given in Table 1. The Dormand-Prince Runge-Kutta Integration

Table 1. Butcher tableau for an explicit Runge-Kutta method

0					
c_2	$a_{2,1}$				
c_3	$a_{3,1}$	$a_{3,2}$			
$\vdots$	$\vdots$		$\ddots$		
c_s	$a_{s,1}$	$\cdots$	$\cdots$	$a_{s,s-1}$	
x	$\hat{b}_1$	$\cdots$	$\cdots$	$\cdots$	$\hat{b}_s$
$\hat{x}$	b_1	$\cdots$	$\cdots$	$\cdots$	b_s
e	$b_1 - \hat{b}_1$	$\cdots$	$\cdots$	$\cdots$	$b_s - \hat{b}_s$

Table 2. Butcher tableau for the DOPRI54 method

0	0	0	0	0	0	0	0
$\frac{1}{5}$	$\frac{1}{5}$	0	0	0	0	0	0
$\frac{3}{10}$	$\frac{3}{40}$	$\frac{9}{40}$	0	0	0	0	0
$\frac{4}{5}$	$\frac{44}{55}$	$\frac{-56}{15}$	$\frac{32}{9}$	0	0	0	0
$\frac{8}{9}$	$\frac{19372}{6561}$	$\frac{-25360}{2187}$	$\frac{64448}{6561}$	$\frac{-212}{729}$	0	0	0
1	$\frac{9017}{3168}$	$\frac{-355}{33}$	$\frac{46732}{5247}$	$\frac{49}{176}$	$\frac{-5103}{18656}$	0	0
1	$\frac{35}{384}$	0	$\frac{500}{1113}$	$\frac{125}{192}$	$\frac{-2187}{6784}$	$\frac{11}{84}$	0
x	$\frac{5179}{57600}$	0	$\frac{7571}{16695}$	$\frac{393}{640}$	$\frac{-92097}{339200}$	$\frac{187}{2100}$	$\frac{1}{40}$
$\hat{x}$	$\frac{35}{384}$	0	$\frac{500}{1113}$	$\frac{125}{192}$	$\frac{-2187}{6784}$	$\frac{11}{84}$	0
e	$\frac{71}{57600}$	0	$\frac{-71}{16695}$	$\frac{71}{1920}$	$\frac{-17253}{339200}$	$\frac{22}{525}$	$\frac{-1}{40}$

scheme (DOPRI54) is an explicit Runge-Kutta scheme with $s = 7$ stages. Asymptotically, the numerical solution generated by DOPRI54 has order 5, while the error estimate has order 4.

Consider the system of ordinary differential equations

$$\dot{x}(t) = f(t, x) \qquad x(t_0) = x_0 \tag{11}$$

The main numerical steps in DOPRI54 for solution of (11) are

$$T_i = t_n + c_i h_n \qquad i = 1, 2, ..., s \tag{12a}$$

$$X_i = x_n + h_n \sum_{j=1}^{s} a_{i,j} f(T_j, X_j) \quad i = 1, 2, ..., s \tag{12b}$$

$$x_{n+1} = x_n + h_n \sum_{j=1}^{s} b_j f(T_j, X_j) \tag{12c}$$

$$e_{n+1} = h_n \sum_{j=1}^{s} d_j f(T_j, X_j) \tag{12d}$$

h_n is the step size. The step size is chosen adaptively using a PI-controller such that the resulting error estimate, e_{n+1}, meets the specifications (Gustafsson, 1992).

The coefficients $a_{i,j}$, b_j, c_j and d_j for DOPRI54 are given by the Butcher tableau in Table 2.

The DOPRI54 method for numerical solution of (11) is modified and tailored to the solution of (5) as well as for the numerical integration computations in the multiple-shooting method for the optimal control problem (Boiroux et al., 2009a).

In summary, we apply a high-order explicit Runge-Kutta method (DOPRI54) with an embedded error estimate and a PI step size controller. The DOPRI54 scheme is used both for numerical integration of the mean-covariance

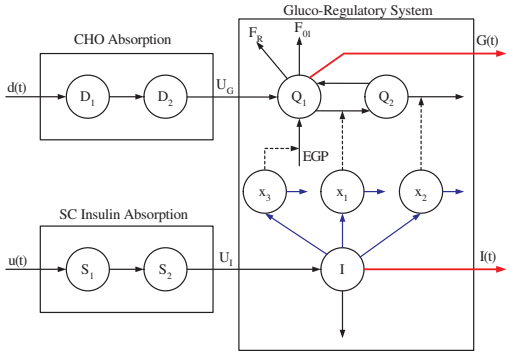

Fig. 2. Diagram of the Hovorka model.

pair and for the numerical integration and sensitivity computation in the multiple shooting algorithm.

4.2 NMPC Algorithm

Algorithm 1 provides the steps in the Nonlinear Model Predictive Controller (NMPC). The algorithm combines the continuous-discrete Extended Kalman Filter for state estimation with a continuous-time optimal control problem for the regulation problem.

The algorithm is initialized by the mean and covariance of the initial state, $\hat{x}_{0|-1}$ and $P_{0|-1}$, as well as the first measurement, y_0. They are used to compute the one step prediction of the mean state and its covariance, $\hat{x}_{1|0}$ and $P_{1|0}$, as well as the first control, u_0. At time step t_k, the algorithm requires $(y_k, \hat{x}_{k|k-1}, P_{k|k-1})$ and computes $(u_k, \hat{x}_{k+1|k}, P_{k+1|k})$.

In the case where one observation y_k is missing, we can update the state and the covariance using

$$\hat{x}_{k|k} = \hat{x}_{k|k-1} \tag{13a}$$
$$P_{k|k} = P_{k|k-1} \tag{13b}$$

The main computational effort in Algorithm 1 is in solving the optimal control problem.

5. SIMULATION RESULTS

In this section, we use the model developed by Hovorka et al. (2004) and also described in Boiroux et al. (2009b) to simulate a subject with type 1 diabetes. A diagram of this model is provided in Fig. 2. This model consists of a submodel describing CHO absorption, a submodel describing subcutaneous-to-intravenous absorption of insulin, a simple lumped model describing the glucose dynamics, and simple lumped models describing insulin dynamics and action mechanisms. We use an implementation of Algorithm 1 to compute the ideal insulin administration profile.

As we want to use the continuous-discrete extended Kalman filter only to estimate the meal size, we choose the variance for the first compartment in the glucose absorption subsystem D_1 as $\mathrm{Var}[D_1] = 5^2$ g^2. This value is a compromise between two contradictory goals: peak detection corresponding to meals intakes (which is improved if $\mathrm{Var}[D_1]$ is big), and sensitivity to measurement noise (the controller is less sensitive to noise if $\mathrm{Var}[D_1]$ is small). We assume that the glucose sensor variance is $R_k = 0.1^2$ (mmol/L)^2. The initial state is assumed to be known by the controller.

We do the optimization in a 24 hour window, i.e. $t_0 = 0$ min and $t_f = 24 \cdot 60$ min, using a sampling time of $T_s = 5$ min. In the scenario considered, the simulated 70 kg subject has a 62 g CHO meal at 6:00, a 55 g CHO meal at 12:00, and a 50 g CHO meal at 18:00.

Fig. 3 shows the simulation results for the case in which the meals are announced to the MPC at mealtime. Hypoglycemia is avoided and only mild hyperglycemic events occur. Insulin related to the meals is delivered at mealtimes following a bolus-like profile. However, the fact that

Algorithm 1 Nonlinear Model Predictive Controller

Require: y_k, $\hat{x}_{k|k-1}$, $P_{k|k-1}$
Return: u_k, $\hat{x}_{k+1|k}$, $P_{k+1|k}$

Filtering:
Compute

$$C_k = \frac{\partial h}{\partial x}(t_k, \hat{x}_{k|k-1})$$
$$R_{k|k-1} = C_k P_{k|k-1} C_k' + R_k$$
$$K_k = P_{k|k-1} C_k' \left(R_{k|k-1}\right)^{-1}$$

Compute the innovation

$$e_k = y_k - h(t_k, \hat{x}_{k|k-1})$$

Compute the filtered state and covariance

$$\hat{x}_{k|k} = \hat{x}_{k|k-1} + K_k e_k$$
$$P_{k|k} = P_{k|k-1} - K_k R_{k|k-1} K_k'$$

Optimal Control Problem:
Solve the optimal control problem

$$\min_{x(\cdot),u(\cdot)} \quad \phi = \int_{t_k}^{t_k+T} g(x(t), u(t))dt + \frac{1}{2} \sum_{i=k}^{k+N-1} \|\Delta u_i\|_{2,S}^2$$
$$s.t. \quad x(t_k) = \hat{x}_{k|k}$$
$$\dot{x}(t) = f(t, x(t), u(t)) \qquad t \in [t_k, t_k + T[$$
$$u_{\min} \le u(t) \le u_{\max} \qquad t \in [t_k, t_k + T[$$

using a zero-order hold parametrization, $\{u_i\}_{i=k}^{k+N-1}$, of the control profile, $[u(t)]_{t_k}^{t_k+T}$. Let $u(t) = u_k$ be the optimal control for $t \in [t_k, t_{k+1}[$.

One-Step Prediction:
Using DOPRI54, compute

$$\hat{x}_{k+1|k} = \hat{x}_k(t_{k+1})$$
$$P_{k+1|k} = P_k(t_{k+1})$$

by solution of the ODE system

$$\frac{d\hat{x}_k(t)}{dt} = f(t, \hat{x}_k(t), u_k), \qquad \hat{x}_k(t_k) = \hat{x}_{k|k}$$
$$\frac{dP_k(t)}{dt} = A_k(t)P_k(t) + P_k(t)A_k(t)' + \sigma\sigma', \quad P_k(t_k) = P_{k|k}$$

with

$$A_k(t) = \frac{\partial f}{\partial x}(t, \hat{x}_k(t), u_k)$$

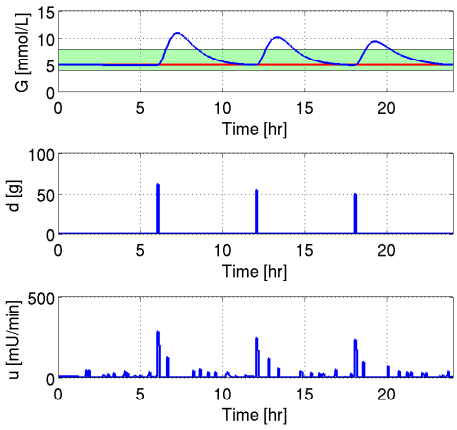

Fig. 3. Optimal insulin administration with meal announcement at meal time.

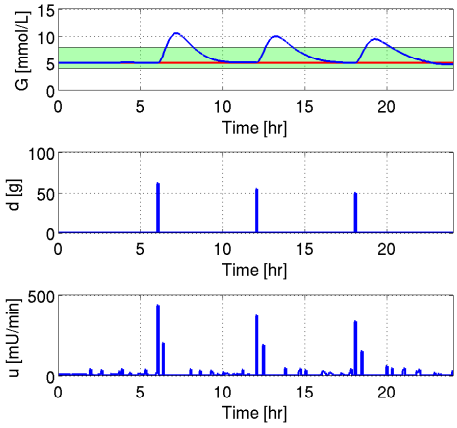

Fig. 4. Optimal insulin administration with meal announcement at meal time. Meal size is overestimated by 50%.

the subject knows with accuracy the meal size is not practical.

Fig. 4 shows the simulation results for the case in which the meals are announced to the MPC at mealtime, but the meal size is overestimated by 50%. The glucose profile looks similar to the one in Fig. 3. However, the insulin profile shows a big bolus instead of two smaller consecutive boluses.

Fig. 5 shows the actual and the estimated values for the two compartments in the CHO absorption subsystem D_1 and D_2. Although the peaks corresponding to the meal intakes are overestimated for D_1, the EKF allows to reconstruct the correct profile for D_2.

Fig. 6 shows the simulation results for the case in which the meals are not announced. Hypoglycemia is still avoided.

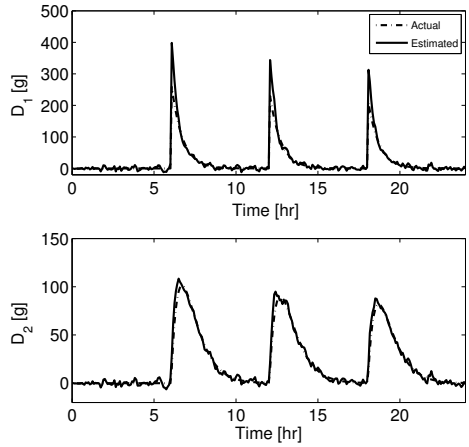

Fig. 5. Actual (dash-dotted line) and reconstructed (solid line) profiles for the two compartments in the CHO absorption subsystem. Meal size is overestimated by 50%.

However, the hyperglycemic events are more important. Insulin delivery is more spread out over time than in the case where the meals are announced. Consequently, the performance of the controller is compromised, but still satisfactory.

Fig. 7 shows the actual and the estimated values for the two compartments in the CHO absorption subsystem D_1 and D_2 for the case in which the meals are not announced. Although the peaks for the the first compartment D_1 are not correctly reconstructed by the continuous-discrete extended Kalman filter, it is possible to reconstruct—with some lag—the profile for D_2. Peak reconstruction could be improved by having a higher value for the variance of D_1 in the EKF, but it would also make the reconstruction more sensitive to noise. This tradeoff, i.e., peak detection and sensitivity to noise, limits the performance of the controller in the case where the meals are not announced.

These results show that it is possible to obtain reasonably good control if the meals are announced only at mealtimes, but it is obvious that the performance of the controller suffers if the meals are not announced. Performance can be improved if the meal (but not the meal size) is announced in advance by the subject. It would allow the administration of a preemptive insulin bolus prior to the meal.

6. CONCLUSION

In this paper we described a nonlinear model predictive control (NMPC) algorithm based on a continuous-discrete extended Kalman filter for state estimation and a multiple shooting for solving the optimal control problem (OCP). This algorithm is used to compute the optimal insulin administration. This filter uses the DOPRI54 for numerical computation of the meal-covariance pair. Numerical simulations have been performed in the case where the exact meal sizes are announced, in the case where erro-

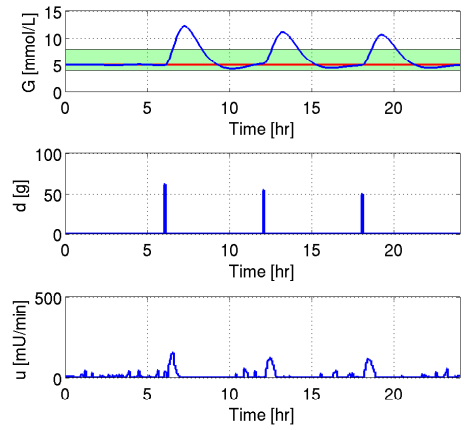

Fig. 6. Optimal insulin administration without meal announcement at meal time.

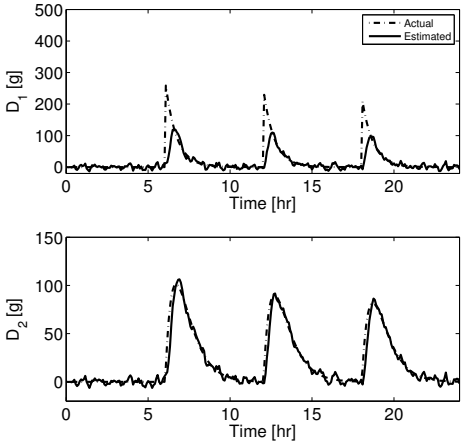

Fig. 7. Actual (dash-dotted line) and reconstructed (solid line) profiles for the two compartments in the CHO absorption subsystem for the case in which the meals are not announced.

neous (overestimated) meal sizes are announced, and in the case where the meals are not announced to the controller. The results provide a practical upper-bound of the control quality to be expected for these three cases.

REFERENCES

Binder, T., Blank, L., Bock, H.G., Burlisch, R., Damen, W., Diehl, M., Kronseder, T., Marquardt, W., Schlöder, J.P., and von Stryk, O. (2001). Introduction to model based optimization of chemical processes on moving horizons. In M. Grötschel, S.O. Krumke, and J. Rambau (eds.), *Online Optimization of Large Scale Systems*, 295–339. Springer, Berlin.

Bock, H. and Plitt, K. (1984). A multiple shooting method for direct solution of optimal control problems. 242–247. Proc. of the IFAC 9th World Congress, Budapest, Hungary.

Boiroux, D., Finan, D.A., Poulsen, N.K., Madsen, H., and Jørgensen, J.B. (2009a). Nonlinear model predictive control for an artificial β-cell. In *Belgian-French-German Conference in Optimization 2009*. BFG'09. Accepted.

Boiroux, D., Finan, D.A., Poulsen, N.K., Madsen, H., and Jørgensen, J.B. (2009b). Optimal insulin administration for people with type 1 diabetes. In *Dynamics and Control of Process Systems 2010*. DYCOPS 2010. Accepted.

Breton, M.D. (2008). Physical activity - the major unaccounted impediment to closed loop control. *Journal of Diabetes Science and Technology*, 2(1), 169–174.

Cobelli, C., Dalla Man, C., Sparacino, G., Magni, L., De Nicolao, G., and Kovatchev, B.P. (2009). Diabetes: Models, signals, and control. *IEEE Reviews in Biomedical Engineering*, 2, 54–96.

Diehl, M., Ferreau, H.J., and Haverbeke, N. (2009). Efficient numerical methods for nolinear MPC and moving horizon estimation. In L. Magni, D.M. Raimondo, and F. Allgöwer (eds.), *Nonlinear Model Predictive Control. Towards New Challenging Applications*, 391–417. Springer, Berlin.

Dormand, J.R. and Prince, P.J. (1980). A family of embedded Runge-Kutta formulae. *Journal of Computational and Applied Mathematics*, 6(1), 19 – 26.

Gustafsson, K. (1992). *Control of Error and Convergence in ODE Solvers*. Ph.D. thesis, Department of Automatic Control, Lund Institute of Technology.

Hovorka, R., Canonico, V., Chassin, L.J., Haueter, U., Massi-Benedetti, M., Federici, M.O., Pieber, T.R., Schaller, H.C., Schaupp, L., Vering, T., and Wilinska, M.E. (2004). Nonlinear model predictive control of glucose concentrations in subjects with type 1 diabetes. *Physiological Measurement*, 25, 905–920.

Jazwinski, A.H. (1970). *Stochastic Processes and Filtering Theory*. Academic Press, San Diego, CA.

Jørgensen, J.B., Kristensen, M.R., Thomsen, P.G., and Madsen, H. (2007). A numerically robust ESDIRK-based implementation of the continuous-discrete extended kalman filter. In *European Control Conference 2007*. ECC 2007, Kos, Greece.

Klonoff, D.C., Cobelli, C., Kovatchev, B., and Zisser, H.C. (2009). Progress in development of an artificial pancreas. *Journal of Diabetes Science and Technology*, 3, 1002–1004.

Magni, L., Raimondo, D., Dalla Man, C., De Nicolao, G., Kovatchev, B., and Cobelli, C. (2009). Model predictive control of glucose concentration in type I diabetic patients: An in silico trial. *Biomedical Signal Processing and Control*, 4(4), 338–346.

Nørgaard, M., Poulsen, N.K., and Ravn, O. (2000). New developments in state estimation for nonlinear systems. *Automatica*, (36), 1627–1638.

APPENDIX F

Paper E

Strategies for glucose control in people with type 1 diabetes

Authors:

Dimitri Boiroux, Daniel Aaron Finan, Niels Kjølstad Poulsen, Henrik Madsen, and John Bagterp Jørgensen

Published in:

Preprints of the 18th IFAC World Congress,, pages 3765-3770, 2011.

Preprints of the 18th IFAC World Congress
Milano (Italy) August 28 - September 2, 2011

Strategies for Glucose Control in People with Type 1 Diabetes ⋆

Dimitri Boiroux * **Daniel A. Finan** * **John Bagterp Jørgensen** *
Niels Kjølstad Poulsen * **Henrik Madsen** *

* *Department of Informatics and Mathematical Modeling, Technical University of Denmark, DK-2800 Kgs Lyngby, Denmark (e-mail: {dibo,dafi,jbj,nkp,hm}@imm.dtu.dk)*

Abstract: In this paper we apply a robust feedforward-feedback control strategy to people with type 1 diabetes. The feedforward controller consists of a bolus calculator which compensates the disturbance coming from meals. The feedback controller is based on a linearized description of the model describing the patient. We minimize the risk of hypoglycemia by introducing a time-varying glucose setpoint based on the announced meal size and the physiological model of the patient. The simulation results are based on a virtual patient simulated by the Hovorka model. They include the cases where the insulin sensitivity changes, and mismatches in meal estimation. They demonstrate that the designed controller is able to achieve offset-free control when the insulin sensitivity change, and that having a time-varying reference signal enables more robust control of blood glucose in the cases where the meal size is known, but also when the ingested meal does not match the announced one.

1. INTRODUCTION

The World Health Organization (2009) estimates that more than 220 million people worldwide have diabetes. This number is likely to double by 2030. In the USA, the budget for diabetes represents 10% of the health care budget, i.e. more than 130 billion dollars (132 billion dollars in 2002).

For healthy people, the blood glucose is tightly held at around 90 mg/dL (or 5 mmol/L). Diabetes is a chronic disease characterized by an insufficient production of insulin and/or a decrease in its effectiveness. Therefore, people with diabetes tend to have a too high blood glucose level, also called hyperglycemia. Long periods of hyperglycemia can lead to complications like nerve diseases, kidney diseases, or blindness. However, the dosing of insulin must be done carefully, because a too high dosage of insulin may lead to hypoglycemia, which has immediate effects, such as insulin shock, coma or even death.

In particular, people with type 1 diabetes must rely on injection of exogenous insulin to survive. The current insulin therapy for people with type 1 diabetes consists of the injection of slow acting insulin once a day and fast acting insulin several times per day, usually before mealtimes. The slow acting insulin is used to counteract the continuous glucose production from the liver. The fast acting insulin compensates the intake of carbohydrates (CHO) during the meals. The decision on the amount of short and fast acting insulin is based on 3-4 blood glucose measurements per day.

Continuous glucose monitors (CGMs) can improve the insulin therapy. In addition, insulin pumps can be used to adjust the insulin infusion rate, and insulin pens can be used to administrate insulin boluses. These devices can be used in an artificial pancreas, which is described in Fig. 1. Various research groups work on aspects of control algorithms integrating the CGM and the insulin pump; see, e.g. Klonoff et al. (2009), Cobelli et al. (2009) and Magni et al. (2009).

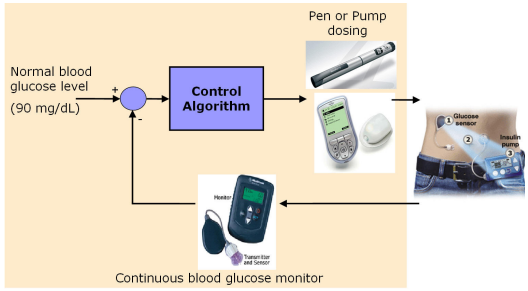

Fig. 1. Closed-loop glucose control. Glucose is measured subcutaneously using a continuous glucose monitor (CGM). Insulin is dosed either continuously by an insulin pump or discretely using an insulin pen.

In this paper we use a feedforward-feedback controller based on linear MPC. The feedforward controller computes the optimal bolus size to compensate the CHO ingested through meals. The feedback controller adjusts the basal insulin infusion rate.

The paper is structured as follows. Section 2 introduces the model used to simulate a virtual patient with type 1 diabetes. Section 3 describes the controller used to compute the optimal closed-loop insulin profiles. Section 4 presents the numerical results in the cases where the insulin sensitivity changes under fasting conditions, and

⋆ Funding for this research as part of the DIACON project from the Danish Council for Strategic Research is gratefully acknowledged.

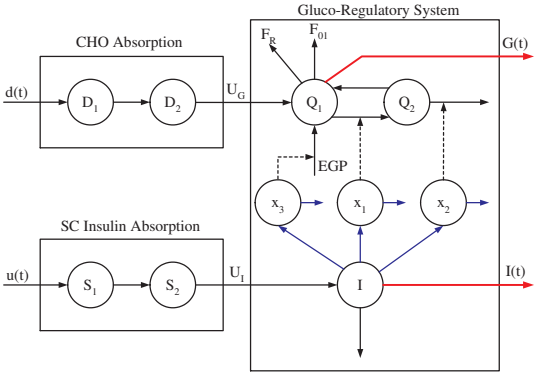

Fig. 2. Diagram of the Hovorka model.

in the case where the patient has one 75g CHO meal. Conclusions are provided in Section 5.

2. PHYSIOLOGICAL MODELS

Several nonlinear physiological models have been developed to simulate virtual patients with type 1 diabetes, see e.g. Bergman et al. (1981), Hovorka et al. (2004), Dalla Man et al. (2007) and the review article written by Wilinska and Hovorka (2009). In this paper, we use the Hovorka model to simulate people with type 1 diabetes. The models for CHO absorption, subcutaneous insulin absorption and the glucose-insulin dynamics for the Hovorka model are described in Fig. 2.

The delays associated to insulin and CHO absorption and the nonlinearities of the model limit the control quality, see e.g. Boiroux et al. (2010a). Indeed, the time constant associated to CHO absorption is $\tau_G = 40$ minutes, while the one associated to insulin absorption is $\tau_I = 55$ minutes. The main source of nonlinearity in the Hovorka model arises from the bilinear term involving the action of insulin x_1 on glucose transport and the glucose in the main blood stream Q_1. This nonlinearity leads to an inaccurate description of linear models when the state of the system is not close to a steady state, e.g. during meals.

An other issue is that these models may be non-identifiable for some subjects (Pillonetto et al. (2003)).

3. CONTROLLER DESIGN

In this section we describe the feedforward-feedback controller used to compute the optimal insulin administration profiles. The controller is based on linear MPC, where the model is a linearized version of the Hovorka model. The reference signal is time-varying. The states of the system are estimated using a stationary Kalman filter with an integrated disturbance.

3.1 Linear model

We consider a system of ordinary differential equations (ODEs) in the form

$$\dot{x}(t) = f(x(t), u(t), d(t)) \tag{1a}$$
$$y(t) = g(x(t)) \tag{1b}$$

in which $x(t) \in \mathbf{R}^{n_x}$ describes the states of the system, $u(t) \in \mathbf{R}^{n_u}$ describes the manipulated variables (insulin infusion rate) $d(t) \in \mathbf{R}^{n_d}$ are disturbances (meals), and $y(t)$ depicts the measured output (blood glucose).

The system (1) can approximated by a linear state space system at a steady state (x_{ss}, u_{ss}, d_{ss}). In this paper we choose the target value $\bar{G} = 5$ mmol/L. The linear state space description in continuous time is

$$\delta\dot{x}(t) = A_c\delta x(t) + B_c\delta u(t) + E_c\delta d(t) \tag{2a}$$
$$\delta y(t) = C_c\delta x(t) \tag{2b}$$

In equation (2), $\delta x(t)$, $\delta u(t)$, $\delta d(t)$ and $\delta y(t)$ are deviation variables from the steady state (x_{ss}, u_{ss}, d_{ss}), i.e.

$$\begin{aligned} \delta x(t) &= x(t) - x_{ss} \quad \delta u(t) = u(t) - u_{ss} \\ \delta d(t) &= d(t) - d_{ss} \quad \delta y(t) = y(t) - \bar{G}(t) \end{aligned} \tag{3}$$

and the time-invariant matrices A_c, B_c, E_c and C_c are

$$\begin{aligned} A_c &= \frac{\partial f}{\partial x}(x_{ss}, u_{ss}, d_{ss}) \quad B_c = \frac{\partial f}{\partial u}(x_{ss}, u_{ss}, d_{ss}) \\ E_c &= \frac{\partial f}{\partial d}(x_{ss}, u_{ss}, d_{ss}) \quad C_c = \frac{\partial g}{\partial x}(x_{ss}) \end{aligned} \tag{4}$$

We now assume a zero-order hold parametrization of the controlled input u and the disturbance d with the sampling time $T_s = 5$ min. Under this assumption, the continuous-time linear state space system (2) is equivalent to the deterministic linear discrete-time state space description

$$\delta x_{k+1} = \bar{A}\delta x_k + \bar{B}\delta u_k + \bar{E}\delta d_k \tag{5a}$$
$$\delta y_k = \bar{C}\delta x_k \tag{5b}$$

3.2 Time-varying reference signal

Boiroux et al. (2010b) demonstrates that a constant glucose reference signal usually leads to an overdose of insulin when the meal size becomes too large. A time-varying glucose setpoint has been extensively used to reduce the risk of hypoglycemia, see e.g. Marchetti et al. (2006), Garcia-Gabin et al. (2008) and Eren-Oruklu et al. (2009). It has also been noticed that the optimal insulin administration profile in the case where the meals are announced at mealtime only is close to a bolus-like profile (see Boiroux et al. (2010c) and Fig. 3). Consequently, the insulin administration can be separated between

- The basal insulin, which must compensate for endogenous glucose production. It must be adjusted to reject disturbances caused by changes in physiological parameters, e.g. changes in the insulin sensitivity (feedback control)

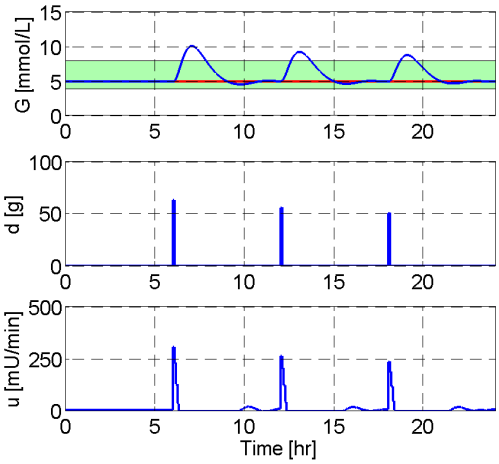

Fig. 3. Glucose profile (top), meal disturbances (middle) and optimal insulin administration profile (bottom) with meal announcement at meal time. Most insulin is taken in bolus like form at meal time.

- Insulin boluses, which are used to limit postprandial hyperglycemic event. The size of the bolus depends on the meal size announced by the patient (feedforward control)

The control strategy described above is a feedforward-feedback control strategy similar to the one described in Marchetti et al. (2008). When a meal is announced to the controller, the optimal bolus and the optimal postprandial blood glucose trajectory are computed by solving the univariate constrained optimization problem

$$\min_{u^{bolus}} \ \psi = \frac{1}{2}\sum_{k=0}^{N-1} \|y^0_{k+1} - \bar{G}\|_2^2 \tag{6a}$$

$$s.t. \quad \dot{x}^0(t) = f(x^0(t), u_k, d_k) \quad t \in [t_k, t_{k+1}[\tag{6b}$$
$$x^0_0 = x_{ss} \tag{6c}$$
$$u^0_0 = u_{ss} + u^{bolus} \tag{6d}$$
$$u^0_k = u_{ss}, \quad k = 1, 2, \ldots, N-1 \tag{6e}$$
$$y^0_k = Cx_k \tag{6f}$$
$$y^0_k \geq \bar{G} \tag{6g}$$

In other words, we want to find the optimal bolus such that the reference signal is above the desired glucose target $\bar{G} = 5$ mmol/L for all times. In this case, the predictions on the future states of the system are made using the continuous-time nonlinear model.

The solution of (6) gives the reference insulin profile u^0_k, the reference states x^0_k and the reference blood glucose setpoint y^0_k. Thus, we introduce the deviation variables from the reference state δy_k, δx_k and δu_k such that

$$y_k = y^0_k + \delta y_k \quad x_k = x^0_k + \delta x_k \quad u_k = u^0_k + \delta u_k \tag{7}$$

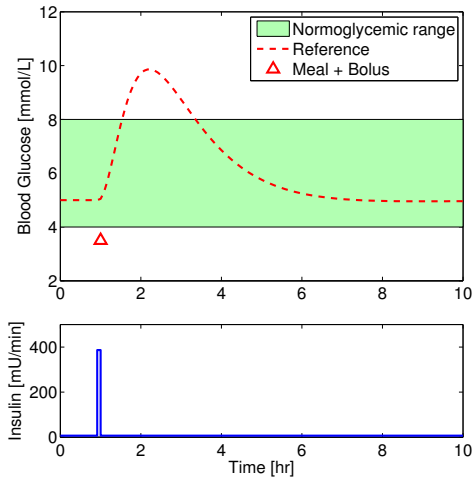

Fig. 4. Example of time-varying reference signal for the blood glucose. The meal size is 50g CHO.

Fig. 4 gives an example of reference signal in the case where the patient has a 50g CHO meal.

3.3 Offset-free MPC

Accordingly to Pannocchia and Rawlings (2003), offset-free control can be achieved by augmenting the state vector with an integrated disturbance z_k. In a fasting state, the stochastic linear discrete-time augmented state space description is

$$\begin{bmatrix}\delta x \\ z\end{bmatrix}_{k+1} = \begin{bmatrix}\bar{A} & B_z \\ 0 & I\end{bmatrix}\begin{bmatrix}\delta x \\ z\end{bmatrix}_k + \begin{bmatrix}\bar{B} \\ 0\end{bmatrix}\delta u_k + \begin{bmatrix}\xi \\ \zeta\end{bmatrix}_k \tag{8a}$$

$$\delta y_k = \begin{bmatrix}\bar{C} & C_z\end{bmatrix}\begin{bmatrix}\delta x \\ z\end{bmatrix}_k + w_k \tag{8b}$$

in which $B_z \in \mathbf{R}^{n_x \times n_z}$, and $C_z \in \mathbf{R}^{n_y \times n_z}$. The processes ξ_k, ζ_k and w_k are zero-mean white noise processes, and we assume that ξ_k and ζ_k are uncorrelated. For convenience, we will denote

$$A = \begin{bmatrix}\bar{A} & B_z \\ 0 & I\end{bmatrix} \quad B = \begin{bmatrix}\bar{B} \\ 0\end{bmatrix} \quad E = \begin{bmatrix}\bar{E} \\ 0\end{bmatrix} \quad C = \begin{bmatrix}\bar{C} & C_z\end{bmatrix}$$
$$\delta \underline{x}_k = \begin{bmatrix}\delta x \\ z\end{bmatrix}_k \tag{9}$$

and we define the time-invariant covariance matrices

$$R_1 = \mathrm{Cov}\left(\begin{bmatrix}\xi \\ \zeta\end{bmatrix}_k\right) \quad R_2 = \mathrm{Cov}\,(v_k) \tag{10}$$

We set $\mathrm{Var}[\xi_k] = 0$. Hence, the variances of the white noise processes ζ_k and v_k are tuning parameters. For the simulations we set

$$\mathrm{Var}[\zeta_k] = 0.7^2 \quad R_2 = 0.5^2 \tag{11}$$

The integrated disturbance process z_k can be added either to the insulin infusion, or to the meal ingestion, or the the blood glucose measurements. In this paper, we choose to add the disturbance to the insulin infusion, i.e.

$$B_z = \bar{B}, \quad C_z = 0 \tag{12}$$

It must be pointed out that the reference glucose trajectory determined in section 3.2 already includes the effects of the meal intake and the associated bolus. Consequently, the one-step ahead prediction for the state vector $\delta\hat{x}_{k+1|k}$ is

$$\delta\hat{\underline{x}}_{k+1|k} = A\delta\hat{\underline{x}}_{k|k} + B\delta u_k \tag{13}$$

and the filtered state $\delta\hat{\underline{x}}_{k+1|k+1}$ is computed as

$$e_{k+1} = \delta y_{k+1} - C\delta\hat{\underline{x}}_{k+1|k} \tag{14a}$$
$$\delta\hat{\underline{x}}_{k+1|k+1} = \delta\hat{\underline{x}}_{k+1|k} + Ke_{k+1} \tag{14b}$$

in which K is the stationary Kalman gain. The one-step ahead prediction and the filtering step are expressed in terms of deviation variables from the reference signal.

3.4 Linear MPC with soft output constraints

At each time sample, it is required to solve an open-loop constrained optimization problem. Let N be the prediction horizon length. The linear problem with hard input constraints and soft output constraints at time t_k is formulated as

$$\min_{\{u_i, v_i\}_{i=0}^{N-1}} \phi = \frac{1}{2}\sum_{i=0}^{N-1} \|\delta\hat{y}_{k+i+1|k}\|_2^2 + \lambda\|\Delta u_{k+i}\|_2^2 + \kappa\|v_i\|_2^2 \tag{15a}$$

$$s.t. \quad \delta\hat{\underline{x}}_{k+i+1|k} = A\delta\hat{\underline{x}}_{k+i|k} + B\delta u_{k+i} \tag{15b}$$
$$\delta\hat{y}_{k+i|k} = C\delta\hat{\underline{x}}_{k+i|k} \tag{15c}$$
$$u_{\min} \le \delta u_{k+i} \le u_{\max} \tag{15d}$$
$$\Delta u_{\min} \le \Delta\delta u_{k+i} \le \Delta u_{\max} \tag{15e}$$
$$y_{\min} - y^0_{k+i} - \delta\hat{y}_{k+i|k} \le v_i \tag{15f}$$
$$v_i \ge 0 \tag{15g}$$

The slack variables v_i are introduced to penalize hypoglycemia. The hard input constraints (15d-15e) limit the insulin infusion rate and the increment of the insulin infusion rate respectively. The penalty term $\kappa\|v_i\|_2^2$ is used to avoid hypoglycemia and the penalty term $\lambda\|\Delta u_i\|_2^2$ prevents the insulin infusion rate from varying too aggressively.

For the simulations we choose $N = 120$, i.e. a 10 hour prediction horizon, such that the computed optimal insulin profile is similar to the one in the case where the prediction horizon is infinite. Thus, the prediction horizon is not considered as a tuning parameter. The tuning parameters of (15) are the weights λ and κ.

For the simulations we choose

$$u_{min} = -\frac{u_{ss}}{2}, \quad \lambda = 400, \quad \kappa = 100 \tag{16}$$

The choice of $u_{min} = -\frac{u_{ss}}{2}$ instead of $u_{min} = -u_{ss}$ does not allow the controller to switch off the insulin pump. Instead, switching off the pump can be implemented as a safety layer in case of an (upcoming) hypoglycemic event.

4. NUMERICAL RESULTS

In this section, we use the Hovorka model and the described linear MPC algorithm to compute the optimal insulin administration profiles for people with type 1 diabetes. We consider two cases:

- A 36 hour simulation with a decrease in insulin sensitivity by 50% under fasting conditions. We both consider the case where the sensor is noise-free, and the case where the sensor is affected by white noise.
- A 24 hour simulation with one 75g CHO meal. The meal is given 6 hours after the beginning of the simulation. We consider the cases where the correct meal size is announced, the meal size is underestimated by 50%, the meal size is overestimated by 50% and the meal is not announced at all.

For the first case, the insulin sensitivity is changed by modifying the insulin sensitivities for the three insulin action compartments after 1 hour. The insulin sensitivities are described by the parameters $S_{I,1}$, $S_{I,2}$ and $S_{I,3}$ in the Hovorka model (the model is described in Hovorka et al. (2004) and Boiroux et al. (2010b)). A decrease by 33% of these parameters will give a new insulin infusion basal rate

$$\tilde{u}_{ss} = 1.5u_{ss} \tag{17}$$

We assume that the noise process of the glucose sensor is a zero-mean white noise process which follows a Gaussian distribution with the standard deviation

$$\sigma = 0.5 \text{ mmol/L} \tag{18}$$

Fig. 5 illustrates the blood glucose and the insulin profiles in the case where a change in the insulin sensitivity occurs while the patient is fasting, with and without sensor noise (5(a) and 5(a)). The insulin infusion rate increases to reject the disturbance caused by the decrease in insulin sensitivity. In the uncontrolled case where the basal insulin infusion rate is not adjusted, the blood glucose tends to a new steady state in the hyperglycemic range.

Fig. 6 shows the insulin and blood glucose profiles in the case where the patient has a 75g CHO meal, but the meal is not announced to the controller. In that case, a severe hypoglycemia cannot be avoided. A similar hypoglycemic event occurs if we allow to switch off the insulin pump and if we use noise-free blood glucose measurements instead (results not shown).

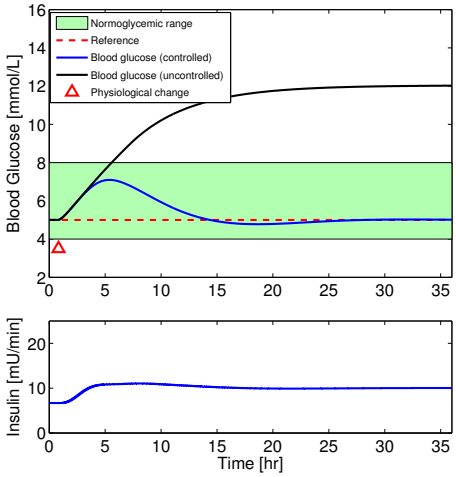

(a) Noise-free sensor

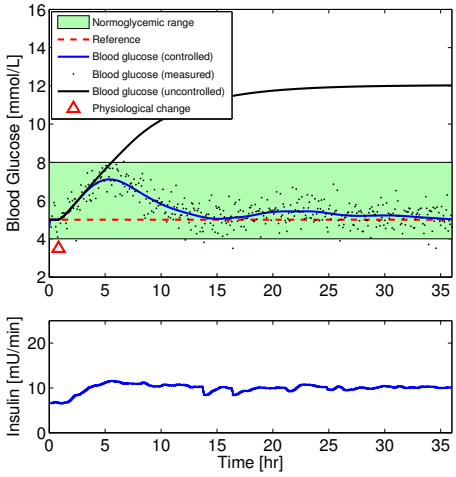

(b) Noisy sensor

Fig. 5. Insulin and blood glucose profile in the case where the insulin sensitivity decreases by 50% after 1 hour.

Fig. 7 illustrates the blood glucose and the insulin profiles in the case where the patient has a 75g CHO meal. For the case where the exact meal size is announced (Fig. 7(a)), the insulin infusion rate remains close to the basal rate. Consequently, the blood glucose follows tightly the glucose setpoint. For the case where the meal size is underestimated (Fig. 7(b)), the basal rate increases after the mealtime to compensate for the too low bolus. For the case where the meal size is overestimated (Fig. 7(c)), the insulin infusion rate is at the minimum after the meal to compensate for the too high bolus. No hypoglycemic events occur when a meal is announced. However, the postprandial blood glucose excursion is bigger when the meal size is underestimated by the patient.

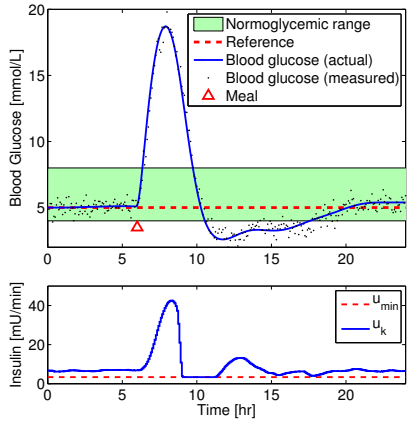

Fig. 6. Blood glucose and insulin profiles in the case where the meal is not announced.

These results show that reasonably good control can be obtained when a feedforward-feedback strategy is used. However, the main limitation of this strategy is that a fairly good nonlinear model description of the patient must be available.

5. CONCLUSION

In this paper, we described a feedforward-feedback predictive control. The feedback part of the controller is a model predictive controller based on a linearized version of the Hovorka model. The state is augmented with an integrated disturbance to ensure an offset-free control of the blood glucose. We used the feedforward-feedback control algorithm to compute insulin administration profiles in the cases where the insulin sensitivity decreases by 50%, and in the case where the patient has one 75g CHO meal. In the case where the patient has a meal, we consider the cases where the correct meal size is announced, the meal size is underestimated, the meal size is overestimated, and the meal is not announced at all. The results demonstrate that the control of blood glucose can be achieved without offset, and that a feedforward-feedback control strategy is superior to a feedback control only, assuming that a good model description of the patient can be obtained.

REFERENCES

R. N. Bergman, L. S. Phillips, and C. Cobelli. Physiologic evaluation of factors controlling glucose tolerance in man: measurement of insulin sensitivity and beta-cell glucose sensitivity from the response to intravenous glucose. *Journal of Clinical Investigation*, 68(6):1456 – 1467, 1981.

D. Boiroux, D. A. Finan, N. K. Poulsen, H. Madsen, and J. B. Jørgensen. Nonlinear model predictive control for an artificial β-cell. In *Recent Advances in Optimization and its Applications in Engineering*, pages 299 – 308. Springer, 2010a.

D. Boiroux, D. A. Finan, N. K. Poulsen, H. Madsen, and J. B. Jørgensen. Optimal insulin administration for people with type 1 diabetes. In *Proceedings of the*

9th International Symposium on Dynamics and Control of Process Systems (DYCOPS 2010), pages 234 – 239, 2010b.

D. Boiroux, D. A. Finan, N. K. Poulsen, H. Madsen, and J. B. Jørgensen. Implications and limitations of ideal insulin administration for people with type 1 diabetes. In *UKACC International Conference on Control 2010*, pages 156 – 161, 2010c.

C. Cobelli, C. Dalla Man, G. Sparacino, L. Magni, G. De Nicolao, and B. P. Kovatchev. Diabetes: Models, signals, and control. *IEEE Reviews in Biomedical Engineering*, 2:54–96, 2009.

C. Dalla Man, R. Rizza, and C. Cobelli. Meal simulation model of the glucose-insulin system. *IEEE Transactions on Biomedical Engineering*, 54(10):1740–1749, 2007.

M. Eren-Oruklu, A. Cinar, L. Quinn, and D. Smith. Adaptive control strategy for regulation of blood glucose levels in patients with type 1 diabetes. *Journal of Process Control*, 19:1333 – 1346, 2009.

W. Garcia-Gabin, J. Vehí, J. Bondia, C. Tarín, and R. Calm. Robust sliding mode closed-loop glucose control with meal compensation in type 1 diabetes mellitus. In *Proceedings of the 17th World Congress, The International Federation of Automatic Control*, pages 4240 – 4245, 2008.

R. Hovorka, V. Canonico, L. J. Chassin, U. Haueter, M. Massi-Benedetti, M. O. Federici, T. R. Pieber, H. C. Schaller, L. Schaupp, T. Vering, and M. E. Wilinska. Nonlinear model predictive control of glucose concentration in subjects with type 1 diabetes. *Physiological Measurement*, 25:905–920, 2004.

D. C. Klonoff, C. Cobelli, B. Kovatchev, and H. C. Zisser. Progress in development of an artificial pancreas. *Journal of Diabetes Science and Technology*, 3:1002–1004, 2009.

L. Magni, D. M. Raimondo, C. Dalla Man, G. De Nicolao, B. P. Kovatchev, and C. Cobelli. Model predictive control of glucose concentration in type I diabetic patients: An in silico trial. *Biomedical Signal Processing and Control*, 4(4):338–346, 2009.

G. Marchetti, M. Barolo, L. Jovanovič, H. Zisser, and D. E. Seborg. An improved PID switching control strategy for type 1 diabetes. In *2006 International Conference of the IEEE Engineering in Medicine and Biology Society*, pages 5041–5044, New York City, USA, 2006.

G. Marchetti, M. Barolo, L. Jovanovič, H. Zisser, and D. E. Seborg. A feedforward-feedback glucose control strategy for type 1 diabetes mellitus. *Journal of Process Control*, 18(2):149–162, 2008.

G. Pannocchia and J. B. Rawlings. Disturbance models for offset-free model-predictive control. *AIChE Journal*, 49(2):426–437, 2003.

G. Pillonetto, G. Sparacino, and C. Cobelli. Numerical non-identifiability regions of the minimal model of glucose kinetics: superiority of bayesian estimation. *Mathematical Biosciences*, 184:53 – 67, 2003.

M. E. Wilinska and R. Hovorka. Simulations models for in-silico testing of closed-loop glucose controllers in type i diabetes. *Drug Discovery Today: Disease Models*, 5(4): 289 – 298, 2009.

World Health Organization. Diabetes (fact sheet no. 312), November 2009. WHO Web site: http://www.who.int/mediacentre/factsheets/fs312/en/.

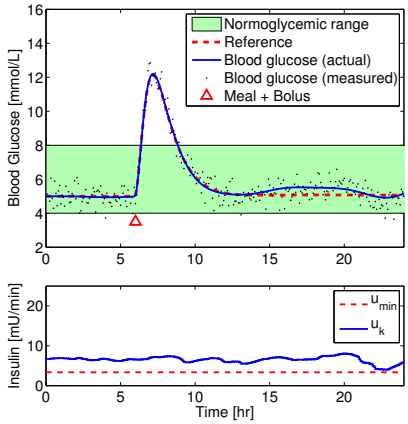

(a) Correct meal size

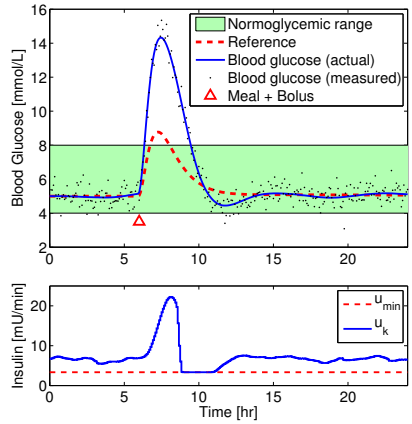

(b) Meal size underestimated by 50%

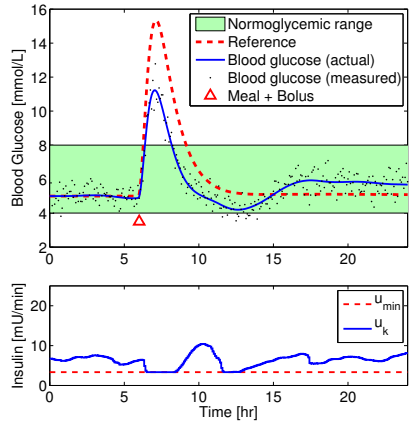

(c) Meal size overestimated by 50%

Fig. 7. Blood glucose and insulin profiles for the 24 hour simulations with one 75g CHO meal.

APPENDIX G

Paper F

Insulin Administration for People with Type 1 Diabetes

Authors:

Dimitri Boiroux, Daniel Aaron Finan, Henrik Madsen, Niels Kjølstad Poulsen, and John Bagterp Jørgensen

Published in:

21st European Symposium on Computer-Aided Process Engineering (ESCAPE-21), pages 1558-1562, 2011.

21st European Symposium on Computer Aided Process Engineering – ESCAPE 21
E.N. Pistikopoulos, M.C. Georgiadis and A.C. Kokossis (Editors)

Insulin Administration for People with Type 1 diabetes

Dimitri Boiroux, Daniel Aaron Finan, Niels Kjølstad Poulsen, Henrik Madsen and John Bagterp Jørgensen

[a]*Department of Informatics and Mathematical Modeling, Technical University of Denmark, DK - 2800 Kgs. Lyngby(e-mail: {dibo,dafi,nkp,hm,jbj}@imm.dtu.dk)*

Abstract

In this paper, we apply model predictive control (MPC) for control of blood glucose in people with type 1 diabetes. The two first control strategies are based on nonlinear model predictive control (NMPC). The first control strategy is based on meal announcement in advance, while the second one considers meal announcement at mealtimes only. They give a quantitative upper bound on the achievable control performance. The third control strategy is a feedforward-feedback control strategy. This strategy uses a time-varying setpoint to reduce the risk of hypoglycemia. The feedback controller computes the optimal basal insulin infusion rate. The feedforward controller consists of a bolus calculator. It computes the optimal bolus, along with the time-varying glucose setpoint. We test these three strategies on a virtual patient with type 1 diabetes. The numerical results demonstrate the robustness of the last control strategy with respect to changes in the model parameters and incorrect meal announcement.

Keywords: Type 1 diabetes, Nonlinear model predictive control, feedforward-feedback control

1. Introduction

The World Health Organization (WHO) estimates that more than 220 million people worldwide have diabetes. This number is likely to double by 2030. In the USA, the budget for diabetes represents 10% of the health care budget, i.e. more than 130 billion dollars (132 billion dollars in 2002).

In people without diabetes, the blood glucose is controlled tightly around 90 mg/dL (5 mmol/L). Type 1 diabetes is a chronic disease characterized by an insufficient (effectively nonexistent) endogenous production of insulin, which leads to poor regulation of glucose concentrations in the blood. In particular, the deficiency of insulin causes sustained high glucose levels (hyperglycemia) that result in serious long-term health problems like eye, nerve, and kidney disease. On the other hand, too much insulin can result in very low glucose levels (hypoglycemia) which can pose immediate health risks. Consequently, exogenous insulin must be injected to regulate the blood glucose concentration as tightly as possible.

Usually, insulin treatment consists of the administration of rapid acting insulin through boluses (i.e., discrete insulin administration) at the time of meals. The size of the bolus is based on a measurement of the current blood glucose at mealtime and the (estimated) size of the meal. However, having measurements only at mealtime does not provide enough information about blood glucose. Consequently, people with diabetes often tolerate hyperglycemia in order to avoid hypoglycemia and its immediate effects.

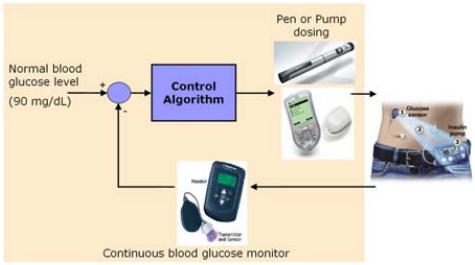

Fig. 1. Closed-loop glucose control. Glucose is measured subcutaneously using a continuous glucose monitor (CGM). Insulin is dosed either continuously by an insulin pump or discretely using an insulin pen

Continuous glucose monitors (CGM) can help to provide a better control of blood glucose. They measure the glucose concentration in the subcutaneous depot. Insulin pumps that continuously inject fast acting insulin have also been developed. Combining a CGM with an insulin pump can enable automatic insulin administration for people with type 1 diabetes. Such a medical device is called an artificial pancreas, and its principle is illustrated in Fig. 1. Several research groups work on aspects of control algorithms integrating the CGM and the insulin pump to automatically adjust insulin administration for people with type 1 diabetes, such as Cobelli et al. (2009) and Klonoff et al. (2009).

In this paper we use the model developed by Hovorka et al. (2004) and described in Boiroux et al. (2010b) to simulate a patient with type 1 diabetes. In the Hovorka model, the quality of the glucose control is limited by the time lag associated with subcutaneous-to-intravenous insulin absorption. This system property fundamentally limits the control quality that can be achieved in closed-loop insulin administration, as demonstrated in Boiroux et al. (2010a).

2. Nonlinear Model Predictive Control

In this section, we state the continuous-time optimal control problem and apply it to the computation of the optimal insulin profiles for people with type 1 diabetes. The optimal insulin administration is formulated as a bound constrained continuous-time Bolza problem

$$\begin{aligned} \min_{[x(t),u(t)]_{t_0}^{t_f}} \quad & \phi = \int_{t_0}^{t_f} g(x(t),u(t))dt + h(x(t_f)) \\ s.t. \quad & x(t_0) = x_0 \\ & \dot{x}(t) = f(x(t),u(t),d(t)) \\ & u_{\min} \leq u(t) \leq u_{\max} \end{aligned} \tag{1}$$

in which $x(t) \in \mathrm{R}^{n_x}$ is the state vector, $u(t) \in \mathrm{R}^{n_u}$ is the vector of manipulated inputs (insulin injection), and $d(t) \in \mathrm{R}^{n_d}$ is the vector of known disturbances (meals). We assume the state vector x(t) and the input vector u(t) to be constant between the sampling times and a constant sampling time $T_s = 5$ min. Thus, we can use the multiple-

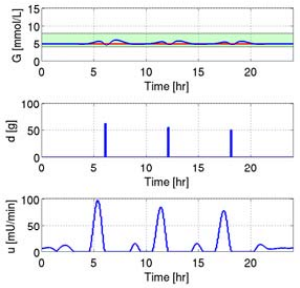

Fig. 2. Glucose profile (top), meal disturbances profile (middle) and insulin administration profile with meal announcement in advance.

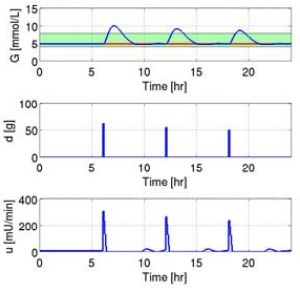

Fig. 3. Glucose profile (top), meal disturbances profile (middle) and insulin administration profile with meal announcement at mealtime.

shooting based algorithm described in Boiroux et al. (2009a) to solve the nonlinear program (1).

In the scenario considered, the simulated 70 kg subject has a 62 g CHO meal at 6:00, a 55 g CHO meal at 12:00, and a 50 g CHO meal at 18:00. Fig. 2 illustrates an optimal insulin administration profile for the described scenario in the case where the controller knows the size and time of all meals in advance. Knowing the meal times and sizes allows the controller to deliver anticipatory insulin to avoid postprandial hyperglycaemia. However, the assumption that the patient would know in advance - and with accuracy - the meal times and sizes is not practical. Safety considerations would preclude significant amounts of insulin from being delivered prior to mealtime (as in this ideal scenario).

Fig. 3 shows the simulation results for the case in which the meals are announced to the MPC only at mealtime. Thus, the controller can deliver no anticipatory insulin prior to meals. The limitations for this case force the subject into (mild) hyperglycaemia, but hypoglycaemia is avoided. The insulin delivery profile for this case looks quite similar to bolus delivery of insulin by a pen; most of the meal-related insulin is delivered in bolus form in the few samples after the meals are taken (and announced).

3. Bolus calculator and control

In this section we describe an offset-free feedforward-feedback controller to compute optimal insulin profiles. Garcia-Gabin et al (2008) and Marchetti et al. (2008) established that a time-varying glucose setpoint can reduce the risk of hypoglycemia. The feedforward controller consists of a bolus calculator. It computes the optimal bolus size and the glucose setpoint, based on the meal size announced by the patient. The feedback controller adjusts the basal insulin infusion rate to compensate for mismatches in meal announcement and variations in the physiological parameters of the patient. The calculation of the basal insulin is based on a linear MPC algorithm.

We use the Hovorka model and the offset-free linear MPC algorithm developed in Boiroux et al. (2011) to compute the optimal insulin administration profiles for people with type 1 diabetes. In the scenario considered, the glucose sensor provides a signal perturbated by a normally distributed white noise. We consider two cases. In the first case, we decrease the insulin sensitivity by 50% under fasting conditions. In the second

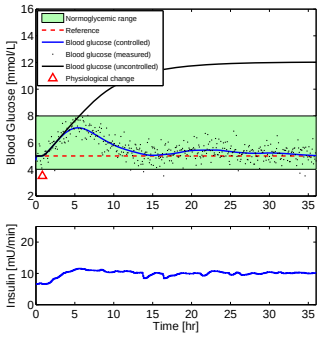

Fig. 4. and insulin administration (bottom) profile in the case wherethe insulin sensitivity decreases by 50% after 1 hour.

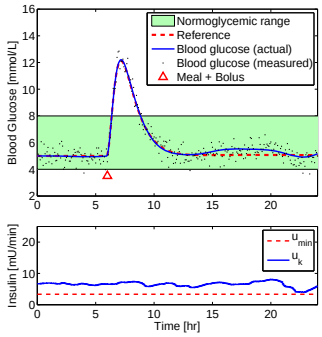

Fig. 5. Blood glucose (top) and insulin administration (bottom) profile in the case where the right meal size is announced

case, the patient has one 75g CHO meal 6 hours after the beginning of the simulation. In the case where the patient has a meal, we consider the cases where the correct meal size is announced, the meal size is underestimated by 50% and the meal size is overestimated by 50%.

Fig. 4 illustrates the blood glucose and the insulin profiles in the case where a change in the insulin sensitivity occurs while the patient is fasting, with sensor noise. The insulin infusion rate increases to reject the disturbance caused by the decrease in insulin sensitivity. In the uncontrolled case where the basal insulin infusion rate is not adjusted, the blood glucose tends to a new steady state in the hyperglycemic range.

For the case where the exact meal size is announced (Fig. 5), the insulin infusion rate remains close to the basal rate. Consequently, the blood glucose follows tightly the glucose setpoint. For the case where the meal size is underestimated (Fig. 6), the basal rate increases after the mealtime to compensate for the too low bolus. For the case where the meal size is overestimated (Fig. 7), the insulin infusion rate is at the minimum after the meal to compensate for the too high bolus. No hypoglycemic events occur when a meal is announced. However, the postprandial blood glucose excursion is bigger when the meal size is underestimated by the patient.

These results show that reasonably good control can be obtained when a feedforward-feedback strategy is used, even for uncertain systems. However, the main limitation of this strategy is that a fairly good nonlinear model description of the patient must be available.

4. Conclusion

In this paper we applied nonlinear model predictive control to compute the optimal insulin profiles for people with type 1 diabetes. These profiles give an upper-bound on the maximal achievable performance in the cases where the meals are announced beforehand, and in the case where meals are announced at mealtimes only. We utilized the bolus-like nature of the optimal insulin profile to design an offset-free feedforward-feedback controller. The feedforward part is a model-based bolus calculator, while the

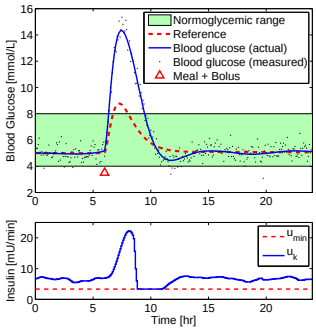

Fig. 6. Blood glucose profile(top) and insulin profile (bottom). Meal size underestimated by 50%.

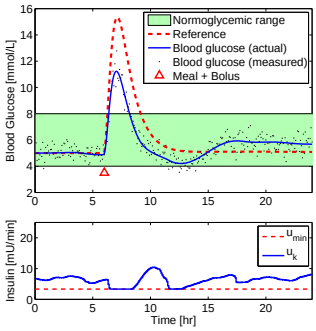

Fig. 7. Blood glucose profile(top) and insulin profile (bottom). Meal size overestimated by 50%.

feedback part adjusts the basal insulin infusion rate. The numerical results demonstrate that a rather good control of blood glucose can be obtained, assuming that a fairly good physiological model of the patient can be identified.

References

Boiroux, D.; Finan, D.A.; Jørgensen, J.B.; Poulsen, N.K.; Madsen, H.: Implications and limitations of ideal insulin administration for people with type 1 diabetes, UKACC International Conference on Control 2010, pages 156-161, 2010a

Boiroux, D.; Finan, D.; Jørgensen, J.; Poulsen, N.; Madsen, H.: Optimal insulin administration for People with Type 1 Diabetes, proceedings of the 9th International Symposium on Dynamics and Control of Process Systems (DYCOPS 2010), pages 234-239, 2010b

Boiroux, D.; Finan, D.; Jørgensen, J.B.; Poulsen, N.K.; Madsen, H.: Strategies for glucose control in people with type 1 diabetes, IFAC world congress 2011. *Submitted*

Cobelli, C.; Dalla-Man, C.; Sparacino, G.; Magni, L.; De Nicolao, G.; Kovatchev, B.P.: Diabetes: models, signals, and control, IEEE Reviews in Biomedical Engineering, **2**, 2009, 54-96

Garcia-Gabin, W.; Vehi, J.; Bondia, J.; Tarin, C.; Calm, R.: Robust sliding mode closed-loop glucose control with meal compensation in type 1 diabetes mellitus, proceedings of the 18th world congress, the international federation of automatic control, pages 4240-4245, 2008

Hovorka, R.; Canonico, V.; Chassin, L.J.; Haueter, U.; Massi-Benedetti, M.; Frederici, M.O.; Pieber, T.R.; Schaller, H.C.; Schaupp, L.; Vering, T.; Wilinska, E.: Nonlinear model predictive control of glucose concentration in subjects with type 1 diabetes, Physiological measurements, **25**, 2004, 905-920

Klonoff, D.C.; Cobelli, C.; Kovatchev, B.; Zisser, H.C.: Progress in development of an artificial pancreas, Journal of Diabetes Science and Technology, **3**, 2009, 1002-1004

Marchetti, G.; Barolo, M.; Jovanovič, L.; Zisser, H.; Seborg, D.E.: A feedforward-feedback glucose control strategy for type 1 diabetes mellitus, Journal of process control, 2008, **18**(2), 149-162

APPENDIX H

Paper G

Model Predictive Control Based on ARX Model for People with type 1 Diabetes

Authors:

Dimitri Boiroux, Niels Kjølstad Poulsen, Henrik Madsen, and John Bagterp Jørgensen
Technical Report, DTU Informatics, Technical University of Denmark, 2011

Model Predictive Control Based on ARX Model for People with type 1 Diabetes

Dimitri Boiroux, Niels Kjølstad Poulsen, Henrik Madsen and John Bagterp Jørgensen

***Abstract*— In this paper we describe and test a controller for regulation of blood glucose in people with type 1 diabetes. The purpose of the controller is to stabilize the overnight blood glucose. The controller is a model predictive controller (MPC) based on a low-order extended ΔARX (autoregressive with exogenous input) model. We robustify the controller by introducing a time-varying glucose setpoint based based on an estimation of the current blood glucose. The feedback is provided by a noisy glucose sensor. The controller is tested on a cohort of seven patients simulated by the Hovorka model. The numerical simulations demonstrate the ability of the controller to handle variations in the insulin sensitivity that can occur during the night.**

I. Introduction

Type 1 diabetes is an autoimmune disease caused by destruction of the beta-cells in the pancreas. The most important consequence for people with type 1 diabetes is an elevated blood glucose. Blood glucose values in non-diabetics will stay in the range 4.0-8.0 mmol/l. Long periods of too high blood glucose (also called hyperglycemia) can lead to complications like nerve diseases, kidney diseases, or blindness. However, the dosing of insulin must be done carefully, because a too high dosage of insulin may lead to a too low blood glucose (hypoglycemia), which has immediate effects, such as insulin shock, coma or even death.

The current insulin therapy for people with type 1 diabetes consists of the injection of slow acting insulin once a day and fast acting insulin several times per day, usually before mealtimes. The slow acting insulin is used to counteract the continuous glucose production from the liver. The fast acting insulin compensates the intake of carbohydrates (CHO) during the meals. The decision on the amount of short and fast acting insulin is based on 3-4 blood glucose measurements per day.

Continuous glucose monitors (CGMs) can improve the insulin therapy by providing more frequent blood glucose measurements. In addition, insulin pumps can be used to adjust the insulin infusion rate, and insulin pens can be used to administrate insulin boluses. These devices can be used in an artificial pancreas, which is described in Fig. 1. Various research groups work on aspects of control algorithms integrating the CGM and the insulin pump [1], [2], [3].

Although insulin pumps and CGMs can improve blood glucose control quality overnight, nocturnal hypoglycemia is still common [4]. For instance, alcohol consumption at dinner have been identified as responsible for nocturnal hypoglycemia [5]. Nocturnal hyperglycemia (also called dawn effect) may also occur.

Technical University of Denmark, DTU Informatics, Richard Petersen's Plads, Building 321, DK-2800 Kgs Lyngby, Denmark.
Corresponding author: jbj@imm.dtu.dk

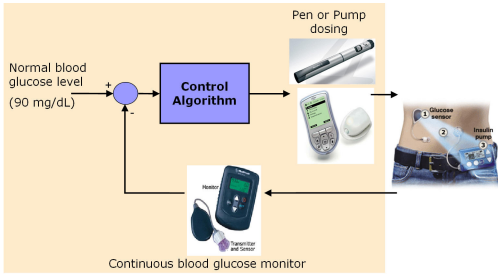

Fig. 1. Closed-loop glucose control. Glucose is measured subcutaneously using a continuous glucose monitor (CGM). Insulin is dosed either continuously by an insulin pump or discretely using an insulin pen.

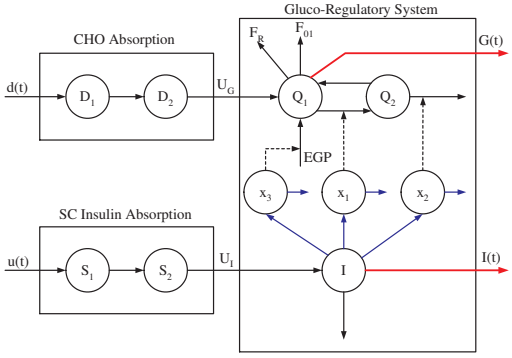

Fig. 2. Diagram of the Hovorka model [7].

In this paper we use a controller based on a low order extended ΔARX model. We test the controller in silico on a cohort of seven virtual patient with type 1 diabetes. The simulations imitate an overnight protocol to stabilize overnight blood glucose in people with type 1 diabetes [6]. In these simulations we assume that the insulin sensitivity of the subjects varies during the night.

The paper is structured as follows. Section 2 introduces the model used to simulate the virtual patients with type 1 diabetes. Section 3 describes the controller used to compute the optimal closed-loop insulin profiles. Section 4 presents the numerical results in the cases where the insulin sensitivity changes overnight. Conclusions are provided in Section 5.

TABLE I

PARAMETERS FOR THE SEVEN PATIENTS [14].THE UNITS ARE: EGP_0 IN $\mu mol/kg/min$, F_{01} IN $\mu mol/kg/min$, k_{12} ($\times 10^{-2}$ UNITLESS), k_{a1} IN 10^{-3} min^{-1}, k_{a2} IN 10^{-3} min^{-1}, k_{a3} IN $10^{-3} \times min^{-1}$, $S_{IT}^f = k_{b1}/k_{a1}$ IN $10^{-4}/min/mU/L$, $S_{ID}^f = k_{b2}/k_{a2}$ IN $10^{-4}/min/mU/L$, $S_{IE}^f = k_{b3}/k_{a3}$ IN $10^{-4}/mU/L$, k_e IN min^{-1}, V_I IN L/kg, V_G IN L/kg, τ_I IN min, τ_G IN min AND BW IN kg

Subject	1	2	3	4	5	6	7
EGP_0	14.8	14.3	15.6	21.3	20.0	10.5	16.1
F_{01}	12.1	7.5	10.3	11.9	7.1	9.2	9.7
k_{12}	3.43	8.71	8.63	9.68	3.90	4.58	6.49
k_{a1}	3.1	15.7	2.9	8.8	0.7	1.7	5.5
k_{a2}	75.2	23.1	49.5	30.2	163.1	68.9	68.3
k_{a3}	47.2	14.3	69.1	11.8	11.4	28.5	30.4
S_{IT}^f	29.4	18.7	81.2	86.1	72.4	19.1	51.2
S_{ID}^f	0.9	6.1	20.1	4.7	15.3	2.2	8.2
S_{IE}^f	401	379	578	720	961	81	520
k_e	0.138	0.138	0.138	0.138	0.138	0.138	0.138
V_I	0.18	0.13	0.22	0.14	0.14	0.13	0.16
V_G	0.18	0.13	0.22	0.14	0.14	0.13	0.12
τ_I	55	55	55	55	55	55	55
τ_G	40	40	40	40	40	40	40
BW	70	70	70	70	70	70	70

II. PHYSIOLOGICAL MODELS

Several nonlinear physiological models have been developed to simulate virtual patients with type 1 diabetes [7], [8], [9], [10], [11]. However, even the simplest nonlinear physiological models, such as the minimal model developed by Bergman et al. may present identifiability issues [12]. In this paper, we use the Hovorka model to simulate people with type 1 diabetes. The models for CHO absorption, subcutaneous insulin absorption and the glucose-insulin dynamics for the Hovorka model are described in Fig. 2.

As the time constants associated to insulin absorption can vary from individual to individual (inter-patient variability) and even for the same person at different times (intra-patient variability), there is no doubt that the quality control is limited by these lags [13]. Furthermore, the complexity of the physiological mechanisms associated to the glucose-insulin dynamics make predictions of the blood glucose inaccurate when the state of the system is not close to the steady state, e.g. during meals.

III. CONTROLLER SETUP

In this section we describe the controller used to compute the optimal insulin administration profiles. The controller is based on an extended ΔARX MPC, where the model is rewritten in the state space innovation form. We use a time-varying glucose setpoint based on an estimation of the current blood glucose. The optimal control problem is formulated as a convex quadratic program with soft output constraints.

A. ARX model

In this paper we use the following discrete-time, linear ARX model

$$A(q^{-1})y(t) = q^{-n_k}B(q^{-1})u(t) + \varepsilon(t) \tag{1}$$

where q^{-1} is the backward shift operator, $\varepsilon(t) \sim N_{iid}(0,\sigma^2)$ and A and B are polynomials of degree n_a and n_b respectively, i.e.

$$\begin{aligned} A(q^{-1}) &= 1 + a_1 q^{-1} + ... + a_{n_a} q^{-n_a} \\ B(q^{-1}) &= b_1 q^{-1} + ... + b_{n_b} q^{-n_b} \end{aligned} \tag{2}$$

The ARX model (1) may be realized as a stationary state space model in innovation form

$$x_{k+1} = Ax_k + Bu_k + K\varepsilon_k \tag{3}$$

$$y_k = Cx_k + \varepsilon_k \tag{4}$$

where the matrices A, B, C and K are written in the canonical form

$$\begin{aligned} A &= \begin{bmatrix} -a_1 & 1 & 0 & \cdots & 0 \\ -a_2 & 0 & 1 & \cdots & 0 \\ \vdots & \vdots & \vdots & \ddots & \vdots \\ -a_{n-1} & 0 & 0 & \cdots & 1 \\ -a_n & 0 & 0 & 0 & 0 \end{bmatrix} B = \begin{bmatrix} b_1 \\ b_2 \\ \vdots \\ b_{n-1} \\ b_n \end{bmatrix} \\ K &= \begin{bmatrix} -a_1 \\ -a_2 \\ \vdots \\ -a_{n-1} \\ -a_n \end{bmatrix} C = \begin{bmatrix} 1 & 0 & \cdots & 0 \end{bmatrix} \end{aligned} \tag{5}$$

It must be pointed out that the process noise and the measurement noise are completely correlated.

Consequently, the one-step ahead predictions of the states and the outputs are

$$\hat{x}_{k+1|k} = A\hat{x}_{k|k} + Bu_{k|k} + K\varepsilon_k \tag{6a}$$

$$\hat{y}_{k+1|k} = C\hat{x}_{k+1|k} \tag{6b}$$

in which ε_k is the innovation term

$$\varepsilon_k = y_k - C\hat{x}_{k|k-1} \tag{7}$$

Similarly, the $j+1$ steps ahead predictions of the states and the outputs are

$$\hat{x}_{k+j+1|k} = A\hat{x}_{k+j|k} + Bu_{k+j|k} \tag{8a}$$

$$\hat{y}_{k+j+1|k} = C\hat{x}_{k+j+1|k} \tag{8b}$$

B. Extended Δ-ARX

We now assume that the process noise $\varepsilon(t)$ is an integrated white noise, i.e.

$$\varepsilon(t) = \frac{1-\alpha q^{-1}}{1-q^{-1}} e(t) \tag{9}$$

, the extended Δ-ARX model is

$$\bar{A}(q^{-1})y(t) = \bar{B}(q^{-1})u(t) + (1-\alpha q^{-1})e(t) \tag{10}$$

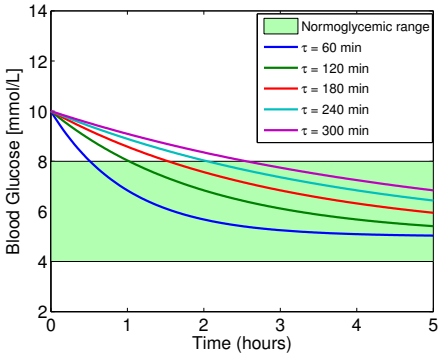

Fig. 3. Example of time-varying reference signal for different values of the time constant τ.

where $e(t)$ is a white noise process and

$$\bar{A}(q^{-1}) = (1-q^{-1})A(q^{-1}) \tag{11}$$
$$\bar{B}(q^{-1}) = (1-q^{-1})B(q^{-1}) \tag{12}$$
$$(1-\alpha q^{-1})e(t) = (1-q^{-1})\varepsilon(t) \tag{13}$$

The extended Δ-ARX model (10) is able to provide offset-free tracking due to the integrator [15]. The choice of the tuning parameter $\alpha \in [0;1]$ determines the aggressiveness of the controller. $\alpha = 0$ corresponds to the pure ΔARX model, and $\alpha = 1$ is equivalent to the ARX model without the integrator (1). Larger values of α decrease the input and output variance, but provide a slower disturbance rejection.

In this paper, the input $u(t)$ is the deviation of insulin infusion rate from the steady state u_{ss} and the output $y(t)$ is the deviation of blood glucose from the steady state $\bar{G}$. For the numerical simulations, we choose $\bar{G} = 6$ mmol/L.

We still can use the innovation form (3) for the realization of the extended model (10) by substracting α to the first row in K.

C. Time-varying glucose setpoint

The glucose trajectory is exponentially decreasing when the blood glucose is above the target, which robustifies the controller with respect to plant-model mismatches. Consequently, the reference blood glucose is

$$\hat{r}_{k+j|k}(t) = \hat{y}_{k|k} \exp\left(-\frac{t_j}{\tau}\right) \tag{14}$$

The choice of the tuning parameters τ has an influence on the rapidness and the robustness of the controller. Small values of τ provide a faster return to the euglycemic range, while larger values of τ ensure a more robust control. The glucose setpoint profiles for different values of the time constant τ are shown in Fig. 3.

D. Model Predictive Control with Soft Constraints

At the time t_k, the open loop convex quadratic program solved is

$$\min_{\{u_k+j,v_j\}_{j=0}^{N-1}} \phi = \frac{1}{2}\sum_{j=0}^{N-1} \|\hat{y}_{k+j+1|k} - \hat{r}_{k+j+1|k}\|_2^2 + \lambda\|\Delta u_{k+j}\|_2^2 + \kappa_1\|v_{k+j}\|_2^2 \tag{15a}$$

$$s.t. \quad \hat{x}_{k+1|k} = A\hat{x}_{k|k-1} + Bu_k + Ke_k \tag{15b}$$
$$\hat{y}_{k+1|k} = C\hat{x}_{k+1|k} \tag{15c}$$
$$\hat{x}_{k+j+1|k} = A\hat{x}_{k+j|k} + Bu_k \tag{15d}$$
$$\hat{y}_{k+j+1|k} = C\hat{x}_{k+j+1|k} \tag{15e}$$
$$u_{\min} \le u_{k+j} \le u_{\max} \tag{15f}$$
$$\Delta u_{\min} \le \Delta u_{k+j} \le \Delta u_{\max} \tag{15g}$$
$$G_{\min} - y_{k+1} \le v_{k+j} \tag{15h}$$
$$v_j \ge 0 \tag{15i}$$

in which $\hat{x}_{k|k-1}$ and $e_k = y_k - C\hat{x}_{k|k-1}$ are given. $u_{\min}$ and $u_{\max}$ are the minimum and the maximum insulin infusion rates allowed by the pump. $\Delta u_{k+j} = u_{k+j} - u_{k+j-1}$ is the variation in the insulin infusion rate. $G_{\min}$ depicts the lower bound on blood glucose.

The slack variables v_j are introduced to penalize hypoglycemia. The hard input constraints (15f-15g) limit the insulin infusion rate and the increment of the insulin infusion rate respectively. The penalty term $\kappa\|v_{k+j}\|_2^2$ is used to avoid hypoglycemia and the penalty term $\lambda\|\Delta u_{k+j}\|_2^2$ prevents the insulin infusion rate from varying too aggressively.

For the simulations we choose $N = 120$, i.e. a 10 hour prediction horizon, and

$$u_{min} = -u_{ss}, \quad u_{max} = u_{ss}, \quad \lambda = \frac{10}{u_{ss}^2}, \quad \kappa = 500 \tag{16}$$

We remind here that the input avariables are deviation variables from the steady state u_{ss}. Consequently, the choice of $u_{min} = -u_{ss}$ allows the controller to switch off the insulin pump, and $u_{max} = u_{ss}$ prevents the pump from overdosing the insulin.

IV. Numerical Results

In this section, we use a cohort of seven virtual patients and the controller presented above to compute insulin and blood glucose profiles. We illustrate both overnight simulations and 36 hour simulations without meals. For overnight simulations we consider the case where the insulin sensitivity decreases during the night (also called dawn phenomenon) and the case where the insulin sensitivity increases, which might cause nocturnal hypoglycemia. We compare the closed-loop controller where the patient wears a blood glucose sensor with open-loop simulations where the insulin infusion remains constant during the night.

TABLE II

CONTROLLER PARAMETERS FOR THE SEVEN PATIENTS.

Subject	a_1	b_1 ($\times 10^{-3}$)
1	-0.9995	-7.7
2	-0.9966	-13.4
3	-0.9961	-12.9
4	-0.9974	-25.9
5	-0.9944	-23.5
6	-0.9984	-3.3
7	-0.9958	-20.7

A. Clinical protocol

The clinical protocol for the seven patients is the following:

- The patient arrives at 17:00 at the clinic.
- The patient gets a 70 g CHO dinner and an insulin bolus at 18:00.
- The closed loop starts at 22:00.
- The insulin sensitivity varies by $\pm 30\%$ at 02:00.
- The patient gets a 50 g CHO breakfast and an insulin bolus at 08:00. The closed-loop controller is switched off.
- The patient leaves the clinic at 12:00.

The insulin sensitivity is changed by modifying the insulin sensitivities for the three insulin action compartments at 3AM. The insulin sensitivities are described by the parameters $S_{I,1}$, $S_{I,2}$ and $S_{I,3}$ in the Hovorka model (the model is described in [7] and [16]) accordingly. The bolus sizes are provided by a bolus calculator.

For the simulations, we assume that the sensor noise is a white noise with the standard deviation $\sigma = 0.2$mmol/L

B. Model for the patients

The model is a low order ARX model with $n_a = n_b = 1$, $n_k = 0$

$$(1 + a_1 q^{-1})\Delta y(t) = b_1 \Delta u(t) + (1 - \alpha q^{-1})\varepsilon(t) \qquad (17)$$

in which we choose $\alpha = 0.99$. This choice of α will make the disturbance rejection slow, however smaller values of α would make the controller unstable.

The two parameters a_1 and b_1 have been identified off-line and are individualized for each patient. The parameters for each patient are shown on Table II.

C. Fasting simulation results

Fig. 4 illustrates the blood glucose and the insulin profiles in the case where the insulin sensitivity decreases by 30% while the patient is fasting. In the controlled case (Fig. 4(b)), the insulin infusion rate increases to reject the disturbance. In the uncontrolled case where the basal insulin infusion rate is not adjusted (Fig. 4(a)), the blood glucose tends to a new steady state in the hyperglycemic range for all the patients.

Fig. 5 illustrates the blood glucose and the insulin profiles in the case where the insulin sensitivity increases by 30% while the patient is fasting. In the controlled case (Fig. 5(b)), the insulin infusion rate decreases to avoid hypoglycemia.

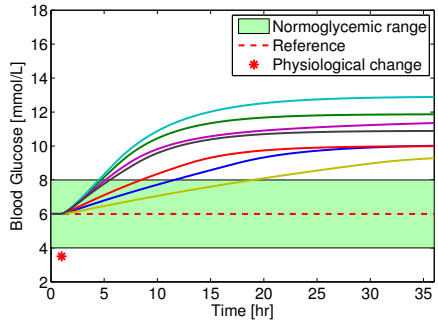

(a) Open-loop

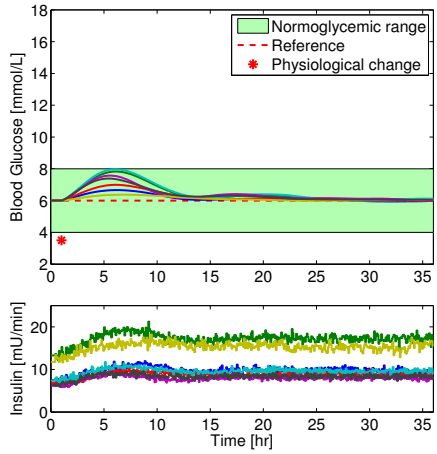

(b) Closed-loop

Fig. 4. Insulin and blood glucose profile in the case where the insulin sensitivity decreases by 30% after one hour.

In the uncontrolled case where the basal insulin infusion rate is not adjusted (Fig. 5(a)), all the subjects fall into mild hypoglycemia, and some of them fall into severe hypoglycemia.

These simulations demonstrate that the controller is able to avoid prolonged periods of hypoglycemia and hyperglycemia. They also show that the controller can achieve offset-free control in the case where the insulin sensitivity varies.

D. Overnight simulation results

Fig. 6 illustrate the blood glucose and the insulin profiles in the case where the insulin sensitivity does not vary during the night. The blood glucose remains within the euglycemic range during the whole night.

Fig. 7(a) and 7(b) depict the blood glucose and the insulin profiles in the case where an increase by 30% in the insulin sensitivity occurs during the night. The insulin infusion rate

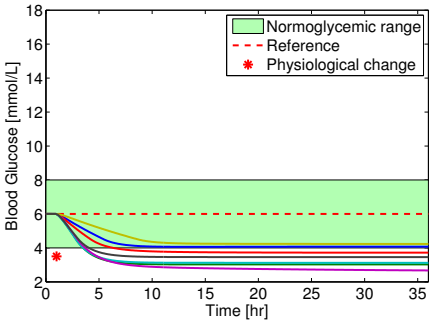

(a) Open-loop

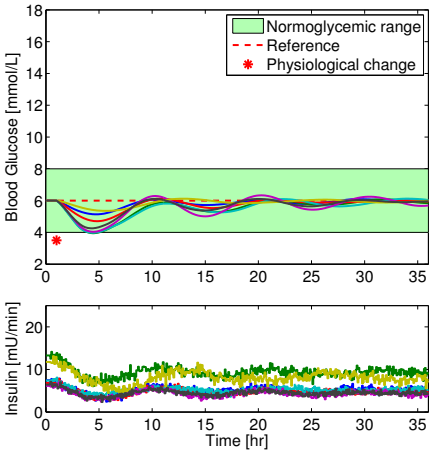

(b) Closed-loop

Fig. 5. Insulin and blood glucose profile in the case where the insulin sensitivity increases by 30% after during the night.

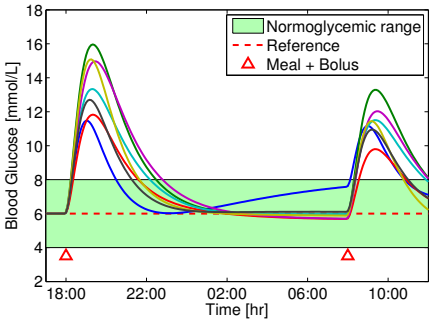

Fig. 6. Insulin and blood glucose profile in the case where the insulin sensitivity does not change during the night.

decreases to reject the disturbance caused by the change in insulin sensitivity. In the case where the insulin infusion

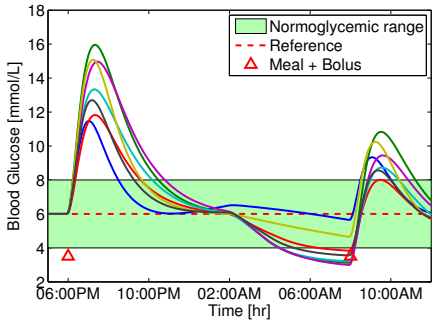

(a) Open-loop

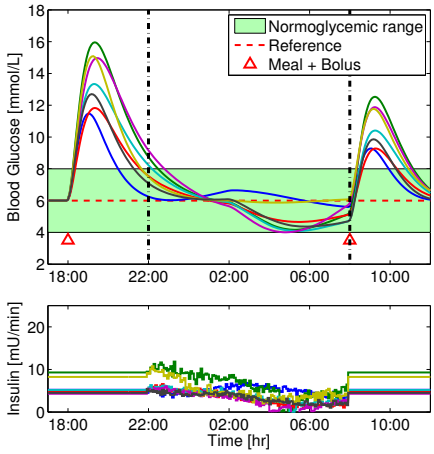

(b) Closed-loop

Fig. 7. Insulin and blood glucose profile in the case where the insulin sensitivity increases by 30% during the night.

rate does not vary during the night (Fig. 7(a)), most of the patients fall into hypoglycemia. Hypoglycemic events can be avoided for all the subjects when the closed-loop controller is active (Fig. 7(b)). Therefore, it can be concluded that the closed-loop controller can reduce the risk of nocturnal hypoglycemia.

Fig. 8(a) and 8(b) depict the blood glucose and the insulin profiles in the case where a decrease by 30% in the insulin sensitivity occurs during the night. It can be seen that the blood glucose before the breakfast is closer to the euglycemic range for the closed-loop controller than for the open-loop one. Even more important, the postprandial blood glucose excursions are smaller when the closed-loop controller is active.

V. Conclusion

In this paper we described and tested a controller for regulation of blood glucose in people with type 1 diabetes.

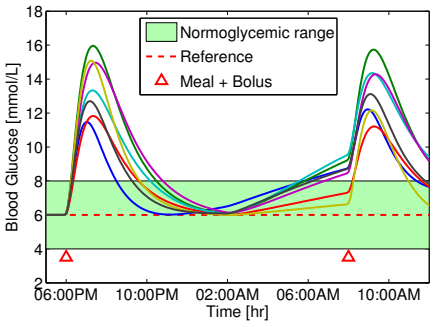

(a) Open-loop

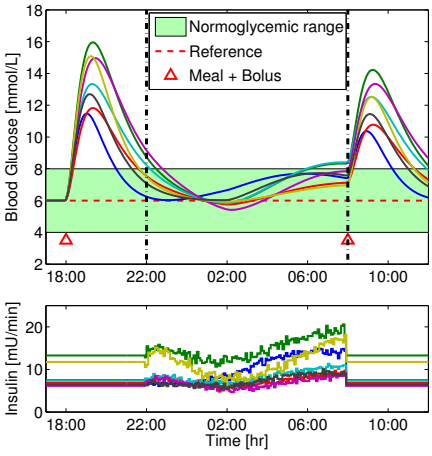

(b) Closed-loop

Fig. 8. Insulin and blood glucose profile in the case where the insulin sensitivity decreases by 30% during the night.

The controller is based on a low-order extended ΔARX model of the patient. We considered the cases where the dawn phenomenon occurs during the night, and the case where the blood glucose suddenly decreases. The numerical results demonstrate that a closed loop controller based on MPC can significantly reduce the risk of hypoglycemia and hyperglycemia during the night. Closed-loop controllers can also reduce the amplitude of the postprandial blood glucose excursion in the case where the blood glucose increases during the night.

REFERENCES

[1] D. C. Klonoff, C. Cobelli, B. Kovatchev, and H. C. Zisser, "Progress in development of an artificial pancreas," *Journal of Diabetes Science and Technology*, vol. 3, pp. 1002–1004, 2009.

[2] C. Cobelli, C. Dalla Man, G. Sparacino, L. Magni, G. De Nicolao, and B. P. Kovatchev, "Diabetes: Models, signals, and control," *IEEE Reviews in Biomedical Engineering*, vol. 2, pp. 54–96, 2009.

[3] L. Magni, D. M. Raimondo, C. Dalla Man, G. De Nicolao, B. P. Kovatchev, and C. Cobelli, "Model predictive control of glucose concentration in type I diabetic patients: An in silico trial," *Biomedical Signal Processing and Control*, vol. 4, no. 4, pp. 338–346, 2009.

[4] R. W. Beck, "Prolonged nocturnal hypoglycemia is common during 12 months of continuous glucose monitoring in children and adults with type 1 diabetes," *Diabetes Care*, pp. 992 – 1007, 2010.

[5] B. C. Turner, E. Jenkins, D. Kerr, R. S. Sherwin, and D. A. Cavan, "The effect of evening alcohol consumption on next-morning glucose control in type 1 diabetes," *Diabetes care*, vol. 24, pp. 1888 – 1893, 2001.

[6] R. Hovorka, J. M. Allen, D. Elleri, L. J. Chassin, J. Harris, D. Xing, C. Kollman, T. Hovorka, A. M. F. Larsen, M. Nodale, A. De Palma, M. E. Wilinska, C. L. Acerini, and D. B. Dunger, "Manual closed-loop insulin delivery in children and adolescents with type 1 diabetes: a phase 2 randomised crossover trial," *Lancet*, vol. 375, pp. 743 – 751, 2010.

[7] R. Hovorka, V. Canonico, L. J. Chassin, U. Haueter, M. Massi-Benedetti, M. O. Federici, T. R. Pieber, H. C. Schaller, L. Schaupp, T. Vering, and M. E. Wilinska, "Nonlinear model predictive control of glucose concentration in subjects with type 1 diabetes," *Physiological Measurement*, vol. 25, pp. 905–920, 2004.

[8] R. N. Bergman, L. S. Phillips, and C. Cobelli, "Physiologic evaluation of factors controlling glucose tolerance in man: measurement of insulin sensitivity and beta-cell glucose sensitivity from the response to intravenous glucose," *Journal of Clinical Investigation*, vol. 68, no. 6, pp. 1456 – 1467, 1981.

[9] C. Dalla Man, R. Rizza, and C. Cobelli, "Meal simulation model of the glucose-insulin system," *IEEE Transactions on Biomedical Engineering*, vol. 54, no. 10, pp. 1740–1749, 2007.

[10] M. E. Wilinska and R. Hovorka, "Simulations models for in-silico testing of closed-loop glucose controllers in type i diabetes," *Drug Discovery Today: Disease Models*, vol. 5, no. 4, pp. 289 – 298, 2009.

[11] J. T. Sorensen, "A physiologic model of glucose metabolism in man and its use to design and assess improved insulin therapies for diabetes," Ph.D. dissertation, Massachusetts Institute of Technology, 1985.

[12] G. Pillonetto, G. Sparacino, and C. Cobelli, "Numerical non-identifiability regions of the minimal model of glucose kinetics: superiority of bayesian estimation," *Mathematical Biosciences*, vol. 184, pp. 53 – 67, 2003.

[13] D. Boiroux, D. A. Finan, N. K. Poulsen, H. Madsen, and J. B. Jørgensen, "Nonlinear model predictive control for an artificial β-cell," in *Recent Advances in Optimization and its Applications in Engineering*. Springer, 2010, pp. 299 – 308.

[14] R. Hovorka, F. Shojaee-Moradie, P. V. Caroll, L. J. Chassin, I. J. Gowrie, N. C. Jackson, R. S. Tudor, A. M. Umpleby, and R. H. Jones, "Partitioning glucose distribution/transport, disposal, and endogenous production during IVGTT," *Am. J. Physiol.*, vol. 282, pp. 992–1007, 2002.

[15] J. K. Huusom, N. K. Poulsen, S. B. Jørgensen, and J. B. Jørgensen, "Tuning of methods for offset free MPC based on ARX model representations," in *2010 American Control Conference (ACC)*, Baltimore, MD, USA, 2010, pp. 2355–2360.

[16] D. Boiroux, D. A. Finan, N. K. Poulsen, H. Madsen, and J. B. Jørgensen, "Optimal insulin administration for people with type 1 diabetes," in *Proceedings of the 9th International Symposium on Dynamics and Control of Process Systems (DYCOPS 2010)*, 2010, pp. 234 – 239.

APPENDIX I

Paper H

Control of Blood Glucose for People with Type 1 Diabetes: an in-vivo Study

Authors:

Dimitri Boiroux, Signe Schmidt, Laurits Frøssing, Kirsten Nørgaard, Sten Madsbad, Ole Skyggebjerg, Anne Katrine Duun-Henriksen, Niels Kjølstad Poulsen, Henrik Madsen, and John Bagterp Jørgensen

Published in:

Proceedings of the 17th Nordic Process Control Workshop, pages 133-140, 2012.

Control of Blood Glucose for People with Type 1 Diabetes: an in Vivo Study

Dimitri Boiroux * **Signe Schmidt** **
Anne Katrine Duun-Henriksen * **Laurits Frøssing** **
Kirsten Nørgaard ** **Sten Madsbad** ** **Ole Skyggebjerg** *
Niels Kjølstad Poulsen * **Henrik Madsen** *
John Bagterp Jørgensen *

* *Department of Informatics and Mathematical Modeling, Technical University of Denmark, 2800 Kgs Lyngby, Denmark.*
** *Department of Endocrinology, Hvidovre Hospital, 2650 Hvidovre, Denmark*

Abstract:
Since continuous glucose monitoring (CGM) technology and insulin pumps have improved recent years, a strong interest in a closed-loop artificial pancreas for people with type 1 diabetes has arisen. Presently, a fully automated controller of blood glucose must face many challenges, such as daily variations of patient's physiology and lack of accuracy of glucose sensors. In this paper we design and discuss an algorithm for overnight closed-loop control of blood glucose in people with type 1 diabetes. The algorithm is based on Model Predictive Control (MPC). We use an offset-free autoregressive model with exogenous input and moving average (ARMAX) to model the patient. Observer design and a time-varying glucose reference signal improve robustness of the algorithm. We test the algorithm in two clinical studies conducted at Hvidovre Hospital. The first study took place overnight, and the second one took place during daytime. These trials demonstrate the importance of observer design in ARMAX models and show the possibility of stabilizing blood glucose during the night.

1. INTRODUCTION

Type 1 diabetes is a disease caused by destruction of the insulin producing beta-cells in the pancreas. Therefore, patients with type 1 diabetes must rely on exogenous insulin administration in order to tightly regulate their blood glucose. Blood glucose should preferably be kept in the range 4.0-8.0 mmol/l. Long periods of high blood glucose (hyperglycemia) can lead to long-term complications like nerve diseases, kidney diseases, or blindness. However, the dosing of insulin must be done carefully, because a too high dosage of insulin may lead to a too low blood glucose (hypoglycemia). Low blood glucose has immediate effects, such as coma or even death.

The conventional insulin therapy for people with type 1 diabetes consists of the injection of slow acting insulin once a day and rapid acting insulin several times per day. The slow acting insulin is used to counteract the continuous glucose production from the liver. The fast acting insulin compensates the intake of carbohydrates (CHO) during the meals. The decision on the dosage of short and fast acting insulin is based on several blood glucose measurements per day.

However, an increasing number of patients with type 1 diabetes use an intensive insulin therapy based on continuous glucose monitors (CGMs) and insulin pumps instead of the conventional therapy described above. This regime can reduce the risk of complications. CGMs can provide more frequent blood glucose measurements. In addition, insulin pumps can adjust to daily variations in insulin needs.

Nevertheless, the patients still need to be constantly involved in their decisions on the insulin treatment based on their CGMs and/or fingersticks measurements. A system consisting of a CGM, an insulin pump and a control algorithm that computes the insulin dose based on glucose measurements is called an artificial pancreas. The artificial pancreas provides closed-loop control of the blood glucose by manipulation of the insulin injection. The artificial pancreas has the potential to ease the life and reduce complications for people with type 1 diabetes. Its principle is illustrated in Fig. 1. Several review papers about closed-loop control of blood glucose for people with type 1 diabetes have been published (Hovorka et al. (2006), Cobelli et al. (2011), Bequette (2011)).

Previous publications have proven that model predictive control (MPC) has great potential for design of an artificial pancreas. Magni et al. (2009) established that MPC could reduce oscillatory behaviors compared to proportional integral derivative (PID) controllers. Boiroux et al. (2010) applied open-loop constrained nonlinear optimal control. Hovorka et al. (2010) tested an MPC-based controller on children and adolescents with type 1 diabetes.

In this paper we focus on overnight blood glucose control for people with type 1 diabetes using a CGM, an insulin

⋆ Funding for this research as part of the DIACON project from the Danish Council for Strategic Research (NABIIT project 2106-07-0034) is gratefully acknowledged.

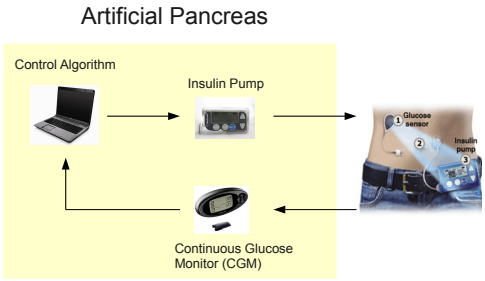

Fig. 1. Closed-loop glucose control. Glucose is measured subcutaneously using a continuous glucose monitor (CGM). Insulin is dosed by an insulin pump.

Fig. 2. Picture of the pilot trial.

pump, and a controller based on MPC. Many factors, such as meal intake, physical exercise, stress, illness, alcohol consumption etc. affect insulin needs. Also, hormone release during the night may cause elevated blood glucose in the early morning. This particular phenomenon is called the dawn phenomenon. The main goal of a closed-loop controller is to compensate these effects by adjusting the amount of injected insulin based on frequent glucose measurements coming from a CGM.

The paper is structured as following. Section 2 describes the material and methods used for the studies. We discuss the design of the controller in Section 3. Section 4 shows the results for the two clinical studies conducted at Hvidovre Hospital. Conclusions are provided in Section 5.

2. METHODS AND MATERIAL

This section describes the clinical protocol and the internally developed graphical user interface for the clinical studies.

2.1 Clinical protocol

The clinical trial consists of a randomized cross-over study including 12 patients with type 1 diabetes. The goal is to compare overnight glucose control during open-loop and closed-loop insulin administration. We investigate the cases where

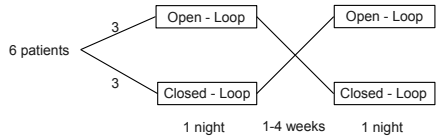

Fig. 3. Study design.

- The insulin bolus matches the evening meal (6 patients in total)
- The insulin bolus is underdosed (6 patients in total)

The study design for the 2 cases is illustrated in Fig. 3.

The scenario during the clinical studies is the following:

- The patient arrives at 16:00.
- A meal is consumed at 18:00 and an insulin bolus is administrated. The meal size is determined by the weight of the patient. The bolus size depends on the patient and the scenario (meal with the correct bolus or underbolused meal).
- The loop is closed at 22:00 (for closed-loop studies only).
- The closed-loop ends at 07:00 the following day (for closed-loop studies only).

The purpose of the first part of the study (when the insulin bolus matches the evening meal) is to validate the ability of the controller to compensate for overnight physiological changes in patients. The second part of the study (when meals are underbolused) must ensure that the controller can bring and keep blood glucose in the range 4.0-8.0 mmol/L.

The patient is equipped with 2 Dexcom Seven Plus CGMs and a Medtronic Paradigm insulin pump. The CGMs provide glucose measurements every 5 minutes. The clinician decides on the sensor used by the controller, based on the accuracy of the sensor during the days before the study. The other CGM can be used as a backup device. Insulin is administrated to the patient through small discrete insulin injections (also called microboluses) every 15 minutes.

It must be pointed out that the pump used for the trials has discrete increments of 0.025U for the microboluses, and a minimum continuous insulin injection (or basal rate) of 0.025 U/hr. The controller handles these restrictions by using hard constraints on the minimal insulin infusion rate and by rounding the suggested microbolus to the nearest 0.025U (see Section 3.6).

In addition, blood samples are taken every 30 minutes in order to measure more accurately the blood glucose (in case of prolonged period of low blood glucose, the sampling time is set to 15 minutes). The blood glucose was measured by Hemocue and after the trial by YSI. These values are not provided to the controller.

The clinician has the authority to prevent severe hypoglycemia by injection of intravenous glucose. Such a decision is based on the glucose history.

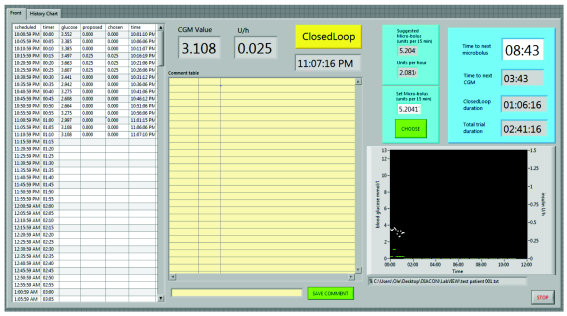

Fig. 4. Graphical User Interface screenshot

2.2 Graphical User Interface

Fig 4 provides an overview of the graphical user interface developed for the artificial pancreas. The glucose sensor provides a glucose measurement every 5 minutes. The glucose measurements are transmitted from the sensor to the software via a wireless receiver.

The graphical user interface returns a new insulin microbolus suggestion every 15 minutes. At these times, it also returns the glucose prediction and insulin prediction profiles. The decision on the insulin microbolus can be overruled if there is a safety risk for the patient. The exact time before the next microbolus suggestion is provided by the graphical user interface.

It is also possible to add comments if necessary. These comments have no influence on the microboluses computation, but are stored.

3. CONTROLLER DESIGN

This section presents the detailed description of the controller. The controller computes a discrete-time offset-free ARMAX model. This model is then used to optimize the future injections of insulin. The controller must be designed in a robust and safe way for the patient, especially regarding low blood glucose. We use here a time-varying glucose setpoint to avoid insulin overdose.

3.1 Model computation

Several research groups investigated low-order models to describe glucose-insulin dynamics. Kirchsteiger et al. (2011) used a third order transfer function, Finan et al. (2009) identified ARX models and Percival et al. (2010) applied a first order transfer function with a delay. In this paper we use a Single Input-Single Output (SISO) second order continuous-time transfer function

$$Y(s) = G(s)U(s), \quad G(s) = \frac{K}{(\tau s + 1)^2} \tag{1}$$

The input $U(s)$ is the insulin intake and the output $Y(s)$ is the blood glucose, both expressed in terms of deviation variables from a steady state, K is the static gain and τ is the time constant. The gain and the time constant are computed from known patient-specific parameters. These parameters are the insulin action time and the insulin sensitivity factor (ISF). They can be estimated for each individual patient by looking at the impulse response for a small insulin bolus. The insulin action time τ corresponds to the time that blood glucose takes to reach its minimum. The insulin sensitivity factor (ISF) corresponds to the maximum decrease in blood glucose per unit of insulin bolus. These parameters are empirically estimated by the patient and his/her physician. However, these parameters may dramatically vary from day to day for a given patient.

The impulse response in the temporal domain of the transfer function (1) is

$$y(t) = K \frac{t}{\tau^2} \exp(-t/\tau) \tag{2}$$

We shall now relate the insulin sensitivity factor and the insulin action time to the gain K and the time constant τ in (2). The insulin action time corresponds to the time to reach the minimum blood glucose, it is therefore equal to τ. We find K by computing the output of the impulse response (2) at its minimum, i.e. at time $t = \tau$. It gives

$$y(\tau) = -I_{SF} = \frac{K}{\tau} \exp(-1) \tag{3}$$

Isolating K in the above equation yields to

$$K = -\tau \exp(1) I_{SF} \tag{4}$$

The transfer function (1) can be reformulated as a discrete-time transfer function model in the form

$$y(t) = G(q^{-1})u(t), \quad G(q^{-1}) = \frac{\bar{B}(q^{-1})}{\bar{A}(q^{-1})} \tag{5}$$

which is equivalent to

$$\bar{A}(q^{-1})y(t) = q^{-n_k}\bar{B}(q^{-1})u(t) \tag{6}$$

$\bar{A}(q^{-1})$ and $\bar{B}(q^{-1})$ are

$$\bar{A}(q^{-1}) = 1 + \bar{a}_1 q^{-1} + \bar{a}_2 q^{-2} \tag{7a}$$
$$\bar{B}(q^{-1}) = \bar{b}_1 q^{-1} + \bar{b}_2 q^{-2} \tag{7b}$$

Fig 5 depicts the exact impulse response and its second order approximation for a virtual patient. This patient is simulated using the model developed by Hovorka et al. (2004). The figure demonstrates that a second order model can provide a fairly good approximation of a patient with type 1 diabetes. Current insulin, such as the Novorapid insulin documented in Nov (2002) has a similar impulse response shape, but can provide even faster action (the minimum in glucose is reached in 60-90 minutes).

3.2 Observer design for the first study

Odelson et al. (2006), Jørgensen and Jørgensen (2007) and Åkesson et al. (2008) proposed several methods for Kalman filter tuning. In our controller we use the following discrete-time, linear ARMAX model

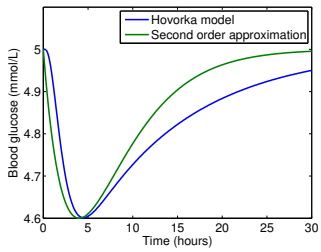

Fig. 5. Example of second order approximation compared to the exact impulse response. The bolus size is here 0.1U. The parameters are: τ=4 hours and $I_{SF} = 4$ mmol/L/U.

$$A(q^{-1})y(t) = q^{-n_k}B(q^{-1})u(t) + C(q^{-1})\varepsilon(t) \quad (8)$$

A, B and C are polynomials, and q^{-1} is the backward shift operator. We assume that $\varepsilon(t) \sim N_{iid}(0, \sigma)$. In the first pilot study we used the following ARMAX model description

$$A(q^{-1})y(t) = B(q^{-1})u(t) + (1 - \alpha q^{-1})e(t) \quad (9)$$

in which

$$A(q^{-1}) = (1 - q^{-1})\bar{A}(q^{-1}) \quad (10)$$
$$B(q^{-1}) = (1 - q^{-1})\bar{B}(q^{-1}) \quad (11)$$

The model (9) is able to provide offset-free tracking due to the integrator. The parameter $\alpha \in [0; 1]$ is a tuning parameter. $\alpha = 0$ corresponds to an integrated ARX model, while $\alpha = 1$ corresponds to an ARX model without integrator. For further details about the choice of α, see e.g. Huusom et al. (2010).

The ARX model (9) may be realized as a stationary state space model in innovation form

$$x_{k+1} = Ax_k + Bu_k + K\varepsilon_k \quad (12)$$
$$y_k = Cx_k + \varepsilon_k \quad (13)$$

The matrices A, B, C and K are written in the canonical form

$$A = \begin{bmatrix} -a_1 & 1 & 0 \\ -a_2 & 0 & 1 \\ -a_3 & 0 & 0 \end{bmatrix} \quad B = \begin{bmatrix} b_1 \\ b_2 \\ b_3 \end{bmatrix}$$
$$K = \begin{bmatrix} -\alpha - a_1 \\ -a_2 \\ -a_3 \end{bmatrix} \quad C = [1\ 0\ 0] \quad (14)$$

Fig. 6 shows the glucose and insulin predictions for the first study. It can be noticed that the prediction is mostly based on the two previous observations (which show an increasing blood glucose) rather than on the global trend (which shows a decreasing blood glucose).

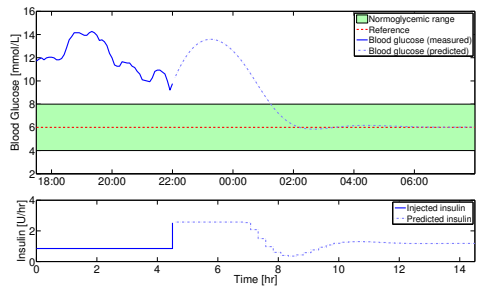

Fig. 6. Example of blood glucose prediction for the first study. It can be seen that the controller relies more on the local trend than on the global trend.

3.3 Observer design for the second study

In this section we consider the general ARMAX model (8) in which we assume

$$C(q^{-1}) = 1 + c_1q^{-1} + c_2q^{-2} + c_3q^{-3} \quad (15)$$

and

$$A(q^{-1}) = (1 - q^{-1})\bar{A}(q^{-1}) \quad (16)$$
$$B(q^{-1}) = (1 - q^{-1})\bar{B}(q^{-1}) \quad (17)$$

in order to preserve the offset-free control property. Therefore, the Kalman gain K in equation (14) becomes

$$K = \begin{bmatrix} c_1 - a_1 \\ c_2 - a_2 \\ c_3 - a_3 \end{bmatrix} \quad (18)$$

(the matrices A, B and C remain unchanged). The design of observer consists of setting the eigenvalues of $A - KC$. Having the eigenvalues close to 0 makes the state estimation error rapidly vanish, but on the other hand the observer will be more sensitive to noise. Having the eigenvalues close to 1 makes the observer less sensitive to noise (and therefore more relying on the global trend) but introduces a delay in the predictions. It can be shown that these eigenvalues are the roots of the polynomial

$$\chi(z) = z^3 + c_1z^2 + c_2z + c_3 \quad (19)$$

$\chi(z)$ is the characteristic polynomial of $A - KC$, and the coefficients c_i, $i = 1, 2, 3$ are the same as the ones in equations (15) and (18). Let α, β_1 and β_2 be the roots of (19). We assume that $\alpha \in \mathbf{R}$, and that β_1 and β_2 are either real or complex conjugate. Furthermore, these roots must all lie inside the unit circle.

As for the first study, we fixed $\alpha = 0.99$. The choice of β_1 and β_2 has been made using data from the first pilot study. For modeling purpose, we considered the stochastic continuous-time model and measurements at discrete times, i.e.

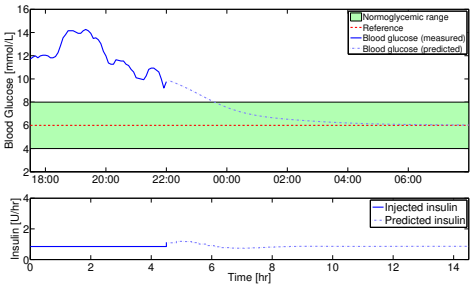

Fig. 7. Example of blood glucose prediction for the first study with the new observer. The controller is able to predict more accurately the blood glucose trend.

$$dx(t) = f(t, x(t), u(t))dt + \sigma d\omega(t) \tag{20a}$$
$$y_k = h(t_k, x(t_k)) + v_k \tag{20b}$$

$x(t)$ are the system states, $u(t)$ are the known inputs (insulin injections, meals and intravenous glucose injections) and y_k are discrete outputs (CGM measurements). The function f is a continuous-time state-space description of the transfer function (1).

We used the internally developed software "Continuous Time Stochastic Modelling" (CTSM) to estimate the variances (variance of process noise and measurement noise) with the maximum likelihood method. We took these variances to compute the predictive Kalman gain K, and hence β_1 and β_2. The computation of β_1 and β_2 yielded

$$\beta_{1,2} = 0.8078 \pm 0.1581i \tag{21}$$

These roots give

$$c_1 = -2.6056 \quad c_2 = 2.2770 \quad c_3 = -0.6708 \tag{22}$$

Fig. 7 illustrates an other example of blood glucose and insulin prediction. We have generated these prediction plots by taking the same data sequence in which we designed the observer. Unlike the previous case in Fig. 6, the controller is able to predict more accurately the blood glucose trend.

3.4 Computing the j-steps ahead predictions

If the k-th glucose measurement y_k is available, the one-step ahead prediction of the states and outputs is

$$\hat{x}_{k+1|k} = A\hat{x}_{k|k} + Bu_{k|k} + K\varepsilon_k \tag{23a}$$
$$\hat{y}_{k+1|k} = C\hat{x}_{k+1|k} \tag{23b}$$

ε_k is the innovation term

$$\varepsilon_k = y_k - C\hat{x}_{k|k-1} \tag{24}$$

In the case where the k-th glucose measurement y_k is not available, the one-step ahead prediction of the states and outputs is

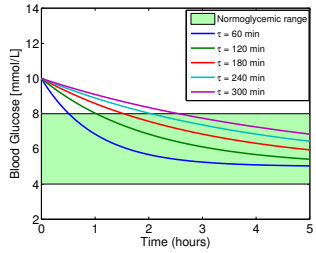

Fig. 8. Example of time-varying reference signal for different values of the time constant τ_r.

$$\hat{x}_{k+1|k} = A\hat{x}_{k|k} + Bu_{k|k} \tag{25a}$$
$$\hat{y}_{k+1|k} = C\hat{x}_{k+1|k} \tag{25b}$$

Similarly, the $j+1$ steps ahead predictions of the states and the outputs for $j = 1, 2, ...$ are

$$\hat{x}_{k+j+1|k} = A\hat{x}_{k+j|k} + Bu_{k+j|k} \tag{26a}$$
$$\hat{y}_{k+j+1|k} = C\hat{x}_{k+j+1|k} \tag{26b}$$

3.5 Time-varying glucose setpoint

The glucose trajectory is exponentially decreasing when the blood glucose is above the target, which robustifies the controller with respect to plant-model mismatches. Consequently, the reference blood glucose is

$$\hat{r}_{k+j|k}(t) = \hat{y}_{k|k} \exp\left(-\frac{t_j}{\tau_r}\right) \tag{27}$$

The choice of the tuning parameters τ_r has an influence on the rapidness and the robustness of the controller. Small values of τ_r provide a faster return to the euglycemic range, while larger values of τ ensure a more robust control. The glucose setpoint profiles for different values of the time constant τ_r are shown in Fig. 8.

3.6 Model Predictive Control with Soft Constraints

At the time t_k, the open loop convex quadratic program solved online is

$$\min_{\{u_k+j, v_j\}_{j=0}^{N-1}} \phi = \frac{1}{2}\sum_{j=0}^{N-1} \|\hat{y}_{k+j+1|k} - \hat{r}_{k+j+1|k}\|_2^2 + \lambda\|\Delta u_{k+j}\|_2^2 + \kappa\|v_{k+j}\|_2^2 \tag{28a}$$

$$s.t. \quad \hat{x}_{k+1|k} = A\hat{x}_{k|k-1} + Bu_k + Ke_k \tag{28b}$$
$$\hat{y}_{k+1|k} = C\hat{x}_{k+1|k} \tag{28c}$$
$$\hat{x}_{k+j+1|k} = A\hat{x}_{k+j|k} + Bu_k \tag{28d}$$
$$\hat{y}_{k+j+1|k} = C\hat{x}_{k+j+1|k} \tag{28e}$$
$$u_{\min} \leq u_{k+j} \leq u_{\max} \tag{28f}$$
$$G_{\min} - y_{k+1} \leq v_{k+j} \tag{28g}$$
$$v_j \geq 0 \tag{28h}$$

in which $\hat{x}_{k|k-1}$ and $e_k = y_k - C\hat{x}_{k|k-1}$ are given. $u_{\min}$ and $u_{\max}$ are the minimum and the maximum insulin infusion rates allowed by the pump. $\Delta u_{k+j} = u_{k+j} - u_{k+j-1}$ is the variation in the insulin infusion rate. $G_{\min}$ depicts the lower bound on blood glucose. The reference signal $\hat{r}_{k+j+1|k}$ is time-varying and its computation is given in section 3.5.

The slack variables v_j are introduced to penalize hypoglycemia. The hard input constraints (28f) limit the insulin infusion rate. The penalty term $\kappa\|v_{k+j}\|_2^2$ is used to avoid hypoglycemia and the penalty term $\lambda\|\Delta u_{k+j}\|_2^2$ prevents the insulin infusion rate from varying too aggressively.

For the study we choose $N = 120$, i.e. a 10 hour prediction horizon, and

$$u_{min} = -u_{ss} + 0.025, \quad u_{max} = u_{ss}, \\ \lambda = \frac{10}{u_{ss}^2}, \quad \kappa = 1000 \tag{29}$$

We remind here that the input variables are deviation variables from the steady state u_{ss}. Consequently, the choice of $u_{min} = -u_{ss} + 0.025$ allows the controller to deliver the minimum basal rate (0.025U/hr), and $u_{max} = u_{ss}$ prevents the pump from overdosing the insulin. The high value of κ makes hypoglycemia undesirable.

4. STUDIES RESULTS

In this section we discuss the two studies conducted at Hvidovre Hospital on the same patient. The patient has an insulin sensitivity factor equal to 5 mmol/L/U and an insulin action time equal to 5 hours. Her basal insulin is $u_{ss} = 0.85$ U/hr.

4.1 Pilot studies results

Fig. 9 depicts the blood glucose and insulin profiles for the first pilot study. The study started at 17:30. A meal has been consumed at 18:00. An insulin overdosing led to severe hypoglycemia and an intravenous glucose injection at approximately 00:00. A microbolus decision has been overruled at 01:30.

Fig. 10 depicts the blood glucose and insulin profiles for the second pilot study. Intravenous glucose has been administrated at 10:00 and 12:00 to compensate for a too high insulin sensitivity. The sensor has to be calibrated at 12:15 and 14:45. In despite of these disturbances, the controller was able to keep the blood glucose within the range 4.0-8.0 mmol/L after the second glucose administration. In addition, the intravenous glucose is not included in the model, and therefore can be considered as an unknown disturbance. However, it can be noticed that insulin is still slightly overdosed.

5. CONCLUSION

This contribution presents a closed-loop controller for people with type 1 diabetes. We described a practical way of computing the glucose-insulin dynamics model. The controller has been tested two times on the same patient. The most noticeable difference between the two studies was the observer design. The trial results illustrated the importance of observer design in state space models in innovation form, and how modelling based on prior data can be used to design the observer. Improvements are being implemented on the controller in order to ensure a more robust control of blood glucose and avoid the observed insulin overdosing during the second pilot study.

REFERENCES

Novorapid Product Monograph. Can be downloaded at: http://www.novonordisk.com/images/diabetes/pdf /Novorapid%20Product%20Monograph.pdf, 2002.

B. M. Åkesson, J. B. Jørgensen, N. K. Poulsen, and S. B. Jørgensen. A generalized autocovariance least-squares method for kalman filter tuning. *Journal of Process Control*, 18:769 – 779, 2008.

B. W. Bequette. Challenges and progress in the development of a closed-loop artificial pancreas. In *American Control Conference 2012 (ACC 2012)*, 2011. Submitted.

D. Boiroux, D. A. Finan, N. K. Poulsen, H. Madsen, and J. B. Jørgensen. Implications and limitations of ideal insulin administration for people with type 1 diabetes. In *UKACC International Conference on Control 2010*, pages 156 – 161, 2010.

C. Cobelli, E. Renard, and B. Kovatchev. Artificial pancreas: past, present, future. *Diabetes*, 60:2672 – 2682, 2011.

D. A. Finan, F. J. Doyle, C. C. Palerm, W. C. Bevier, H. C. Zisser, L. Jovanovič, and D. E. Seborg. Experimantal evaluation of a recursive model identification technique for type 1 diabetes. *J Diabetes Sci Technol*, 3:1192 – 1202, 2009.

R. Hovorka, V. Canonico, L. J. Chassin, U. Haueter, M. Massi-Benedetti, M. O. Federici, T. R. Pieber, H. C. Schaller, L. Schaupp, T. Vering, and M. E. Wilinska. Nonlinear model predictive control of glucose concentration in subjects with type 1 diabetes. *Physiological Measurement*, 25:905–920, 2004.

R. Hovorka, M. E. Wilinska, L. J. Chassin, and D. B. Dunger. Roadmap to the artificial pancreas. *Diabetes Research and Clinical Practice*, 74:178 – 182, 2006.

R. Hovorka, J. M. Allen, D. Elleri, L. J. Chassin, J. Harris, D. Xing, C. Kollman, T. Hovorka, A. M. F. Larsen, M. Nodale, A. De Palma, M. E. Wilinska, C. L. Acerini, and D. B. Dunger. Manual closed-loop insulin delivery in children and adolescents with type 1 diabetes: a phase 2 randomised crossover trial. *Lancet*, 375:743 – 751, 2010.

Jakob Kjøbsted Huusom, Niels Kjølstad Poulsen, Sten Bay Jørgensen, and John Bagterp Jørgensen. Tuning of methods for offset free MPC based on ARX model representations. In *2010 American Control Conference (ACC)*, pages 2355–2360, Baltimore, MD, USA, 2010.

J. B. Jørgensen and S. B. Jørgensen. Comparison of prediction-error modelling criteria. In *Proceedings of the 2007 American Control Conference (ACC 2007)*, 2007.

Harald Kirchsteiger, Giovanna Castillo Estrada, Stephan Pölzer, Eric Renard, and Luigi del Re. Estimating interval process models for type 1 diabetes for robust control design. In *Preprints of the 18th IFAC World Congress*, pages 11761 – 11766, 2011.

L. Magni, D. M. Raimondo, C. Dalla Man, G. De Nicolao, B. P. Kovatchev, and C. Cobelli. Model predictive con-

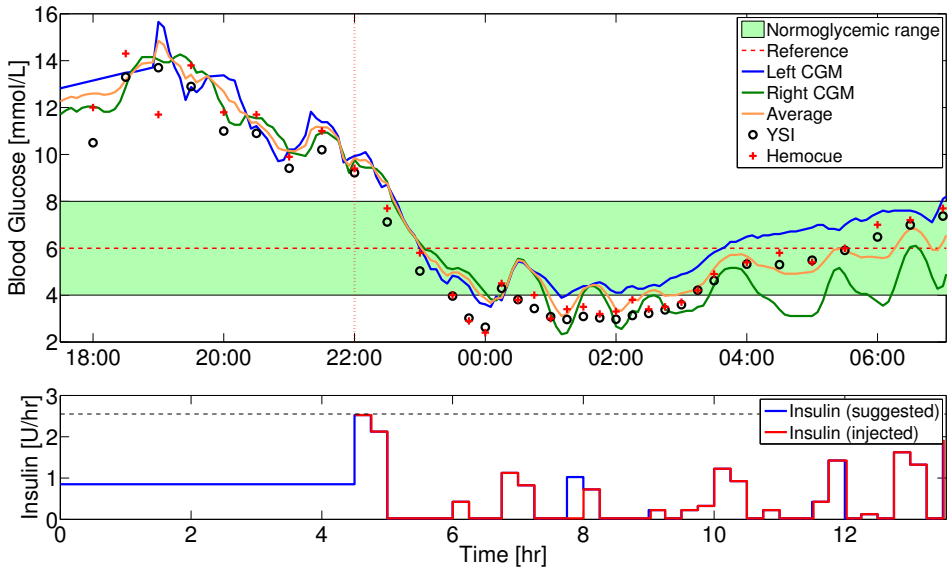

Fig. 9. Blood glucose and insulin profiles for the first pilot study. The insulin infusion rates are computed based on the right CGM (green curve).

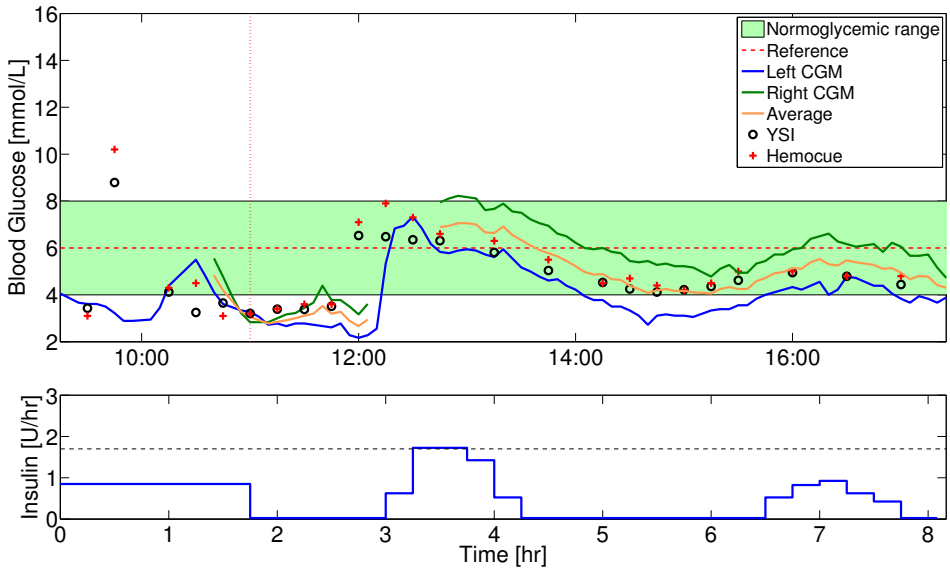

Fig. 10. Blood glucose and insulin profiles for the second pilot study. The insulin infusion rates are computed based on the left CGM (blue curve).

trol of glucose concentration in type I diabetic patients: An in silico trial. *Biomedical Signal Processing and Control*, 4(4):338–346, 2009.

B. J. Odelson, A. Lutz, and J. B. Rawlings. The autocovariance least-squares method for estimating covariances: application to model-based control of chemical reactors. *IEEE transactions on control systems technology*, 14(3):532 – 540, 2006.

M. W. Percival, W. C. Bevier, Y. Wang, E. Dassau, H Zisser, L. Jovanovič, and F. J. Doyle III. Modeling the effects of subcutaneous insulin administration and carbohydrate consumption on blood glucose. *Diabet Sci Technol*, 4(5):1214–1228, 2010.

APPENDIX J

Paper I

Overnight Control of Blood Glucose in People with Type 1 Diabetes

Authors:

Dimitri Boiroux, Anne Katrine Duun-Henriksen, Signe Schmidt, Kirsten Nørgaard, Sten Madsbad, Ole Skyggebjerg, Peter Ruhdal Jensen, Niels Kjølstad Poulsen, Henrik Madsen, and John Bagterp Jørgensen

Published in:

8th IFAC Symposium on Biological and Medical Systems, 2012

Overnight Control of Blood Glucose in People with Type 1 Diabetes

Dimitri Boiroux [*] **Anne Katrine Duun-Henriksen** [*]
Signe Schmidt [***] **Kirsten Nørgaard** [***] **Sten Madsbad** [***]
Ole Skyggebjerg [****] **Peter Ruhdal Jensen** [**]
Niels Kjølstad Poulsen [*] **Henrik Madsen** [*]
John Bagterp Jørgensen [*]

[*] *DTU Informatics, Technical University of Denmark, Denmark*
[**] *DTU Systems Biology, Technical University of Denmark, Denmark*
[***] *Dept. of Endocrinology, Hvidovre Hospital, Denmark*
[****] *Horus ApS, Copenhagen, Denmark*

Abstract:
In this paper, we develop and test a Model Predictive Controller (MPC) for overnight stabilization of blood glucose in people with type 1 diabetes. The controller uses glucose measurements from a continuous glucose monitor (CGM) and its decisions are implemented by a continuous subcutaneous insulin infusion (CSII) pump. Based on a priori patient information, we propose a systematic method for computation of the model parameters in the MPC. Safety layers improve the controller robustness and reduce the risk of hypoglycemia. The controller is evaluated in silico on a cohort of 100 randomly generated patients with a representative inter-subject variability. This cohort is simulated overnight with realistic variations in the insulin sensitivities and needs. Finally, we provide results for the first tests of this controller in a real clinic.

1. INTRODUCTION

People with type 1 diabetes need several blood measurements and insulin injections per day to regulate their blood glucose properly. Too small doses of insulin result in high blood glucose (hyperglycemia), which has long-term complications such as nerve diseases, kidney diseases, and blindness. In contrast, too high doses lead to low blood glucose (hypoglycemia) with immediate adverse effects such as seizure, coma or even death.

Closed-loop control of blood glucose, also known as the artificial pancreas (AP), has been suggested to overcome the burden and complications associated with management of the blood glucose level in people with type 1 diabetes. An AP using subcutaneous (sc) measurements and subcutaneous delivery consists of a continuous glucose monitor (CGM), a control algorithm, and a continuous subcutaneous insulin infusion (CSII) pump. Fig. 1 illustrates the principal components of an AP. It has been a subject of interest for almost 40 years (Albisser et al. (1974)) and is still an active field of research (Cobelli et al. (2011), Nicolao et al. (2011)).

Model Predictive Control is a useful control method for the AP due to its ability to handle constraints and out-of-zone glucose levels in a systematic and proactive fashion. Prototypes of AP using MPC have been successfully tested both in silico (Magni et al., 2009) and in vivo (Hovorka et al., 2010).

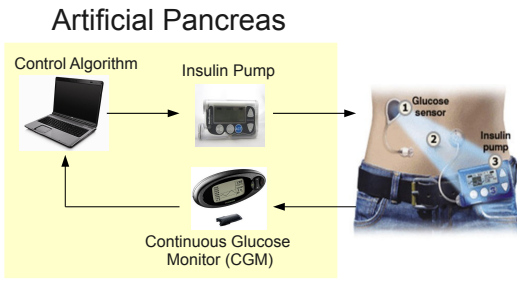

Fig. 1. Closed-loop glucose control. Glucose is measured subcutaneously using a continuous glucose monitor (CGM). Insulin is dosed by an insulin pump.

In this paper we implement an AP using a CGM for glucose feedback, an insulin pump and a control algorithm based on MPC. We present a method exploiting a priori available patient information for computing a personalized set of model parameters. In the considered setup, the patient information required by the controller is: The basal insulin infusion rate, the insulin sensitivity factor (also called the correction factor), and the insulin action time. Safety layers limit the occurrence of hypoglycemic events. The controller is tested in silico on a cohort of 100 patients. We simulate an overnight clinical trial and induce realistic variations in insulin needs. We also present glucose and

⋆ Funding for this research as part of the DIACON project from the Danish Council for Strategic Research (NABIIT project 2106-07-0034) is gratefully acknowledged.
Corresponding author: J.B. Jørgensen, jbj@imm.dtu.dk

Table 1. Parameters and distribution for the simulated cohort.

Parameter	Unit	Distribution
EGP_0	mmol/kg/min	$EGP_0 \sim N(0.0161, 0.0039^2)$
F_{01}	mmol/kg/min	$F_{01} \sim N(0.0097, 0.0022^2)$
k_{12}	min^{-1}	$k_{12} \sim N(0.0649, 0.0282^2)$
k_{a1}	min^{-1}	$k_{a1} \sim N(0.0055, 0.0056^2)$
k_{a2}	min^{-1}	$k_{a2} \sim N(0.0683, 0.0507^2)$
k_{a3}	min^{-1}	$k_{a3} \sim N(0.0304, 0.0235^2)$
S^f_{IT}	$\text{min}^{-1}/(\text{mU/L})$	$S^f_{IT} \sim N(51.2, 32.09^2)$
S^f_{ID}	$\text{min}^{-1}/(\text{mU/L})$	$S^f_{ID} \sim N(8.2, 7.84^2)$
S^f_{IE}	L/mU	$S^f_{IE} \sim N(520, 306.2^2)$
k_e	min^{-1}	$k_e \sim N(0.14, 0.035^2)$
V_I	L/kg	$V_I \sim N(0.12, 0.012^2)$
V_G	L/kg	$\exp(V_G) \sim N(\ln(0.15), 0.23^2)$
τ_I	min	$\frac{1}{\tau_I} \sim N(0.018, 0.0045^2)$
τ_G	min	$\frac{1}{\ln(\tau_G)} \sim N(-3.689, 0.25^2)$
A_g	Unitless	$A_g \sim U(0.7, 1.2)$
BW	kg	$BW \sim U(65, 95)$

insulin profiles from an initial test of the controller in a real clinic.

This paper is structured as follows. In Section 2 we describe the model and the methods used to simulate a cohort of patients with type 1 diabetes. Section 3 presents a procedure for computation of the MPC model parameters from prior patient information. Section 4 describes the controller. In Section 5 we evaluate and discuss the controller performance on a cohort of 100 patients and provide in vivo test results. Conclusions are provided in Section 6.

2. PHYSIOLOGICAL MODELS FOR PEOPLE WITH TYPE 1 DIABETES

Several physiological models have been developed to simulate virtual patients with type 1 diabetes (Hovorka et al. (2004); Bergman et al. (1981); Dalla Man et al. (2007)). They describe subcutaneous insulin transport, intake of carbohydrates through meals and include a model of glucose-insulin dynamics.

In this paper, we use the Hovorka model to simulate people with type 1 diabetes. Using the parameters and distribution provided in Hovorka et al. (2002) and Wilinska et al. (2010), we generate a cohort of 100 patients. These parameters and their distribution are summarized in Table 1.

In addition, we use a CGM for glucose feedback in our controller setup. For the numerical simulations, we generate noisy CGM data based on the model and the parameters determined by Breton and Kovatchev (2008). This model consists of two parts. The first part describes the glucose transport from blood to interstitial tissues. The second part models non-Gaussian sensor noise.

3. PREDICTION OF SUBCUTANEOUS GLUCOSE

In this section, we derive a prediction model for subcutaneous glucose, $y(t)$. The model has a deterministic part describing the effect of sc injected insulin, $u(t)$, and a stochastic part describing the effect of other unknown factors. The prediction model is an autoregressive integrated moving average with exogenous input (ARIMAX) model

$$A(q^{-1})y(t) = B(q^{-1})u(t) + \frac{C(q^{-1})}{1-q^{-1}}\varepsilon(t) \tag{1}$$

The ARIMAX model structure is used do have offset free control when the filter and predictor of this model are used in an MPC. A and B are individualized and derived from known patient information. C is identified from data for one real patient and this C is used for the cohort of virtual and real patients. This model identification technique turns out to give a good compromise between data requirements, performance and robustness of the resulting controller for the overnight study described in this paper.

3.1 Deterministic Model

All the physiological models presented in Section 2 contain a large number of parameters, and even the minimal model developed by Bergman et al. (1981) may be difficult to identify (Pillonetto et al., 2003). To overcome this issue, we use a low-order linear model to describe the glucose-insulin dynamics. Similar approaches have been investigated previously. Kirchsteiger et al. (2011) used a third order transfer function and Percival et al. (2010) applied a first order transfer function with a time delay. In this paper we use a continuous-time second order transfer function

$$G(s) = \frac{Y(s)}{U(s)} = \frac{K_u}{(\tau s + 1)^2} \tag{2}$$

to model the effect of sc injected insulin on sc glucose. The gain, K_u, and the time constant, τ, are computed from known subject-specific parameters; the insulin action time and the insulin sensitivity factor (ISF).

The insulin action time and the insulin sensitivity factor are related to the response of blood glucose to an insulin bolus. If we assume that blood glucose is approximately identical to sc glucose, this is the impulse response of (2). The insulin action time is the time for blood glucose to reach its minimum. The ISF corresponds to the maximum decrease in blood glucose per unit of insulin bolus. These parameters are empirically estimated by the patient and his/her physician. These parameters may vary from day to day for a given patient but gives an estimate of the effect of insulin on blood glucose and sc glucose.

In the temporal domain, the impulse response of (2) is described by

$$y(t) = K_u \frac{t}{\tau^2} \exp(-t/\tau) \tag{3}$$

The insulin action time corresponds to the time to reach the minimum blood glucose. Consequently, this insulin action time is equal to τ. We determine K_u using (3) and the fact that the insulin sensitivity factor is equal to the minimal blood glucose (sc glucose), $y(\tau) = -ISF$, such that

$$K_u = -\tau \exp(1) ISF \tag{4}$$

Using a zero-order-hold insulin profile, the continuous-time transfer function (2) may be used to determine the A and B polynomials in the ARIMAX model (1). They are

$$A(q^{-1}) = 1 + a_1 q^{-1} + a_2 q^{-2} \tag{5a}$$

$$B(q^{-1}) = b_1 q^{-1} + b_2 q^{-2} \tag{5b}$$

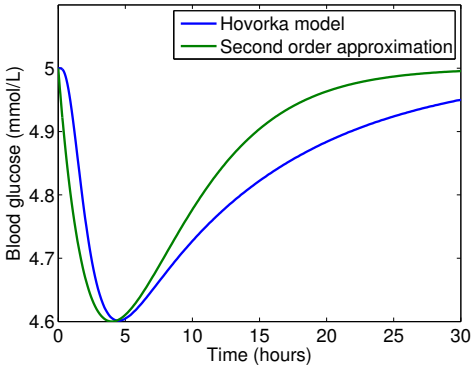

Fig. 2. Impulse responses for a second order model and the nonlinear Hovorka model. The bolus size is 0.1U and the parameters for the second order model are: τ=4 hours and $ISF = 0.4$ mmol/L/0.1 U $= 4.0$ mmol/L/U.

with the coefficients a_1, a_2, b_1 and b_2 computed as

$$a_1 = -2\exp(-T_s/\tau) \tag{6a}$$
$$a_2 = \exp(-2T_s/\tau) \tag{6b}$$
$$b_1 = K_u(1-\exp(-T_s/\tau)(1+T_s/\tau)) \tag{6c}$$
$$b_2 = K_u\exp(-T_s/\tau)(-1+\exp(-T_s/\tau)+T_s/\tau) \tag{6d}$$

T_s is the sample time.

Fig 2 depicts the impulse response for a virtual patient with type 1 diabetes and its second order approximation (2). This patient is simulated using the model developed by Hovorka et al. (2004). The figure demonstrates that a second order model provides an acceptable approximation of a patient with type 1 diabetes.

3.2 Stochastic Model

The stochastic part, $C(q^{-1})$, of the ARIMAX model (1) is assumed to be a third order polynomial of the form

$$\begin{aligned} C(q^{-1}) &= 1 + c_1q^{-1} + c_2q^{-2} + c_3q^{-3} \\ &= (1-\alpha q^{-1})(1-\beta_1 q^{-1})(1-\beta_2 q^{-1}) \end{aligned} \tag{7}$$

$\alpha = 0.99$ is a fixed parameter. It has been determined based on performance studies of the resulting MPC. β_1 and β_2 are determined from clinical data for one real patient (Boiroux et al., 2012).

We compute β_1 and β_2 by estimating the process and measurement noise characteristics, σ and r, in the following continuous-discrete stochastic linear model

$$dx(t) = (A_cx(t) + B_cu(t))dt + \sigma d\omega(t) \tag{8a}$$
$$y_k = h(t_k, x(t_k)) + v_k \tag{8b}$$

A_c and B_c are realizations of (2). $\omega(t)$ is a standard Wiener process. The matrix σ is time-invariant and the measurement noise v_k is normally distributed, i.e. $v_k \sim N_{iid}(0, r^2)$. We estimate, σ and r, using a maximum likelihood criteria for the one-step prediction error (Kristensen et al., 2004; Jørgensen and Jørgensen, 2007). By zero-order hold (zoh) discretization, Kalman filter design, and z-transformation, (8) may be represented as

$$y_k = G(q^{-1})u_k + H(q^{-1})\epsilon_k \tag{9}$$

with

$$G(q^{-1}) = B(q^{-1})/A(q^{-1}) \tag{10a}$$
$$H(q^{-1}) = \tilde{C}(q^{-1})/A(q^{-1}) \tag{10b}$$

The parameters, β_1 and β_2, in

$$\tilde{C}(q^{-1}) = (1-\beta_1 q^{-1})(1-\beta_2 q^{-1}) \tag{11}$$

are extracted from $H(q^{-1})$. The coefficients β_1 and β_2 computed in this way are $\beta_{1,2} = 0.81 \pm 0.16i$.

The difference equation (9) corresponding to the SDE (8) is related to the ARIMAX model (1) by

$$\epsilon_k = \frac{1-\alpha q^{-1}}{1-q^{-1}}\varepsilon_k \tag{12}$$

This specification introduces a model-plant mismatch. ϵ_k is white noise in (9) while (12) models ϵ_k as filtered integrated white noise. This model-plant mismatch is necessary to have offset free control in the resulting predictive control system. (12) implies that

$$C(q^{-1}) = (1-\alpha q^{-1})\tilde{C}(q^{-1}) \tag{13}$$

such that $c_1 = -2.61$, $c_2 = 2.28$ and $c_3 = -0.67$.

3.3 Realization and Predictions with ARIMAX Models

The ARIMAX model (1) with A, B and C given by (5) and (7) may be represented as a discrete-time state space model in innovation form

$$x_{k+1} = Ax_k + Bu_k + K\varepsilon_k \tag{14a}$$
$$y_k = Cx_k + \varepsilon_k \tag{14b}$$

with the observer canonical realization

$$A = \begin{bmatrix} 1-a_1 & 1 & 0 \\ a_1-a_2 & 0 & 1 \\ a_2 & 0 & 0 \end{bmatrix} \quad B = \begin{bmatrix} b_1 \\ b_2-b_1 \\ -b_2 \end{bmatrix} \quad K = \begin{bmatrix} c_1+1-a_1 \\ c_2+a_1-a_2 \\ c_3+a_2 \end{bmatrix}$$
$$C = [1\ 0\ 0]$$

The innovation of (14) is

$$e_k = y_k - C\hat{x}_{k|k-1} \tag{15}$$

and the corresponding predictions are (Jørgensen et al., 2011)

$$\hat{x}_{k+1|k} = A\hat{x}_{k|k-1} + B\hat{u}_{k|k} + Ke_k \tag{16a}$$
$$\hat{x}_{k+1+j|k} = A\hat{x}_{k+j|k} + B\hat{u}_{k+j|k}, \quad j = 1, \ldots, N-1 \tag{16b}$$
$$\hat{y}_{k+j|k} = C\hat{x}_{k+j|k}, \quad j = 1, \ldots, N \tag{16c}$$

The innovation (15) and the predictions (16) constitute the feedback and the predictions in the model predictive controller.

4. MODEL PREDICTIVE CONTROL

Control algorithms for glucose regulation in people with type 1 diabetes must be able to handle intra- and inter-patient variability. In addition, the controller must administrate insulin in a safe way to minimize the risk of hypoglycemia. Due to the nonlinearity in the glucose-insulin interaction the risk of hypoglycemic episodes as consequence of too much insulin is particular prominent.

In this section we describe an MPC formulation with soft output constraints and hard input constraints. This formulation is based on the individualized prediction model for glucose computed in Section 3. Along with other features

we introduce a modified time-varying reference signal to robustify the controller and mitigate the effect of glucose-insulin nonlinearities and model-plant mismatch in the controller action.

The MPC algorithm computes the insulin dose by solution of an open-loop optimal control problem. Only the control action corresponding to the first sample interval is implemented and the process is repeated at the next sample interval. This is called a moving horizon implementation. The innovation (15) provides feedback from the CGM, y_k, and the open-loop optimal control problem solved in each sample interval is the convex quadratic program

$$\min_{\{\hat{u}_{k+j|k},\hat{v}_{k+j+1|k}\}_{j=0}^{N-1}} \phi \tag{17a}$$

$$s.t. \qquad (16) \tag{17b}$$

$$u_{\min} \leq \hat{u}_{k+j|k} \leq u_{\max} \tag{17c}$$

$$\hat{y}_{k+j+1|k} \geq y_{\min} - \hat{v}_{k+j+1|k} \tag{17d}$$

$$\hat{v}_{k+j+1|k} \geq 0 \tag{17e}$$

with the objective function ϕ defined as

$$\begin{aligned}\phi =& \frac{1}{2}\sum_{j=0}^{N-1} \|\hat{y}_{k+j+1|k} - \hat{r}_{k+j+1|k}\|_2^2 \\ &+ \lambda\|\Delta\hat{u}_{k+j|k}\|_2^2 + \kappa\|\hat{v}_{k+j+1|k}\|_2^2\end{aligned} \tag{18}$$

N is the control and prediction horizon. We choose a prediction horizon equivalent to 10 hours, such that the insulin profile of the finite horizon optimal control problem (17) is similar to the insulin profile of the infinite horizon optimal control problem, (17) with $N \to \infty$. $\|\hat{y}_{k+j+1|k} - \hat{r}_{k+j+1|k}\|_2^2$ penalizes glucose deviation from the time-varying glucose setpoint and aims to drive the glucose concentration to 6 mmol/L. $\lambda\|\Delta u_{k+j|k}\|_2^2$ is a regularization term that prevents the insulin infusion rate from varying too aggressively. For the simulations and the in vivo clinical studies we set $\lambda = 100/u_{ss}^2$. The soft output constraint (17d) penalizes glucose values below 4 mmol/L. Since hypoglycemia is highly undesirable, we choose the weight on the soft output constraint to be rather high i.e. $\kappa = 100$.

To guard against model-plant mismatch we modify the maximal allowable insulin injection, $u_{\max}$, and let it depend on the current glucose concentration. If the glucose concentration is low (below the target of 6 mmol/L) we prevent the controller from taking future hyperglycemia into account by restricting the maximal insulin injection. If the glucose concentration is high (4 mmol/L above the target) we increase the maximal allowable insulin injection rate. In the range 0 - 4 mmol/L above target we allow the controller to double the basal insulin injection rate. These considerations lead to

$$u_{\max} = \begin{cases} 1.5u_{ss} & 4 \leq y_k \leq \infty \\ u_{ss} & 0 \leq y_k \leq 4 \\ 0.5u_{ss} & -\infty \leq y_k \leq 0 \end{cases} \tag{19}$$

in which u_{ss} is the basal insulin infusion rate. Due to pump restrictions, the minimum insulin injection rate, $u_{\min}$, is a low value but not exactly zero.

Garcia-Gabin et al. (2008) and Eren-Oruklu et al. (2009) use a time-varying glucose reference signal to robustify the controller and reduce the risk of hypoglycemic events. In this paper, we use an asymmetric time-varying glucose reference signal. The idea of the asymmetric reference signal is to induce safe insulin injections in hyperglycemic periods and fast recovery in hypoglycemic and below target periods. The asymmetric time-varying setpoint is given by

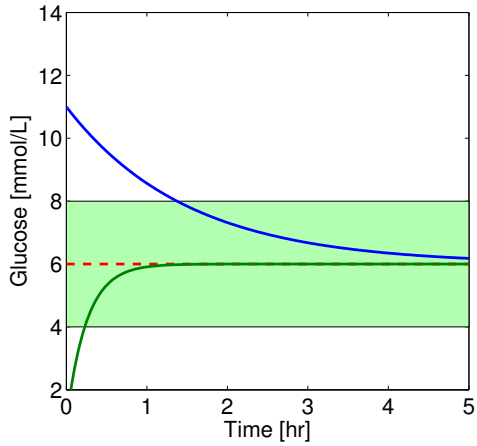

Fig. 3. Time-varying reference signals for glucose above (blue curve) and below (green curve) the target of 6 mmol/L.

$$\hat{r}_{k+j|k}(t) = \begin{cases} y_k \exp\left(-t_j/\tau_r^+\right) & y_k \geq 0 \\ y_k \exp\left(-t_j/\tau_r^-\right) & y_k < 0 \end{cases} \tag{20}$$

Since we want to avoid hypoglycemia, we make the controller react more aggressively if the blood glucose level is below 6 mmol/L, so we choose $\tau_r^- = 15$ min and $\tau_r^+ = 90$ min. Fig 3 provides an illustration of the time-varying reference signal.

5. NUMERICAL RESULTS AND DISCUSSION

In this section we discuss the performance of the MPC for a randomly generated cohort of 100 patients. The 100 patients are generated from the probability distribution presented in Section 2. We compare the performance of the controller with simulated conventional insulin therapy in which the basal insulin infusion rate remains constant during the night. Variations in metabolism and insulin need is simulated by a sudden change in the insulin sensitivity parameters of the Hovorka model.

The clinical protocol for the 100 in silico patients is:

- The patient arrives at the clinic at 17:00.
- The patient gets a 75 g CHO dinner and an insulin bolus at 18:00.
- The closed loop starts at 22:00.
- The insulin sensitivity is modified by ±30% at 01:00.
- The patient gets a 60 g CHO breakfast and an insulin bolus at 08:00. The controller is switched off.

The MPC is individualized using the insulin basal rate (u_{ss}), the insulin sensitivity factor (ISF), and the insulin action time for each individual patient. In the virtual clinic these numbers are computed from an impulse response

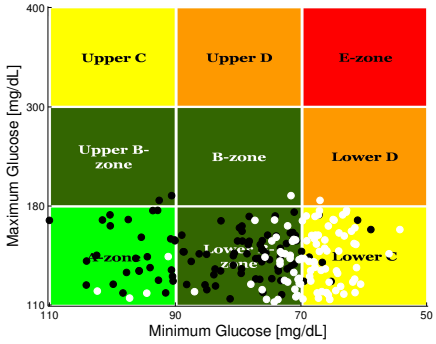

(a) Insulin sensitivity increases by 30%

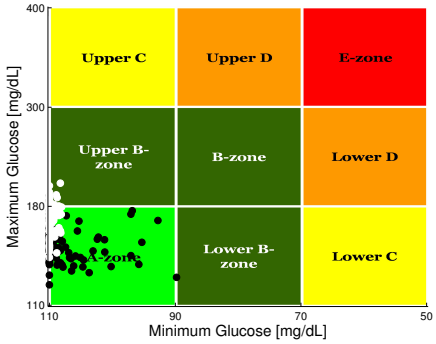

(b) Insulin sensitivity decreases by 30%

Fig. 4. CVGA (Magni et al. (2008)) plot of the 100 in silico patients. White: Without MPC. Black: With MPC.

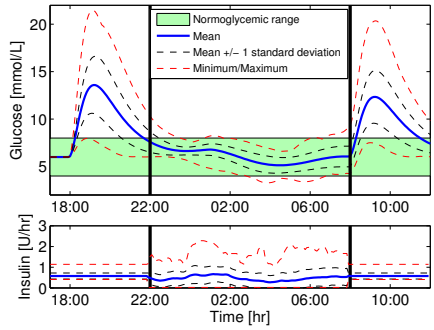

(a) Insulin sensitivity increases by 30%

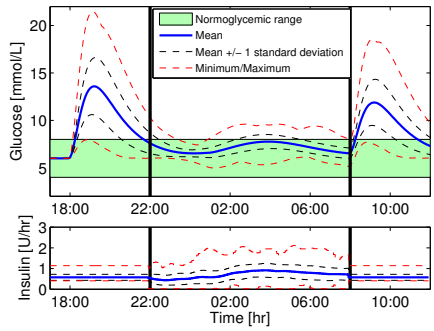

(b) Insulin sensitivity decreases by 30%

Fig. 5. Glucose and insulin profiles envelopes. Closed-loop control takes place between the 2 vertical black lines.

starting at a steady state. The meal boluses are determined using a bolus calculator similar to the one presented in Boiroux et al. (2011). The glucose is provided to the controller every 5 minutes by a noise-corrupted CGM. The pump insulin infusion rate is changed every 5 minutes.

Fig. 4 shows the control variability grid analysis (CVGA) of the period between 22:00 and 08:00 for the case without MPC (white circles) and the case with MPC (black circles). In Fig. 4(a) we depict the case where the insulin sensitivity is increased by 30%, and in Fig. 4(b) we depict the case where the insulin sensitivity is decreased by 30%. These figures show that our control algorithm reduces the risk of nocturnal hypoglycemia. Although the improvement is less significant, they also show that it can slightly reduce the risk of nocturnal hyperglycemia. Fig. 5 depicts the mean, standard deviation and minimum/maximum blood glucose and insulin profiles for the closed-loop simulations. In the case where insulin sensitivity is increased by 30% (Fig. 4(a) and 5(a)), mild hypoglycemic events occur for some of the patients. However, no severe hypoglycemia (i.e. blood glucose concentrations below 50 mg/dL) is observed, and the choice of the tuning parameters in the controller allows for a fast recovery. In the case where insulin sensitivity is decreased by 30% (Fig. 4(b) and 5(b)), all the patients are well controlled during the study period.

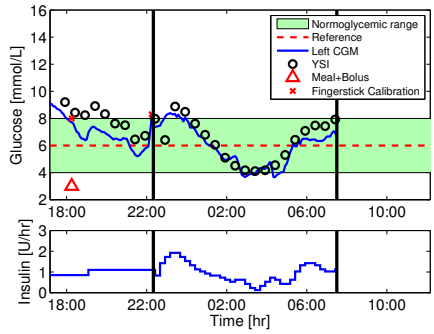

Fig. 6. Glucose and insulin profiles for an in vivo clinical study. Glucose input is provided by a CGM (blue curve). Closed-loop control takes place between the 2 vertical black lines.

Fig. 6 illustrates the glucose and insulin profiles for a real clinical test of the MPC. The glucose input is provided by a CGM (blue curve). Actual blood glucose measurements are provided by a glucose analyzer of blood samples (YSI). Although a mild hyperglycemic event occurred at approximately 23:00 and a few CGM values are below

4 mmol/L at approximately 03:00 and 04:00, this study shows the capability of the controller to stabilize blood glucose during the study night. Currently, the controller is being tested in a real clinical study.

6. CONCLUSION

This paper presents a subject-specific MPC controller designed for overnight stabilization of blood glucose in people with type 1 diabetes. The model parameters in the MPC are personalized based on easily available patient information. The main advantage of this method is its ease of implementation in real clinical studies due to the moderate model parameter requirement. The design of the controller allows for both a conservative control strategy in case of high glucose values, and a more aggressive control strategy in case of low glucose values. The controller is tested in silico on a cohort of 100 patients with temporal insulin sensitivity variations. A single test study from a real clinic is also presented. The proposed MPC is able to stabilize blood glucose overnight and reduces the risk of nocturnal hypoglycemia and hyperglycemia.

REFERENCES

A. Albisser, B. Leibel, T. Ewart, Z. Davidovac, C. Botz, and W. Zingg. An artificial endocrine pancreas. *Diabetes*, 23:389 – 396, 1974.

R. N. Bergman, L. S. Phillips, and C. Cobelli. Physiologic evaluation of factors controlling glucose tolerance in man: measurement of insulin sensitivity and beta-cell glucose sensitivity from the response to intravenous glucose. *Journal of Clinical Investigation*, 68(6):1456 – 1467, 1981.

D. Boiroux, D. A. Finan, J. B. Jørgensen, N. K. Poulsen, and H. Madsen. Strategies for glucose control in people with type 1 diabetes. In *17th IFAC World Congress*, 2011.

D. Boiroux, A. K. Dunn-Henriksen, S. Schmidt, L. Frøssing, K. Nørgaard, S. Madsbad, O. Skyggebjerg, N.K. Poulsen, H. Madsen, and J.B. Jørgensen. Control of blood glucose for people with type 1 diabetes: an in vivo study. In *Proceedings of the 17th Nordic Process Control Workshop*, pages 133 – 140, 2012.

M. Breton and B. Kovatchev. Analysis, modeling, and simulation of the accuracy of continuous glucose sensors. *Journal of Diabetes Science and Technology*, 2:853–862, 2008.

C. Cobelli, E. Renard, and B. Kovatchev. Artificial pancreas: past, present, future. *Diabetes*, 60:2672 – 2682, 2011.

C. Dalla Man, R. Rizza, and C. Cobelli. Meal simulation model of the glucose-insulin system. *IEEE Transactions on Biomedical Engineering*, 54(10):1740–1749, 2007.

M. Eren-Oruklu, A. Cinar, L. Quinn, and D. Smith. Adaptive control strategy for regulation of blood glucose levels in patients with type 1 diabetes. *Journal of Process Control*, 19:1333 – 1346, 2009.

W. Garcia-Gabin, J. Vehí, J. Bondia, C. Tarín, and R. Calm. Robust sliding mode closed-loop glucose control with meal compensation in type 1 diabetes mellitus. In *Proceedings of the 17th World Congress, The International Federation of Automatic Control*, pages 4240 – 4245, 2008.

R. Hovorka, F. Shojaee-Moradie, P. V. Caroll, L. J. Chassin, I. J. Gowrie, N. C. Jackson, R. S. Tudor, A. M. Umpleby, and R. H. Jones. Partitioning glucose distribution/transport, disposal, and endogenous production during IVGTT. *Am. J. Physiol.*, 282:992–1007, 2002.

R. Hovorka, V. Canonico, L. J. Chassin, U. Haueter, M. Massi-Benedetti, M. O. Federici, T. R. Pieber, H. C. Schaller, L. Schaupp, T. Vering, and M. E. Wilinska. Nonlinear model predictive control of glucose concentration in subjects with type 1 diabetes. *Physiological Measurement*, 25:905–920, 2004.

R. Hovorka, J. M. Allen, D. Elleri, L. J. Chassin, J. Harris, D. Xing, C. Kollman, T. Hovorka, A. M. F. Larsen, M. Nodale, A. De Palma, M. E. Wilinska, C. L. Acerini, and D. B. Dunger. Manual closed-loop insulin delivery in children and adolescents with type 1 diabetes: a phase 2 randomised crossover trial. *Lancet*, 375:743 – 751, 2010.

J. B. Jørgensen and S. B. Jørgensen. Comparison of prediction-error modelling criteria. In *Proceedings of the 2007 American Control Conference (ACC 2007)*, pages 140–146, 2007.

J. B. Jørgensen, J. K. Huusom, and J. B. Rawlings. Finite horizon MPC for systems in innovation form. In *50th IEEE Conference on Decision and Control and European Control Conference (CDC-ECC 2011)*, pages 1896 – 1903, 2011.

H. Kirchsteiger, G. C. Estrada, S. Pölzer, E. Renard, and L. del Re. Estimating interval process models for type 1 diabetes for robust control design. In *Preprints of the 18th IFAC World Congress*, pages 11761 – 11766, 2011.

N. R. Kristensen, H. Madsen, and S. B. Jørgensen. Parameter estimation in stochastic grey-box models. *Automatica*, 40:225 – 237, 2004.

L. Magni, D. Raimondo, C. Dalla Man, M. Breton, S. Patek, G. De Nicolao, C. Cobelli, and B. Kovatchev. Evaluating the efficacy of closed-loop glucose regulation via control-variability grid analysis. *Journal of Diabetes Science and Technology*, 2(4):630 – 635, 2008.

L. Magni, D. M. Raimondo, C. Dalla Man, G. De Nicolao, B. P. Kovatchev, and C. Cobelli. Model predictive control of glucose concentration in type I diabetic patients: An in silico trial. *Biomedical Signal Processing and Control*, 4(4):338–346, 2009.

G. De Nicolao, L. Magni, C. Dalla Man, and C. Cobelli. Modeling and control of diabetes: Towards the artificial pancreas. In *Preprints of the 18th IFAC World Congress*, pages 7092 – 7101, 2011.

M. W. Percival, W. C. Bevier, Y. Wang, E. Dassau, H Zisser, L. Jovanovič, and F. J. Doyle III. Modeling the effects of subcutaneous insulin administration and carbohydrate consumption on blood glucose. *Diabet Sci Technol*, 4(5):1214–1228, 2010.

G. Pillonetto, G. Sparacino, and C. Cobelli. Numerical non-identifiability regions of the minimal model of glucose kinetics: superiority of bayesian estimation. *Mathematical Biosciences*, 184:53 – 67, 2003.

M. E. Wilinska, L. J. Chassin, C. L. Acerini, J. M. Allen, D. B. Dunger, and R. Hovorka. Simulation environment to evaluate closed-loop insulin delivery systems in type 1 diabetes. *Journal of Diabetes Science and Technology*, 4(1):132 – 144, 2010.

APPENDIX K

Paper J

A Strategy for Overnight Glucose Control in People with Type 1 Diabetes

Authors:

Dimitri Boiroux, Anne Katrine Duun-Henriksen, Signe Schmidt, Kirsten Nørgaard, Sten Madsbad, Ole Skyggebjerg, Peter Ruhdal Jensen, Niels Kjølstad Poulsen, Henrik Madsen, and John Bagterp Jørgensen

Submitted in:

Computer Methods and Programs in Biomedicine, 2012

A Strategy for Overnight Glucose Control in People with Type 1 Diabetes

Dimitri Boiroux[a], Anne Katrine Duun-Henriksen[a], Signe Schmidt[c], Kirsten Nørgaard[c], Sten Madsbad[c], Ole Skyggebjerg[d], Peter Ruhdal Jensen[b], Niels Kjølstad Poulsen[a], Henrik Madsen[a], John Bagterp Jørgensen[a,*]

[a]*DTU Informatics, Technical University of Denmark, Denmark*
[b]*DTU Systems Biology, Technical University of Denmark, Denmark*
[c]*Dept. of Endocrinology, Hvidovre Hospital, Denmark*
[d]*Horus ApS, Copenhagen, Denmark*

Abstract

This paper investigates overnight blood glucose stabilization in people with type 1 diabetes using a Model Predictive Controller (MPC). We compute the model parameters in the MPC in a systematic way based on a priori available patient information. The controller uses frequent glucose measurements from a continuous glucose monitor (CGM) and its decisions are implemented by a continuous subcutaneous insulin infusion (CSII) pump. Safety layers improve the controller robustness and reduce the risk of hypoglycemia. We validate the controller on a cohort of 100 randomly generated virtual patients with a representative inter-subject variability. Finally, we provide preliminary results of this controller in a real overnight clinical study.

Keywords: Model Predictive Control, Glucose control, Artificial pancreas, Type 1 diabetes, Closed-loop control

1. Introduction

Diabetes is a disease characterized by blood glucose concentrations outside the safe range (4.0-8.0 mmol/l). In 2010, approximately 280 million people suffered from diabetes, and this number is expected to increase by 150 million by 2030 [1]. Type 1 diabetes represent 5-10% of diabetes. In addition, the global health care expenditure to treat long-term complications related to diabetes is also going to significantly increase within the next years [2].

In people with type 1 diabetes, the pancreas does not produce insulin. Patients with type 1 diabetes need exogenous insulin administration in order to tightly regulate their blood glucose. However, the dosage of insulin must be done carefully. An insulin overdose may lead to low blood glucose (hypoglycemia). Hypoglycemia has immediate effects, such as seizures, coma or even death. In contrast, prolonged periods of too high blood glucose (hyperglycemia) has long-term clinical complications, such as blindness, nerve diseases or kidney diseases.

The conventional insulin therapy for people with type 1 diabetes consists of the injection of slow acting insulin once or twice a day and rapid acting insulin several times per day, usually before mealtimes. The slow acting insulin is used to counteract the continuous glucose production from the liver. The rapid acting insulin reduces postprandial glucose excursions by increasing acutely peripheral glucose uptake in the skeletal muscles and inhibiting glucose production. The decision on the amount of short and fast acting insulin is based on several finger stick blood glucose measurements per day.

An increasing number of patients with type 1 diabetes use an intensive insulin therapy based on continuous glucose monitors (CGMs) and continuous subcutaneous insulin infusion (CSII) pumps instead of the conventional therapy described above. This regime can reduce the risk of complications significantly [3]. CGMs provide more frequent subcutaneous (sc) glucose measurements. In addition, insulin pumps can be adjusted to daily variations in insulin needs.

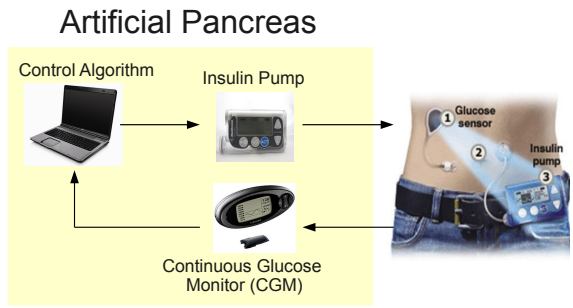

Figure 1: Closed-loop glucose control. Glucose is measured subcutaneously using a continuous glucose monitor (CGM). Insulin is dosed by an insulin pump.

Closed-loop control of blood glucose, also known as the artificial pancreas (AP), has been a subject of interest for almost 40 years [4, 5] and is still an active field of research [6, 7, 8, 9, 10]. An AP consists of a CGM, a control algorithm and a CSII pump. It has the potential to ease the life and reduce the burden and complications for people with type 1 diabetes. Fig. 1 illustrates the principle of an AP.

Several research groups worked on the implementation of APs both on virtual patients [11, 12, 13] and on human clinical studies [14, 15, 16]. Currently, the most popular control

*Corresponding author. E-mail: jbj@imm.dtu.dk

algorithms are proportional integral derivative (PID) control [17, 18], model predictive control (MPC) [19, 20, 21], sliding mode control [22], fuzzy logic [23, 24] and H_∞ control [25]. Nevertheless, the performance of current APs is limited by several factors, such as the intra- and inter-patient variability, along with the lags and delays associated to the choice of sc route for glucose monitoring and insulin administration [26].

MPC is one of the most commonly used methods for the AP. The main advantages of MPC are the ability to handle constraints both on input and output variables in a systematic way. An MPC controller with insulin on board (IOB) constraints can reduce the risk of overdosing insulin due to nonlinearities in glucose-insulin dynamics [27]. Feedforward-feedback control strategies can reduce the postprandial glucose peak by administrating meal boluses in anticipation of meals [28, 29].

In this paper, we present an AP using a CGM for glucose feedback, an insulin pump and a control algorithm based on MPC. The method described in this article exploits a priori available patient information for computing a personalized set of model parameters. In the considered setup, the patient information required by the controller is: The basal insulin infusion rate, the insulin sensitivity factor (also called the correction factor), and the insulin action time. Safety layers limit the occurrence of hypoglycemic events and improve the controller robustness. The controller is tested in silico on a cohort of 100 patients. These simulations mimic an overnight clinical trial and induce realistic variations in insulin needs.

The paper is structured as follows. In Section 2 we describe the model and the methods used to simulate a cohort of patients with type 1 diabetes. Section 3 describes the material and the software used for the in vivo clinical studies. Section 4 presents a procedure for computation of the MPC model parameters from prior patient information. Section 5 describes the controller. In Section 6 we evaluate and discuss the controller performance on a cohort of 100 virtual patients and also provide in vivo test results. Conclusions are provided in Section 7.

2. Physiological models for people with type 1 diabetes

Several physiological models have been developed to simulate virtual patients with type 1 diabetes [30, 31, 32]. They describe subcutaneous insulin transport, intake of carbohydrates through meals and include a model of glucose-insulin dynamics.

In this paper, we use the model developed by *Hovorka et al.* to simulate people with type 1 diabetes. Using the parameters and distributions provided in [33, 26] and [34], we generate a cohort of 100 virtual patients. These parameters and their distribution are summarized in Table 1.

2.1. CGM Model

In addition, we use a CGM for glucose feedback in our controller setup. For the numerical simulations, we generate noisy CGM data based on the model and the parameters stated in [35]. This model consists of two parts. The first part describes the glucose transport from blood to interstitial tissues, which is

Table 1: Parameters and distribution for the simulated cohort.

Parameter	Unit	Distribution
EGP_0	mmol/kg/min	$EGP_0 \sim N(0.0161, 0.0039^2)$
F_{01}	mmol/kg/min	$F_{01} \sim N(0.0097, 0.0022^2)$
k_{12}	min^{-1}	$k_{12} \sim N(0.0649, 0.0282^2)$
k_{a1}	min^{-1}	$k_{a1} \sim N(0.0055, 0.0056^2)$
k_{a2}	min^{-1}	$k_{a2} \sim N(0.0683, 0.0507^2)$
k_{a3}	min^{-1}	$k_{a3} \sim N(0.0304, 0.0235^2)$
S^f_{IT}	min^{-1}/(mU/L)	$S^f_{IT} \sim N(51.2, 32.09^2)$
S^f_{ID}	min^{-1}/(mU/L)	$S^f_{ID} \sim N(8.2, 7.84^2)$
S^f_{IE}	L/mU	$S^f_{IE} \sim N(520, 306.2^2)$
k_e	min^{-1}	$k_e \sim N(0.14, 0.035^2)$
V_I	L/kg	$V_I \sim N(0.12, 0.012^2)$
V_G	L/kg	$\exp(V_G) \sim N(\ln(0.15), 0.23^2)$
τ_I	min	$\frac{1}{\tau_I} \sim N(0.018, 0.0045^2)$
τ_G	min	$\frac{1}{\ln(\tau_G)} \sim N(-3.689, 0.25^2)$
A_g	Unitless	$A_g \sim U(0.7, 1.2)$
BW	kg	$BW \sim U(65, 95)$

Table 2: Parameters for the CGM model [35].

Parameter	Value
τ_{sub}	15 min
λ	15.96
ξ	-5.471
δ	1.6898
γ	-0.5444

$$\frac{dG_{sub}}{dt} = \frac{1}{\tau_{sub}} \left(G(t) - G_{sub}(t)\right) \tag{1}$$

$G_{sub}(t)$ is the subcutaneous glucose and $G(t)$ is the blood glucose. τ_{sub} is the time constant associated to glucose transport from blood to subcutaneous tissues.

The second part models non-Gaussian sensor noise. It is given by

$$\begin{cases} e_1 &= v_1 \\ e_k &= 0.7(e_{k-1} + v_n) \end{cases} \tag{2}$$

$$v_k \sim N_{iid}(0, 1) \tag{3}$$

$$\eta_k = \xi + \lambda \sinh\left(\frac{e_k - \gamma}{\delta}\right) \tag{4}$$

Consequently, the glucose value returned by the CGM is

$$G_{CGM}(t_k) = G_{sub}(t_k) + \eta_k \tag{5}$$

3. Methods and material

This section describes the clinical protocol and the developed graphical user interface for the clinical studies.

3.1. Clinical protocol

The patient is equipped with two Dexcom Seven Plus CGMs and a Medtronic Paradigm Veo insulin pump. The CGMs provide glucose measurements every 5 minutes. The clinician decides on the sensor used by the controller, based on the accuracy of the sensor during the days before the study. The other CGM can be used as a backup device. Insulin is administrated to the patient through small discrete insulin injections (also called microboluses) every 15 minutes.

The pump used for the clinical studies has discrete increments of 0.025U, and a minimum continuous insulin injection (or basal rate) of 0.025 U/hr. The controller handles these restrictions by using hard constraints on the minimal insulin infusion rate and by rounding the suggested microbolus to the nearest 0.025U.

In addition, blood samples are taken at least every 30 minutes in order to measure the blood glucose. In case of a prolonged period of low blood glucose, the sampling time is set to 15 minutes. The blood glucose was measured by Hemocue and after the study by YSI. These values are not provided to the controller.

The clinician has the authority to prevent severe hypoglycemia by injection of intravenous glucose. Such a decision is based on the glucose history.

3.2. Graphical User Interface

Fig 2 provides an overview of the graphical user interface of our controller developed for the artificial pancreas. The glucose sensor provides a glucose measurement every 5 minutes. The glucose measurements are transmitted from the sensor to the software via a wireless receiver.

The graphical user interface returns a new insulin microbolus suggestion every 15 minutes. At these times, it also returns the glucose prediction and insulin prediction profiles. The decision on the insulin microbolus can be overruled if there is a safety risk for the patient. The exact time before the next microbolus suggestion is provided by the graphical user interface.

The clinician also has the possibility to add comments if needed. These comments have no influence on the microboli computations.

4. Prediction of Subcutaneous Glucose

In this section, we derive a prediction model for subcutaneous glucose, $y(t)$. The model has a deterministic part describing the effect of sc injected insulin, $u(t)$, and a stochastic part describing the effect of other unknown factors. The prediction model is an autoregressive integrated moving average with exogenous input (ARIMAX) model

$$A(q^{-1})y(t) = B(q^{-1})u(t) + \frac{C(q^{-1})}{1-q^{-1}}\varepsilon(t) \tag{6}$$

The ARIMAX model structure (6) is used to achieve offset-free control when the filter and predictor of this model are used in an MPC. A and B are individualized and derived from known patient information. C is identified from data for one real patient and this C is used for the entire cohort of virtual and real patients. This model identification technique turns out to give a good compromise between data requirements, performance and robustness of the resulting controller for the overnight study described in this paper.

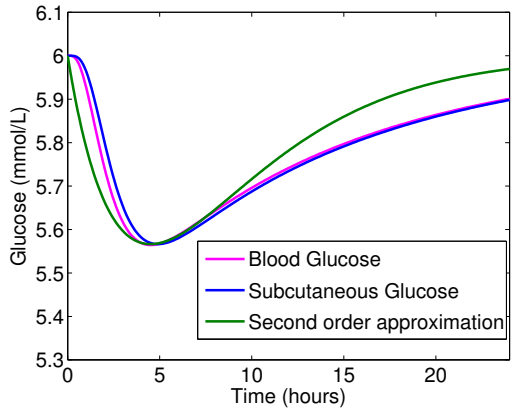

Figure 3: Impulse responses for a second order model and the nonlinear Hovorka model. The bolus size is 0.1U and the parameters for the second order model are: τ=4 hours and ISF = 0.4 mmol/L/0.1 U = 4.0 mmol/L/U.

4.1. Deterministic Model

All the physiological models mentioned in Section 2 contain a large number of parameters, and even the minimal model developed by *Bergman et al.* [31] may be difficult to identify [36]. To overcome this issue, we use a low-order linear model to describe the glucose-insulin dynamics. Similar approaches have been investigated previously. *Kirchsteiger et al.* [37] used a third order transfer function and *Percival et al.* [38] applied a first order transfer function with a time delay. In this paper we use a continuous-time second order transfer function

$$G(s) = \frac{Y(s)}{U(s)} = \frac{K_u}{(\tau s + 1)^2} \tag{7}$$

to model the effect of sc injected insulin on sc glucose. The gain, K_u, and the time constant, τ, are computed from known subject-specific parameters; the insulin action time and the insulin sensitivity factor (ISF).

Fig 3 depicts the impulse response for a virtual patient with type 1 diabetes and its second order approximation (7). This patient is simulated using the model developed by [30]. The figure demonstrates that a second order model provides an acceptable approximation of a patient with type 1 diabetes.

The insulin action time and the insulin sensitivity factor are related to the response of blood glucose to an insulin bolus. If we assume that blood glucose is approximately identical to sc glucose, this is the impulse response of (7). The insulin action time is the time for blood glucose to reach its minimum. The ISF corresponds to the maximum decrease in blood glucose per

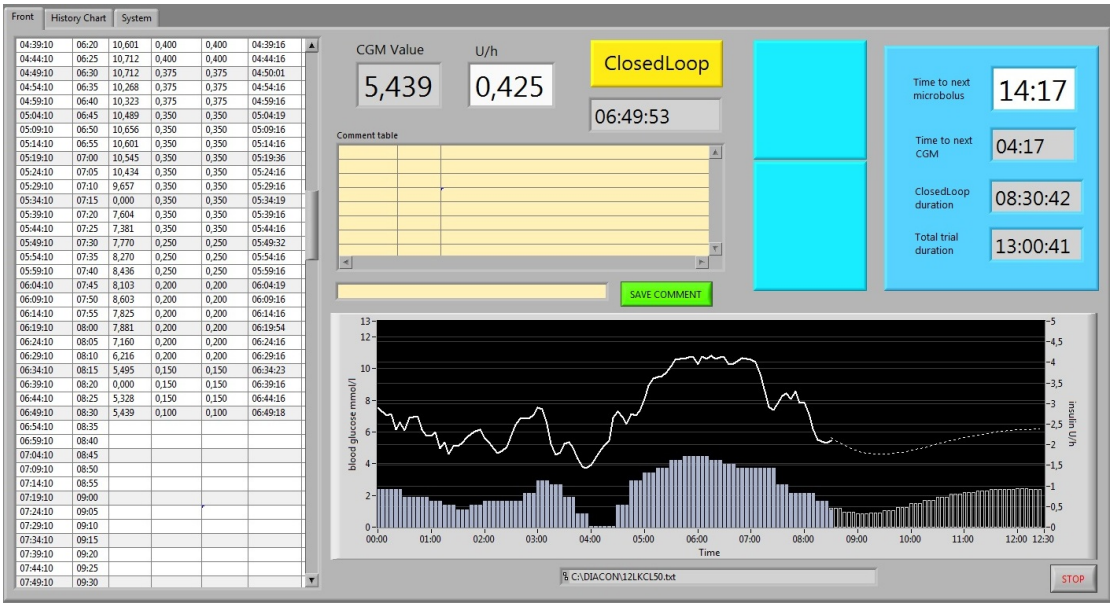

Figure 2: Graphical User Interface screenshot. The left panel provides the glucose and insulin history. The middle panel displays the current CGM value and insulin microbolus and the comments. The right panel indicates the time before the next microbolus administration, the time before the next CGM measurement, the duration of closed-loop and the total study duration. The plot depicts the glucose and insulin profiles (solid lines) and the predictions for glucose and insulin (dashed lines).

unit of insulin bolus. These parameters are empirically estimated by the patient and his/her physician. These parameters may vary from day to day for a given patient but gives an estimate of the effect of insulin on blood glucose and sc glucose.

In the temporal domain, the impulse response of (7) is described by

$$y(t) = K_u \frac{t}{\tau^2} \exp(-t/\tau) \tag{8}$$

The insulin action time corresponds to the time to reach the minimum blood glucose. Consequently, this insulin action time is equal to τ. We determine K_u using (8) and the fact that the insulin sensitivity factor is equal to the minimal blood glucose (sc glucose), $y(\tau) = -IS\,F$, such that

$$K_u = -\tau \exp(1) IS\,F \tag{9}$$

Using a zero-order-hold insulin profile, the continuous-time transfer function (7) may be used to determine the A and B polynomials in the ARIMAX model (6). They are

$$A(q^{-1}) = 1 + a_1 q^{-1} + a_2 q^{-2} \tag{10a}$$
$$B(q^{-1}) = b_1 q^{-1} + b_2 q^{-2} \tag{10b}$$

with the coefficients a_1, a_2, b_1 and b_2 computed as

$$a_1 = -2\exp(-T_s/\tau) \tag{11a}$$
$$a_2 = \exp(-2T_s/\tau) \tag{11b}$$
$$b_1 = K_u(1 - \exp(-T_s/\tau)(1 + T_s/\tau)) \tag{11c}$$
$$b_2 = K_u \exp(-T_s/\tau)(-1 + \exp(-T_s/\tau) + T_s/\tau) \tag{11d}$$

T_s is the sample time.

4.2. Stochastic Model

The stochastic part, $C(q^{-1})$, of the ARIMAX model (6) is assumed to be a third order polynomial of the form

$$\begin{aligned} C(q^{-1}) &= 1 + c_1 q^{-1} + c_2 q^{-2} + c_3 q^{-3} \\ &= (1 - \alpha q^{-1})(1 - \beta_1 q^{-1})(1 - \beta_2 q^{-1}) \end{aligned} \tag{12}$$

$\alpha = 0.99$ is a fixed parameter. α has been determined based on performance studies of the resulting MPC. β_1 and β_2 are determined from clinical data for one real patient [15, 39].

We compute β_1 and β_2 by estimating the process and measurement noise characteristics, σ and r, in the following continuous-discrete stochastic linear model

$$dx(t) = (A_c x(t) + B_c u(t))dt + \sigma d\omega(t) \tag{13a}$$
$$y_k = h(t_k, x(t_k)) + v_k \tag{13b}$$

A_c and B_c are realizations of (7). $\omega(t)$ is a standard Wiener process. The matrix σ is time-invariant and the measurement noise v_k is normally distributed, i.e. $v_k \sim N_{iid}(0, r^2)$. We estimate, σ and r, using a maximum likelihood criteria for the one-step prediction error [40, 41]. By zero-order hold (zoh) discretization, Kalman filter design, and z-transformation, (13) may be represented as

$$y_k = G(q^{-1})u_k + H(q^{-1})\epsilon_k \tag{14}$$

with

$$G(q^{-1}) = B(q^{-1})/A(q^{-1}) \tag{15a}$$
$$H(q^{-1}) = \tilde{C}(q^{-1})/A(q^{-1}) \tag{15b}$$

The parameters, β_1 and β_2, in

$$\tilde{C}(q^{-1}) = (1-\beta_1 q^{-1})(1-\beta_2 q^{-1}) \tag{16}$$

are extracted from $H(q^{-1})$. The coefficients β_1 and β_2 computed in this way are $\beta_{1,2} = 0.81 \pm 0.16i$.

The difference equation (14) corresponding to the Stochastic Differential Equation (SDE) (13) is related to the ARIMAX model (6) by

$$\epsilon_k = \frac{1-\alpha q^{-1}}{1-q^{-1}}\varepsilon_k \tag{17}$$

This specification introduces a model-plant mismatch. ϵ_k is white noise in (14) while (17) models ϵ_k as filtered integrated white noise. This model-plant mismatch is necessary to have offset free control in the resulting predictive control system. (17) implies that

$$C(q^{-1}) = (1-\alpha q^{-1})\tilde{C}(q^{-1}) \tag{18}$$

such that $c_1 = -2.61$, $c_2 = 2.28$ and $c_3 = -0.67$.

4.3. Realization and Predictions with ARIMAX Models

The ARIMAX model (6) with A, B and C given by (10) and (12) may be represented as a discrete-time state space model in innovation form

$$x_{k+1} = Ax_k + Bu_k + K\varepsilon_k \tag{19a}$$
$$y_k = Cx_k + \varepsilon_k \tag{19b}$$

with the observer canonical realization

$$A = \begin{bmatrix} 1-a_1 & 1 & 0 \\ a_1-a_2 & 0 & 1 \\ a_2 & 0 & 0 \end{bmatrix} B = \begin{bmatrix} b_1 \\ b_2-b_1 \\ -b_2 \end{bmatrix} K = \begin{bmatrix} c_1+1-a_1 \\ c_2+a_1-a_2 \\ c_3+a_2 \end{bmatrix}$$
$$C = \begin{bmatrix} 1 & 0 & 0 \end{bmatrix}$$

The innovation of (19) is

$$e_k = y_k - C\hat{x}_{k|k-1} \tag{20}$$

and the corresponding predictions are [42]

$$\hat{x}_{k+1|k} = A\hat{x}_{k|k-1} + B\hat{u}_{k|k} + Ke_k \tag{21a}$$
$$\hat{x}_{k+1+j|k} = A\hat{x}_{k+j|k} + B\hat{u}_{k+j|k}, \quad j = 1,\ldots,N-1 \tag{21b}$$
$$\hat{y}_{k+j|k} = C\hat{x}_{k+j|k}, \qquad j = 1,\ldots,N \tag{21c}$$

The innovation (20) and the predictions (21) constitute the feedback and the predictions in the model predictive controller.

5. Model Predictive Control

Control algorithms for glucose regulation in people with type 1 diabetes must be able to handle intra- and inter-patient variability. In addition, the controller must administrate insulin in a safe way to minimize the risk of hypoglycemia. Due to the nonlinearity in the glucose-insulin interaction, the risk of hypoglycemic episodes as consequence of too much insulin is particularly prominent.

In this section we describe an MPC formulation with soft output constraints and hard input constraints. This formulation is based on the individualized prediction model for glucose computed in Section 4. Along with other features we introduce a modified time-varying reference signal to robustify the controller and mitigate the effect of glucose-insulin nonlinearities and model-plant mismatch in the controller action.

The MPC algorithm computes the insulin dose by solution of an open-loop optimal control problem. Only the control action corresponding to the first sample interval is implemented and the process is repeated at the next sample interval when a new glucose measurement arrives. This is called a moving horizon implementation. The innovation (20) provides feedback from the CGM, y_k, and the open-loop optimal control problem solved in each sample interval is the convex quadratic program

$$\min_{\{\hat{u}_{k+j|k},\hat{v}_{k+j+1|k}\}_{j=0}^{N-1}} \phi \tag{22a}$$

$$\text{s.t.} \qquad (21) \tag{22b}$$
$$u_{\min} \le \hat{u}_{k+j|k} \le u_{\max} \tag{22c}$$
$$\hat{y}_{k+j+1|k} \ge y_{\min} - \hat{v}_{k+j+1|k} \tag{22d}$$
$$\hat{v}_{k+j+1|k} \ge 0 \tag{22e}$$

with the objective function ϕ defined as

$$\phi = \frac{1}{2}\sum_{j=0}^{N-1} \|\hat{y}_{k+j+1|k} - \hat{r}_{k+j+1|k}\|_2^2 + \lambda\|\Delta\hat{u}_{k+j|k}\|_2^2 + \kappa\|\hat{v}_{k+j+1|k}\|_2^2 \tag{23}$$

N is the control and prediction horizon. We choose a prediction horizon equivalent to 10 hours, such that the insulin profile of the finite horizon optimal control problem (22) is similar to the insulin profile of the infinite horizon optimal control problem, i.e. (22) with $N \to \infty$. $\|\hat{y}_{k+j+1|k} - \hat{r}_{k+j+1|k}\|_2^2$ penalizes glucose deviation from the time-varying glucose setpoint and aims to drive the glucose concentration to 6 mmol/L. $\lambda\|\Delta u_{k+j|k}\|_2^2$ is a regularization term that prevents the insulin infusion rate from varying too aggressively. For the simulations and the in vivo clinical studies we set $\lambda = 100/u_{ss}^2$. The soft output constraint (22d) penalizes glucose values below 4 mmol/L. Since hypoglycemia is highly undesirable, we choose the weight on the soft output constraint to be rather high i.e. $\kappa = 100$. The penalty function profile is illustrated in Fig. 4.

To guard against model-plant mismatch we modify the maximal allowable insulin injection, $u_{\max}$, and let it depend on the current glucose concentration. If the glucose concentration is low (below the target of 6 mmol/L) we prevent the controller from taking future hyperglycemia into account by restricting the maximal insulin injection. If the glucose concentration is high (4 mmol/L above the target) we increase the maximal allowable insulin injection rate. In the range 0 - 4 mmol/L above

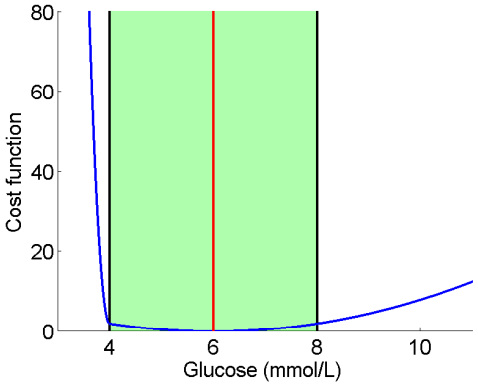

Figure 4: The penalty function

target we allow the controller to double the basal insulin injection rate. These considerations lead to

$$u_{\max} = \begin{cases} 1.5u_{ss} & 4 \le y_k \le \infty \\ u_{ss} & 0 \le y_k \le 4 \\ 0.5u_{ss} & -\infty \le y_k \le 0 \end{cases} \tag{24}$$

in which u_{ss} is the basal insulin infusion rate. Due to pump restrictions, the minimum insulin injection rate, $u_{\min}$, is a low value but not exactly zero.

[22] and [11] use a time-varying glucose reference signal to robustify the controller and reduce the risk of hypoglycemic events. In this paper, we use an asymmetric time-varying glucose reference signal. The idea of the asymmetric reference signal is to induce safe insulin injections in hyperglycemic periods and fast recovery in hypoglycemic and below target periods. The asymmetric time-varying setpoint is given by

$$\hat{r}_{k+j|k}(t) = \begin{cases} y_k \exp\left(-t_j/\tau_r^+\right) & y_k \ge 0 \\ y_k \exp\left(-t_j/\tau_r^-\right) & y_k < 0 \end{cases} \tag{25}$$

Since we want to avoid hypoglycemia, we make the controller react more aggressively if the blood glucose level is below 6 mmol/L, so we choose $\tau_r^- = 15$ min and $\tau_r^+ = 90$ min. Fig 5 provides an illustration of the time-varying reference signal.

6. Numerical results and discussion

In this section, we discuss the performance of the MPC for a randomly generated cohort of 100 virtual patients. These 100 virtual patients are generated from the probability distribution presented in Section 2. We compare the performance of the controller with simulated conventional insulin therapy in which the basal insulin infusion rate remains constant during the night. The change in insulin sensitivity is simulated by a step change in the insulin sensitivity parameters of the Hovorka model. We also provide glucose and insulin profiles for a test clinical study using the same MPC controller and the setup presented in Section 3.

The clinical protocol for the 100 in silico patients is:

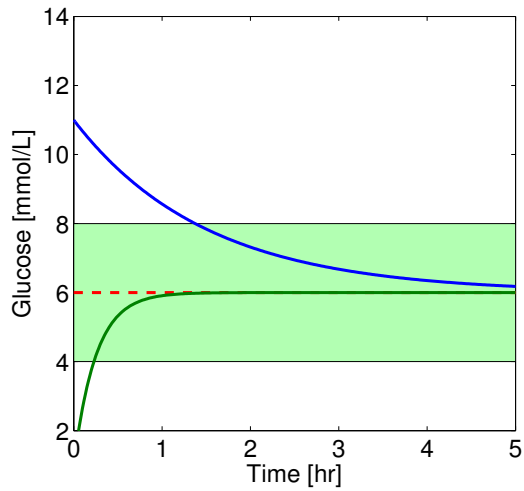

Figure 5: Time-varying reference signals for glucose above (blue curve) and below (green curve) the target of 6 mmol/L.

- The patient arrives at the clinic at 17:00. The Kalman filter is activated.
- The patient gets a 75 g CHO dinner and an insulin bolus at 18:00.
- The closed loop starts at 22:00. In addition to the Kalman filter, the MPC is activated.
- The insulin sensitivity is modified by ±30% at 01:00.
- The patient gets a 60 g CHO breakfast and an insulin bolus at 08:00. The controller is switched off.

The MPC is individualized using the insulin basal rate (u_{ss}), the insulin sensitivity factor (ISF), and the insulin action time for each individual patient. In the virtual clinic these numbers are computed from an impulse response starting at a steady state. The meal boluses are determined using a bolus calculator similar to the one presented in [21]. The glucose is provided to the controller every 5 minutes by a noise-corrupted CGM. The pump insulin infusion rate is changed every 5 minutes.

Fig. 6 depicts the mean blood glucose and insulin profiles, along with blood glucose and insulin profiles for 3 representative patients. It shows a well-controlled patient (black curve), a decently controlled patient (purple curve) and a badly controlled patient (red curve), both in the case where insulin sensitivity increases (Fig. 6(a)) and in the case where insulin sensitivity decreases (Fig. 6(b)).

Fig. 7 shows the control variability grid analysis (CVGA) of the period between 22:00 and 08:00 for the case without MPC (white circles) and the case with MPC (black circles). In Fig. 7(a) we depict the case where the insulin sensitivity is increased by 30%, and in Fig. 7(b) we depict the case where the insulin

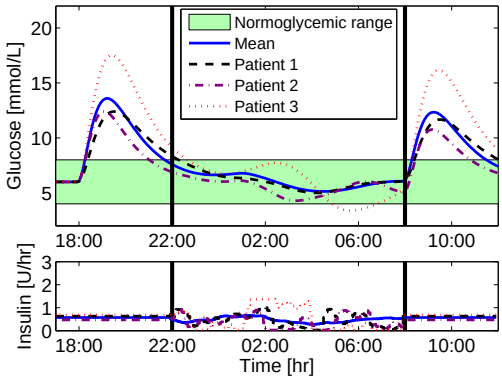

(a) Insulin sensitivity increases by 30%

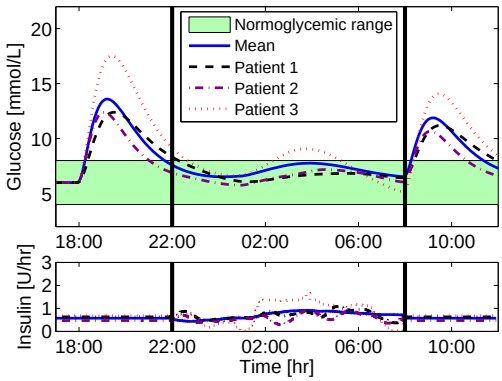

(b) Insulin sensitivity decreases by 30%

Figure 6: Glucose and insulin profiles for 3 representative patients.

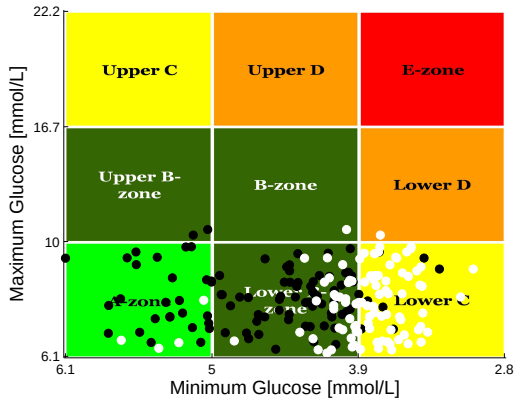

(a) Insulin sensitivity increases by 30%

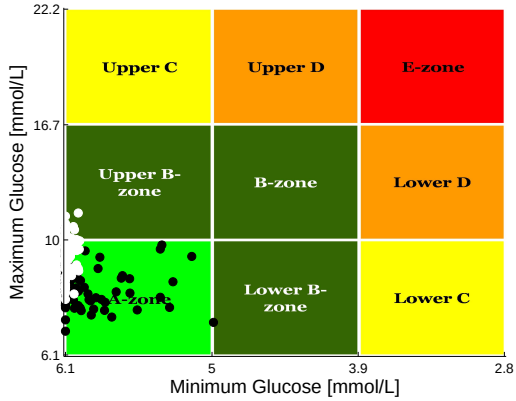

(b) Insulin sensitivity decreases by 30%

Figure 7: CVGA ([43]) plot of the 100 in silico patients. White: Without MPC. Black: With MPC.

sensitivity is decreased by 30%. These figures show that our control algorithm reduces the risk of nocturnal hypoglycemia. Although the improvement is less significant, they also show that it can slightly reduce the risk of nocturnal hyperglycemia.

In the case where insulin sensitivity is increased by 30% (Fig. 7(a)), mild hypoglycemic events occur for some of the patients. However, only few hypoglycemc events (i.e. blood glucose concentrations below 3.5 mmol/L) are observed, and the choice of the tuning parameters in the controller allows for a fast recovery. In the case where insulin sensitivity is decreased by 30% (Fig. 7(b)), all the patients are well controlled during the study period.

Table 3 provides the percentage of time spent in various glycemic regimes in the period between 22:00 and 08:00 for the 100 simulated patients. These glycemic ranges are the euglycemic range (3.9-8 mmol/L), hyperglycemia(>10 mmol/L), slight hypoglycemia(<3.9 mmol/L) and severe hypoglycemia (<3.5 mmol/L). This table show that MPC reduces the risk of hyperglycemia and significantly reduces the time spent in hypoglycemia in the case where the insulin sensitivity increases during the night.

Fig. 8 illustrates the glucose and insulin profiles for a real clinical test of the MPC. The glucose input is provided by a CGM (blue curve). Actual blood glucose measurements are provided by a glucose analyzer of blood samples (YSI). Although a mild hyperglycemic event occurred at approximately 23:00 and a few CGM values are below 4 mmol/L at approximately 03:00 and 04:00, this study shows the capability of the controller to stabilize blood glucose during the study night. Currently, the controller is being tested in an in vivo clinical study.

Table 3: Evaluation of the MPC versus constant insulin infusion rate.

Blood Glucose (mmol/L)	w/o. MPC -30%	w. MPC -30%	w/o. MPC +30%	w. MPC +30%
% $BG \geq 10$	2.2	<0.01	<0.01	<0.01
% $5 \leq BG \leq 10$	97.9	99.9	53.2	83.1
% $3.9 \leq BG \leq 5$	0	<0.01	30.7	16.0
% $BG \leq 3.9$	0	0	16.1	0.9

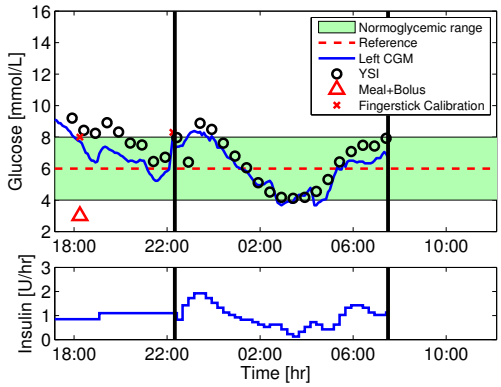

Figure 8: Glucose and insulin profiles for an in vivo clinical study. Glucose input is provided by a CGM (blue curve). Closed-loop control takes place between the 2 vertical black lines.

7. Conclusion

This paper presents a personalized controller designed for overnight stabilization of blood glucose in people with type 1 diabetes. The controller is tested on a cohort of 100 virtual patients with insulin sensitivity variations. Due to the low number of required model parameters, this controller can easily be implemented in real clinical studies. The controller both allows for safe control of blood glucose in case of high glucose and a more aggressive control strategy in case of low blood glucose. This controller is tested on 100 virtual patients with a representative parameter distribution, where we simulate an insulin sensitivity variation. Results from a clinical study is also presented. These results demonstrate that the proposed control strategy has the potential to ensure a better stabilization of overnight blood glucose in people with type 1 diabetes.

References

[1] J. Shaw, R. Sicree, P. Zimmet, Global estimates of the prevalence of diabetes for 2010 and 2030, Diabetes Research and Clinical Practice 87 (2010) 4 – 14.

[2] P. Zhang, X. Zhang, J. Brown, D. Vistisen, R. Sicree, J. Shaw, G. Nichols, Global healthcare expenditure on diabetes for 2010 and 2030, Diabetes Research and Clinical Practice 87 (2010) 293 – 301.

[3] R. M. Bergenstal, W. V. Tamborlane, A. Ahmann, J. B. Buse, G. Dailey, S. N. Davis, C. Joyce, T. Peoples, B. A. Perkins, J. B. Welsh, S. M. Willi, M. A. Wood, Effectiveness of sensor-augmented insulin-pump therapy in type 1 diabetes, New England Journal of Medicine 363 (2010) 311 – 320.

[4] A. Albisser, B. Leibel, T. Ewart, Z. Davidovac, C. Botz, W. Zingg, An artificial endocrine pancreas, Diabetes 23 (1974) 389 – 396.

[5] E. Pfeiffer, C. Thum, A. Clemens, The artificial beta cell - a continuous control of blood sugar by external regulation of insulin infusion (glucose controller insulin infusion system), Hormone and Metabolic Research 6 (5) (1974) 339 – 342.

[6] R. Hovorka, M. E. Wilinska, L. J. Chassin, D. B. Dunger, Roadmap to the artificial pancreas, Diabetes Research and Clinical Practice 74 (2006) 178 – 182.

[7] C. Cobelli, C. Dalla Man, G. Sparacino, L. Magni, G. De Nicolao, B. P. Kovatchev, Diabetes: Models, signals, and control, IEEE Reviews in Biomedical Engineering 2 (2009) 54–96.

[8] C. Cobelli, E. Renard, B. Kovatchev, Artificial pancreas: past, present, future, Diabetes 60 (2011) 2672 – 2682.

[9] G. D. Nicolao, L. Magni, C. D. Man, C. Cobelli, Modeling and control of diabetes: Towards the artificial pancreas, in: Preprints of the 18th IFAC World Congress, 2011, pp. 7092 – 7101.

[10] B. W. Bequette, Challenges and progress in the development of a closed-loop artificial pancreas, in: American Control Conference 2012 (ACC 2012), 2012.

[11] M. Eren-Oruklu, A. Cinar, L. Quinn, D. Smith, Adaptive control strategy for regulation of blood glucose levels in patients with type 1 diabetes, Journal of Process Control 19 (2009) 1333 – 1346.

[12] L. Magni, D. M. Raimondo, C. Dalla Man, G. De Nicolao, B. P. Kovatchev, C. Cobelli, Model predictive control of glucose concentration in type I diabetic patients: An in silico trial, Biomedical Signal Processing and Control 4 (4) (2009) 338–346.

[13] P. Soru, G. De Nicolao, C. Toffanin, C. Dalla Man, C. Cobelli, L. Magni, MPC based artificial pancreas: Strategies for individualization and meal compensation, Annual reviews in control 36 (2012) 118 – 128.

[14] R. Hovorka, J. M. Allen, D. Elleri, L. J. Chassin, J. Harris, D. Xing, C. Kollman, T. Hovorka, A. M. F. Larsen, M. Nodale, A. De Palma, M. E. Wilinska, C. L. Acerini, D. B. Dunger, Manual closed-loop insulin delivery in children and adolescents with type 1 diabetes: a phase 2 randomised crossover trial, Lancet 375 (2010) 743 – 751.

[15] D. Boiroux, A. K. Dunn-Henriksen, S. Schmidt, L. Frøssing, K. Nørgaard, S. Madsbad, O. Skyggebjerg, N. Poulsen, H. Madsen, J. Jørgensen, Control of blood glucose for people with type 1 diabetes: an in vivo study, in: Proceedings of the 17th Nordic Process Control Workshop, 2012, pp. 133 – 140.

[16] D. Boiroux, A. K. Duun-Henriksen, S. Schmidt, K. Nørgaard, S. Madsbad, O. Skyggebjerg, P. R. Jensen, N. K. Poulsen, H. Madsen, J. B. Jørgensen, Overnight control of blood glucose in people with type 1 diabetes, in: 8th IFAC Symposium on Biological and Medical Systems, BMS 2012, Budapest, Hungary, 2012.

[17] G. Marchetti, M. Barolo, L. Jovanovič, H. Zisser, D. E. Seborg, An improved PID switching control strategy for type 1 diabetes, in: 2006 International Conference of the IEEE Engineering in Medicine and Biology Society, New York City, USA, 2006, pp. 5041–5044.

[18] S. Weinzimer, G. Steil, K. Swan, J. Dziura, N. Kurtz, W. Tamborlane, Fully automated closed-loop insulin delivery versus semiautomated hybrid control in pediatric patients with type 1 diabetes using an artificial pancreas, Diabetes care 31 (5) (2008) 934 – 939.

[19] E. Dassau, C. Palerm, H. Zisser, B. Buckingham, L. Jovanovič, , F. Doyle III, In silico evaluation platform for artificial pancreatic beta-cell development - a dynamic simulator for closed-loop control with hardware-in-the-loop, Diabetes Technology and Therapeutics 11 (3) (2009) 187 – 194.

[20] F. El-Khatib, S. Russell, D. Nathan, R. Sutherlin, E. Damiano, A bihormonal closed-loop artificial pancreas for type 1 diabetes, Science Translational Medicine 2 (27) (2010) 27ra27.

[21] D. Boiroux, D. A. Finan, J. B. Jørgensen, N. K. Poulsen, H. Madsen,

Strategies for glucose control in people with type 1 diabetes, in: 17th IFAC World Congress, 2011.

[22] W. Garcia-Gabin, J. Vehí, J. Bondia, C. Tarín, R. Calm, Robust sliding mode closed-loop glucose control with meal compensation in type 1 diabetes mellitus, in: Proceedings of the 17th World Congress, The International Federation of Automatic Control, 2008, pp. 4240 – 4245.

[23] R. Mauseth, Y. Wang, E. Dassau, R. Kircher, D. Matheson Jr., H. Zisser, L. Jovanovič, , F. Doyle III, Proposed clinical application for tuning fuzzy logic controller of artificial pancreas utilizing a personalization factor, Journal of Diabetes Science and Technology 4 (4) (2010) 913–922.

[24] E. Atlas, R. Nimri, S. Miller, E. Grunberg, M. Phillip, Md-logic artificial pancreas system: a pilot study in adults with type 1 diabetes, Diabetes Care 33 (4) (2010) 1072–1076.

[25] L. Kovács, P. Szalay, B. Benyó, J. Chase, Robust tight glycaemic control of icu patients, in: Proceedings of the 17th World Congress, The International Federation of Automatic Control, 2011, pp. 4995 – 5000.

[26] D. Boiroux, D. A. Finan, N. K. Poulsen, H. Madsen, J. B. Jørgensen, Optimal insulin administration for people with type 1 diabetes, in: Proceedings of the 9th International Symposium on Dynamics and Control of Process Systems (DYCOPS 2010), 2010, pp. 234 – 239.

[27] C. Ellingsen, E. Dassau, H. Zisser, B. Grosman, M. W. Percival, L. Jovanovič, F. J. D. III, Safety constraints in an artificial pancreatic β cell: An implementation of model predictive control with insulin on board, Journal of diabetes science and technology 3 (2009) 536 – 544.

[28] G. Marchetti, M. Barolo, L. Jovanovič, H. Zisser, D. E. Seborg, A feedforward-feedback glucose control strategy for type 1 diabetes mellitus, Journal of Process Control 18 (2) (2008) 149–162.

[29] A. Abu-Rmileh, W. Garcia-Gabin, Feedforward-feedback multiple predictive controllers for glucose regulation in type 1 diabetes, Computer Methods and Programs in Biomedicine 99 (2010) 113–123.

[30] R. Hovorka, V. Canonico, L. J. Chassin, U. Haueter, M. Massi-Benedetti, M. O. Federici, T. R. Pieber, H. C. Schaller, L. Schaupp, T. Vering, M. E. Wilinska, Nonlinear model predictive control of glucose concentration in subjects with type 1 diabetes, Physiological Measurement 25 (2004) 905–920.

[31] R. N. Bergman, L. S. Phillips, C. Cobelli, Physiologic evaluation of factors controlling glucose tolerance in man: measurement of insulin sensitivity and beta-cell glucose sensitivity from the response to intravenous glucose, Journal of Clinical Investigation 68 (6) (1981) 1456 – 1467.

[32] C. Dalla Man, R. Rizza, C. Cobelli, Meal simulation model of the glucose-insulin system, IEEE Transactions on Biomedical Engineering 54 (10) (2007) 1740–1749.

[33] R. Hovorka, F. Shojaee-Moradie, P. V. Caroll, L. J. Chassin, I. J. Gowrie, N. C. Jackson, R. S. Tudor, A. M. Umpleby, R. H. Jones, Partitioning glucose distribution/transport, disposal, and endogenous production during IVGTT, Am. J. Physiol. 282 (2002) 992–1007.

[34] M. E. Wilinska, L. J. Chassin, C. L. Acerini, J. M. Allen, D. B. Dunger, R. Hovorka, Simulation environment to evaluate closed-loop insulin delivery systems in type 1 diabetes, Journal of Diabetes Science and Technology 4 (1) (2010) 132 – 144.

[35] M. Breton, B. Kovatchev, Analysis, modeling, and simulation of the accuracy of continuous glucose sensors, Journal of Diabetes Science and Technology 2 (2008) 853–862.

[36] G. Pillonetto, G. Sparacino, C. Cobelli, Numerical non-identifiability regions of the minimal model of glucose kinetics: superiority of bayesian estimation, Mathematical Biosciences 184 (2003) 53 – 67.

[37] H. Kirchsteiger, G. C. Estrada, S. Pölzer, E. Renard, L. del Re, Estimating interval process models for type 1 diabetes for robust control design, in: Preprints of the 18th IFAC World Congress, 2011, pp. 11761 – 11766.

[38] M. W. Percival, W. C. Bevier, Y. Wang, E. Dassau, H. Zisser, L. Jovanovič, F. J. D. III, Modeling the effects of subcutaneous insulin administration and carbohydrate consumption on blood glucose, Diabet Sci Technol 4 (5) (2010) 1214–1228.

[39] A. K. Duun-Henriksen, D. Boiroux, S. Schmidt, K. Nørgaard, S. Madsbad, O. Skyggebjerg, P. R. Jensen, N. K. Poulsen, J. B. Jørgensen, H. Madsen, Tuning of controller for type 1 diabetes treatment with stochastic differential equations, in: 8th IFAC Symposium on Biological and Medical Systems, BMS 2012, Budapest, Hungary, 2012.

[40] N. R. Kristensen, H. Madsen, S. B. Jørgensen, Parameter estimation in stochastic grey-box models, Automatica 40 (2004) 225 – 237.

[41] J. B. Jørgensen, S. B. Jørgensen, Comparison of prediction-error modelling criteria, in: Proceedings of the 2007 American Control Conference (ACC 2007), 2007, pp. 140–146.

[42] J. B. Jørgensen, J. K. Huusom, J. B. Rawlings, Finite horizon MPC for systems in innovation form, in: 50th IEEE Conference on Decision and Control and European Control Conference (CDC-ECC 2011), 2011, pp. 1896 – 1903.

[43] L. Magni, D. Raimondo, C. D. Man, M. Breton, S. Patek, G. D. Nicolao, C. Cobelli, B. Kovatchev, Evaluating the efficacy of closed-loop glucose regulation via control-variability grid analysis, Journal of Diabetes Science and Technology 2 (4) (2008) 630 – 635.

APPENDIX L

Paper K

Adaptive Control for People with Type 1 Diabetes

Authors:

Dimitri Boiroux, Anne Katrine Duun-Henriksen, Signe Schmidt, Kirsten Nørgaard, Sten Madsbad, Ole Skyggebjerg, Peter Ruhdal Jensen, Niels Kjølstad Poulsen, Henrik Madsen, and John Bagterp Jørgensen

To be Submitted

Adaptive Control for People with Type 1 Diabetes

Dimitri Boiroux[a], Anne Katrine Duun-Henriksen[a], Signe Schmidt[c], Kirsten Nørgaard[c], Sten Madsbad[c], Ole Skyggebjerg[d], Peter Ruhdal Jensen[b], Niels Kjølstad Poulsen[a], Henrik Madsen[a], John Bagterp Jørgensen[a,*]

[a]*DTU Informatics, Technical University of Denmark, Denmark*
[b]*DTU Systems Biology, Technical University of Denmark, Denmark*
[c]*Dept. of Endocrinology, Hvidovre Hospital, Denmark*
[d]*Horus ApS, Copenhagen, Denmark*

Abstract

In this paper, we discuss overnight blood glucose stabilization in people with type 1 diabetes using a Model Predictive Controller (MPC). We compute the model parameters in the MPC using a simple and systematic way based on a priori available patient information. We describe and compare 3 different model structures. The first one is an autoregressive integrated moving average with exogenous input (ARIMAX) structure. The second one is an autoregressive moving average with exogenous input (ARMAX) model, ie. without integrator. The third one is an adaptive ARMAX model in which we use a Recursive Least Square (RLS) method to estimate parameters of the stochastic part. Safety layers improve the controller robustness and reduce the risk of hypoglycemia. We test and compare our control strategies on a virtual clinic of 100 randomly generated patients with a representative inter-subject variability. This virtual clinic is based on the Hovorka model. We consider the case where only half of the meal bolus is administrated at mealtime, and the case where the insulin sensitivity increases during the night.

Keywords: Model Predictive Control, Glucose control, Artificial pancreas, Type 1 diabetes, Closed-loop control

1. Introduction

Type 1 diabetes is a metabolic disease characterized by a destruction of the insulin-producing β-cells in the pancreas. Therefore, patients with type 1 diabetes need exogenous insulin administration in order to survive. However, the dosage of insulin must be done carefully. An insulin overdose may lead to low blood glucose (hypoglycemia). Hypoglycemia has immediate effects, such as seizures, coma or even death. In contrast, prolonged periods of too high blood glucose (hyperglycemia) has long-term clinical complications, such as blindness, nerve diseases or kidney diseases.

The conventional insulin therapy for people with type 1 diabetes consists of the injection of slow acting insulin once a day and rapid acting insulin several times per day, usually before mealtimes. The slow acting insulin is used to counteract the continuous glucose production from the liver. The rapid acting insulin compensates the intake of carbohydrates (CHO) during the meals. The decision on the amount of short and fast acting insulin is based on several blood glucose measurements per day.

An increasing number of patients with type 1 diabetes use an intensive insulin therapy based on continuous glucose monitors (CGMs) and continuous subcutaneous insulin infusion (CSII) pumps instead of the conventional therapy described above. This regime can reduce the risk of complications significantly. CGMs provide more frequent subcutaneous (sc) glucose measurements. In addition, insulin pumps can be adjusted to daily variations in insulin needs.

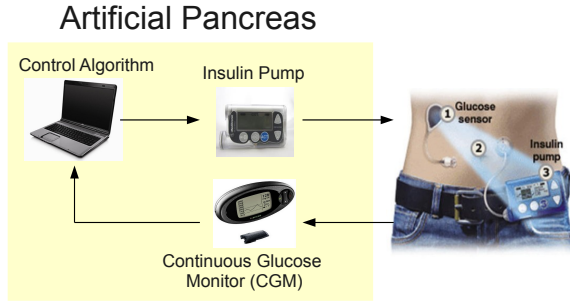

Figure 1: Closed-loop glucose control. Glucose is measured subcutaneously using a continuous glucose monitor (CGM). Insulin is dosed by an insulin pump.

Closed-loop control of blood glucose, also known as the artificial pancreas (AP) has the potential to ease the life and reduce the burden and complications for people with type 1 diabetes. It has been a subject of interest for almost 40 years [1, 2] and is still an active field of research [3, 4, 5, 6, 7]. An AP consists of a CGM, a control algorithm and a CSII pump. Fig. 1 illustrates the principle of an AP.

Several research groups worked on the implementation of APs both on virtual patients [8, 9, 10] and on in vivo clinical studies [11, 12]. Currently, the most popular control algorithms are proportional integral derivative (PID) control

*Corresponding author. E-mail: jbj@imm.dtu.dk

[13, 14], model predictive control (MPC) [15, 16], sliding mode control [17], fuzzy logic [18, 19] and $\mathcal{H}_\infty$ control [20]. Nevertheless, the performance of current APs is limited by several factors, such as the intra- and inter-patient variability, along with the lags and delays associated to the choice of sc route for glucose monitoring and insulin administration [21].

MPC is one of the most commonly used methods for the AP. The main advantages of MPC are the ability to handle constraints both on input and output variables in a systematic way. An MPC controller with insulin on board (IOB) constraints can reduce the risk of overdosing insulin due to nonlinearities in glucose-insulin dynamics [22]. Feedforward-feedback control strategies can reduce the postprandial glucose peak by administrating meal boluses in anticipation of meals [23, 24].

In this paper, we describe an AP using a CGM for glucose feedback, an insulin pump and a control algorithm based on MPC. The considered control strategy requires a priori available patient information for computing a subject-specific set of parameters. The required information is: The basal insulin infusion rate, the insulin sensitivity factor (also called the correction factor), and the insulin action time. We discuss three different model structures for the stochastic part. The first one is an autoregressive integrated moving average with exogenous input (ARIMAX) structure. The second one is an autoregressive moving average with exogenous input (ARMAX) model, ie. without integrator. The third one is an adaptive ARMAX model in which we use a Recursive Least Square (RLS) method to estimate parameters of the stochastic part. The controller is tested on a cohort of 100 virtual patients.

The paper is structured as follows. In section 2, we describe the model and the methods used to simulate a cohort of patients with type 1 diabetes and noise-corrupted CGM measurements. Section 3 presents a procedure for computation of the MPC model parameters from prior patient information, which is common to the three control strategies. In section 4, we state the three choices for the stochastic part. In section 6, we evaluate and discuss the controller performance on a cohort of 100 virtual patients. We consider the case where half of the ideal meal bolus is administrated at mealtime, and the case where the insulin sensitivity increases during the night. Conclusions are provided in section 7.

2. Physiological models for people with type 1 diabetes

Several physiological models have been developed to simulate virtual patients with type 1 diabetes [25, 26, 27]. They describe subcutaneous insulin transport, intake of carbohydrates through meals and include a model of glucose-insulin dynamics.

In this paper, we use the Hovorka model to simulate people with type 1 diabetes. Using the parameters and distributions provided in [28, 21] and [29], we generate a cohort of 100 virtual patients. The Hovorka model is illustrated in Fig. 2. The parameters and their distribution are summarized in Table 1.

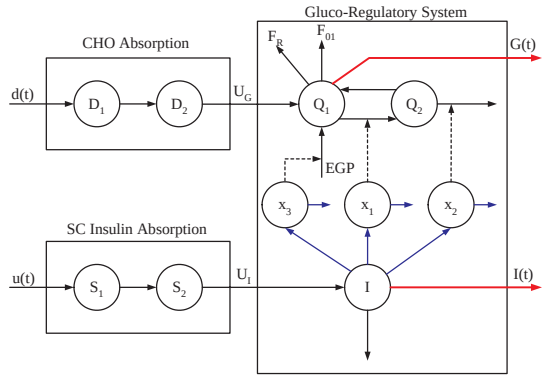

Figure 2: The Hovorka model.

Table 1: Parameters and distribution for the simulated cohort.

Parameter	Unit	Distribution
EGP_0	mmol/kg/min	$EGP_0 \sim N(0.0161, 0.0039^2)$
F_{01}	mmol/kg/min	$F_{01} \sim N(0.0097, 0.0022^2)$
k_{12}	min^{-1}	$k_{12} \sim N(0.0649, 0.0282^2)$
k_{a1}	min^{-1}	$k_{a1} \sim N(0.0055, 0.0056^2)$
k_{a2}	min^{-1}	$k_{a2} \sim N(0.0683, 0.0507^2)$
k_{a3}	min^{-1}	$k_{a3} \sim N(0.0304, 0.0235^2)$
S^f_{IT}	min^{-1}/(mU/L)	$S^f_{IT} \sim N(51.2, 32.09^2)$
S^f_{ID}	min^{-1}/(mU/L)	$S^f_{ID} \sim N(8.2, 7.84^2)$
S^f_{IE}	L/mU	$S^f_{IE} \sim N(520, 306.2^2)$
k_e	min^{-1}	$k_e \sim N(0.14, 0.035^2)$
V_I	L/kg	$V_I \sim N(0.12, 0.012^2)$
V_G	L/kg	$\exp(V_G) \sim N(\ln(0.15), 0.23^2)$
τ_I	min	$\frac{1}{\tau_I} \sim N(0.018, 0.0045^2)$
τ_G	min	$\frac{1}{\ln(\tau_G)} \sim N(-3.689, 0.25^2)$
A_g	Unitless	$A_g \sim U(0.7, 1.2)$
BW	kg	$BW \sim U(65, 95)$

2.1. CGM Model

In addition, we use a CGM for glucose feedback in our controller setup. For the numerical simulations, we generate noisy CGM data based on the model and the parameters determined by [30]. This model consists of two parts. The first part describes the glucose transport from blood to interstitial tissues, which is

$$\frac{dG_{sub}}{dt} = \frac{1}{\tau_{sub}} \left(G(t) - G_{sub}(t)\right) \tag{1}$$

$G_{sub}(t)$ is the subcutaneous glucose and $G(t)$ is the blood glucose. τ_{sub} is the time constant associated to glucose transport from blood to subcutaneous tissues.

The second part models non-Gaussian sensor noise. It is given by

Table 2: Parameters for the CGM model [30].

Parameter	Value
τ_{sub}	15 min
λ	15.96
ξ	-5.471
δ	1.6898
γ	-0.5444

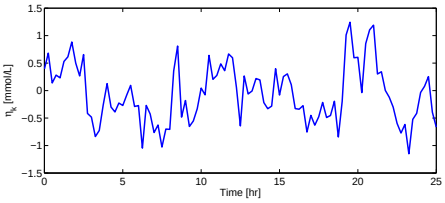

Figure 3: Example of a CGM noise realization.

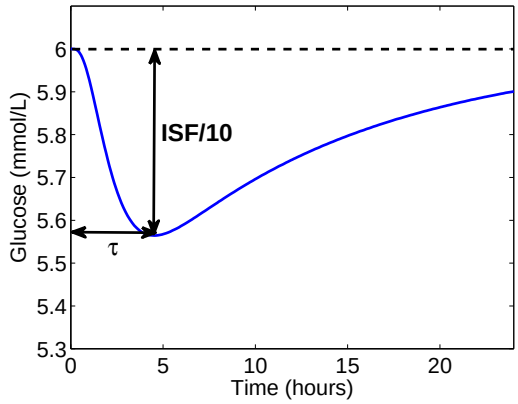

Figure 4: Impulse response for the nonlinear Hovorka model. The bolus size is 0.1U.

$$\begin{cases} e_1 &= v_1 \\ e_k &= 0.7(e_{k-1} + v_n) \end{cases} \tag{2}$$

$$v_k \sim N_{iid}(0, 1) \tag{3}$$

$$\eta_k = \xi + \lambda \sinh\left(\frac{e_k - \gamma}{\delta}\right) \tag{4}$$

Fig. 3 provides an example of a CGM noise sequence η_k. The glucose value returned by the CGM is

$$G_{CGM}(t_k) = G_{sub}(t_k) + \eta_k \tag{5}$$

3. Modeling of Glucose-Insulin Dynamics

In this section, we derive a prediction model for subcutaneous glucose, $y(t)$. The model has a deterministic part describing the effect of sc. injected insulin, $u(t)$, and a stochastic part describing the effect of other unknown factors. This model identification technique turns out to give a good compromise between data requirements, performance and robustness of the resulting controller.

3.1. Choice of the deterministic model

All the physiological models listed in section 2 contain a large number of parameters, and even the minimal model may be difficult to identify [31]. To overcome this issue, we use a low-order linear model to describe the glucose-insulin dynamics. Similar approaches have been investigated previously. [32] used a third order transfer function with an integrator, [33] used a third order discrete transfer function model and [34] applied a first order transfer function with a time delay. In this thesis we use a continuous-time second order transfer function

$$G(s) = \frac{Y(s)}{U(s)} = \frac{K_u}{(\tau s + 1)^2} \tag{6}$$

to model the effect of sc injected insulin on sc glucose. The gain, K_u, and the time constant, τ, are computed from known subject-specific parameters; the insulin action time and the insulin sensitivity factor (ISF).

The insulin action time and the insulin sensitivity factor are related to the response of blood glucose to an insulin bolus. If we assume that blood glucose is approximately identical to sc glucose, this is the impulse response of (6). The insulin action time is the time for blood glucose to reach its minimum. The ISF corresponds to the maximum decrease in blood glucose per unit of insulin bolus. These parameters are empirically estimated by the patient and his/her physician. These parameters may vary from day to day for a given patient but gives an estimate of the effect of insulin on blood glucose and sc glucose. An illustration of the ISF and the insulin action time is provided in Fig. 4.

Fig 5 depicts the impulse response for a virtual patient with type 1 diabetes and its second order approximation (6). This patient is simulated using the model developed by [25]. The figure demonstrates that a second order model provides an acceptable approximation of a patient with type 1 diabetes.

In the temporal domain, the impulse response of (6) is described by

$$y(t) = K_u \frac{t}{\tau^2} \exp(-t/\tau) \tag{7}$$

The insulin action time corresponds to the time to reach the minimum blood glucose. Consequently, this insulin action time is equal to τ. We determine K_u using (7) and the fact that the insulin sensitivity factor is equal to the minimal blood glucose (sc glucose), $y(\tau) = -ISF$, such that

$$K_u = -\tau \exp(1) ISF \tag{8}$$

We discretize the transfer function (6) in the form

$$y(t) = \frac{B(q^{-1})}{A(q^{-1})} u(t) \tag{9}$$

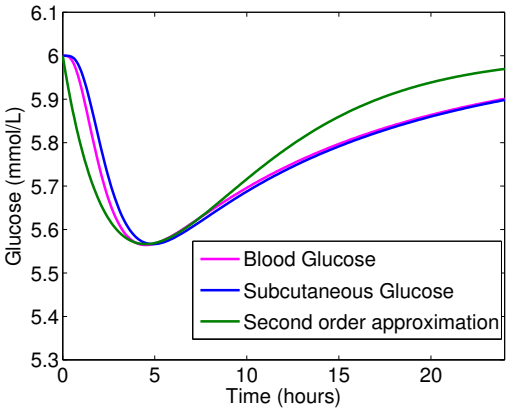

Figure 5: Impulse responses for a second order model and the nonlinear Hovorka model. The bolus size is 0.1U and the parameters for the second order model are: τ=4 hours and ISF = 0.4 mmol/L/0.1 U = 4.0 mmol/L/U.

Using a zero-order-hold insulin profile, the continuous-time transfer function (6) may be used to determine the A and B polynomials in the model (9). They are

$$A(q^{-1}) = 1 + a_1 q^{-1} + a_2 q^{-2} \tag{10a}$$
$$B(q^{-1}) = b_1 q^{-1} + b_2 q^{-2} \tag{10b}$$

with the coefficients a_1, a_2, b_1 and b_2 computed as [35]

$$a_1 = -2\exp(-T_s/\tau) \tag{11a}$$
$$a_2 = \exp(-2T_s/\tau) \tag{11b}$$
$$b_1 = K_u(1 - \exp(-T_s/\tau)(1 + T_s/\tau)) \tag{11c}$$
$$b_2 = K_u \exp(-T_s/\tau)(-1 + \exp(-T_s/\tau) + T_s/\tau) \tag{11d}$$

T_s is the sample time.

4. Stochastic Model

We take into account the process and measurement noise by adding a term describing the effect of unknown factors to the discrete-time model (9). We assume the model describing the glucose-insulin dynamics to be in the form

$$A(q^{-1})y(t) = B(q^{-1})u(t) + \frac{C(q^{-1})}{D(q^{-1})}\varepsilon(t) \tag{12}$$

The model (12) has a deterministic part describing the effects of insulin injections $u(t)$ and a stochastic part. We assume either $D(q^{-1}) = 1 - q^{-1}$, which turns the model (12) into an ARIMAX model or $D(q^{-1}) = 1$, which turns the model (12) into an ARMAX model.

In this section we propose and discuss three different choices for the stochastic model in (12). The two first choices estimate the $C(q^{-1})$ based on a previous clinical study, while the last method estimate it recursively using a Recursive Least Square (RLS) algorithm.

4.1. ARIMAX modeling

The stochastic part, $C(q^{-1})$, of the ARIMAX model

$$A(q^{-1})y(t) = B(q^{-1})u(t) + \frac{C(q^{-1})}{1 - q^{-1}}\varepsilon(t) \tag{13}$$

is assumed to be a third order polynomial of the form

$$\begin{aligned} C(q^{-1}) &= 1 + c_1 q^{-1} + c_2 q^{-2} + c_3 q^{-3} \\ &= (1 - \alpha q^{-1})(1 - \beta_1 q^{-1})(1 - \beta_2 q^{-1}) \end{aligned} \tag{14}$$

$\alpha = 0.99$ is a fixed parameter. α has been determined based on performance studies of the resulting MPC. The choice of α is discussed in [36]. β_1 and β_2 are determined from clinical data for one real patient [37, 38].

We compute β_1 and β_2 by estimating the process and measurement noise characteristics, σ and r, in the following continuous-discrete stochastic linear model

$$dx(t) = (A_c x(t) + B_c u(t))dt + \sigma d\omega(t) \tag{15a}$$
$$y_k = h(t_k, x(t_k)) + v_k \tag{15b}$$

A_c and B_c are realizations of (6). $\omega(t)$ is a standard Wiener process. The matrix σ is time-invariant and the measurement noise v_k is normally distributed, i.e. $v_k \sim N_{iid}(0, r^2)$. We estimate, σ and r, using a maximum likelihood criteria for the one-step prediction error [39, 40]. By zero-order hold (zoh) discretization, Kalman filter design, and z-transformation, (15) may be represented as

$$y_k = G(q^{-1})u_k + H(q^{-1})\epsilon_k \tag{16}$$

with

$$G(q^{-1}) = B(q^{-1})/A(q^{-1}) \tag{17a}$$
$$H(q^{-1}) = \tilde{C}(q^{-1})/A(q^{-1}) \tag{17b}$$

The parameters, β_1 and β_2, in

$$\tilde{C}(q^{-1}) = (1 - \beta_1 q^{-1})(1 - \beta_2 q^{-1}) \tag{18}$$

are extracted from $H(q^{-1})$. The coefficients β_1 and β_2 computed in this way are $\beta_{1,2} = 0.81 \pm 0.16i$.

The difference equation (16) corresponding to the SDE (15) is related to the ARIMAX model (13) by

$$\epsilon_k = \frac{1 - \alpha q^{-1}}{1 - q^{-1}}\varepsilon_k \tag{19}$$

This specification introduces a model-plant mismatch. ϵ_k is white noise in (16) while (19) models ϵ_k as filtered integrated white noise. This model-plant mismatch is necessary to have offset free control in the resulting predictive control system. (19) implies that

$$C(q^{-1}) = (1 - \alpha q^{-1})\tilde{C}(q^{-1}) \tag{20}$$

such that $c_1 = -2.61$, $c_2 = 2.28$ and $c_3 = -0.67$.

4.2. ARMAX modeling

The stochastic part, $C(q^{-1})$, of the ARMAX model

$$A(q^{-1})y(t) = B(q^{-1})u(t) + C(q^{-1})\varepsilon(t) \tag{21}$$

is now assumed to be a second order polynomial of the form

$$\begin{aligned} C(q^{-1}) &= 1 + c_1 q^{-1} + c_2 q^{-2} \\ &= (1 - \beta_1 q^{-1})(1 - \beta_2 q^{-1}) \end{aligned} \tag{22}$$

We use the same way as in Section 4.1 for computing β_1 and β_2, i.e. $\beta_{1,2} = 0.81 \pm 0.16i$. This yields

$$C(q^{-1}) = 1 - 1.62q^{-1} + 0.68q^{-2} \tag{23}$$

Unlike the ARIMAX model structure described in Section 4.1, this model structure does not ensure offset-free control. However, it does not introduce a supplementary model-plant mismatch.

4.3. Adaptive control

Here, we consider again the ARMAX model structure (21). A similar approach has been proposed by [8].

The parameters c_1 and c_2 are estimated at each iteration using the recursive least square (RLS) method

$$y_k = \phi_k' \hat{\theta}_{k-1} + \varepsilon_k \tag{24a}$$

$$K_k = \frac{P_{k-1}\phi_k}{\mu + \phi_k' P_{k-1}\phi_k} \tag{24b}$$

$$\hat{\theta}_k = \hat{\theta}_{k-1} + K_k\left(y_k - \phi_k'\hat{\theta}_{k-1}\right) \tag{24c}$$

$$P_k = \frac{1}{\mu}\left(P_{k-1} - \frac{P_{k-1}\phi_k\phi_k' P_{k-1}}{\mu + \phi_k' P_{k-1}\phi_k}\right) \tag{24d}$$

ϕ_k is a vector of past observations

$$\phi_k = \begin{bmatrix} y_{k-1} & y_{k-2} & u_{k-1} & u_{k-2} & e_k & e_{k-1} \end{bmatrix} \tag{25}$$

θ_k is a vector of model parameters

$$\theta_k = \begin{bmatrix} -a_1 & -a_2 & b_1 & b_2 & c_1 & c_2 \end{bmatrix}' \tag{26}$$

P_k is the model parameters covariance matrix. Since we want to estimate c_1 and c_2 only, we initialize it with

$$P_0 = diag(0, 0, 0, 0, 100, 100) \tag{27}$$

Finally, μ is the forgetting factor. This parameter has an influence on the weight of previous observations. When $\mu = 1$, all the past observations are equally weighted. Smaller values of μ give more importance to recent observations [41].

An approximation of the memory length (in time samples) is

$$\frac{1}{1-\mu} \tag{28}$$

In this Chapter, we chose $\mu = 0.95$, ie. the corresponding memory length is approximately $1/(1 - 0.95) = 20$ time samples, or 100 minutes.

This model structure allows for a personalized stochastic model description.

4.4. Realization and predictions

The ARIMAX model (13) and the ARMAX model (21) may be represented as a discrete-time state space model in innovation form

$$x_{k+1} = Ax_k + Bu_k + K\varepsilon_k \tag{29a}$$

$$y_k = Cx_k + \varepsilon_k \tag{29b}$$

The observer canonical realization for the ARMAX model (21) is

$$\begin{aligned} A &= \begin{bmatrix} -a_1 & 1 \\ -a_2 & 0 \end{bmatrix} B = \begin{bmatrix} b_1 \\ b_2 \end{bmatrix} K = \begin{bmatrix} c_1 - a_1 \\ c_2 - a_2 \end{bmatrix} \\ C &= \begin{bmatrix} 1 & 0 \end{bmatrix} \end{aligned}$$

and the observer canonical realization for the ARIMAX model (13) is

$$\begin{aligned} A &= \begin{bmatrix} 1 - a_1 & 1 & 0 \\ a_1 - a_2 & 0 & 1 \\ a_2 & 0 & 0 \end{bmatrix} B = \begin{bmatrix} b_1 \\ b_2 - b_1 \\ -b_2 \end{bmatrix} K = \begin{bmatrix} c_1 + 1 - a_1 \\ c_2 + a_1 - a_2 \\ c_3 + a_2 \end{bmatrix} \\ C &= \begin{bmatrix} 1 & 0 & 0 \end{bmatrix} \end{aligned}$$

The innovation of (29) is

$$e_k = y_k - C\hat{x}_{k|k-1} \tag{30}$$

and the corresponding predictions are [42]

$$\hat{x}_{k+1|k} = A\hat{x}_{k|k-1} + B\hat{u}_{k|k} + Ke_k \tag{31a}$$

$$\hat{x}_{k+1+j|k} = A\hat{x}_{k+j|k} + B\hat{u}_{k+j|k}, \quad j = 1, \ldots, N-1 \tag{31b}$$

$$\hat{y}_{k+j|k} = C\hat{x}_{k+j|k}, \qquad j = 1, \ldots, N \tag{31c}$$

The innovation (30) and the predictions (31) constitute the feedback and the predictions in the model predictive controller.

5. Model Predictive Control

Control algorithms for glucose regulation in people with type 1 diabetes must be able to handle intra- and inter-patient variability. In addition, the controller must administrate insulin in a safe way to minimize the risk of hypoglycemia. Due to the nonlinearity in the glucose-insulin interaction, the risk of hypoglycemic episodes as consequence of too much insulin is particularly prominent.

In this section we describe an MPC formulation with soft output constraints and hard input constraints. This formulation is based on the individualized prediction model for glucose computed in Section 4.2. Along with other features, we introduce a modified time-varying reference signal to robustify the controller and mitigate the effect of glucose-insulin nonlinearities and model-plant mismatch in the controller action.

The MPC algorithm computes the insulin dose by solution of an open-loop optimal control problem. Only the control action corresponding to the first sample interval is implemented and the process is repeated at the next sample interval. This is

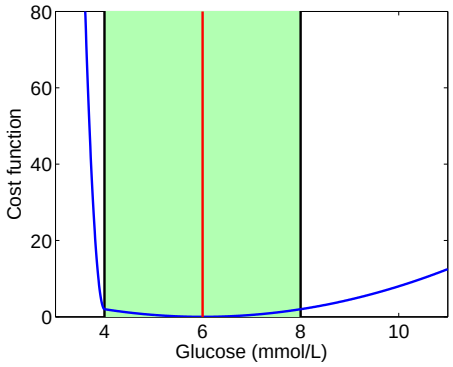

Figure 6: The penalty function $\rho = \|y - r\|_2^2 + \kappa\|\min\{y - y_{\min}, 0\}\|_2^2$.

called a moving horizon implementation. The innovation (30) provides feedback from the CGM, y_k, and the open-loop optimal control problem solved in each sample interval is the convex quadratic program

$$\min_{\{\hat{u}_{k+j|k}, \hat{v}_{k+j+1|k}\}_{j=0}^{N-1}} \phi \tag{32a}$$

$$s.t. \qquad (31) \tag{32b}$$

$$u_{\min} \leq \hat{u}_{k+j|k} \leq u_{\max} \tag{32c}$$

$$\hat{y}_{k+j+1|k} \geq y_{\min} - \hat{v}_{k+j+1|k} \tag{32d}$$

$$\hat{v}_{k+j+1|k} \geq 0 \tag{32e}$$

with the objective function ϕ defined as

$$\begin{aligned}\phi = &\frac{1}{2}\sum_{j=0}^{N-1} \|\hat{y}_{k+j+1|k} - \hat{r}_{k+j+1|k}\|_2^2 \\ &+ \lambda\|\Delta\hat{u}_{k+j|k}\|_2^2 + \kappa\|\hat{v}_{k+j+1|k}\|_2^2\end{aligned} \tag{33}$$

N is the control and prediction horizon. We choose a prediction horizon equivalent to 10 hours, such that the insulin profile of the finite horizon optimal control problem (32) is similar to the insulin profile of the infinite horizon optimal control problem, (32) with $N \to \infty$. $\|\hat{y}_{k+j+1|k} - \hat{r}_{k+j+1|k}\|_2^2$ penalizes glucose deviation from the time-varying glucose setpoint and aims to drive the glucose concentration to 6 mmol/L. $\lambda\|\Delta u_{k+j|k}\|_2^2$ is a regularization term that prevents the insulin infusion rate from varying too aggressively. For the simulations and the in vivo clinical studies we set $\lambda = 100/u_{ss}^2$. The soft output constraint (32d) penalizes glucose values below 4 mmol/L. Since hypoglycemia is highly undesirable, we choose the weight on the soft output constraint to be rather high, i.e. $\kappa = 100$. The penalty function profile is illustrated in Fig. 6.

To guard against model-plant mismatch we modify the maximal allowable insulin injection, $u_{\max}$, and let it depend on the current glucose concentration. If the glucose concentration is low (below the target of 6 mmol/L), we prevent the controller from taking future hyperglycemia into account by restricting

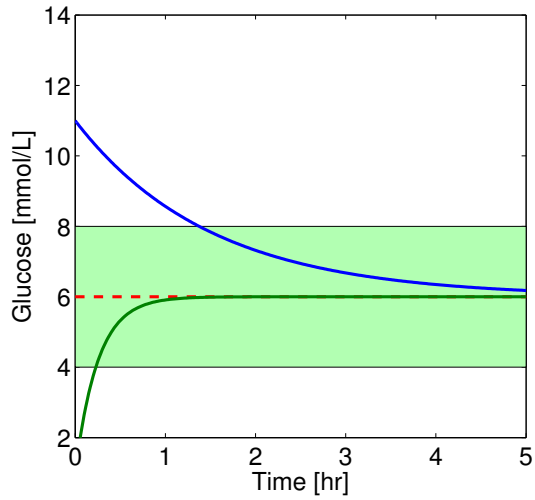

Figure 7: Time-varying reference signals for glucose above (blue curve) and below (green curve) the target of 6 mmol/L.

the maximal insulin injection. If the glucose concentration is high (4 mmol/L above the target) we increase the maximal allowable insulin injection rate. In the range 0 - 4 mmol/L above target we allow the controller to double the basal insulin injection rate. These considerations lead to

$$u_{\max} = \begin{cases} 1.5u_{ss} & 4 \leq y_k \leq \infty \\ u_{ss} & 0 \leq y_k \leq 4 \\ 0.5u_{ss} & -\infty \leq y_k \leq 0 \end{cases} \tag{34}$$

in which u_{ss} is the basal insulin infusion rate. Due to pump restrictions, the minimum insulin injection rate, $u_{\min}$, is a low value but not exactly zero.

[17] and [8] use a time-varying glucose reference signal to robustify the controller and reduce the risk of hypoglycemic events. In this paper, we use an asymmetric time-varying glucose reference signal. The idea of the asymmetric reference signal is to induce safe insulin injections in hyperglycemic periods and fast recovery in hypoglycemic and below target periods. The asymmetric time-varying setpoint is given by

$$\hat{r}_{k+j|k}(t) = \begin{cases} y_k \exp\left(-t_j/\tau_r^+\right) & y_k \geq 0 \\ y_k \exp\left(-t_j/\tau_r^-\right) & y_k < 0 \end{cases} \tag{35}$$

Since we want to avoid hypoglycemia, we make the controller react more aggressively if the blood glucose level is below 6 mmol/L, so we choose $\tau_r^- = 15$ min and $\tau_r^+ = 90$ min. Fig 7 provides an illustration of the time-varying reference signal.

6. Comparison between ARIMAX, ARMAX and adaptive ARMAX model structures

In this section we compare three different versions of our Model Predictive Controller on a cohort of 100 virtual patients.

These three versions are the ARIMAX formulation presented in Section 4.1, the ARMAX formulation presented in Section 4.2 and the adaptive ARMAX model formulation presented in Section 4.3. We compare the performance of the controllers for the case where the meal is underbolused and the case where the insulin sensitivity is increased by 30% during the night. The change in insulin sensitivity is simulated by a step change in the insulin sensitivity parameters of the Hovorka model.

The ARMAX based controllers do not contain an integrator and cannot guarantee steady-state offset-free control. However, the tuning of the MPC based ARMAX models may be simpler than the tuning of the MPC based on the ARIMAX model. The reason is that no artificial model-plant mismatch is introduced in the MPC based on ARMAX models, while the ARIMAX based controller deliberately include such a mismatch to ensure steady-state offset free control.

The MPC is individualized using the insulin basal rate (u_{ss}), the insulin sensitivity factor (ISF), and the insulin action time for each individual patient. In the virtual clinic these numbers are computed from an impulse response starting at a steady state. The meal boluses are determined using a bolus calculator similar to the one presented in [16]. The glucose is provided to the controller every 5 minutes by a noise-corrupted CGM. The pump insulin infusion rate is changed every 5 minutes.

The clinical protocol for the 100 in silico patients is:

- The patient arrives at the clinic at 17:00. The Kalman filter is activated.
- The patient gets a 75 g CHO dinner and an insulin bolus at 18:00.
- The closed loop starts at 22:00. In addition to the Kalman filter, the MPC is activated.
- The patient gets a 60 g CHO breakfast and an insulin bolus at 08:00. The controller is switched off.

6.1. Underbolused meal

Fig. 9 shows the CVGA plot for the three different strategies in the case where only 50% of the meal bolus is administrated at mealtime. The control strategy based on an ARIMAX model shows several cases of mild hypoglycemia due to an insulin overdose. The two control strategies based on an ARMAX model are able to avoid this undershoot.

Table 3 shows the time spent in the euglycemic range, hypoglycemia and hyperglycemia for the three different strategies in the case where only 50% of the meal bolus is administrated at mealtime. The results show that the control strategy based on an ARIMAX model structure reduce the time spent in hyperglycemia. The adaptive ARMAX model structure shows the best compromise between the time spent in euglycemia and safety concerning the risk of insulin overdose.

6.2. Change in insulin sensitivity

Fig. 10 shows the CVGA plot for the three different strategies for the case where the insulin sensitivity is increased by

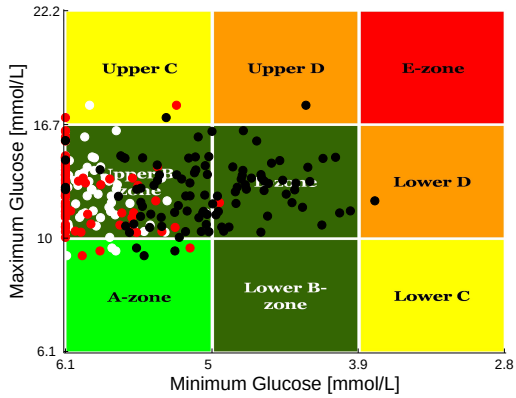

Figure 9: Control Variability Grid Analysis (CVGA) plot for the three different stochastic model structures. 50% of the meal bolus is administrated at mealtime. Black: ARIMAX. Red: ARMAX. White: Adaptive ARMAX.

Table 3: Evaluation of the controller for the different control strategies in the case where only 50% of the meal bolus is administrated at mealtime. The numbers show the total percentage of time spent in different glucose ranges for the 100 virtual patients during the period 22:00 - 08:00.

Glucose (mmol/L)	ARIMAX	ARMAX	Adaptive ARMAX
$G > 10$	17.8	23.9	20.8
$G > 8$	31.6	58.1	42.2
$3.9 \leq G \leq 10$	82.1	76.1	79.2
$3.9 \leq G \leq 8$	68.3	41.9	57.8
$G < 3.9$	0.1	0	0
$G < 3.5$	0	0	0

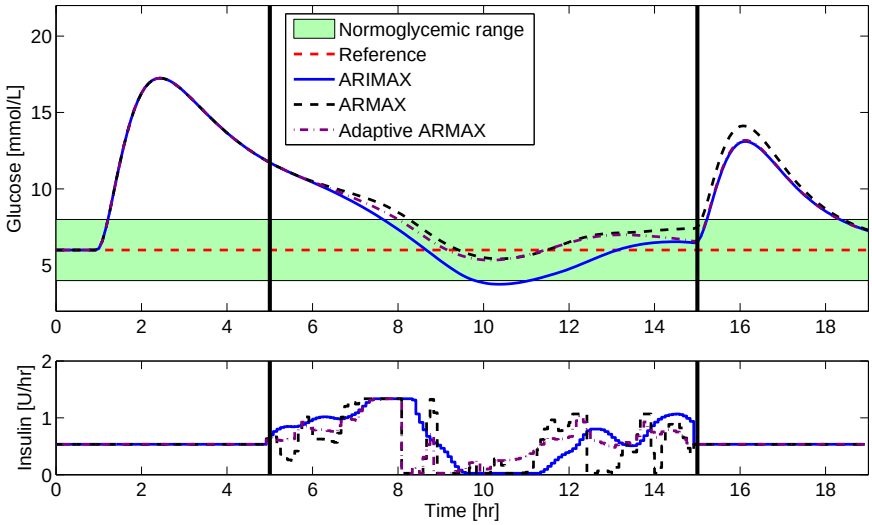

Figure 8: Glucose and insulin profiles of a specific patient for the different control strategies. The patients gets half of the optimal bolus at mealtime.

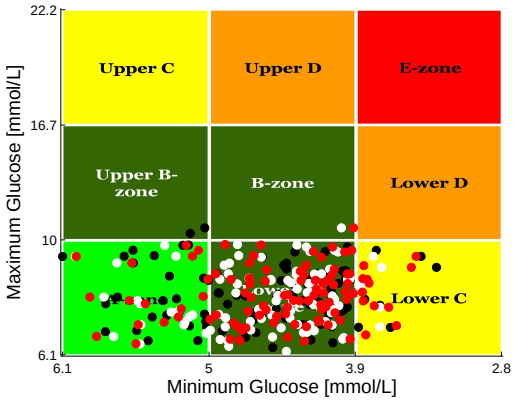

Figure 10: Control Variability Grid Analysis (CVGA) plot for the three different stochastic model structures in the case where the insulin sensitivity is increased by 30% during the night. Black: ARIMAX. Red: ARMAX. White: Adaptive ARMAX.

30% during the night. Table 4 shows the time spent in the euglycemic range, hypoglycemia and hyperglycemia for the three different strategies in the case where the insulin sensitivity is increased by 30% during the night. The control strategies based on an ARMAX model structure, i.e. the controllers without the integrator, reduces the occurrences of hypoglycemia, and avoid severe hypoglycemia (ie. glucose values below 3.5 mmol/L).

Table 4: Evaluation of the controller for the different control strategies in the case where the insulin sensitivity is increased by 30% during the night. The numbers show the total percentage of time spent in different glucose ranges for the 100 virtual patients during the period 22:00 - 08:00.

Glucose (mmol/L)	ARIMAX	ARMAX	Adaptive ARMAX
$G > 10$	<0.1	<0.1	<0.1
$G > 8$	3.2	2.5	2.2
$3.9 \leq G \leq 10$	99.1	99.4	99.7
$3.9 \leq G \leq 8$	95.9	96.9	97.5
$G < 3.9$	0.9	0.6	0.3
$G < 3.5$	0.2	0	0

7. Conclusion

This paper presents subject-specific control strategies designed for overnight stabilization of blood glucose in people with type 1 diabetes. This controller is tested on 100 virtual patients with a representative parameter distribution, where we simulate an underbolused meal or an insulin sensitivity variation. The choice of the model structure for the stochastic part is a tradeoff between offset-free control and model-plant mismatch. In our case, the ARMAX and the adaptive ARMAX formulations presented in this paper have the potential to improve the controller performance, but would need a further investigation before being tested on real patients.

References

[1] A. Albisser, B. Leibel, T. Ewart, Z. Davidovac, C. Botz, W. Zingg, An artificial endocrine pancreas, Diabetes 23 (1974) 389 – 396.
[2] E. Pfeiffer, C. Thum, A. Clemens, The artificial beta cell - a continuous control of blood sugar by external regulation of insulin infusion (glucose

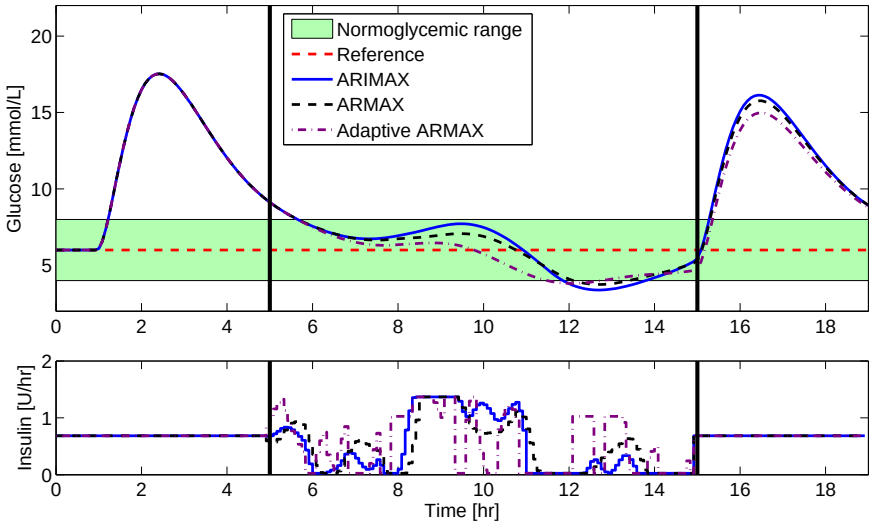

Figure 11: Glucose and insulin profiles of a specific patient for the different control strategies. The insulin sensitivity increases by 30% during the night.

controller insulin infusion system), Hormone and Metabolic Research 6 (5) (1974) 339 – 342.

[3] R. Hovorka, M. E. Wilinska, L. J. Chassin, D. B. Dunger, Roadmap to the artificial pancreas, Diabetes Research and Clinical Practice 74 (2006) 178 – 182.

[4] C. Cobelli, C. Dalla Man, G. Sparacino, L. Magni, G. De Nicolao, B. P. Kovatchev, Diabetes: Models, signals, and control, IEEE Reviews in Biomedical Engineering 2 (2009) 54–96.

[5] C. Cobelli, E. Renard, B. Kovatchev, Artificial pancreas: past, present, future, Diabetes 60 (2011) 2672 – 2682.

[6] G. D. Nicolao, L. Magni, C. D. Man, C. Cobelli, Modeling and control of diabetes: Towards the artificial pancreas, in: Preprints of the 18th IFAC World Congress, 2011, pp. 7092 – 7101.

[7] B. W. Bequette, Challenges and progress in the development of a closed-loop artificial pancreas, in: American Control Conference 2012 (ACC 2012), 2011.

[8] M. Eren-Oruklu, A. Cinar, L. Quinn, D. Smith, Adaptive control strategy for regulation of blood glucose levels in patients with type 1 diabetes, Journal of Process Control 19 (2009) 1333 – 1346.

[9] L. Magni, D. M. Raimondo, C. Dalla Man, G. De Nicolao, B. P. Kovatchev, C. Cobelli, Model predictive control of glucose concentration in type I diabetic patients: An in silico trial, Biomedical Signal Processing and Control 4 (4) (2009) 338–346.

[10] P. Soru, G. De Nicolao, C. Toffanin, C. Dalla Man, C. Cobelli, L. Magni, MPC based artificial pancreas: Strategies for individualization and meal compensation, Annual reviews in control 36 (2012) 118 – 128.

[11] R. Hovorka, J. M. Allen, D. Elleri, L. J. Chassin, J. Harris, D. Xing, C. Kollman, T. Hovorka, A. M. F. Larsen, M. Nodale, A. De Palma, M. E. Wilinska, C. L. Acerini, D. B. Dunger, Manual closed-loop insulin delivery in children and adolescents with type 1 diabetes: a phase 2 randomised crossover trial, Lancet 375 (2010) 743 – 751.

[12] D. Boiroux, A. K. Duun-Henriksen, S. Schmidt, K. Nørgaard, S. Madsbad, O. Skyggebjerg, P. R. Jensen, N. K. Poulsen, H. Madsen, J. B. Jørgensen, Overnight control of blood glucose in people with type 1 diabetes, in: 8th IFAC Symposium on Biological and Medical Systems, BMS 2012, Budapest, Hungary, 2012.

[13] G. Marchetti, M. Barolo, L. Jovanovič, H. Zisser, D. E. Seborg, An improved PID switching control strategy for type 1 diabetes, in: 2006 International Conference of the IEEE Engineering in Medicine and Biology Society, New York City, USA, 2006, pp. 5041–5044.

[14] S. Weinzimer, G. Steil, K. Swan, J. Dziura, N. Kurtz, W. Tamborlane, Fully automated closed-loop insulin delivery versus semiautomated hybrid control in pediatric patients with type 1 diabetes using an artificial pancreas, Diabetes Care 31 (5) (2008) 934 – 939.

[15] E. Dassau, C. Palerm, H. Zisser, B. Buckingham, L. Jovanovič, , F. Doyle III, In silico evaluation platform for artificial pancreatic beta-cell development - a dynamic simulator for closed-loop control with hardware-in-the-loop, Diabetes Technology and Therapeutics 11 (3) (2009) 187 – 194.

[16] D. Boiroux, D. A. Finan, J. B. Jørgensen, N. K. Poulsen, H. Madsen, Strategies for glucose control in people with type 1 diabetes, in: 17th IFAC World Congress, 2011.

[17] W. Garcia-Gabin, J. Vehí, J. Bondia, C. Tarín, R. Calm, Robust sliding mode closed-loop glucose control with meal compensation in type 1 diabetes mellitus, in: Proceedings of the 17th World Congress, The International Federation of Automatic Control, 2008, pp. 4240 – 4245.

[18] R. Mauseth, Y. Wang, E. Dassau, R. Kircher, D. Matheson Jr., H. Zisser, L. Jovanovič, , F. Doyle III, Proposed clinical application for tuning fuzzy logic controller of artificial pancreas utilizing a personalization factor, Journal of Diabetes Science and Technology 4 (4) (2010) 913–922.

[19] E. Atlas, R. Nimri, S. Miller, E. Grunberg, M. Phillip, Md-logic artificial pancreas system: a pilot study in adults with type 1 diabetes, Diabetes Care 33 (4) (2010) 1072–1076.

[20] L. Kovács, P. Szalay, B. Benyó, J. Chase, Robust tight glycaemic control of icu patients, in: Proceedings of the 17th World Congress, The International Federation of Automatic Control, 2011, pp. 4995 – 5000.

[21] D. Boiroux, D. A. Finan, N. K. Poulsen, H. Madsen, J. B. Jørgensen, Optimal insulin administration for people with type 1 diabetes, in: Proceedings of the 9th International Symposium on Dynamics and Control of Process Systems (DYCOPS 2010), 2010, pp. 234 – 239.

[22] C. Ellingsen, E. Dassau, H. Zisser, B. Grosman, M. W. Percival, L. Jovanovič, F. J. D. III, Safety constraints in an artificial pancreatic β cell: An implementation of model predictive control with insulin on board, Journal of Diabetes Science and Technology 3 (2009) 536 – 544.

[23] G. Marchetti, M. Barolo, L. Jovanovič, H. Zisser, D. E. Seborg, A feedforward-feedback glucose control strategy for type 1 diabetes mellitus, Journal of Process Control 18 (2) (2008) 149–162.

[24] A. Abu-Rmileh, W. Garcia-Gabin, Feedforward-feedback multiple predictive controllers for glucose regulation in type 1 diabetes, Computer

Methods and Programs in Biomedicine 99 (2010) 113–123.
[25] R. Hovorka, V. Canonico, L. J. Chassin, U. Haueter, M. Massi-Benedetti, M. O. Federici, T. R. Pieber, H. C. Schaller, L. Schaupp, T. Vering, M. E. Wilinska, Nonlinear model predictive control of glucose concentration in subjects with type 1 diabetes, Physiological Measurement 25 (2004) 905–920.
[26] R. N. Bergman, L. S. Phillips, C. Cobelli, Physiologic evaluation of factors controlling glucose tolerance in man: measurement of insulin sensitivity and beta-cell glucose sensitivity from the response to intravenous glucose, Journal of Clinical Investigation 68 (6) (1981) 1456 – 1467.
[27] C. Dalla Man, R. Rizza, C. Cobelli, Meal simulation model of the glucose-insulin system, IEEE Transactions on Biomedical Engineering 54 (10) (2007) 1740–1749.
[28] R. Hovorka, F. Shojaee-Moradie, P. V. Caroll, L. J. Chassin, I. J. Gowrie, N. C. Jackson, R. S. Tudor, A. M. Umpleby, R. H. Jones, Partitioning glucose distribution/transport, disposal, and endogenous production during IVGTT, Am. J. Physiol. 282 (2002) 992–1007.
[29] M. E. Wilinska, L. J. Chassin, C. L. Acerini, J. M. Allen, D. B. Dunger, R. Hovorka, Simulation environment to evaluate closed-loop insulin delivery systems in type 1 diabetes, Journal of Diabetes Science and Technology 4 (1) (2010) 132 – 144.
[30] M. Breton, B. Kovatchev, Analysis, modeling, and simulation of the accuracy of continuous glucose sensors, Journal of Diabetes Science and Technology 2 (2008) 853–862.
[31] G. Pillonetto, G. Sparacino, C. Cobelli, Numerical non-identifiability regions of the minimal model of glucose kinetics: superiority of bayesian estimation, Mathematical Biosciences 184 (2003) 53 – 67.
[32] H. Kirchsteiger, G. C. Estrada, S. Pölzer, E. Renard, L. del Re, Estimating interval process models for type 1 diabetes for robust control design, in: Preprints of the 18th IFAC World Congress, 2011, pp. 11761 – 11766.
[33] K. van Heusden, E. Dassau, H. C. Zisser, D. E. Seborg, F. J. Doyle III, Control-relevant models for glucose control using a priori patient characteristics, IEEE transactions on biomedical engineering 59 (7) (2012) 1839 – 1849.
[34] M. W. Percival, W. C. Bevier, Y. Wang, E. Dassau, H. Zisser, L. Jovanovič, F. J. D. III, Modeling the effects of subcutaneous insulin administration and carbohydrate consumption on blood glucose, Diabet Sci Technol 4 (5) (2010) 1214–1228.
[35] B. Wittenmark, K. J. Åström, K.-E. Årzén, Computer control: An overview, in: IFAC Professional Brief.
[36] J. K. Huusom, N. K. Poulsen, S. B. Jørgensen, J. B. Jørgensen, Tuning SISO offset-free model predictive control based on ARX models, Journal of Process ControlWeb-address: http://dx.doi.org/10.1016/j.jprocont.2012.08.007.
[37] D. Boiroux, A. K. Dunn-Henriksen, S. Schmidt, L. Frøssing, K. Nørgaard, S. Madsbad, O. Skyggebjerg, N. Poulsen, H. Madsen, J. Jørgensen, Control of blood glucose for people with type 1 diabetes: an in vivo study, in: Proceedings of the 17th Nordic Process Control Workshop, 2012, pp. 133 – 140.
[38] A. K. Duun-Henriksen, D. Boiroux, S. Schmidt, K. Nørgaard, S. Madsbad, O. Skyggebjerg, P. R. Jensen, N. K. Poulsen, J. B. Jørgensen, H. Madsen, Tuning of controller for type 1 diabetes treatment with stochastic differential equations, in: 8th IFAC Symposium on Biological and Medical Systems, BMS 2012, Budapest, Hungary, 2012.
[39] N. R. Kristensen, H. Madsen, S. B. Jørgensen, Parameter estimation in stochastic grey-box models, Automatica 40 (2004) 225 – 237.
[40] J. B. Jørgensen, S. B. Jørgensen, Comparison of prediction-error modelling criteria, in: Proceedings of the 2007 American Control Conference (ACC 2007), 2007, pp. 140–146.
[41] J. K. Huusom, N. K. Poulsen, S. B. Jørgensen, J. B. Jørgensen, Adaptive disturbance estimation for offset-free SISO model predictive control, in: 2011 American Control Conference on O'Farrell Street, San Francisco, CA, USA, ACC 2011, 2011, pp. 2417–2422.
[42] J. B. Jørgensen, J. K. Huusom, J. B. Rawlings, Finite horizon MPC for systems in innovation form, in: 50th IEEE Conference on Decision and Control and European Control Conference (CDC-ECC 2011), 2011, pp. 1896 – 1903.